A 1,000 YEAR HIGH-RESOLUTION HURRICANE HISTORY FOR THE BOSTON AREA BASED ON THE VARVED SEDIMENTARY RECORD FROM THE LOWER MYSTIC LAKE (MEDFORD/ARLINGTON, MA)

A Dissertation Presented

by

MARK R. BESONEN

Submitted to the Graduate School of the
University of Massachusetts Amherst in partial fulfillment
of the requirements for the degree of

DOCTOR OF PHILOSOPHY

September 2006

Geosciences

A 1,000 YEAR HIGH-RESOLUTION HURRICANE HISTORY FOR THE BOSTON AREA BASED ON THE VARVED SEDIMENTARY RECORD FROM THE LOWER MYSTIC LAKE (MEDFORD/ARLINGTON, MA)

A Dissertation Presented

by

MARK R. BESONEN

Approved as to style and content by:

_____
Raymond S. Bradley, Chair

_____
R. Mark Leckie, Member

_____
Mark B. Abbott, Member

_____
Pierre Francus, Member

_____
Stuart D. Ludlam, Member

_____
Michael L. Williams, Department Head
Department of Geosciences

ACKNOWLEDGEMENTS

The completion of this project is due, by no small measure, to the many people who have either supported, inspired, or lent a hand to the project over the years.

Without a doubt, my patient and loving wife, Olga, falls at the top of the list of those who deserve my thanks. There are many sacrifices associated with supporting a spouse through graduate school—some big, some small, some obvious, some less visible. For the better part of a decade, Olga has weathered those sacrifices, and provided me the support that I needed to bring this project to completion. For that, sweetheart, I offer you my sincerest thanks and appreciation. Thank you so much, Olga!

Many words of thanks are also due to my advisor, Ray Bradley, who provided the original spark that ignited this project. In particular, in late 1995 or early 1996, Ray presented me with a copy of Liu and Fearn (1993), and suggested a similar project for the New England area, but carrying it over to a higher resolution archive such as a varved lacustrine record. Of course, Ray's patience and wisdom in advising this project over many years cannot be underestimated. Importantly, thanks to his tireless motivation over that last year, I was finally able to bring this project to completion. Finally, Ray provided the lab infrastructure, and in particular, access to two of his stellar post-docs (Mark Abbott and Pierre Francus) who provided fundamental lift-off and propulsion for the project at varying times. Thank you, Ray!

Mark Abbott was instrumental in actually identifying the Lower Mystic Lake as a possible candidate lake after talking with Stuart Ludlam, and importantly, for introducing this then neophyte to the world of hands-on lacustrine research beginning with our first reconnaissance coring trip to the lake in May 1996. For certain, it was Mark's extensive

experience that allowed him to guide a whole crew of us greenhorns to successfully retrieve two long piston cores from the lake in late 1996. The first of those two cores serves as the backbone for this project. To help the project take off, Mark provided the initial two radiocarbon dates to establish a first order of chronologic control, and to keep the project moving he essentially subsidized some of the later radiocarbon dates as well. And despite his move to Pittsburgh, he continued to provide a sort of big brotherly motivation and an occasional kick in the pants as necessary. Thank you, Mark!

Pierre Francus was responsible for introducing me to the process of impregnating unconsolidated sediments with resin, and then thin sectioning them for microscopic analysis. This started me down the road of developing the Lower Mystic Lake varve chronology, one of the fundamental strengths of this project. Later, Pierre's motivation and guidance introduced me to back-scattered electron microscopy and quantitative image analysis. For certain, the back-scattered electron imagery was an extremely powerful tool that gave me the ability to dissect and examine the sediments in a way which was simply not possible with the light microscope. Pierre's impressive knowledge of laminated sediments and paleo records was a constant source of reference. And like Mark, his guidance and motivation to complete the project continued even after he left UMass for the greener pastures of Quebec. Thank you, Pierre!

Mark Leckie and Stuart Ludlam provided occasional guidance and motivation along the way, but importantly did a fantastic job going through the manuscript to provide thoughtful critiques, comments, and suggestions. Dr. Ludlum was also gracious and generous with information about the lake as this project got off the ground, and along the

way provided plankton tow samples as well as some of the Ekman dredge surface samples that he was able to retrieve in the summer of 1993. Thank you, guys!

John Sweeney, our department MacGyver, was the man who, with just a simple diagram and my sketchy ideas, was able to build the oversized freeze-corer that finally allowed us to retrieve the missing section of the sedimentary record that we had doggedly pursued for many years in vain. And John had the patience to deal with the multiple revisions and modifications that were needed to actually make the corer functional. Thank you, John!

Over the years as multiple trips were made to either the lake or marsh for fieldwork, many people bothered to take time out of their busy schedules at one time or another to lend a hand, and break a sweat. These folks include Mark Abbott, Lesleigh Anderson, Michael Apfelbaum, David E. Besonen, Pierre Francus, Olga Gil, Stephen Healy, Rose Heyer, David Korejwo, Ted Lewis, Falk Lindenmaier, Whit Patridge, Bianca Perren, Neal Price, Jack Ridge, Sheldon Smith, Chloe Stuart, and David Wilson. Thank you, everyone!

Among the multitude of folks named above, my dad, David E. Besonen, deserves special thanks because he is the guy who, besides myself, has dedicated the most time to fieldwork and field "infrastructure" support for both the lake and marsh portions of this project. Importantly, this includes providing the "1 human-power motor" that paddled us around the lake in a canoe to obtain about 13 km of GPS/bathymetric track log. Thank you, Dad!

Though this project was self-funded for the most part, the occasional financial support that was received along the way was greatly appreciated, and must be

acknowledged. The UMass Department of Geosciences provided some help early on in the form of Leo M. Hall and Gloria Radke Memorial Prizes to help defray the cost of summer fieldwork and consumable lab supplies. This was supplemented by a student research grant from the Geological Society of America which was dedicated to similar purposes. As mentioned earlier, Mark Abbott funded the initial two radiocarbon dates, and essentially subsidized some of the later ones as well. The largest boost came from a Doctoral Dissertation Improvement Grant provided by the Geography and Regional Science program of the National Science Foundation. This grant (BCS-0101035) was responsible for funding the ^{210}Pb and ^{137}Cs analyses, a series of ^{14}C dates, construction of the oversized freeze corer, lab supplies for sediment impregnations, and finally for out-of-house thin section production.

Despite these three pages of acknowledgements, I have undoubtedly forgotten to mention some folks who really should be thanked individually for something they helped out with. If you are one of those folks, please forgive my oversight. Another whole group of folks does not have to be named individually, but I thank you for your camaraderie, support, and friendship through the years because it has made my time here in the Pioneer Valley a happy one.

ABSTRACT

A 1,000 YEAR HIGH-RESOLUTION HURRICANE HISTORY FOR THE BOSTON AREA BASED ON THE VARVED SEDIMENTARY RECORD FROM THE LOWER MYSTIC LAKE (MEDFORD/ARLINGTON, MA)

SEPTEMBER 2006

MARK R. BESONEN, B.S., TUFTS UNIVERSITY

M.S., UNIVERSITY OF MINNESOTA DULUTH

Ph.D., UNIVERSITY OF MASSACHUSETTS AMHERST

Directed by: Professor Raymond S. Bradley

The Lower Mystic Lake (Medford/Arlington, MA) is a 24 m deep, ectogenically meromictic, low elevation (1 m a.s.l.), coastal lake directly connected to Boston Harbor by the Mystic River. About 1,000 years ago, steadily rising sea level in the Boston area finally reached a point at which occasional marine water delivery events via the river channel could actually reach the lake basin. Since then, such events have continued with enough frequency to maintain the meromictic condition.

Meromixis has allowed the Lower Mystic Lake to accumulate an exquisitely laminated, annually resolvable (i.e. varved) archive of sedimentation in the lake over the last 1,000 years. A varve chronology was developed from this record. Multiple lines of robust evidence verify and validate the accuracy of the chronology.

A series of anomalous, graded beds was found in the stratigraphy, and they show excellent coordination with known historic hurricanes that have affected the Boston area. The graded beds appear to be the result of intense, hurricane-strength rains which cause erosive overland flow that entrains sediment which is carried into the lake where it is

deposited as a graded bed. This is enhanced by hurricane-strength winds which disturb vegetation, and uproot trees to expose fresh, loose sediment. By analogy, similar graded beds in the prehistoric portion of the stratigraphy probably represent similar hurricane events

This record of hurricane activity was compared to a record of sand layers in nearby Belle Isle Marsh (Boston Harbor) which are presumably the result of storm surge overwash events. Such sand layers in low resolution coastal archives are the main form of proxy evidence that paleotempestology studies have used to piece together longer term records of hurricane activity. Even when using multiple techniques, chronologic control in such archives is difficult, and linking sand layers to any particular storm is only tentative at best. Importantly, the Belle Isle Marsh record shows an apparent 600-year quiescent period. However, this is not due to a lack of hurricanes or storms, but to an unknown geomorphic change which affected the marsh, and it therefore serves as a cautionary note for the use of such archives.

TABLE OF CONTENTS

Page

LIST OF TABLES

LIST OF FIGURES

CHAPTER 1

INTRODUCTION

1.1 Background and description of the problem

1.1.1 The legacy of Hurricane Andrew

In August 1992, Hurricane Andrew made landfall at Homestead, Florida about 45 km south of Miami. At landfall, Andrew was a Category 5 hurricane[1], but it quickly decreased to Category 3 strength as it crossed westward over the peninsula. The hurricane made landfall a second time along the sparsely populated Atchafalaya Bay region of the Louisiana coast.

Despite the fact that Hurricane Andrew did not strike any major urban center, it caused more than $30 billion of property damage. The damage exceeded every single estimate of the maximum likely expected losses that could be caused by a single hurricane—ten insurance companies went bankrupt, and a significant portion of the worldwide insurance capital dedicated to natural disasters was exhausted (IIPLR and IRC, 1995; Michaels et al., 1997; RPI, 1997). Subsequent calculations showed that if a large hurricane were to make a direct strike on one of the many major urban centers in the Gulf of Mexico or along the eastern seaboard of the U.S., the results would be nothing short of

[1] Hurricane Andrew's landfall strength was originally estimated as Category 4 based on measured average wind speeds of 145 mpg. However, in 2002, the NOAA National Hurricane Center upgraded it to Category 5 based on a reanalysis which suggested the sustained wind speeds reached 165 mph (see http://www.noaanews.noaa.gov/stories/s966.htm for details). A brief discussion about the Saffir-Simpson hurricane intensity scale, the category scale used to classify the intensity of a hurricane, is presented in the "5.2.1 Regarding trajectories and intensities of pre-20th century hurricanes" section of Chapter 5 of this dissertation.

a major "economic catastrophe" for the global insurance industry (Diaz and Pulwarty, 1997).

What went wrong? Had the traditional actuarial approach for predicting damage, assigning risks, and specifying appropriate insurance premiums failed? Not exactly. An analysis of the situation pointed to the inadequacy of our present record of the natural variability of hurricane activity. This record extends back just 50-100 years reliably (Diaz and Pulwarty, 1997; RPI, 1997), and before that is supplemented by historical records which are increasingly sparse back in time (Ludlum, 1963). This short record is hardly sufficient to predict "100 year" catastrophe events, let alone events with longer recurrence intervals.

1.1.2 The spectre of global warming

Concern is heightened in the face of global warming (IPCC, 2001; Mann et al., 1998 and 1999) because simple atmospheric circulation models suggest the frequency and intensity of hurricane and tropical storm activity should increase in a CO_2-warmed climate (Emanuel, 1987 and 1997; Broccoli and Manabe, 1990; Knutson et al., 1998). Complicating this issue is the fact that more than 53% of the total U.S. population is concentrated along the coasts, and coastal populations are expected to swell another 20% by 2015 (NOAA, 1998). The grim question hanging in the mind of the global insurance industry, as well as that of civic planners and disaster management agencies alike, is whether Hurricane Andrew was simply a precursor to an increasing number of even more costly and deadly tropical storms we should expect in the coming decades.

1.1.3 Addressing the problem

Our experience with Andrew clearly indicated the need for longer-term proxy records of hurricane and tropical storm activity. An obvious place to look for such records are coastal zones as these areas bear the brunt of destructive storm surge and hurricane-force winds and precipitation before a storm begins to weaken over land. These environments may experience abrupt changes in physical sedimentology, or disturbances to vegetation and fauna related to the passage of a storm. If such changes or disturbances are somehow recorded in the sedimentary record, these "signatures" may serve as a proxy witness for such events, and allow us to develop longer-term proxy records of storm activity back in time.

1.2 The science of paleotempestology

1.2.1 Sedimentary signatures and the birth of paleotempestology

Sedimentary signatures related to storm activity have been recognized in a variety of coastal and nearshore environments including:

a.) lakes/ponds (Liu and Fearn, 1993 and 2000; Williams, 1995; Parsons, 1998; Dix et al., 1999; Collins et al., 1999)

b.) marshes (Nyman et al., 1995; Donnelly et al., 2001a,b and 2004; Hilterman, 1998; Rejmanek et al., 1988; Scott et al., 2003), and

c.) shallow open water environments (Davis et al., 1989; May, 1990; Keen and Slingerland, 1993; Flowers et al., 1995; Fisher et al., 1998; Kalbfleisch and Jones, 1998).

However, just a handful of these studies have been carried out for the express purpose of developing records of hurricane activity. Liu (2000) has recently dubbed this nascent field as "paleotempestology".

1.2.2 Gulf of Mexico pioneering groundwork and possible synoptic controls

The groundwork was laid by Liu and Fearn (1993). These researchers observed a sand layer in the uppermost sediments of Lake Shelby on the Alabama coast, and related it to a storm surge overwash fan deposited during the passage of Hurricane Frederic in 1979. Using this modern analog, they recognized five other prominent sand layers deposited in the past 3,000 years, and attributed these to direct strikes by Category 4-5 hurricanes. They noted a total lack of overwash deposits before 3,200 ^{14}C years B.P. suggesting control by a large-scale process such as a regional climatic shift. Freshly following on the heels of Hurricane Andrew, the work of Liu and Fearn (1993) served as a catalyst for a series of similar studies which have begun to provide some longer-term proxy records of storm activity.

Applying the same technique to sediments from Western Lake located in the Florida Panhandle, Liu and Fearn (2000) recognized twelve prominent sand layers which were attributed to category 4-5 hurricanes strikes in the last 3,400 years. Importantly, the inferred activity seemed nearly bimodal at the millennial scale. Eleven of the twelve sand layers were deposited between 3,400 and 1,000 ^{14}C years B.P., but in the last millennium only one sand layer was recorded. The authors suggested that hyperactive hurricane activity in the Gulf of Mexico was probably controlled by shifts in the position of the jet stream and Bermuda High (Figure 1).

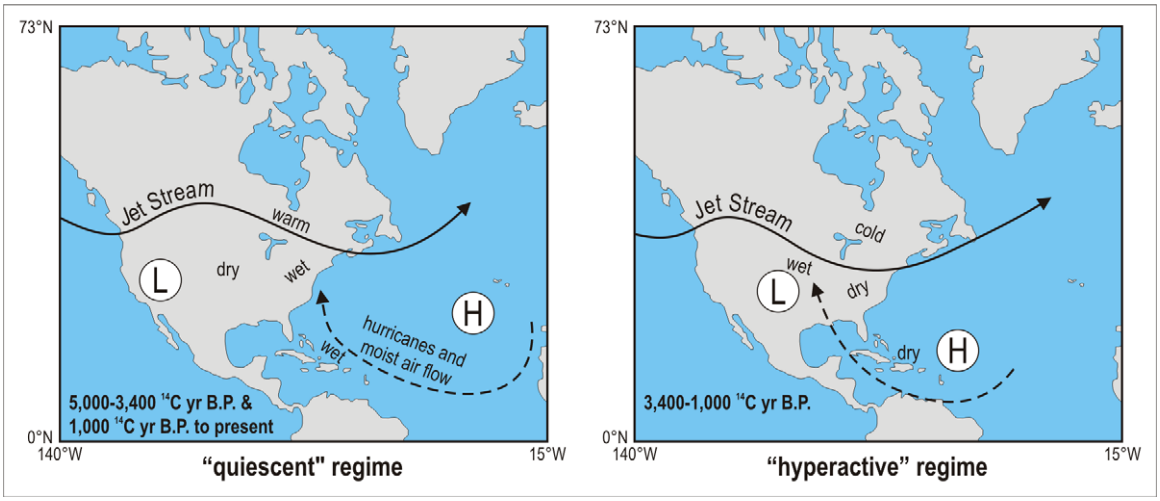

Figure 1—Postulated synoptic control configurations for different hurricane activity regimes in the Gulf of Mexico. This figure is slightly modified from Liu and Fearn (2000).

This relationship was further analyzed by Elsner et al. (2000) who concluded that there was a strong inverse correlation in hurricane activity between the Gulf of Mexico and the eastern seaboard of the U.S. They related this to the position of the subtropical high, and the intensity of the North Atlantic Oscillation. In essence, they suggested that hurricane storm tracks are either funneled into the Gulf of Mexico, or are diverted away from it towards the east coast of the U.S. The implication was that the east coast is currently experiencing a hyperactive regime because the Gulf of Mexico is in quiescent mode.

1.2.3 Records from Rhode Island and New Jersey

Donnelly et al. (2001a,b and 2004) contributed records from several backbarrier coastal marshes along the northeastern U.S. coast. In these marshes, they encountered sand layers which are interpreted as overwash fans related to hurricane storm surge. From Succotash salt marsh (East Matunuck, Rhode Island) in the Narragansett Bay region of southern New England, they developed a 700 year long record, and recognized four

sand layers deposited during historical times, as well as two deposited during prehistoric times (Donnelly et al., 2001a). From Whale Beach, New Jersey, Donnelly et al. (2001b) produced another 700 year long record, and recognized three sand layers (two deposited during historical times, one deposited during prehistoric times). From the beach at Brigantine, New Jersey, Donnelly et al. (2004) generated a record that contains five sand layers deposited in the past 200 years, and two from prehistoric times.

1.2.4 Record from South Carolina

From Singleton Swash, South Carolina, Scott and Collins (1999) and Scott et al. (2003) recognized sand layers in the stratigraphy, and interpreted them to represent overwash deposits from the past 5,000 years. In particular, they noted two deposits around 5,000 years ago, a few more sand layers up to 1800 years B.P., and then a significant increase in sand layers up to the present. Importantly they carried the work a step further than the other studies by examining microfossil assemblages. In particular, they recognized offshore foraminifera in the storm deposits which definitively indicates the sandy deposits are overwash from an offshore locality, and not simply the result of changing coastal geomorphology.

1.3 Contributions of this project to paleotempestology

1.3.1 Limitations of preexisting work

The hurricane proxy records listed above are grounded in sedimentology, and provide a basic foundation for the field of paleotempestology. However, all of the

records come from either shallow coastal lakes or marshes, and have some of the following limitations:

1.) Bioturbation—The existing records are subject to intense bioturbation which decreases event resolution, and may actually skew the number of recorded events. For example, the record of two (or more) hurricane events closely spaced in time may be homogenized and recognized as a single larger event, or the record of more subtle events may be entirely erased.

2.) Chronologic control—Like most Holocene proxy records, the majority of chronologic control is provided by radiometric dating. The limitations and vagaries of radiometric dating, in particular, radiocarbon dating, inevitably allow for improvement especially using annually-resolvable sedimentary records.

3.) Rapid coastal geomorphic evolution—Geomorphic evolution may significantly affect how a coastal lake or marsh records an overwash event; geomorphic changes such as migrating tidal channels, or beach erosion or progradation are common especially when the relative sea level at a location is not static through time

1.3.2 Goal of this project

Since conception of the current project, our goal has been to carry paleotempestology studies to the next level—to develop a hurricane proxy record that significantly overcomes the limitations mentioned above. To do so, we have turned to a varved (i.e. annually laminated) lacustrine record that completely eliminates the issue of bioturbation, and offers exquisite and robust chronologic control that is simply impossible to obtain using sedimentary records from shallow coastal lakes and marshes.

From the beginning, we specifically targeted a sedimentary record that was located slightly inland to minimize issues related to coastal geomorphic evolution, and to serve as a natural filter against frequent winter nor'easter storms which are common along the eastern seaboard of the U.S. Our hurricane proxy record is based on the varved sedimentary record archived in the Lower Mystic Lake, a meromictic coastal lake on the border between Medford and Arlington, Massachusetts which is described further below.

1.3.3 Specific research questions to be addressed and answered

1.3.3.1 What is the average recurrence rate for large intense hurricane strikes near the Boston area during the last millennium?

The 700 year record from Succotash salt marsh in Narragansett Bay (Donnelly et al., 2001a) is the closest preexisting record for the Boston area. Sand layers encountered in the backbarrier marsh stratigraphy were interpreted to represent hurricane overwash fans. Two fans were deposited during prehistoric times (~600 and ~550 years B.P.). Four fans were deposited during historical times, and were attributed to known hurricanes in 1635, 1815, 1938, and 1954. This gives a recurrence interval of approximately 120 years per hurricane strike. However, it may be that other events which should be included are missing. For example, information about the hurricane of 1635 comes from accounts of John Winthrop, Governor of the Massachusetts Bay Colony (Ludlum, 1963). Winthrop wrote that, "The tide rose at Naragansett [sic] fourteen feet higher than ordinary." Yet for another hurricane just three years later in 1638, the very same Winthrop commented that, "about Naragansett [sic], it raised the tide fourteen to fifteen foot [sic] above the ordinary spring tides, upright.". Because both storms produced an

equivalent storm tide, they would presumably produce a similar record at Succotash salt marsh. However, only one sand layer exists in the stratigraphy at the appropriate time. This may be due to the nature of the archive—bioturbation may have combined the results of two closely spaced events into a single perceivable event. Alternatively, either of the storms may not have left a strong physical sedimentological expression in the record (Collins et al., 1999). For the Mystic Lake record, it is not expected that the exact same suite of storms as registered at Succotash salt marsh will be seen, but it is expected that the long term average of hurricane activity will be similar or greater given that bioturbation of the record has not occurred.

1.3.3.2 Do the hyperactive and quiescent modes of hurricane activity reported in the Gulf of Mexico also exist for the eastern seaboard of the U.S., and are they anti-correlated between regions?

This question does not yet have an answer because very few records exist, and geomorphological changes such as shifting channels or migrating dunes may lead to what is interpreted as an on/off signal in hurricane activity. The Succotash record is just 700 years long, so it does not cover the hypothesized transition between regimes at 1,000 years B.P. indicated by Liu and Fearn (2000) and Elsner et al. (2000). And the Singleton Swash record points to a transition between regimes at 1800 years B.P., a significant difference from 1000 years B.P. The 1,200 year[2] Lower Mystic Lake record will contribute another piece of evidence to help resolve this question.

[2] A gap in the varved stratigraphy existed for several years despite multiple unsuccessful attempts to close it. It was finally closed via an oversized freeze core in January 2001. However, prior to this point when this research question was devised, the age of the varve chronology could only be estimated based on a single radiocarbon date towards the base of the laminated section. That radiocarbon date suggested the varves extended back about 1200 years before present, hence the 1200 year figure here.

1.3.3.3 Can any empirical relationship be detected between periods of globally warmer or cooler climate, and hurricane activity which simple atmospheric circulation models suggest should exist?

This relationship has never been documented by empirical or proxy evidence. The Mystic Lake record will be used to ground-truth these model results. The magnitude and frequency of hurricane activity during periods of warmer and cooler climate (i.e. the Medieval Warm Period (Keigwin, 1996), and the Little Ice Age (Grove, 1988), respectively, will be examined in relation to the entire 1,000 year record to see what trends might be expected related to global warming.

1.4 Details about the Lower Mystic Lake and its unique sedimentary record

1.4.1 Location

The Lower Mystic Lake, henceforth referred to as the "LML", is a meromictic coastal lake situated between Medford and Arlington, Massachusetts. It is located 10 km from downtown Boston as the bird flies, and it is directly connected to Boston Harbor via the Mystic River by approximately the same distance (Figure 2). The lake has a low surface elevation of just one meter above sea level (USGS, 1985)[3]. Combined with its slight inland location, the lake is optimally positioned to record the effects of powerful hurricane storm surges, but at the same time protected from the action of smaller winter storm tides[4].

---

[3] The sea level datum used is mean low water.

[4] When this project was being conceived, our working hypothesis was that a hurricane signal in the sediments of the LML would be the result of storm surge deposition from the seaward side of the system. In fact, we specifically searched for a lake with a slightly inland location so it would be subject only to the largest of storm surges like those associated with a hurricane. Nonetheless, as the project evolved, and we

1.4.2 Mystic River tidal prism system

The Mystic River system formerly functioned as an estuarine tidal prism system. Garrison (1993) explains a tidal prism system as follows:

> "...exiting fresh water holds back a wedge of intruding sea water...the seawater wedge moves seaward at times of low tide or strong river flow and returns landward as the tide rises or when river flow diminishes..."

During normal tidal circulation on the Mystic River, the seawater wedge reached upstream to some point past Cradock Dam (Figure 2), but generally not to the LML itself (Totten et al., 1861). However, the lake was often noted as brackish (R. Duffy, personal communication[5]), and the presence of dilute marine water in the basin (see the "1.4.4 Chemical stratification and water column structure" section below) clearly indicated that marine water reached the lake on at least occasions. In 1908/1910[6], the Cradock Dam was built to prevent the regular tidal bore from passing further upriver of this spot. On occasion, the locks at the dam were opened up intentionally to allow marine water to pass upstream (Ludlam and Duval, 2001, and R. Duffy, personal communication). For example, they were opened on a few occasions in the 1930's to help flush out the river system upstream of the dam because bacterial counts there had become too high (R.

---

generated ever more data about the system, we came to the conclusion that our original hypothesis of storm surge deposition was incorrect. In fact, the hurricane-related deposition in the LML comes from the the lake watershed on the landward side of the system. This is briefly mention in the "1.4.8 The varve chronology and paleotempestology" section of this chapter below, and then thoroughly documented in Chapter 5 of this dissertation.

[5] Richard Duffy is a local historian from the town of Arlington. He has a particular interest in the Mystic Lakes and River system, and has spent many years researching their history via various historical sources.

[6] Many different resources cite 1908 as the year in which the Cradock Dam was constructed. However, R. Duffy (personal communication) suggests the dam was not completed until about 1910 based on his research. In particular, his evidence for this conclusion is a Medford Mercury newspaper article from 1910 which mentions that the impending completion of the dam would "bring to an end the annual harvest of thousands of eels."

Figure 2—Location map showing the Lower Mystic Lake and Mystic River system down to Boston Harbor. Other important locations and points of interest referenced in the text are also included.

Area of large map
MA
CT
RI
Belle Isle Marsh
N
0
1
2
3 Km
Logan International Airport
Boston Inner Harbor
Amelia Earhart Dam (1966)
Mystic River
Charles River
Wrights Pond
Cradock Dam (1908)
Aberjona River
Upper Mystic Lake
Lower Mystic Lake
Spy Pond
Alewife Brook
Little Pond
Fresh Pond

Duffy, personal communication). Later, in 1966, the larger Amelia Earhart Dam (Figure 2) was constructed, and estuarine activity on the river upstream from the dam completely ceased.

1.4.3 Setting and general physical limnology

The LML is a small kettle lake (Chute, 1959) with a surface area of approximately 3.76×10^5 m^2 (Figure 3). The main inflow is from the Upper Mystic Lake (henceforth referred to as the "UML") which itself is primarily fed by the Aberjona River (Figure 2). A smaller inflow stream known as Mill Brook (Figure 3) is situated at the southwest corner of the lake, but its contribution is negligible. Water exits from the LML at its southeastern corner via the Mystic River (Figures 2 and 3), and travels 11 km to reach Boston Harbor.

The LML and UML were formerly confluent. However, in 1864[7], a 2-3 m high dam (adjustable by boards) was built between the lakes at a natural constriction known as "The Partings" (Figure 3).

The LML is composed of two sub-basins (Figure 3). The northern sub-basin is shallower, and approaches 16 m depth. The southern sub-basin is deeper, and reaches 24 m depth.

Residence time of water in the lake (calculated as lake volume ÷ inflow rate) is quite short. Based on the bathymetric survey we conducted (discussed in Chapters 3 and 4), the lake has an approximate volume of 3.54×10^6 m^3. A USGS stream gauge exists

[7] There is some slight disagreement in the literature about the actual date when this dam was built. In Brooks and Usher (1886), they cited the date of 1861 as its construction date. But Chapman (1936)

on the Aberjona River about 800 m upstream of where the river empties into the UML. Based on 63 years of stream flow data from this gauge, the river has an average flow rate of 0.838 m^3/sec (Socolow et al., 2003). This suggests that residence time in the LML is on the order of just 49 days.

1.4.4 Chemical stratification and water column structure

In most New England lakes, the entire water column is mixed by a combination of simple wind-driven circulation and density-driven overturn[8] due to seasonal temperature differences. Such lakes which mix completely are termed holomictic. However, the LML is permanently stratified into upper and lower water masses, and the lower mass is entirely excluded from circulation processes. Such a lake is termed meromictic.

The lower water mass, the monimolimnion, is composed of dilute marine water, and the upper mass, the mixolimnion, is composed of fresh water (Figure 4). The stratification between these two water masses is a direct function of their chemical composition—the salinity of the monimolimnion gives it a greater density than the overlying fresh water mass, and the density contrast prevents them from mixing. A chemocline, or zone of rapidly changing chemical composition, separates the two water masses (Figure 4).

---

suggests that it was started in 1863, and completed in 1864. R. Duffy (personal communication) believes the 1863/1864 version to be correct.

[8] This overturn process occurs in the spring and fall because of a peculiar physical property of water—it is densest at ~4°C, and not its freezing point. Thus, in the fall, as the lake surface temperature cools and passes through the 4°C point, the surface water becomes denser, sinks to the bottom, and pushes warmer water to the surface. That water then cools, and sinks to the bottom, and so on, and so forth until the entire water column falls below 4°C. In the spring, the same process occurs, but in reverse as the water column warms up to the 4°C point. This overturn process essentially functions like a conveyor belt to thoroughly mix the water column.

Figure 3—Bathymetry map of the Lower Mystic Lake. This map was produced from our bathymetric survey which is discussed in Chapter 3 of this dissertation.

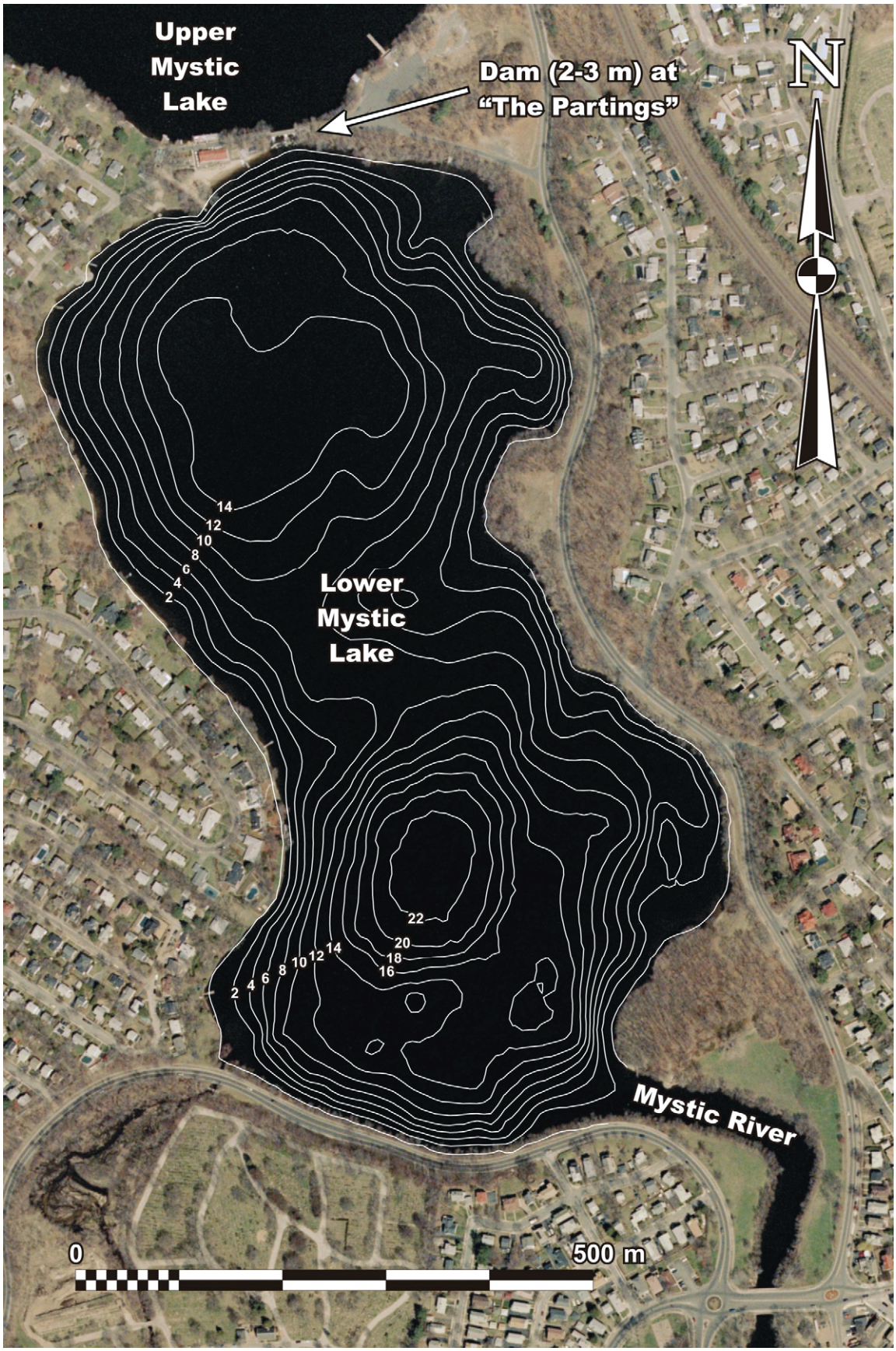
Upper
Mystic
Lake
Dam (2-3 m) at
"The Partings"
N
Lower
Mystic
Lake
2
4
6
8
10
12
14
16
18
20
22
Mystic River
0
500 m

This existence of this denser, dilute marine water mass was recognized as early as 1857 when a water report by Baldwin and Stevenson mentioned the presence of "foul matter" in the water column (Totten et al., 1861). According to Duval and Ludlam (2001) and Ludlam and Duval (2001), this may make the LML the very first meromictic lake reported in the United States. Meromixis is of ectogenic origin, and is discussed in the "1.4.6 Meromixis is of ectogenic origin, and produced by marine water delivery events via the Mystic River" section below.

The top of the monimolimnion is currently situated at approximately 18 m depth (Figure 4), and thus only exists in the deep, southern sub-basin of the LML. The northern sub-basin is currently holomictic. The chemocline extends from the top of the monimolimnion upwards to about 15.5 m water depth where it meets the base of the mixolimnion (Figure 4). The mixolimnion, like other lakes in the region, shows a typical seasonal dimictic (i.e. twice yearly) circulation pattern with overturn in the spring and fall.

Figure 4 presents temperature, dissolved oxygen content, and salinity measurements for the southern sub-basin LML water column during the winter and early summer. As the monimolimnion is excluded from normal lake mixing processes, conditions in it are relatively constant throughout the year. Temperature shows a subtle trend increasing from ~6°C to ~7.5°C from the top of the monimolimnion down to 24 m depth. Oxygen is absent (i.e. it is anoxic)[9], and salinity is constant at around 17 ppt.

[9] While the dissolved oxygen concentrations illustrated in Figure 4 are very low, but non-zero, the monimolimnion is actually completely anoxic (i.e. 0 mg/l dissolved oxygen) as reported elsewhere (Duval and Ludlam, 2001 and Ludlam and Duval, 2001). As a result of S^{2-} poisoning, dissolved oxygen meters almost always indicate oxygen content as > 0 ppm, but < 0.5 ppm even when oxygen is completely absent (S. Ludlam, personal communication).

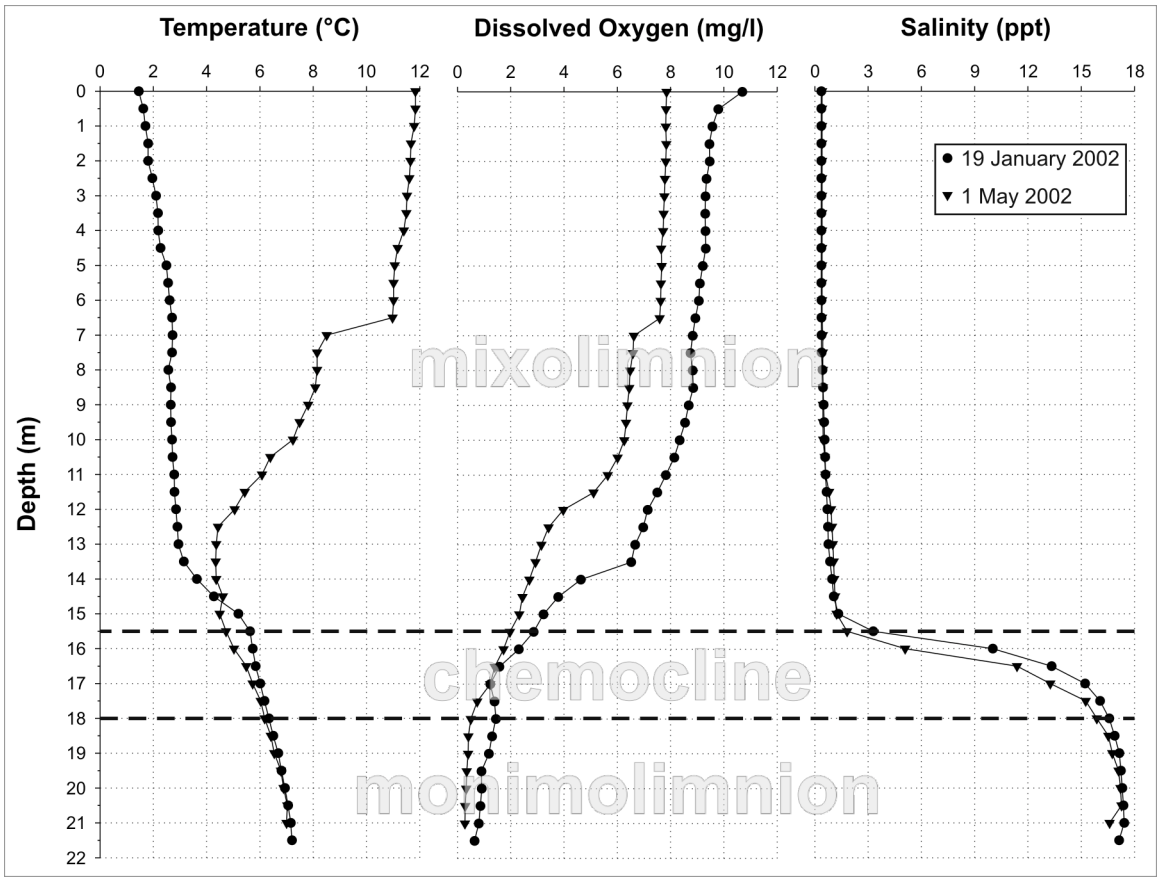

Figure 4—Water column structure, temperature, dissolved oxygen content, and salinity in the southern sub-basin of the Lower Mystic Lake. Note that these profiles were not taken at the very deepest point of the lake where it reaches 24 m depth.

1.4.5 Changing volume of the monimolimnion and chemocline, and their eventual demise

The volume of the monimolimnion and chemocline are not constant. Currently, they compose less than 4% of the total lake volume according to the hypsometric curve produced from our bathymetric survey (Figure 5). But their volume has fluctuated through time according to historical data. For example, analysis of data from Totten et al. (1861) suggests that back in 1860, the top of the chemocline was at approximately 6 m depth, and thus composed about 46% of the total lake volume (Figure 5).

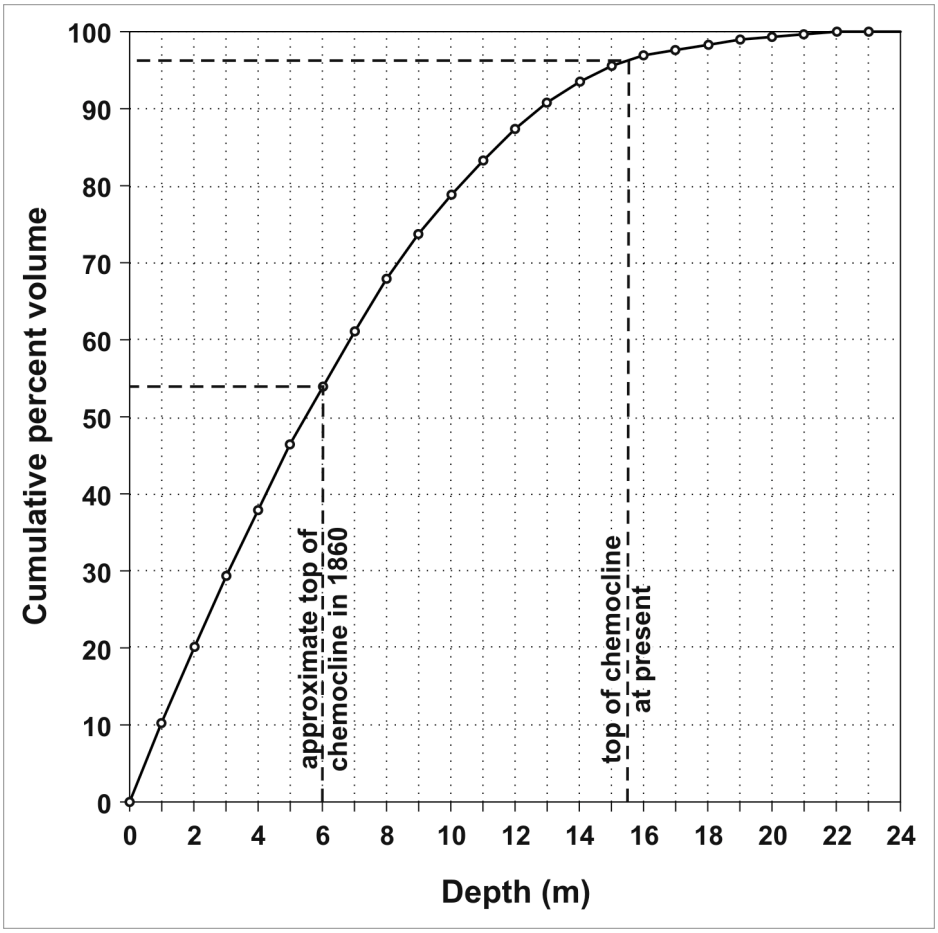

Figure 5—Cumulative percent volume hypsometric curve for the Lower Mystic Lake produced from bathymetric survey data. Tie lines showing the combined volume of monimolimnion and chemocline in 1860 and at present are included.

With the construction of the Amelia Earhart Dam in 1966, sea water can no longer reach the LML, and volume of the chemocline and monimolimnion will only decrease. Ludlam and Duval (2001) provide an in-depth historical analysis of the increasing depth of the chemocline (and hence, decreasing monimolimnetic volume) from 1965-1996, and estimate that the monimolimnion will completely disappear by 2013-2014.

1.4.6 Meromixis is of ectogenic origin, and produced by marine water delivery events via the Mystic River

The presence of the dilute marine water which composes the monimolimnion cannot be attributed to subsurface groundwater intrusion according to the Ghyben-Herzberg principle of salt water intrusion into an unconfined coastal aquifer (Fetter, 1980)[10]. This fact was realized more than 140 years ago when the LML was being evaluated as a possible source for fresh water. After an elaborate civil engineering survey project which extensively studied the tidal prism configuration in the Mystic River (Totten et al., 1861), and an accompanying chemical analysis of the LML water column and sediments (Horsford, 1860), it was concluded that the dilute marine water in the LML was:

> "…due to the inflow, not infiltration of sea water on the occasions of high tide; how frequently, and in what quantity, hydrographic observations only can determine. The foregoing observations are quite in keeping with occasional and rare, rather than frequent, supplies of sea water."

Thus, given this marine water delivery mechanism, meromixis in the LML is of an ectogenic origin (i.e. it is provoked by an external influence).

With what frequency was marine water delivered to the lake? The Horsford (1860) description of "occasional and rare" is vague, and perhaps misleading because no time scale is given. A more informative description is provided by Duffy (1999) who described the situation in the 1850's (before the dam was built at "The Partings"):

---

[10] Given the lake's surface elevation of one meter above sea level, this principle would predict the fresh/salt water interface at an elevation of ~40 m below sea level. But the lake has a maximum depth of only ~24 m (i.e. 23 m below sea level given its surface elevation); thus, the presence of the dilute marine water cannot be attributed to subsurface groundwater intrusion.. There is even less of a possibility of subsurface groundwater intrusion in the past as relative sea level in the Boston area over the late Holocene has always been lower than at present as documented in Chapter 2.

> "The Mystic Pond was also the occasional recipient of saltwater. This came about during periods of drought when the enfeebled outflow of freshwater would be overtaken by the tidal current, or as the result of seasonal flood tides or those due to 'northeaster' storms. These incursions of seawater yielded brackish conditions mostly in the lower section of the pond."

1.4.7 The varved sedimentary record

The LML preserves an exquisite record of sedimentation over the last millennium because the anoxic monimolimnion has protected the sediments beneath it from the homogenizing force of bioturbation. The uppermost 2.5 meters of the sedimentary record are discretely laminated at the millimeter scale. In fact, the sediments are varved—the laminae occur in distinct annual increments of sedimentation with a regularly alternating pattern of lighter-colored biogenic, and darker-colored siliciclastic components[11].

Varved records, by their very nature, possess an exact, continuous, internal, annual chronology that is independent of the vagaries of radiometric dating. The sedimentation is sensitive to changes in the environment, and in particular, to events which have affected the lake. In essence, the LML has preserved a year by year chronicle of sedimentation in the basin over the last 1,000 years.

The varved sedimentary record of the LML offers an unparalleled archive of paleoenvironmental information for Boston and the surrounding area. To the knowledge of the author, no comparable records exist for the greater New England area. In particular, with a 600 year pre-European settlement lead in, the record archives the

[11] This light/biogenic and dark/siliciclastic relationship is generally true when looking at a split sediment core, or a thin section in transmitted light. The color/composition relationship is reversed in other types of imagery with an example given in Figure 40 in Chapter 4.

environmental effects of the birth, growth, and development of a large urban center from a unique perspective at the very heart of that urban center.

1.4.8 The varve chronology and paleotempestology

We have developed a varve chronology to track sedimentation in the LML on a (sub-)annual basis over the last millennium. We have recognized a series of occasional, anomalous graded beds in the stratigraphy that are not part of the annual sedimentary cycle. For the historical portion of the record, these anomalous layers show excellent correspondence with years in which hurricanes have struck the Boston area.

Our original working hypothesis was that such deposits had a seaward origin, in particular, they were related to turbid storm surges which traveled up the Mystic River, and settled out in the LML. However, as the project evolved and we generated ever more data about the system, we have come to the conclusion that the graded beds are, in fact, generated from a landward source, in particular, the lake watershed. The mechanism we propose is that tree blow down and vegetation disturbance which accompany a hurricane allow its heavy precipitation to entrain sediment and carry it into the lake. This is more thoroughly documented in Chapter 5 of this dissertation.

As mentioned above, the varves from the historic period which contain the occasional, anomalous graded beds show excellent correspondence with years in which known historical hurricanes have affected the Boston area. Therefore, by analogy, we infer that similar deposits which occur in the prehistoric portion of the record represent similar events. This study serves as a natural extension to earlier paleotempestology work

such as the pioneering study of Liu and Fearn (1993), but it overcomes many of the limitations of this earlier work by use of a precise, high resolution archive.

1.5 A note about this dissertation regarding imagery and electronic distribution

Computer bitmap imagery (regular optical core photography, optical microscope thin-section imagery, high resolution X-ray densitometry imagery, and BSEM imagery) figures prominently in this dissertation. Besides a few printed copies, it is expected that this dissertation will be primarily made available and distributed in an electronic form such as in Adobe Acrobat PDF format. Therefore, the imagery has been downsampled to 200 dpi resolution to keep the resulting electronic file to a manageable size. Furthermore, some of the imagery such as the BSEM material has simply not been included because it is essentially useless in printed and/or low resolution format. If high resolution originals and/or the excluded imagery is needed at some point in the future, it should be available by getting in touch with the author.

CHAPTER 2

SEA LEVEL RISE AND THE BIRTH OF A LAMINATED SEDIMENTARY RECORD

2.1 Introduction

Meromixis in the LML is a direct result of marine water delivery to the basin via excessive spring tides, storm surge, or simply drought conditions that allow the tidal prism to more easily extend up river. A critical and limiting control for each of these mechanisms is the long-term rise or fall of sea level. A significantly lower sea level would make it impossible for such mechanisms to affect the lake. But a significantly higher sea level would make such marine water delivery events more common and frequent.

Accordingly, this chapter reviews currently available sea level records for the New England area. While the last 1000 years is of the most importance for understanding the birth and development of the LML's laminated sedimentary record, critical context is provided by first briefly examining the sea level history since the Late Glacial. Subsequently, we review the records that are available for the greater New England area over the last 5000 years, and finally, we present a synthesis which represent our best interpretation for the evolution of sea level in the Boston area over the last 1000 years, and its possible significance for the LML storm record.

2.2 Eustatic sea level versus relative sea level

When discussing sea level, it is important to distinguish between eustatic sea level and relative sea level.

Eustatic sea level refers to a global or absolute sea level which on the time scale of ~100,000 years is, in general, controlled by the climate system. The control mechanism is the distribution of water masses in the hydrologic cycle; in particular, the volume of water sequestered into continental ice sheets in the Northern Hemisphere. During warm interglacial epochs such as at present, no large Northern Hemisphere continental ice sheets exist, and eustatic sea level is high. But during cold glacial epochs when water becomes locked up in the ice sheets at the expense of the ocean basins, the eustatic sea level drops. The quantity of water sequestered as ice is significant and measurable. For example, at the point of maximum ice sheet extent during the last (i.e. Wisconsinan) glaciation, it is estimated that eustatic sea level had been lowered by approximately 120 m due to this mechanism (Fairbanks, 1989).

In general, the apparent sea level perceived at any particular coastal locality does not mirror the contemporaneous eustatic sea level trend exactly. In fact, not only may the magnitude of change be different, but the actual direction (i.e. rise vs. fall) may also be out of sync (Figure 6). These differences can be attributed to a variety of local factors. For example, local tectonic upwarping or subsidence of the crust, or simple changes in sediment delivery and/or accommodation are some factors that may cause deviation. In areas directly affected by glaciation such as Boston, another significant factor is isostatic adjustment of the earth's crust under the weight of overriding ice sheets. Thus, the

effective or apparent sea level perceived at any particular locality is actually a local relative sea level (hereafter indicated by RSL).

An important implication of this fact is that if one is interested in the effects of changing sea level at any spot such as the Boston area, one should consider its RSL history, and not simply the eustatic trend.

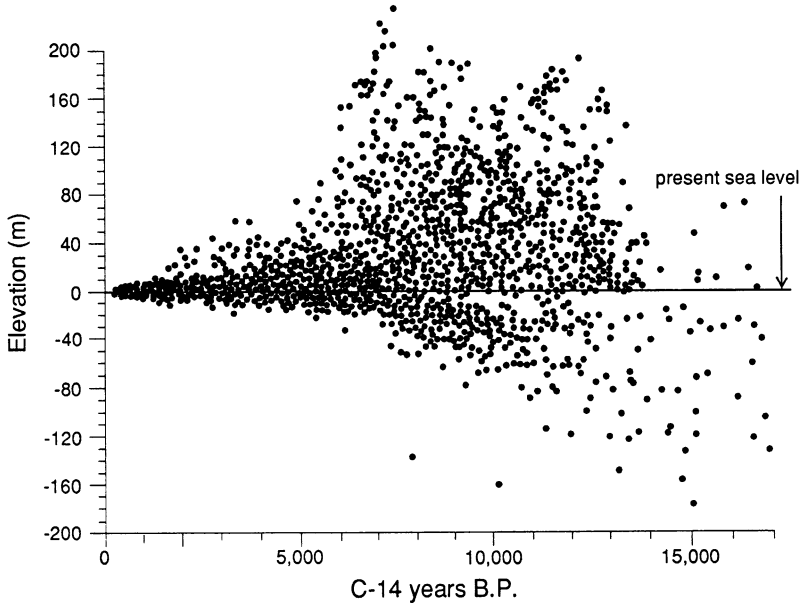

Figure 6—Plot from Stanley (1995) showing sea level data points from many different localities around the globe over the last 17,000 ^{14}C yr BP. The spread of data points indicates that the perceived sea level (i.e. RSL) at any particular spot is not necessarily (nor probably) in sync with global/eustatic trends. Thus, for interpreting the effects of changing sea level at any particular location, one should consider its RSL history, and not the eustatic trend.

2.3 Paleo sea level indicators

The evolution of RSL is usually constrained by paleo sea level indicators (i.e. objects or features which approximate the elevation of a former sea level). There are a wide variety of such indicators (van de Plassche, 1986) each with a different potential to resolve the actual position of a paleo sea level. Some common indicators include 1.) peat deposits from coastal salt marshes (esp. the floral and microfaunal assemblages they contain), 2.) faunal remains of marine organisms such as mollusks, gastropods, corals,

etc., and 3.) many different coastal/strandline geomorphic features such as barrier islands, lagoons, spits, wave-cut platforms, and delta topset/foreset bed contacts. Provided that such indicators are dateable, or at least occur in a dateable context, a curve showing the evolution of RSL through time may be plotted.

2.4 New England salt marshes and their use in RSL studies

In the New England area, the most commonly used indicator for recent RSL studies is peat from coastal salt marshes, and this is the case for two reasons. First, marsh peat is primarily composed of organic matter, and thus can be radiocarbon dated easily. Second, coastal marshes exhibit striking zonations in vegetation assemblages that can be precisely linked to certain water levels (Redfield, 1972; Chapman, 1974; Nixon, 1982; Niering and Warren, 1980). Importantly, those vegetation assemblages can be identified easily and rapidly at the macroscopic scale after simply splitting a marsh sediment core.

Similar zonations are also present in foraminiferal assemblages encountered in salt marsh peats, and these allow for more precise and higher resolution estimates of past water levels (Scott and Medioli, 1978 and 1980; Thomas and Varekamp, 1991; Nydick et al., 1995; Gehrels, 1999 and 2003). An unfortunate trade-off for this significant upgrade is an increased amount of lab time necessary for sample preparation and analysis. Thus, studies based on foraminiferal assemblages are less frequently undertaken than work based on the simple macroscopic analysis of vegetation assemblages.

In general, New England coastal salt marshes can be divided into three elevational subenvironments based on their vegetational assemblages—the low, high, and highest marsh zones (Johnson and York, 1915; Miller and Egler, 1950; Redfield, 1972;

Chapman, 1974; Scott and Medioli, 1978; Niering and Warren, 1980; Nixon, 1982; Long and Mason, 1983; Scott and Leckie, 1990; Bertness, 1991b; and van de Plassche, 1991).

The **low marsh zone** typically extends from MSL (mean sea level) up to MHW (mean high water), and is characterized by the salt-tolerant grass *Spartina alterniflora*. In real life, this zone corresponds to the portion of the marsh that is flooded twice per day (mudflats, channels, etc.).

The **high marsh zone** extends from MHW up to MHWS (mean high water spring tide level), and is characterized by *S. patens* (less salt-tolerant) and *Distichlis spicata*. *S. alterniflora* is also present in the high marsh zone, but only in local patches as the stunted/dwarf variety. The high marsh zone essentially corresponds with the flat marsh surface.

Finally, the **highest marsh zone** extends from MHWS upwards and landwards towards where freshwater input dominates. The highest marsh zone is characterized by a range of fresh to slightly salt-tolerant plants such as *Scirpus robustus*, *Juncus gerardii*, and *Phragmites australis*. Marine water only reaches this environment on rare occasions.

The vegetation assemblages outlined here are flexible, and may show local variations. Table 1 shows a tabular summary of the above data.

Table 1—Summary of marsh zones, elevations, and vegetation types.

Zone	**Elevation**	**Vegetation**
highest marsh	MHWS up	fresh to brackish water plants such as *S. robustus*, *J. gerardii*, and *P. australis*
high marsh	MHW up to MHWS	*S. patens* dominates with lesser amounts of *D. spicata*, and local zones of dwarf *S. alterniflora*
low marsh	MSL up to MHW	*S. alterniflora*

Of particular interest to many RSL studies is the high marsh zone which is easily identifiable in both the field and the lab due to its distinct vegetation assemblage. More importantly, the high marsh zone occupies a very restricted elevational range, and therefore serves as a robust approximation for the position of MHW (Table 2). In fact, many of the RSL curves which exist for the New England area are essentially records of MHW variation.

Table 2—High marsh assemblages, elevational ranges, and MHW relations for several New England marshes.

Study	**High marsh assemblage**	**Elevational range and relation to MHW**
Redfield and Rubin (1962)	*S. patens*, *D. spicata*, and dwarf *S. alterniflora*	**~30 cm range**; from MHW + 0 cm to MHW + 30 cm
van de Plassche (1991)	*S. patens* and *D. spicata*	**18 cm range**; from MHW - 3.5 cm to MHW + 14.5 cm
Kelley et al. (1995)	*S. patens*	**60 cm range**; from MHW - 20 cm to MHW + 40 cm
Donnelly et al. (2004)	*S. patens* and *J. gerardii*	**~20 cm range**; from MHW - 5 cm to MHW + 15 cm

Low marsh peat and highest marsh peat may also be used as paleo sea level indicators, but they are less useful. Low marsh peat, for example, is composed of *S. alterniflora* which exists over the broad elevational range between MSL and MHW. The actual range varies by locality; for example, in the area examined by Redfield and Rubin (1962) it is more than 180 cm, by van de Plassche (1991) approximately 90 cm, and by Kelley et al. (1995) approximately 120 cm. These amounts are comparable or even greater than the actual amount of RSL variation over the last 1000 years. Thus, at this timescale (or during periods when the rate of RSL evolution is slow), low marsh peat is not a useful indicator.

The elevational distribution of the highest marsh environment may also be similarly broad depending on a variety of factors such as fresh water input. However, if it can be suitably demonstrated that its distribution is restricted and that its relationship to MHW is known (see Bloom and Stuiver, 1963 and Donnelly et al., 2004), it may also be useful for shorter timescales.

2.5 Considerations for the use of marsh peat as a paleo RSL indicator

In general, there are two considerations one must keep in mind when using marsh peat for RSL studies.

2.5.1 Compaction and basal fresh water peat

Peat compacts under its own weight (autocompaction), or that of overlying materials (Kaye and Barghoorn, 1964). Thus, a high marsh peat that precisely marked the former position of MHW may be depressed to an elevation that is no longer representative of the original elevation at which it formed. To minimize the problem of compaction, basal high marsh peat samples that directly overly an incompressible substrate are often targeted (Redfield and Rubin, 1962; Donnelly et al., 2004).

One significant caution exists for basal peat samples—in many cases they may actually be composed of fresh water plant remains from the highest marsh zone (or higher) because this is the typical transgressive stratigraphic sequence that should develop during periods of sea level rise. Thus, if one dates a basal sample to minimize compaction, but the sample is composed of fresh water peat, the date returned is not

exactly representative of when the sea (i.e. MHW) actually invaded that point, but is too old (it includes some amount of lead time).

McIntire and Morgan (1964) clearly demonstrated this issue from the marshes at Plum Island, MA (see "2.11.1 Plum Island, MA—McIntire and Morgan (1964)" section below). The stratigraphy in their sediment cores showed the incompressible substrate (glacial till) overlain by a fresh water peat layer which was in turn succeeded by salt water peat. They dated both the bottom of the fresh water peat (directly over the substrate), and the top of it (transition to salt water peat). The second date which marked the true invasion of the sea was 600 years younger. In studies which deal with longer periods of time such as the entire Holocene, the age error resulting from such a lead time is less significant, but for studies on the scale of 1000-2000 years it is substantial.

In the case of McIntire and Morgan (1964), a correction can be applied because the age differential between the basal-most fresh water peat and the overlying salt water peat was determined. Alternatively, one could correct for the issue if the elevational difference between the environment in which the fresh water peat formed, and that of MHW was known. Unfortunately, some studies do not present all of these details.

2.5.2 Root contamination

The second important consideration that one must keep in mind when dealing with marsh peat is that of root contamination. This is especially true if conventional ^{14}C analysis is used to determine ages. The rhizomes of living high marsh grasses typically occur 4-12 cm below the actual marsh surface (van de Plassche et al., 1998), and roots have been observed to extend from the rhizome another 40 cm deeper (Kaye and

Barghoorn, 1964). Thus, modern plant roots may occur as deep as 50 cm within the marsh surface. Even with careful picking, it is not necessarily possible to avoid contamination. The reality of root contamination is clearly illustrated in an observation by Gehrels and Belknap (1993)—AMS (accelerator mass spectrometry) radiocarbon dates on individual grass fragments from a given stratigraphic level were up to 30% older than bulk sample dates from the very same level. Fortunately, the development of the AMS technique is a tremendous tool that helps to minimize this problem.

Both compaction and root contamination could lead to misinterpretation of the RSL history with a potential bias towards assigning ages that are too young to a particular height datum.

2.6 A note on radiocarbon dating and the dates used herein

This chapter reviews the work of many previous studies that, for the most part, have used radiocarbon dating to establish age control. Nowadays we recognize that systematic discrepancies exist between the radiocarbon timescale and the actual calendar/solar year timescale. Unfortunately, this was not the case in the 1960's when several of the studies reviewed herein were published.

Modern convention dictates that raw radiocarbon ages are calibrated into actual calendar/solar ages, and most of the modern studies reviewed below follow this convention. This means that earlier studies are not directly comparable to later studies because they use different timescales. To overcome this issue, all the uncalibrated radiocarbon dates presented in the older studies have been updated to their calibrated,

calendar/solar age equivalents using the Calib v4.4.2 computer program (Stuiver and Reimer, 1993).

Calibrated radiocarbon ages typically include multiple ranges of possibly correct ages as a result of the fact that ^{14}C production in the upper atmosphere has occurred at a non-constant rate back in time. Multiple ranges of possible ages makes plotting results and calculating rates rather inconvenient. Thus, to simplify this, the calibrated ages presented herein are simply the median value of the full possible 2 sigma (i.e. 2 standard deviations, or 95% confidence interval) calibrated calendar age range.

While it is trivial to calibrate a single radiocarbon age date, many of the earlier studies present hand-drawn RSL curves and rate calculations that are based on their uncalibrated dates. Thus, a best effort attempt has been made to "translate" the original intention of the authors by manually adjusting and updating RSL curves and rates to reflect the calibrated ages. Notes about any significant differences introduced due to the uncalibrated to calibrated transition are included for each record if necessary.

As a further aid to differentiate between uncalibrated and calibrated radiocarbon ages, the following convention will be used. All uncalibrated dates (i.e. radiocarbon timescale) will be labeled as "^{14}C (k)yr BP". All calibrated dates (i.e. actual calendar/solar year timescale) will be labeled as "cal (k)yr BP". Note that the starting point for both timescales is actually AD 1950; thus, a calibrated date of 350 cal yr BP is actually equivalent to AD 1600.

2.7 RSL in the Boston area from the Late Glacial through middle Holocene

For the period from the Late Glacial through the middle Holocene, few RSL curves are available for the immediate Boston area, and, in fact, for all of New England. For the most part, this is a direct function of the fact that a general rise in sea level through the entire Holocene has left most paleo sea level indicators submerged in offshore localities. Thus, they are typically difficult to reach and study, and retrieval of dateable materials via sediment cores is simply a matter of luck. The most complete synthesis for the Boston area is that of Oldale et al. (1993) which summarized the sparse preexisting data, and contributed two new uncalibrated radiocarbon dates to provide a RSL curve for the northeastern coast of Massachusetts since deglaciation[12].

The record provided by Oldale et al. (1993) must be considered as generalized simply because of the sparsity of data points, but also because of the quality of samples that produced them. For example, precise elevations are not available for all data points, ^{14}C age dates were sometimes obtained on shell carbonate which was not necessarily in equilibrium with atmospheric carbon when produced, and some of the data points do not directly anchor the RSL curve but simply provide bounds for its position. Nonetheless, for the Boston area, Oldale et al. (1993) is currently the best that exists for the period from the Late Glacial through the middle Holocene. We offer a slightly modified version of that diagram in our Figure 7.

---

[12] The radiocarbon age dates presented in Oldale et al. (1993) are uncalibrated for the most part. The exceptions are the five peat dates from Plum Island, MA that are illustrated as circles and a square in our Figure 7. Though these dates were originally published as uncalibrated in McIntire and Morgan (1964), Bloom (1967) later calibrated them with a rudimentary technique that was available at that time. For unknown reasons, Oldale et al. (1993) used the pseudo-calibrated versions presented by Bloom (1967) despite the fact that all the other dates they presented were uncalibrated.

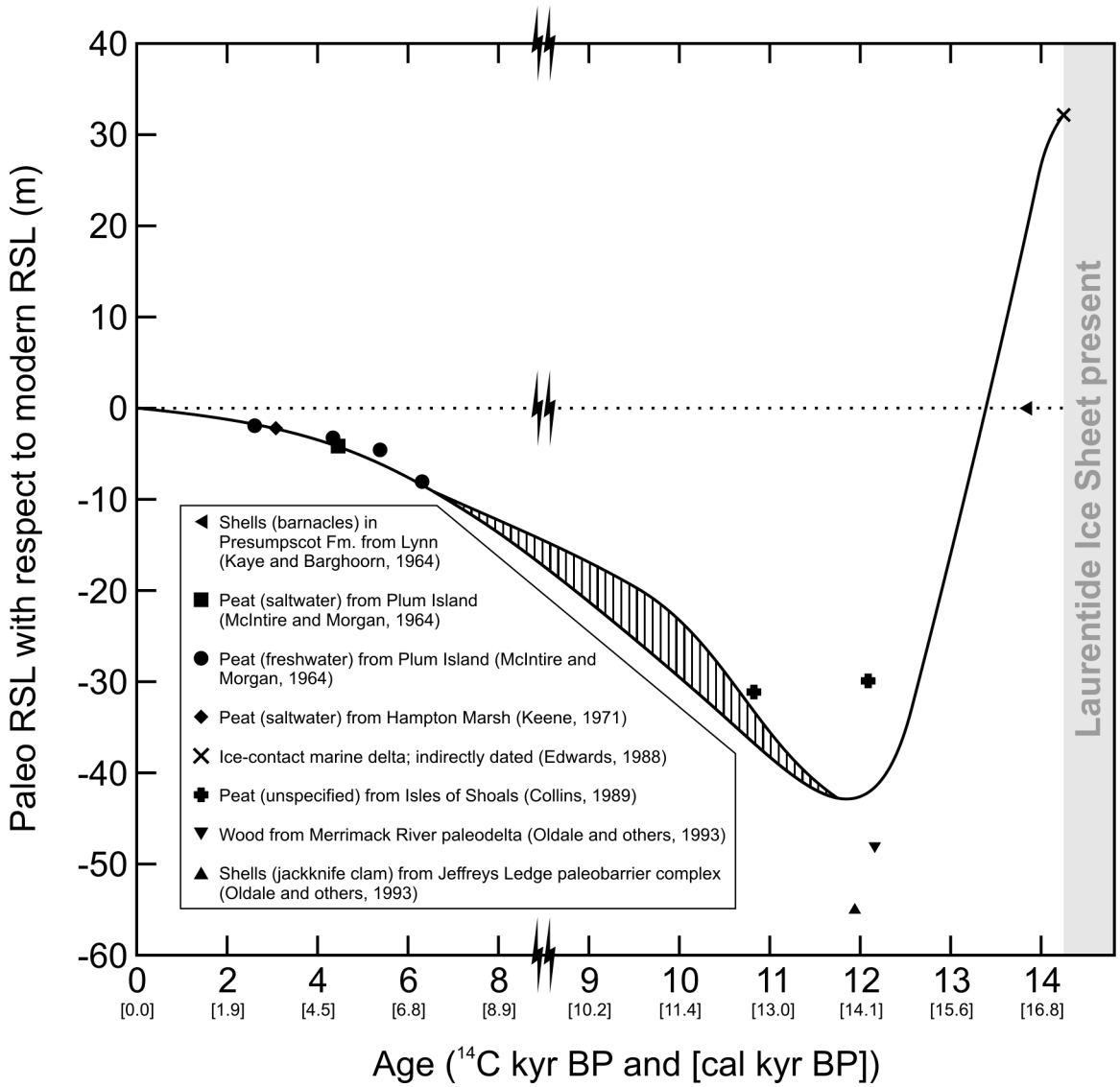

Figure 7—RSL curve for the Boston area from the Late Glacial to the present. This figure is slightly modified from Oldale et al. (1993). Note that the "Age" axis is given in uncalibrated ^{14}C years, but calibrated equivalents are listed in square brackets underneath. There is a change in the scale between 8000 and 9000 ^{14}C yr BP. The Plum Island dates are partially calibrated (see Footnote 12 for more details). From the point of deglaciation to about 12,000 ^{14}C yr BP, isostatic rebound of the crust outpaced eustatic sea level rise leading to a net drop in the RSL in the Boston area. With most of the isostatic rebound completed by 12,000 ^{14}C yr B.P., RSL has continued to rise through the present.

As mentioned earlier, eustatic sea level had dropped by about 120 m at the point of maximum continental ice sheet extent during the last glaciation (Fairbanks, 1989). In the New England area, however, the relative sea level was not 120 m lower. Isostatic depression of the crust had occurred due to the massive weight of the overriding

continental ice sheets. The isostatic depression actually exceeded the eustatic sea level drop; thus, the land surface, though covered with ice, had been depressed to an effective elevation below the RSL.

As deglaciation of New England began, marine waters penetrated inland of the modern coastline, and were in contact with the ice front as it receded northwards. This effectively resulted in a marine transgression (i.e. an apparent RSL highstand), and its maximum inland extent is known as the marine limit (Figure 8). The generally fine-grained sediments deposited in this mixed glaciomarine environment are collectively known as the Presumpscot Formation (Bloom, 1960 and 1963), and their general distribution can be seen in Figure 8. In the Boston area, this deposit is locally known as the Boston Blue Clay.

As the rate of isostatic rebound picked up, it soon outpaced eustatic sea level rise, and resulted in a continuous drop of the RSL (i.e. a marine regression) that lasted about 2000 years. During this time formerly subaqueous environments emerged from the ocean—for example, the glaciomarine Presumpscot Formation became subaerially exposed[13]. By 12000 ^{14}C yr BP, the bulk of isostatic rebound had been completed, and RSL began to rise once again under eustatic influence. In general, the RSL has continued to rise in all of New England, albeit at different rates, through the entire Holocene.

[13] The Presumpscot Formation is still exposed at many localities along the New England coastline. For example, it occurs at least 18 m above modern sea level in the Boston area (Kaye and Barghoorn, 1964), but as high as 130 m above modern sea level in central Maine (Thompson, 1982). This difference probably reflects the fact that isostatic depression was less in the south towards the thin margin of the ice sheet, and greater in the north where the ice sheet was thicker.

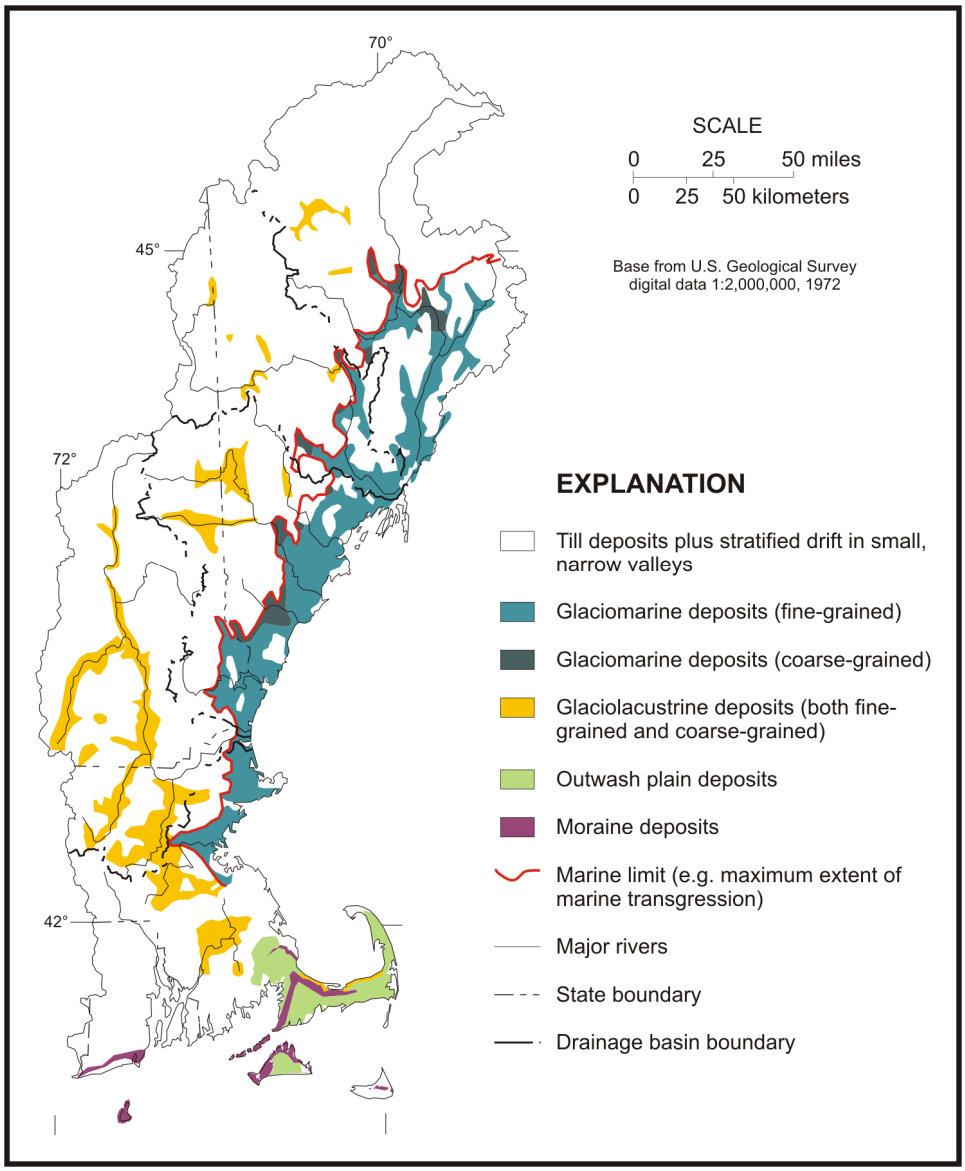

Figure 8—Generalized glacial geology of eastern New England. This figure is reproduced from Figure 5a of Flanagan et al. (1999). Mixed glaciomarine deposits of the Presumpscot Fm. are shaded in aquamarine tones, and the marine limit is indicated by the red line.

2.8 Late Holocene RSL records in New England—introduction

A surprising number of late Holocene[14] RSL records have been published for various spots along the New England coast since the early 1960's. For most recent times,

[14] For convenience, we define "late Holocene" as the last 5000 calendar years.

the paleo records are supplemented by historical tide gauge measurements which offer direct observation of sea level evolution, but on a short time scale. For our purposes, records from the immediate Boston area are of the most interest. Besides the short tide gauge record, two paleo records exist for the immediate area, but only one appears reliable. Therefore, we will supplement these records with others available from the wider New England area.

Most of these late Holocene records are based on peat deposits from coastal salt marshes some of which have a continuous sedimentary record over the last several thousand years. As mentioned above, peat deposits from the high marsh environment are often specifically targeted because they robustly approximate paleo MHW elevations. Thus, following the example of Redfield and Rubin (1962), we will use the local MHW at each locality as a common datum. For the few records that do not use MHW (or the flat marsh surface) as their datum, the RSL curves they provide are simply adjusted upwards or downwards accordingly, and the fact is noted. Provided that the tidal range at these localities has not changed significantly over the late Holocene, this upwards/downwards shift is appropriate.

Of the multiple RSL records reviewed below, the majority are undeniably of low resolution especially for the past 1000 years which is of most interest to us. In many cases, the RSL curves are simply composed of two straight line segments that the authors drafted by hand to illustrate the general trends of RSL evolution for a certain time period. While straight line segments are easy to understand, they undoubtedly reflect natural processes poorly. Many of the curves appear in reduced size in the original publications so enlargement has been necessary. Because of this small cosmetic defects have become

obvious; for example, an RSL curve does not cross the datum zero point at the present day. In all cases, an attempt to remain true to the intentions of the authors has been undertaken.

2.9 Late Holocene RSL records in New England—immediate Boston area

This section reviews the short Boston Harbor tide gauge record, followed by two late Holocene RSL records for the immediate Boston area.

2.9.1 Boston, MA (Boston Harbor tide gauge record)

Hourly tide gauge measurements for Boston Harbor are available back to 1921[15]. An average annual water level value for each year from 1921 to 2004 was derived by taking the average of all the hourly values for the particular year in question, and is plotted up in Figure 9. A linear regression through the data set suggests an average rate of rise of about 2.54 mm/year over the length of the record. This value is comparable to those reported from other regional tide gauges. For example, based on data from 1856-2001, the tide gauge at New York City shows a rise of 2.8 mm/year (Donnelly et al., 2004), and the New London, CT tide gauge shows a rise of 2.1 mm/year based on data from 1939-1986 (Lyles et al., 1988).

[15] "Verified/Historic (Tides) Water Level Data" is freely available via the CO-OPS (Center for Operational Oceanographic Products and Services) Internet website (URL http://www.co-ops.nos.noaa.gov/). CO-OPS is a branch of the NOS/NOAA (National Ocean Service/National Oceanic and Atmospheric Administration).

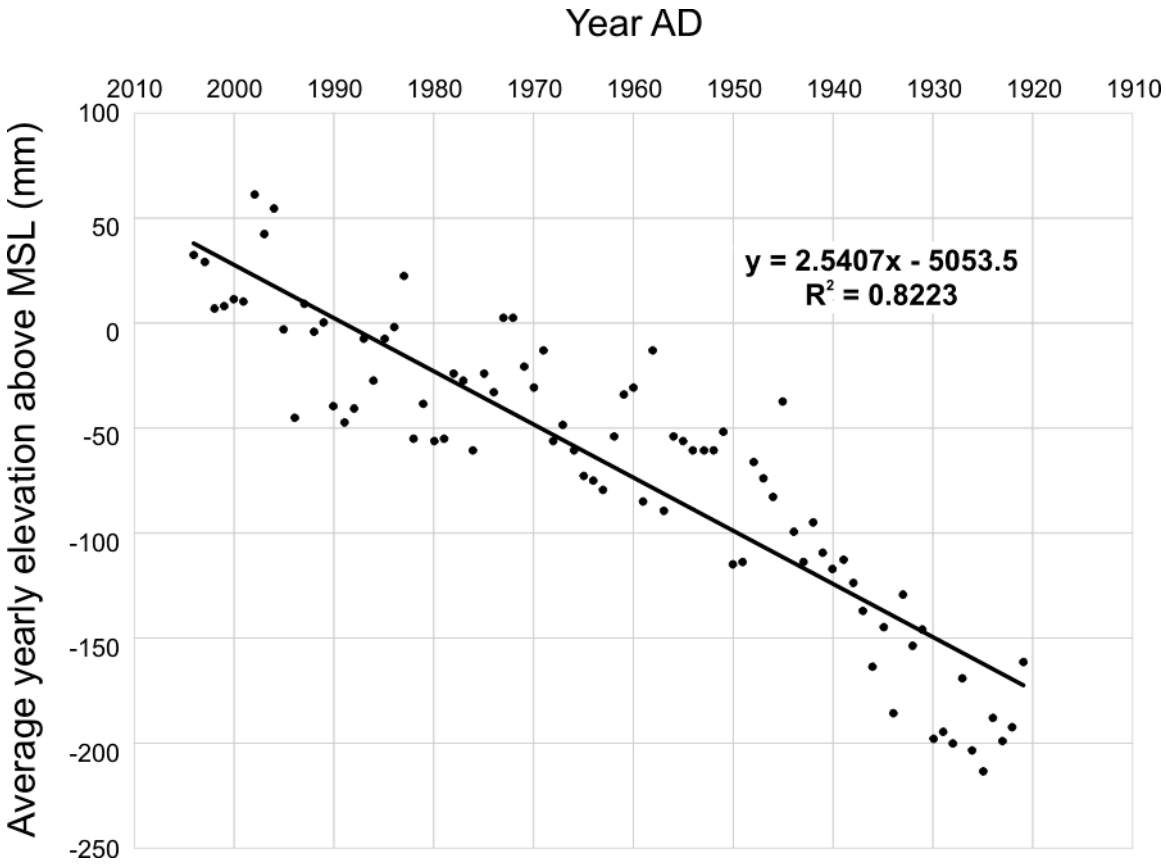

Figure 9—Annually-averaged tide gauge data from Boston Harbor showing the rise in sea level from 1921-2004. A straight line fit to the data suggests an average rise rate of about 2.54 mm/year over this period.

2.9.2 Boston, MA (Boston Common and Back Bay)—Kaye and Barghoorn (1964)

Kaye and Barghoorn (1964) is the first of two late Holocene RSL records published for the immediate Boston area (location #1 in Figure 10). They sampled marsh peat exposures (datum of MHW) that were fortuitously, but only briefly, exposed during construction projects in the Boston area. An unfortunate consequence of this sampling strategy is that the exposures are no longer available for reexamination.

Figure 10—Locations of sea level studies in the New England area

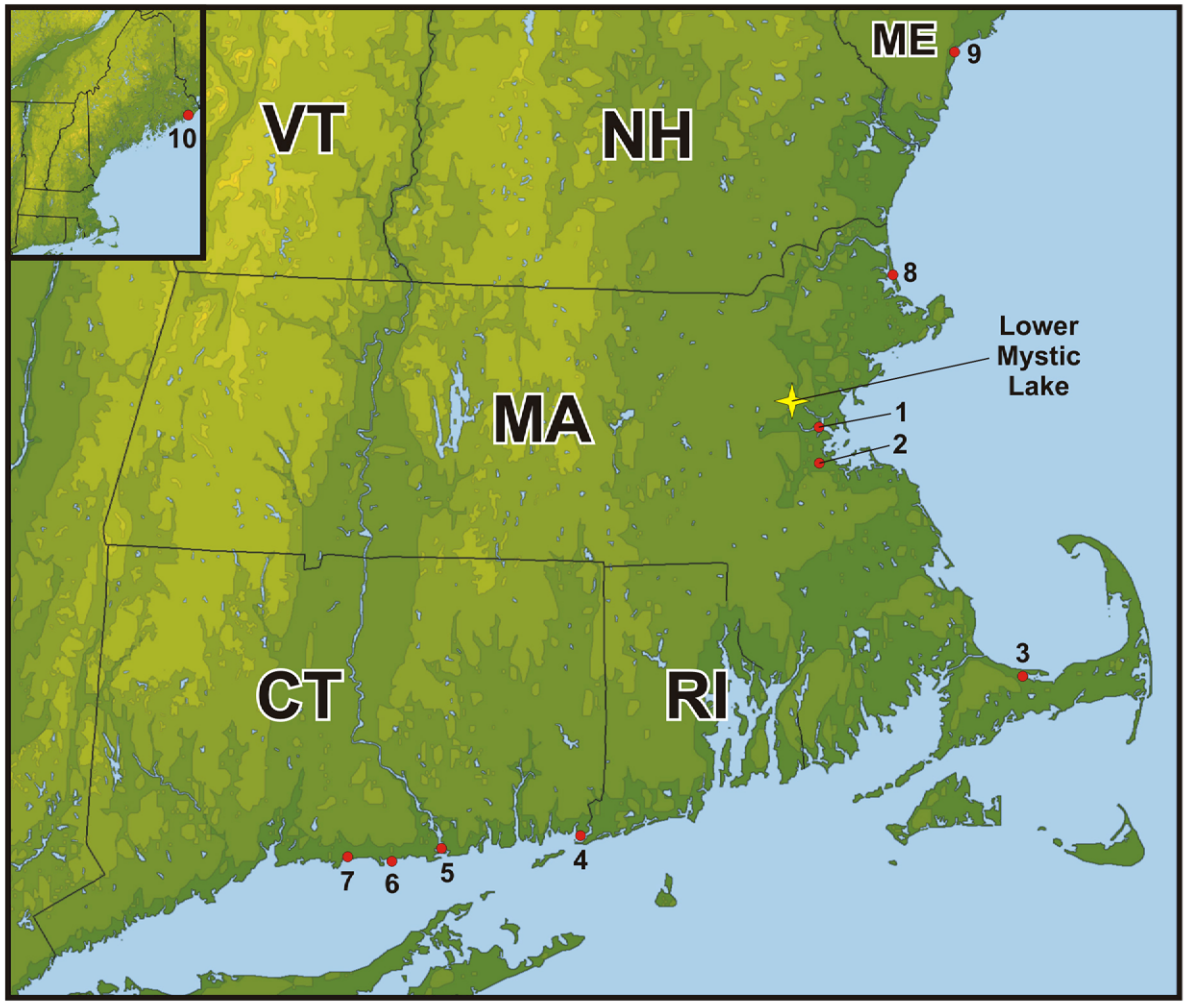

1.) Kaye and Barghoorn (1964)
2.) Redfield (1967)
3.) Redfield and Rubin (1962)
4.) Donnelly and others (2004)
5.) Patton and Horne (1991)
6.) Bloom and Stuiver (1963), Van de Plassche (1991), Thomas and Varekamp (1991), Varekamp and others (1992), and Van de Plassche and others (1998)
7.) Nydick and others (1995)
8.) McIntire and Morgan (1964)
9.) Belknap and others (1985) and Kelley and others (1995)
10.) Gehrels (1999)

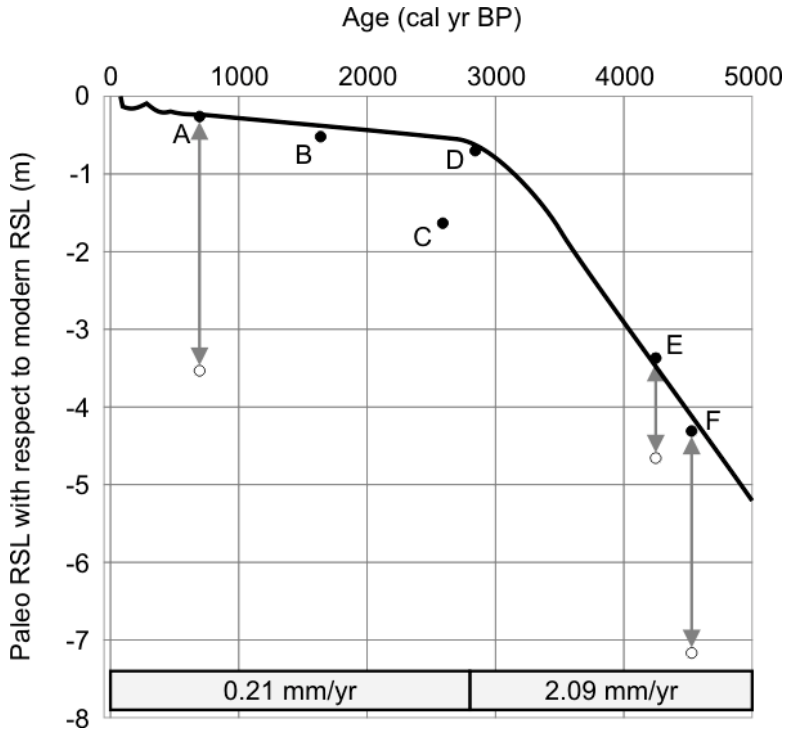

Figure 11—RSL curve from Kaye and Barghoorn (1964). Note that the true elevation at which samples A, E, and F were retrieved is represented by the lower data points. Kaye and Barghoorn (1964) manually adjusted their elevations upwards between 1.3 and 3.3 m (indicated by arrows) so that they fell along the RSL curve as drawn. Average rates of rise for the two segments of the curve are indicated at the base of the diagram.

The study presented uncalibrated results from 16 conventional radiocarbon age dates, but only six of those samples (i.e. their samples A-F) yield ages of less than 5000 cal yr BP when calibrated. Using these data points, they presented a RSL curve with two clear segments. From 5000-2800 cal yr BP the curve shows a total rise of about 4.60 m, or a rate of approximately 2.09 mm/year. From 2800 cal yr BP onwards, however, they illustrated a sharp decrease in the rate of rise. Over this time, the RSL rose just 60 cm total, or a rate of about 0.21 mm/year. In essence, they depict a relatively stable sea level over the last 2800 years. There appear to be some problems with this record, and they are discussed in detail in the "2.13.1 Analysis of Kaye and Barghoorn (1964)" section below.

2.9.3 Boston, MA (Neponset River)—Redfield (1967)

The second late Holocene RSL record published for the immediate Boston area is that of Redfield (1967). From marshes along the Neponset River about 10 km south of downtown Boston (location #2 in Figure 10), the study presented six uncalibrated conventional radiocarbon dates obtained from basal high marsh peat samples[16] so as to minimize the effects of peat autocompaction. The local marsh surface which approximates MHW was used as the datum. When the six radiocarbon dates are calibrated, they define a RSL curve for the area from 3300 cal yr BP up to the present.

Though Redfield's (1967) data points from Neponset only extended back to 3300 cal yr BP, he actually drew the curve further back in time using data from McIntire and Morgan's (1964) research at Plum Island, MA (discussed in the "2.11.1 Plum Island, MA—McIntire and Morgan (1964)" section below) about 55 km north along the Massachusetts coast. The resulting RSL curve can be divided into two clear segments. From 5000-3350 cal yr BP, the curve shows a rise of about 3.70 m total, or an average of about 2.24 mm/year. At 3350 cal yr BP, the rate decreases abruptly, and the curve rises slowly and steadily a total of 2.05 m towards the present at a rate of about 0.67 mm/year[17].

---

[16] Redfield (1967) reviews results from many different areas, and because of this only generically labels the Neponset samples as "peat", and not "fresh water peat", or "salt water peat". However, Redfield was acutely aware of the issues with fresh water peat from earlier work (Redfield and Rubin, 1962). Also, in Redfield (1967), he mentions that, "about 10 percent of recorded data have been disregarded in this study because they depart widely from the general trend of data from the same location. Those samples that appear to be too old are from freshwater deposits that may be suspected of having been formed in freshwater swamps at an elevation above the contemporary sea level." Thus, we conclude that despite the samples being only generically labeled as "peat", they were probably high marsh peat, and truly representative of paleo MHW.

[17] There is a slight cosmetic problem with the RSL curve presented for the Neponset marshes (Figure 2 in Redfield, 1967 and reproduced here as Figure 12). Its most recent segment intersects the modern datum

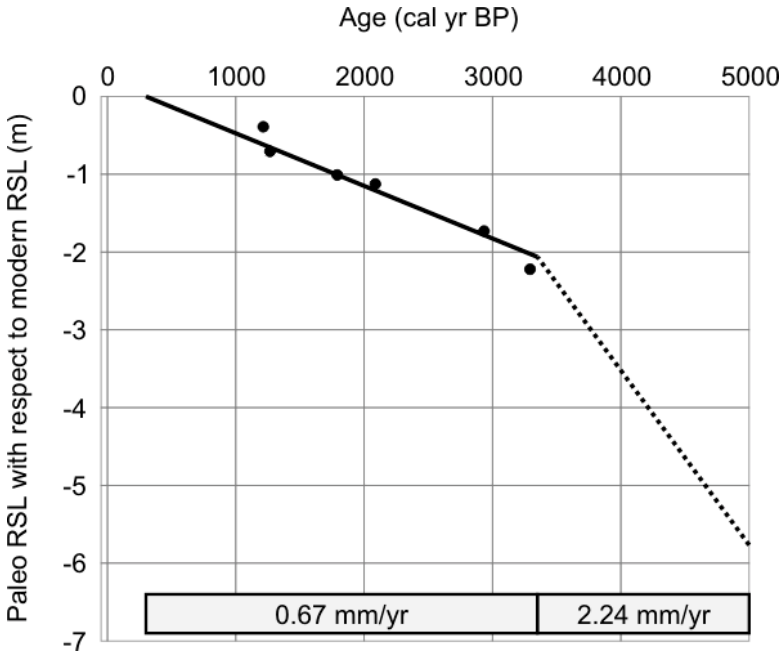

Figure 12—RSL curve from Redfield (1967). Note that the dotted section of the curve is not based on original data from Redfield (1967), but from Plum Island, MA data published in McIntire and Morgan (1964). Note that the curve intersects the modern datum at 300 cal yr BP (see Footnote 17 for a discussion of this). Average rates of rise for the two segments of the curve are indicated at the base of the diagram.

2.10 Late Holocene RSL records in New England—Boston southwards

This section reviews late Holocene RSL records from localities south of the immediate Boston area.

2.10.1 West Barnstable, MA—Redfield and Rubin (1962)

Redfield and Rubin (1962) provide another important study from the marshes of West Barnstable, MA approximately 95 km southeast of Boston along the Massachusetts coast (location #3 in Figure 10). They obtained basal high marsh peat samples to

---

(i.e. the marsh surface) at 300 cal yr BP (AD 1650), and not the present. At face value this is misleading and suggest the sea level has been stable since then. But Redfield clearly knew sea level was rising over the last 300-350 years, and in fact, in the very next figure of the same article he unambiguously demonstrates this as the Neponset RSL curve is shown to rise continuously all the way up to the present day. So despite

minimize the effects of peat autocompaction[18], and used the flat marsh surface as their datum. Uncalibrated conventional radiocarbon age dates were provided for 17 of their samples.

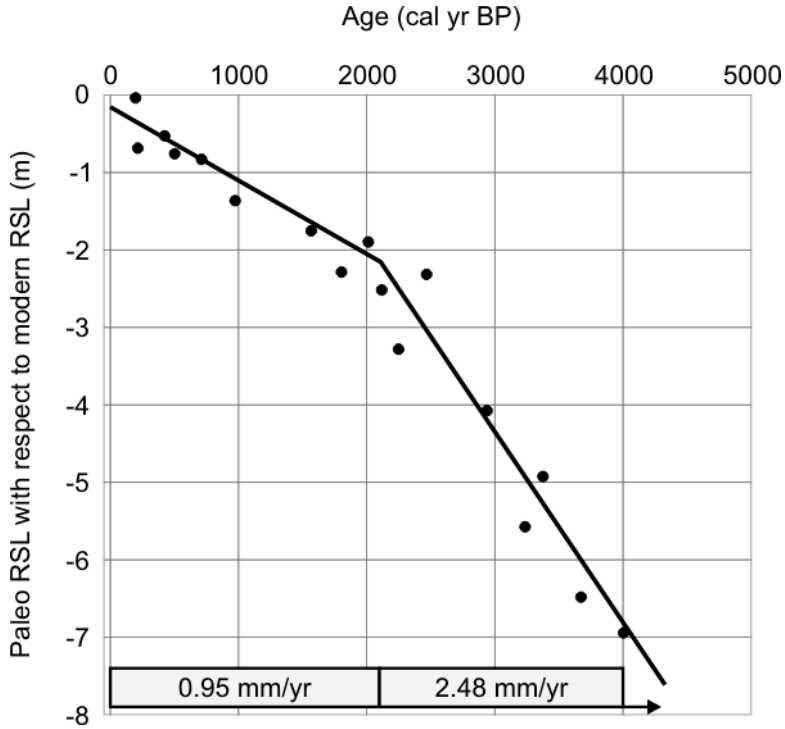

Figure 13—RSL curve from Redfield and Rubin (1962). Average rates of rise for the two segments of the curve are indicated at the base of the diagram.

When their radiocarbon dates are calibrated, they constrain the evolution of RSL from 4300 cal yr BP up to the present. The curve they present has two clear segments. From 4300-2100 cal yr BP, they noted a total rise in the RSL of about 5.45 m, or an average rate of 2.48 mm/year. The curve has an inflection point at 2100 cal yr BP at

---

the fact that Redfield's curve intersect the marsh surface at 300 cal yr BP, we interpret that his true intention was to extend the rate of 0.67 mm/year up to the present day.

[18] Redfield and Rubin (1962) were well aware of the issue with dating basal fresh water peat, and took precautions to avoid it. For example, before actually retrieving the sediment cores they used in the study, they probed and cored the marshes to "determine that the peat was uniform in character throughout its depth, …, and that fresh water peat or depressions in which fresh water peat might have formed … were absent." Their attempts were successful, and 13 of the 17 samples they dated were composed of high marsh salt water peat.

which point the rate of rise slows. From then up the present, the curve steadily rises a total of 2.00 m, or at an average rate of 0.95 mm/year.

2.10.2 Barn Island, CT—Donnelly et al. (2004)

Donnelly et al. (2004) presented a study from Barn Island, CT approximately 135 km southwest of Boston along the Connecticut coast at the CT/RI border (location #4 in Figure 10). They obtained AMS radiocarbon dates on 11 basal peat samples which grew along the top of a glacial erratic so as to avoid the effects of peat autocompaction. They also used pollen assemblages and chemical (i.e. pollution) stratigraphy to provide chronologic control over the last 150 years when radiocarbon dating is impossible. The study specifically targeted high marsh peat, and used local MHW as the datum.

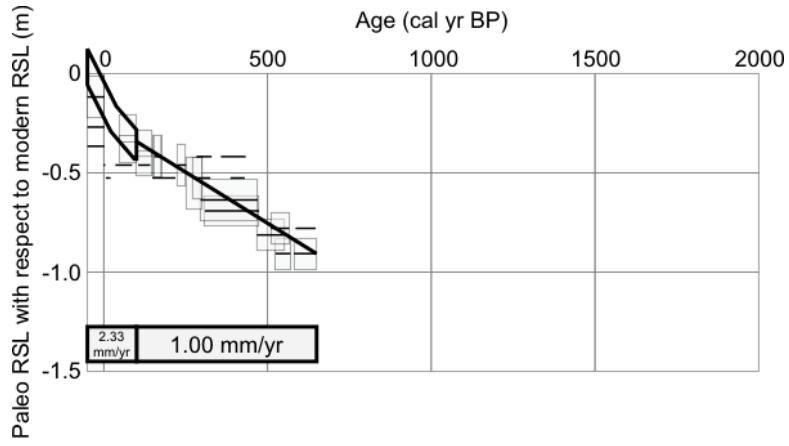

Figure 14—RSL curve from Donnelly et al. (2004). The "window" of ranges from 100 cal yr BP to present (i.e. AD 1850-2000) represents a cloud of actual tidal gauge data points from both New London, CT (AD 1939-2000) and New York City (AD 1856-2000). Average rates of rise for the two segments of the curve are indicated at the base of the diagram.

Combined with modern tide level observations, they presented a RSL rise curve that spanned 700 calendar years back from the present. From 650 to 100 cal yr BP (i.e. AD 1300-1850), their curve rises about 55 cm total, or a rate of 1.00 mm/year. From 100

cal yr BP up to present (AD 2000), the curve rises about 35 cm total, or a rate of about 2.33 mm/year[19]. This rate is very similar to the 2.1 mm/year actually observed at the New London, CT tidal gauge from AD 1939-1986 (Lyles, 1988).

2.10.3 Connecticut River Estuary—Patton and Horne (1991)

Patton and Horne (1991) presented two RSL curves for the last 4300 years from the Connecticut River estuary approximately 160 km southwest of Boston along the Connecticut coast (location #5 in Figure 10). The first curve they presented was based on seven uncalibrated conventional radiocarbon dates from 1.) paleosols on former upland surfaces that were buried by transgressive estuarine deposits, and 2.) drowned floodplain forests. The second curve they presented was based on eight uncalibrated conventional radiocarbon dates obtained on intertidal, basal fresh water peat samples[20] from the estuary, as well as one additional pollen assemblage age date for the historical period.

Both RSL curves are essentially parallel, but offset by about 70 cm elevation reflecting the fact that both track different intertidal environments. We choose to use the marsh peat curve over the upland curve for two reasons. First, it benefits from nine data points (eight ^{14}C dates and one pollen date) spread from 2800 cal yr BP up to the present.

---

[19] Donnelly et al. (2004) did not actually present this calculated rate from their data, nor did they mention the observed rate from the New London tide gauge just 20 km to the west even though the two are similar (2.33 mm/year and 2.1 mm/year, respectively). Instead, they cited the longer term New York City tide gauge record which extends back to AD 1856. This allowed them to patch into their marsh-based RSL curve. Unfortunately, by mentioning only the value for the NYC tide gauge record (2.8 mm/year), it gives the erroneous impression that that was the same value that was actually determined from the marsh stratigraphy they examined.

[20] Vegetation assemblages for the Connecticut River estuary do not have the same indicative meaning as those for regular tidal marshes along the coast. The fresh water peat that Patton and Horne (1991) specify actually forms below MHW whereas in a normal tidal marsh, it typically forms above MHWS. It also

In turn, the upland record has just seven data points, and they are scattered from 4200 to 1350 cal yr BP with nothing to anchor the last millennium. Second, the marsh peat based curve is more similar to the other RSL records from the New England area even if it is not based on high marsh peat.

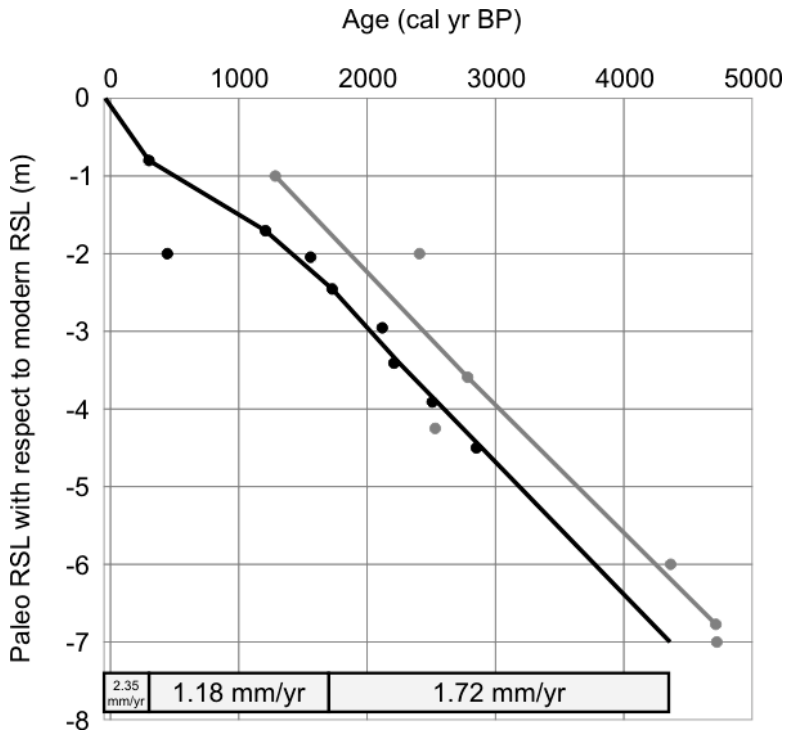

Figure 15—RSL curves from Patton and Horne (1991). The gray curve and data points compose the their "upland"-based RSL curve. The black line and data points compose their marsh-based RSL curve. Average rates of rise for different segments of the marsh-based curve are indicated at the base of the diagram.

Patton and Horne (1991) suggested their marsh peat based RSL curve had three distinct segments. Between 4350 and 1700 cal yr BP, the curve shows a rise of 4.55 m, or an average rate of 1.72 mm/year. Between 1700 and 300 cal yr BP, it rises 1.65 m total, or an average rate of 1.18 mm/year. Finally, between 300 cal yr BP (AD 1650) and

---

contains *S. alterniflora* which is not part of the typical fresh water marsh vegetation assemblage noted in other areas. The difference is simply due to the large flux of fresh water through the estuary.

the present (AD 1991), it rises 80 cm, or an average rate of 2.35 mm/year[21]. This most recent rate is very similar to the value reported from the New London tidal gauge during the middle part of the 20th century (2.2 mm/year from 1940-1971).

2.10.4 Clinton, CT—multiple records

A tremendous amount of highly detailed work has been undertaken at the Hammock River salt marsh in Clinton, CT about 170 km southwest of Boston along the central Connecticut coast (location #6 in Figure 10). The first RSL study from the marsh is that of Bloom and Stuiver (1963) who examined the longer term history from about 8000 cal yr BP onwards. It was later reexamined in great detail by two different groups of investigators; one headed by Orson van de Plassche (Vrije Universiteit), and the other by Ellen Thomas and Johan Varekamp (Wesleyan University). These two groups focused their attention on the most recent portion of the record (i.e. last 1500-2000 years). We systematically examine the records below.

Bloom and Stuiver (1963) presented the first detailed study for the Clinton area based on 16 uncalibrated conventional radiocarbon dates, but we consider just the 10 dates that are younger than 5000 cal yr BP when calibrated. The majority of their dates were obtained on basal (or nearly basal) highest marsh peat samples[22] from the Hammock

---

[21] Patton and Horne (1991) suggested a rise of 2.2 mm/year over the last 300 years, but it is not obvious how they calculated this number. The 300 cal yr BP data point was obtained from ~80 cm depth. If Patton and Horne (1991) used 0 cal yr BP (i.e. AD 1950) as modern, the calculated rate of rise would be 2.67 mm/year. If they used AD 1991 as present, the calculated rate would be 2.35 mm/year. They do mention the New London, CT tide gauge record which they suggest has a average rate of rise of 2.2 mm/year between AD 1940-1971, but to extend that same rate back 300 years may not be appropriate.

[22] Bloom and Stuiver (1963) described the peat that composed their samples as a "sedge peat formed from fragments of *Scirpus*, *Typha*, and *Phragmites*, as well as twigs and leaves of shrubs." This is indicative of the highest marsh zone that is forming at the landward edge of the salt marsh, and not the regular high

River salt marsh with a handful coming from other nearby localities. From 5000 to 3150 cal yr BP, their plotted RSL curve shows a rise of 2.45 m total, or an average rate of 1.32 mm/year. From 3150 cal yr BP up to the present, their curve shows a rise of 2.90 m total, or an average rate of about 0.92 mm/year.

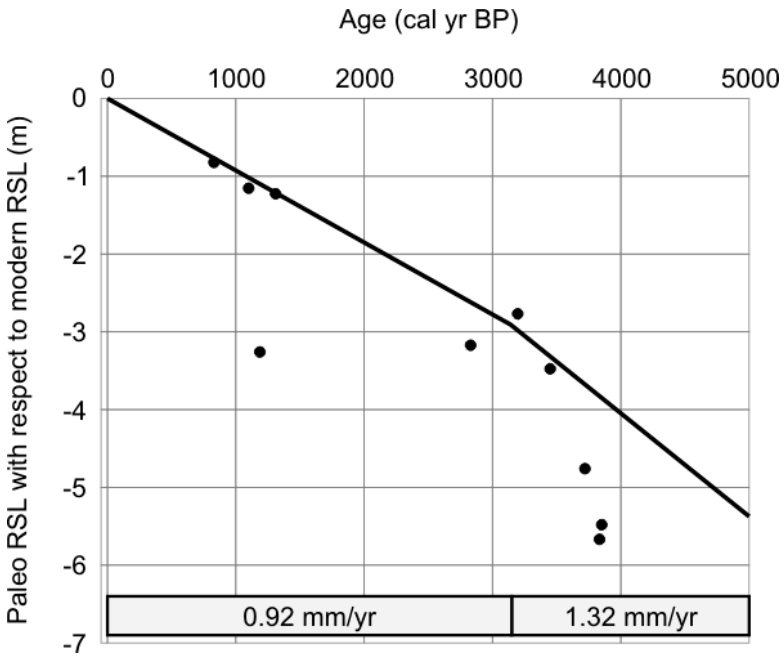

Figure 16—RSL curve from Bloom and Stuiver (1963). The older segment of the plotted RSL curve may not appear well-placed in light of the multiple data points from 4000-3000 cal yr BP, but six other data points older than 5000 cal yr BP are not displayed. When those are considered, the slope of the older segment seems appropriate. Average rates of rise for the two segments of the curve are indicated at the base of the diagram.

Almost three decades after the Bloom and Stuiver (1963) record was published, van de Plassche (1991) presented a complex study of the Hammock River salt marsh stratigraphy deposited over the past 2000 years. The study was performed at a very high resolution, and used more than 400 sediment cores to provide a detailed stratigraphic framework for the marsh. Importantly, it was the first study in the New England area to

---

marsh. Bloom and Stuiver (1963), however, suggested that the assemblage was indicative of MHW or of some elevation slightly above it. Thus, the difference is probably not large. However, it does suggest their RSL might be slightly older than the other curves which track MHW via high marsh peat.

suggest that RSL rise over the last two millennium might not be uniform, and that "steps" of accelerated/decreased rise rates might have occurred. Previous to this point, other RSL studies had typically represented late Holocene RSL rise by straight lines of differing slopes, but the high-resolution nature of van de Plassche's (1991) work suggested short term fluctuations were superimposed on the general trend.

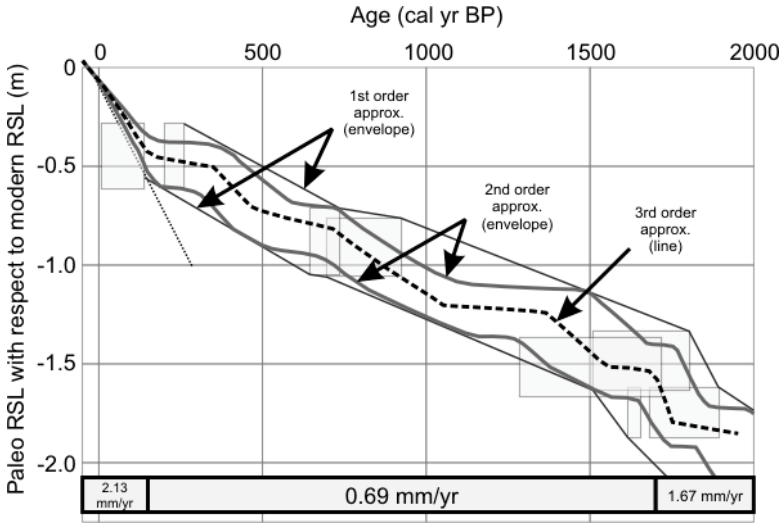

Figure 17—RSL curve from van de Plassche (1991). The first, second, and third order curves as termed by van de Plassche (1991) are labeled. Average rates of rise for different segments of the curve are indicated at the base of the diagram.

Based on the floral composition of the sediment cores, and well as dark horizons which were interpreted to represent transgressive events, five different marsh-wide transgressive/regressive overlap boundaries were recognized in the stratigraphy. Seven uncalibrated conventional radiocarbon dates anchor the chronology[23]. The result was a figure that presented first, second, and third order approximations of RSL evolution over the last 2000 years.

[23] Van de Plassche (1991) used uncalibrated ^{14}C ages including for the presentation of his final results (his Figure 12). However, he did provide calibrated age results at one point in his Figure 11b. The complex nature of his RSL curve and associated error envelopes makes it significantly harder to reproduce than other RSL curves. Thus, using the calibrated timescale framework provided in his Figure 11b, we used a graphical method to transfer his final results over to the calibrated radiocarbon timescale.

Using the slope of the first order approximation (essentially an error envelope) as a guide, three different periods of RSL rise can be distinguished. From 2000-1700 cal yr BP, the curve rises 50 cm total, or an average rate of 1.67 mm/year[24]. Subsequently, the rate decreases, and from 1700-150 cal yr BP, a total rise of 107.5 cm is noted. This yields an average rate 0.69 mm/year. Finally, the rate picks up again starting around 150 cal yr BP, and RSL rises about 42.5 cm total, or an average rate of about 2.13 mm/year. This rate is very similar to the actual rate (2.1 mm/year) observed at the New London tide gauge between AD 1939-1986.

The short term fluctuations superimposed on the longer term trends mentioned above are visible in the third order approximation—they appear as steps in the curve. Periods of accelerated RSL rise begin at 1750, 1550, 1050, 475, and 200 cal yr BP, and periods of slower rise begin at ~1950, 1700, 1375, 700, and 350 cal yr BP. Van de Plassche (1991) attempted to correlate these short term fluctuations with global climate events, but the limited quantity of non-AMS radiocarbon dates available made the correlations mostly speculative.

Thomas and Varekamp (1991) and Varekamp et al. (1992) examined the Hammock River salt marsh stratigraphy deposited over the last 1500 years. They chose an approach different from that of van de Plassche (1991), and concentrated on a small number of cores, but at high resolution. The technique used combined microfaunal and geochemical analyses to reconstruct the history of relative emergence or drowning of the

[24] Van de Plassche (1991) calculated a slightly different rate of 1.40 mm/year for this time period. The difference may be due to the fact that his analysis used uncalibrated dates whereas we employ calibrated equivalents causing the average slope of this portion of the curve to be slightly steeper (see Figure 11b in van de Plassche, 1991).

marsh, and hence the rate of RSL rise. Chronologic control was provided by seven calibrated AMS radiocarbon dates as well as a chemical pollution horizon. Like van de Plassche (1991), they concluded that there were apparent short term RSL fluctuations superimposed on the long term trend.

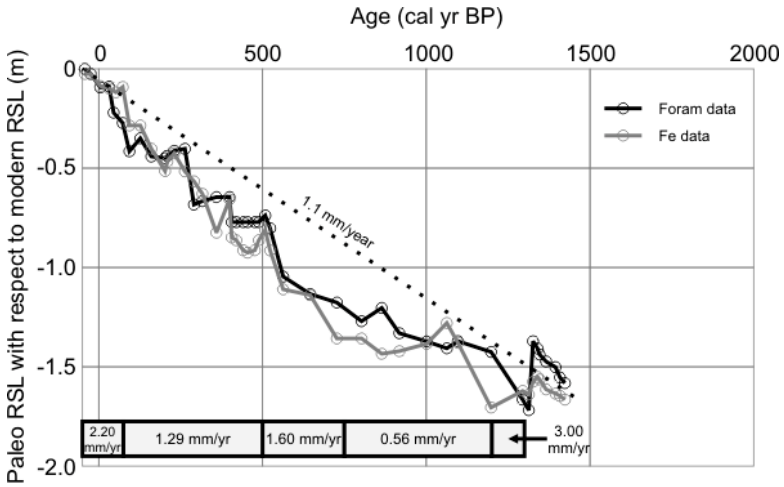

Figure 18—RSL curve from Varekamp et al. (1992). Average rates of rise for different segments of the curve are indicated at the base of the diagram.

Over the entire 1500 year span of their record RSL rose about 1.65 m, or an average rate of 1.10 mm/year. However, they also noted that the rise was not constant, and identified three periods of rapid transgression[25]. The first period of rapid transgression occurred from 1300-1200 cal yr BP (AD 650-750) during which time RSL

[25] Varekamp et al. (1992) displays some frustrating inconsistencies within the text itself, and also in coordination with what is illustrated in the figures. For example, in the text they state that "The T1 event (AD 600) is characterized by a sudden, preceding regression (AD 700)," (p. 297, Varekamp et al., 1992). If the regression occurs at AD 700, how can it precede the T1 event which occurred 100 years earlier? Either one (or both) of the dates is incorrect. One should be able to clarify the issue by consulting their actual RSL curve (Figure 6, Varekamp et al., 1992), and identifying the sudden regression. Unfortunately, this only serves to confuse the issue more as the only sudden regression illustrated occurs from AD 600-650. The same type of inconsistency occurs for a later period of interest—interpretation of their text discussion suggests that the rate of RSL rise increased from AD 1700-1750 and decreased from AD 1750-1880 (p. 297, Varekamp et al., 1992). Yet their Figure 6 (Varekamp et al., 1992) clearly illustrates the RSL jump occurring from AD 1650-1700, and the decrease from AD 1700-1880. We imagine that last minute changes to the manuscript may have caused such discrepancies. We will therefore rely on the illustrations, in particular, their Figure 6 (Varekamp et al., 1992) as definitive, and give them precedence over discrepancies that appear within the text of the article.

rose 30 cm, or an average rate of 3.00 mm/year. This transgression was related to a local change, probably geomorphic, and is therefore only of local use. The second period of rapid transgression occurred from 750-500 cal yr BP (AD 1200-1450) during which time RSL rose about 40 cm, or an average rate of 1.60 mm/year. Finally, the third rapid regression began around 300 cal yr BP, and has continued through modern times. This final transgressive episode was interrupted by a period of relative stability from 250-75 cal yr BP (AD 1700-1875). Over the last 100 years, the rate has increased tremendously. During this time, the foram record suggests an RSL rise of about 22 cm, or a rate of 2.2 mm/year which is very similar to the rate (2.1 mm/year) observed at the New London tide gauge over the last 50 years.

Van de Plassche et al. (1998) built on the microfaunal assemblage work published in Thomas and Varekamp (1991) and Varekamp et al. (1992), but combined it with a suite of 24 new AMS radiocarbon dates obtained from three nearby sediment cores. In the last 1500 years, the long term average rate of RSL rise was about 1.00 mm/year. However, three periods (100-150 years long) of rapid sea level rise that ranged from 2.0-3.5 mm/year were discerned. A variety of concerns were raised about the procedural aspects of van de Plassche et al. (1998) by Varekamp et al. (1999), however, van de Plassche et al. (1999) seemed to adequately deal with the concerns.

2.10.5 Guilford, CT—Nydick et al. (1995)

Nydick et al. (1995) presented a 1700 year long record based on three sediment cores obtained from salt marshes in Guilford, CT about 15 km west of the Hammock River salt marshes in Clinton, CT (location #7 in Figure 10). The study used the same

microfaunal and geochemical techniques employed by Thomas and Varekamp (1991) and Varekamp et al. (1992) to reconstruct the history of relative emergence or drowning of the marsh, and hence the rate of RSL rise. Chronologic control was provided by 17 calibrated conventional radiocarbon dates (approximately five per core), ^{210}Pb analysis, and a chemical pollution horizon.

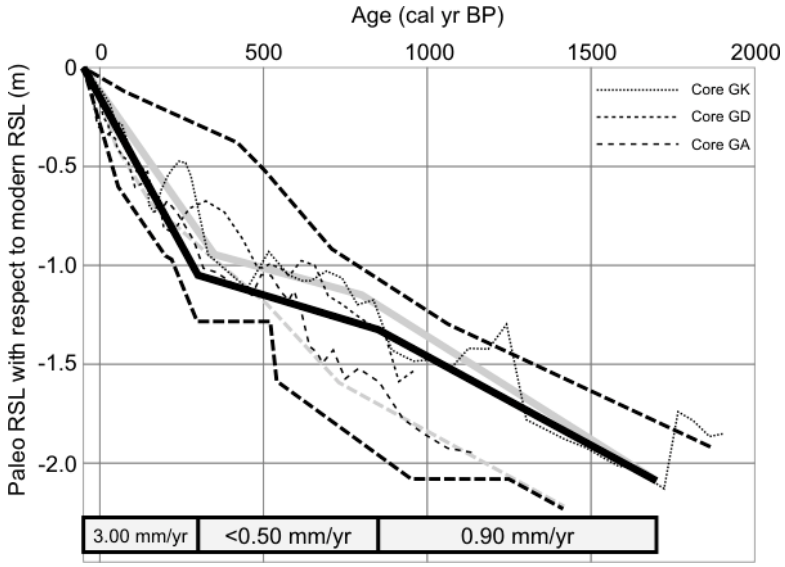

Figure 19—RSL curves from Nydick et al. (1995). The three independent RSL records they presented (cores GA, GD, and GK) are illustrated here as the thin dashed lines[26]. The black, broadly dashed line represents the combined error envelopes of the three records. The thick black line with three segments represents a schematic curve for the general RSL rise trends Nydick et al. (1995) identified from their work. Average rates of RSL rise for the three segments are indicated at the base of the diagram. See Footnote 26 for an explanation of the thick gray and broadly dashed gray lines.

[26] Nydick et al. (1995) illustrated their three independent RSL curves at three different scales. We adjusted each to the same scale, and overlaid them to produce our Figure 19. We observed that the combined upper boundary of the error envelopes for the three curves corresponded exactly with what Nydick et al. (1995) illustrated in their Figure 11e. However, the combined lower boundary was significantly different (larger) than what they illustrated. Additionally, the three segment curve they illustrated in their Figure 11e did not correspond with their own written description which was explicit. They noted this, and referred to the figure as "schematic". In our Figure 19, we have presented the correct lower boundary for the combined error envelope, and the correct three segment curve constructed according to the description provided by Nydick et al. (1995). This is critical for our work because we later graphically overlay records from multiple locations for comparison. The original error envelope for the combined lower boundary and schematic three segment curve as illustrated in Nydick et al. (1995) appear in gray in the background of our Figure 19.

Nydick et al. (1995) provided three independent RSL curves (one for each of the cores examined) which are similar on the broader scale, but differ in many finer scale details. From the three individual records, they produced a master record that illustrates three different RSL trends over the last 1700 years. In general, they concluded that RSL rose at a moderate rate of about 0.90 mm/year from 1700-850 cal yr BP (AD 250-1100) with a possible rate increase from 950-850 cal yr BP (AD 1000-1100). Another possible acceleration was noted in their core GK around 1250 cal yr BP (AD 700), but the records from the other two cores did not extend far enough back in time to confirm or refute this. RSL rise generally slowed from 850-300 cal yr BP (AD 1100-1650) to a rate of less than 0.50 mm/year. Finally, the rate of RSL rise increased to about 3.00 mm/year from 300 cal yr BP (AD 1650) up to the present with a possible slight deceleration between 250-150 cal yr BP (AD 1700-1800).

2.11 Late Holocene RSL records in New England—Boston northwards

This section reviews late Holocene RSL records from localities north of the immediate Boston area.

2.11.1 Plum Island, MA—McIntire and Morgan (1964)

McIntire and Morgan (1964) presented a study focused on the development of Plum Island, a barrier island complex about 45 km north-northeast of Boston along the Massachusetts coast (location #8 in Figure 10). In several deep borings, they encountered marsh peat deposits at depth, and were able to obtain basal fresh water peat samples so as to minimize the effects of peat autocompaction. They published uncalibrated

conventional radiocarbon dates for five samples, but just three of the dates are younger than 5000 cal yr BP when calibrated[27].

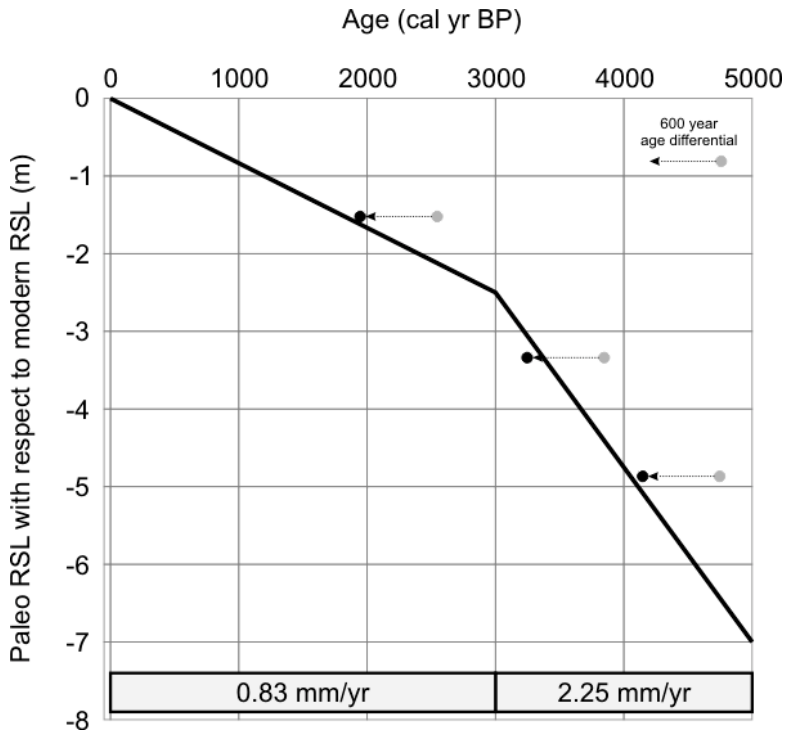

Figure 20—RSL curve constructed from data supplied in McIntire and Morgan (1964). The gray data points represent the actual calibrated radiocarbon ages on the basal fresh water peat samples dated by McIntire and Morgan (1964). However, they determined that these dates preceded the arrival of MHW by about 600 years. Thus, the black data points which represent the level of MHW are shifted 600 years to the left. Two data points older than 5000 cal yr BP are not pictured, but help constrain the slope of the older segment of the curve. Average rates of rise for the two segments of the curve are indicated at the base of the diagram.

McIntire and Morgan (1964) did not provide an actual RSL curve in their study, but did offer enough details and stratigraphy to construct a curve based on their data. They used the local marsh surface (i.e. MHW) as their datum, but dated fresh water peat directly above the substrate. That fresh water peat tracked an environment that was elevationally higher than MHW. Fortunately, from several dates along the length of their

[27] McIntire and Morgan (1964) did not provide errors with their uncalibrated radiocarbon dates, so we assigned a standard error of ± 100 years for the calibration process.

"Parker River B" core, they determined that the basal fresh water peat dates preceded the actual arrival of MHW to that site by about 600 years (see discussion in the "2.5.1 Compaction and basal fresh water peat" section above). To account for this, we shift the data points 600 years younger so they represent MHW, and not an elevationally higher fresh water environment.

McIntire and Morgan (1964) suggested that a significant change in the rate of RSL rise occurred around 3000 years ago as eustatic sea level rise slowed, but subsidence of the land continued. So we have included an inflection point at that time. From the RSL curve we drew based on their data, RSL rises about 4.50 m from 5000-3000 cal yr BP which yields an average rate of 2.25 mm/year. From 3000 cal yr BP up to the present, the curve rises 2.50 m total, or at an average rate of 0.83 mm/year.

2.11.2 Wells, ME—Kelley et al. (1995)

Kelley et al. (1995) presented a RSL record from the marshes around Wells, ME approximately 110 km north-northeast of Boston along the Maine coast (location #9 in Figure 10). They gathered together 19 uncalibrated conventional radiocarbon dates from preexisting studies, and added 18 new conventional and six new AMS radiocarbon dates (both types uncalibrated). All the dates samples were standardized by adjusting them to a common datum[28] as well as classifying them by probable environment of deposition (low marsh, high marsh, etc.).

[28] Kelley et al. (1995) used NGVD (National Geodetic Vertical Datum) as their common datum. According to the authors, MHW has an elevation of 1.43 m above NGVD, so when reproducing their record we adjusted accordingly.

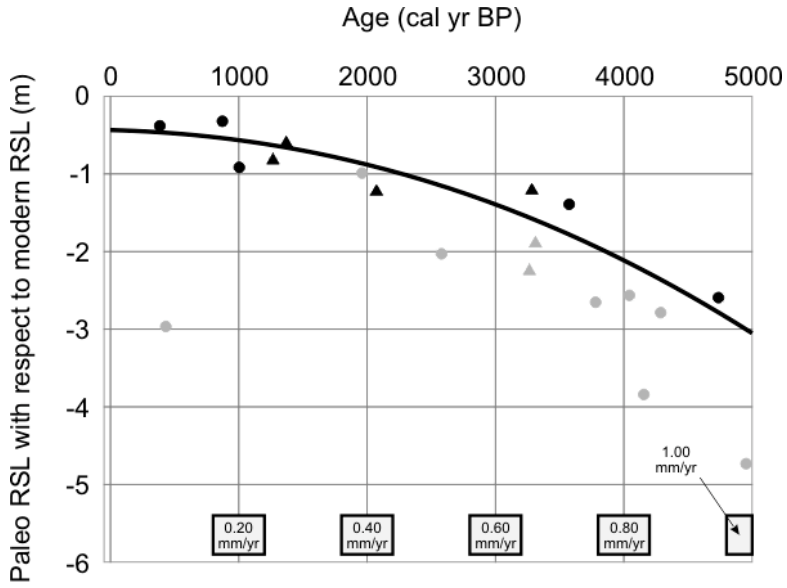

Figure 21—RSL curve from Kelley et al. (1995). The black data points represent the "best data" high marsh data points as determined by Kelley et al. (1995), and on which they based their RSL curve. The gray data points represent other high marsh samples not used in the analysis for various reasons. In both cases, the circles represent conventional radiocarbon dates, and the triangles represent AMS dates. Average rates of rise for different segments of the curve were determined graphically using a 200 year window, and are indicated at the base of the diagram.

From the entire corpus, ten "best data" samples predominantly from the high marsh environment were identified. Nine of the samples (three AMS, six conventional) yield ages younger than 5000 cal yr BP when calibrated, and are considered here. Kelley et al. (1995) drew a smooth, quadratic fit RSL curve based on their data. Around 5000 cal yr BP, the rate of rise was 1.00 mm/year, but it decreased regularly through the late Holocene. However, the rate of rise has picked up significantly in recent times—regional tides gauges have registered rates of 1.0-2.0 mm/year between 1940 and 1990.

2.11.3 Machiasport, ME—Gehrels (1999)

Gehrels (1999) presented two RSL records from the marshes of Machiasport, ME approximately 390 km northeast of Boston along the Maine coast (location #10 in Figure 10). The first record spanned 6000 years back from present, and was constructed using

the traditional technique of dating basal marsh peat samples retrieved from directly above the incompressible substrate. A second high resolution record was produced for the last 2000 years using detailed analyses of foraminiferal stratigraphy in conjunction with the basal peat record. Importantly, this record was corrected for the effect of peat autocompaction. We consider just the shorter, high resolution record here.

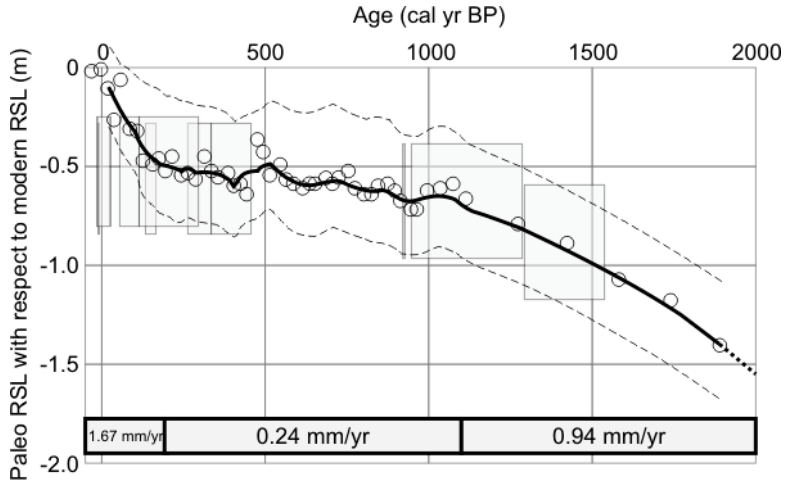

Figure 22—RSL curve from Gehrels (1999). The gray boxes represent four AMS radiocarbon age dates with associated horizontal and vertical error ranges. The original high-resolution curve presented by Gehrels (1999) extended back to only 1900 cal yr BP, but we projected it back to 2000 cal yr BP (dotted segment). Average rates of rise for different segments of the curve are indicated at the base of the diagram.

Four calibrated AMS radiocarbon dates anchor the chronology of the RSL curve over the last 2000 years. In general, three curve segments can be distinguished. From 2000-1100 cal yr BP, the RSL rose approximately 85 cm, or at an average rate of 0.94 mm/year. Subsequent to this, there was a period of relative stability from 1100-250 cal yr BP. During this time, several low amplitude fluctuations of RSL may have occurred, in particular a possible 15 cm rise between 600-400 cal yr BP, but the net rise over the whole period was just 20 cm which yields an average rate of rise of 0.24 mm/year. Since 250 cal yr BP, RSL has risen about 50 cm total, or at an average rate of 1.67 mm/year. However, if one considers just the most recent period since AD 1930, the rate has reached

an unprecedented 2.2 mm/year according to the tide gauge at nearby Eastport (approximately 40 km to the northeast).

2.12 Late Holocene RSL records in New England—summary

Figure 23 presents a compilation of the RSL curves reviewed above. In general, it suggests that the Connecticut area has experienced a greater amount of RSL rise over the late Holocene than localities to the north. In turn, the Massachusetts area appears to have a slightly greater rate of rise than Maine if one excludes the Kaye and Barghoorn (1964) curve which is anomalous, and shallower than not just all the Massachusetts curves, but every single other RSL curve examined[29]. As a group the CT-based curves display a rise of approximately 2.50 m over the last 2000 years whereas the MA-based curves exhibit about 1.70 m rise over the same period, and the ME-based curves about 1.20 m. That the apparent amount of RSL rise diminishes from southern New England northwards is not a new conclusion, and has been known since at least the 1960's (Bloom, 1960; Redfield and Rubin, 1962; Redfield, 1967).

[29] A thorough analysis and discussion of the problems with the Kaye and Barghoorn (1964) record follows in the "2.13.1 Analysis of Kaye and Barghoorn (1964)" section below.

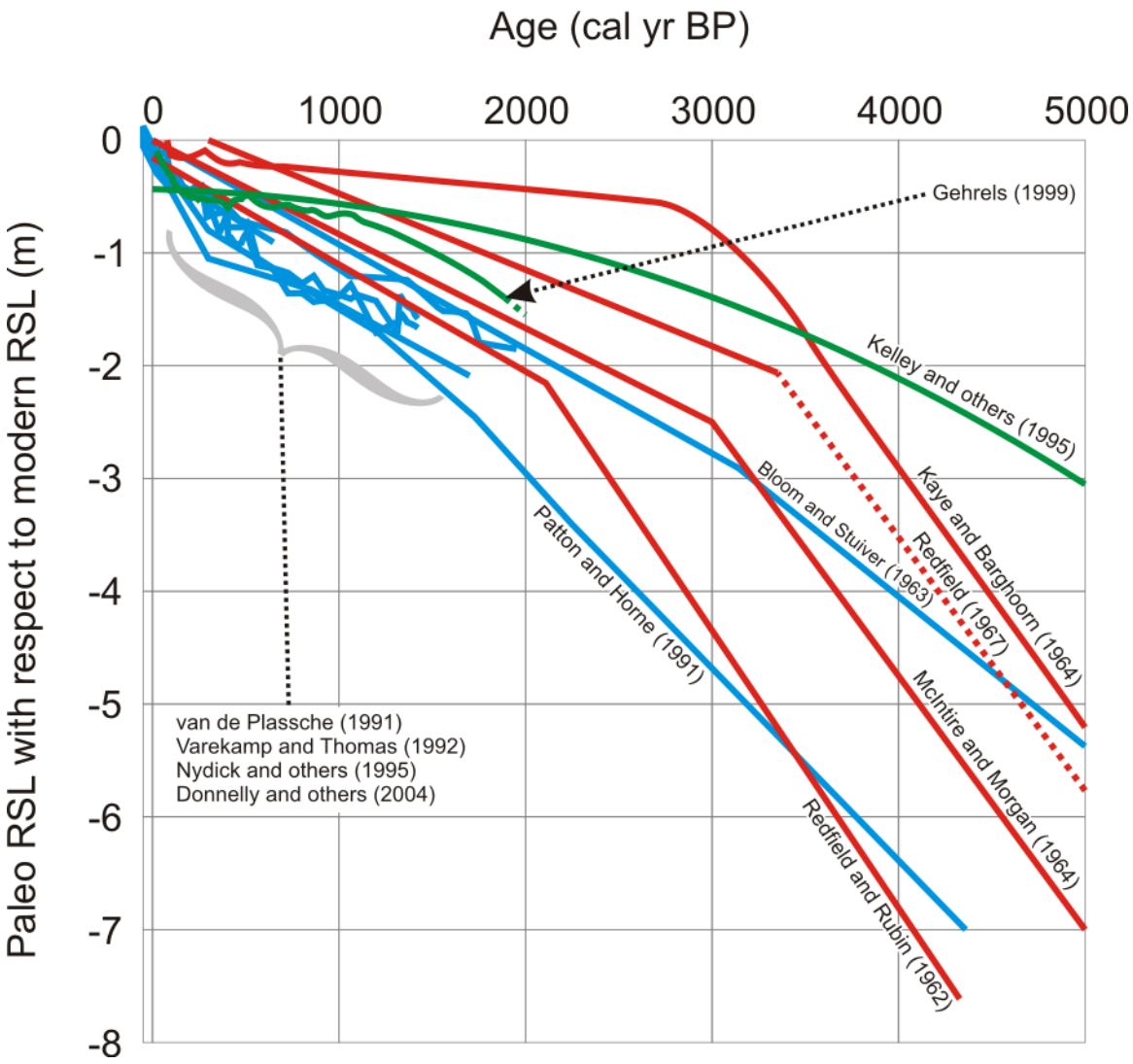

Figure 23—Compilation of late Holocene RSL curves from the New England area. The blue lines represent records from Connecticut, the red lines represent records from Massachusetts, and the green lines represent records from Maine. In general, the Connecticut curves fall deeper than those from areas northwards—this suggests that RSL rise in Connecticut has occurred at a faster rate.

2.13 Relative sea level in the Boston area over the last 1000 years

Given that the RSL records examined can generally be clustered regionally with slightly different rates, the four records from Massachusetts are obviously the best indicators of RSL for the Boston area. To visually compare these four records over the

last 2000 years, they have been aligned to a common calculated age/depth point which is the start of the Boston tide gauge record in Figure 24.

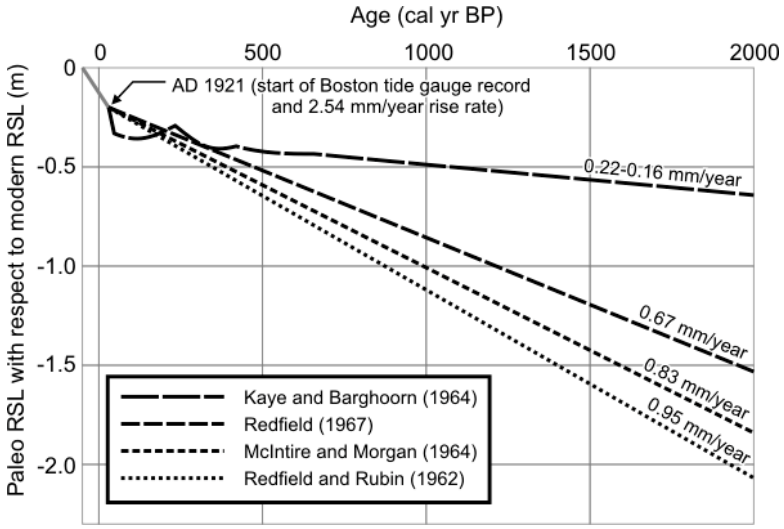

Figure 24—Estimated RSL in the Boston area over the last 2000 years. The four existing Massachusetts RSL curves are aligned to a common point which is the beginning of the Boston tide gauge record. A depth of 20 cm was calculated for this point given the rise rate of 2.54 mm/year during this time (see the Boston Harbor tide gauge record section above). Note that the rise rates calculated for the curves are based on the pre-AD 1921 sections.

An obvious conclusion results—the West Barnstable (Redfield and Rubin, 1962), Neponset River (Redfield, 1967), and Plum Island (McIntire and Morgan, 1964) RSL records are all consistent with one another. Using a simple average, their straight line segments prior to AD 1921 suggest a rise rate of approximately 0.82 mm/year. But despite its location being physically sandwiched between the other three, the Kaye and Barghoorn (1964) record is significantly different. When the 400-0 cal yr BP oscillations of that curve are included, the RSL curve prior to AD 1921 defines a rate of 0.22 mm/year, but if just the straight line segment is considered, it lowers even further to just 0.16 mm/year. Therefore, it is not only the shallowest of all the Massachusetts records, but even shallower than the records from Maine which raises significant questions about

its validity. Something appears to be wrong with the Kaye and Barghoorn (1964) record, and this has been suggested previously (Oldale, 1985).

2.13.1 Analysis of Kaye and Barghoorn (1964)

The Kaye and Barghoorn (1964) record essentially suggests a stable sea level in the Boston area over the last few thousand years. This conclusion was significantly different from contemporaneous records, and the authors clearly acknowledged this. In fact, their conclusion appears to have been heavily influenced by the results of Johnson (1925), Godwin et al.(1958). Gould and McFarlan (1959), Kaye (1959), Fairbridge (1961), and McFarlan (1961) all of which they specifically cited. These studies concluded that eustatically rising seas had reached the modern level between 3000-6000 calendar years before present. Unfortunately, many of these studies were based on results from localities far from Boston, or from areas with significantly different glacial/deglacial histories.

A detailed examination of Kaye and Barghoorn (1964) suggests their record (Figure 11) was problematic. The authors essentially discounted the significance of four of their own six data points (samples A, C, E, and F), and anchored their record on the remaining two (samples B and D). For example, samples A, E, and F neatly fall along the plotted RSL curve, but only because Kaye and Barghoorn (1964) manually adjusted their elevations upwards from 1.3-3.3 m citing compaction. And for sample C which fell below the plotted RSL curve by approximately a meter, the researchers simply ignored it suggesting its significance for representing a paleo sea level was questionable. Thus, the curve is literally anchored by just two data points.

The two data points in question are those for samples B and D, but unfortunately both come from a somewhat questionable context. In particular, they were obtained next to each other from the very feather-edge of a salt marsh deposit that was sandwiched between glacial till, and deformed by a couple of meters of overlying 19th century fill. The researchers additionally noted that the samples had a texture that was different from other peats—it "had a decided parting and in places a faint stratification that paralleled the dished upper surface of the peat body and showed the deformed nature of this surface." Given that samples B and D: 1.) came from the very feather-edge of a deformed deposit, 2.) were directly overlain by 19th century fill which means they were at or close to the surface when buried, and 3.) have a unique texture because of their "decided parting", it is not difficult to imagine that they were somehow disturbed, and may not necessarily represent a primary, in-situ context that has some significance for a paleo RSL. Another simple explanation is that these two samples may have contained fragments of fresh water peat or wood that was not recognized by the researchers. This would have skewed the ages to values that are too old.

Though the location of the Kaye and Barghoorn (1964) RSL record would make it ideal for our work regarding development of the LML laminated sedimentary record, we reluctantly conclude that the results are not robust.

2.13.2 Boston RSL summary and conclusion

The three Massachusetts RSL records presented by Redfield and Rubin (1962), Redfield (1967), and McIntire and Morgan (1964) RSL records are consistent among themselves, and appropriately fit into the regional New England framework of late

Holocene RSL evolution. From these records we conclude that over the last 2000 years, RSL in the Boston area has risen at approximately 0.82 mm/year excluding most recent time when it has accelerated to about 2.54 mm/year. This accelerated rate has been in operation since at least AD 1921 which is the beginning of the Boston tide gauge record.

Over the last 2000 years, non-uniform rates of rise were noted in the high resolution work from Connecticut (van de Plassche, 1991; Thomas and Varekamp, 1991; Varekamp et al., 1992; Nydick et al., 1995; van de Plassche et al., 1998) and Maine (Gehrels, 1999). It is likely that the Boston area would have experienced similar fluctuations, but the resolution of the existing RSL records is simply too low to perceive such fluctuations.

2.14 RSL significance for the LML laminated sediment storm record

Following glacial recession and isostatic rebound, RSL in the Boston area has been rising through the Holocene. By 1000 years ago (Figure 24), the level had reached about 1 m below modern sea level, a level that allowed marine water traveling up the Mystic River to reach the basin of the LML for the very first time. That first marine water delivery event about 1000 years ago initiated chemical stratification and meromixis in the lake, and hence the conditions necessary for developing and preserving the exquisitely laminated sedimentary record archived there. As sea level has continued to rise since that point, occasional marine water delivery events have provided a mechanism to maintain the chemical stratification. Thus, the birth and development of the LML's laminated sedimentary record is intimately linked to the evolution of sea level in the Boston area in recent geologic time.

For the purposes of this study[30], this slowly rising sea level may serve as a natural filter against weaker intensity storm surges going back in time. For example, if a storm surge of a given magnitude could just reach the LML basin in 1900, it would not have been able to reach it several hundred years earlier when the RSL was significantly lower. Another way to look at it is that the storm surge traces found in the earliest part of the record must represent storm surges of the greatest magnitude because they were able to reach the LML basin when the RSL was significantly lower.

There are many significant caveats that may preclude this interpretation. For example, we know that the phase of the diurnal tidal cycle and other phenomena like onshore/offshore winds can greatly moderate the magnitude of a storm surge. While these factors can be somewhat controlled during historical times, they cannot be controlled for the prehistoric part of the record.

[30] This portion of the dissertation was written based on our original working hypothesis that hurricane-related deposition in the LML would be the product of a seaward sourced mechanism, in particular, storm surge. However, based on our ever increasing body of data, we now understand that hurricane-related deposition in the LML is derived from a landward source, in particular, from the lake watershed.

CHAPTER 3

METHODS

3.1 Field work

Between spring 1996 and spring 2002, eight visits were made to the Lower Mystic Lake (LML) for data collection, and to retrieve various portions of the sedimentary record. These visits occurred in May 1996, November 1996, October 1998, April 2000, September and December 2001, and January and May 2002.

Three visits were made to Belle Isle Marsh (BIM) between spring 1999 and fall 2002 for reconnaissance work, and to retrieve the sedimentary record from various locations in the marsh. Those visits occurred in April 1999, June 2002, and September 2002.

3.1.1 Water column observations (LML only)

Temperature and conductivity profiles were obtained for the water column on five visits to the LML. A YSI Model 3000M/3060 temperature-conductivity meter/probe combination was used in May 1996 and April 2000. A Hach Company Hydrolab MiniSonde/Surveyor 4a combination was used in December 2001, and January and May 2002. The Hydrolab combination also allowed the measurement of additional water column parameters such as dissolved oxygen, pH, and salinity.

Figure 25—GPS track log with associated depth sounder data. Approximately 13 km of track log (>1500 data points) was collected.

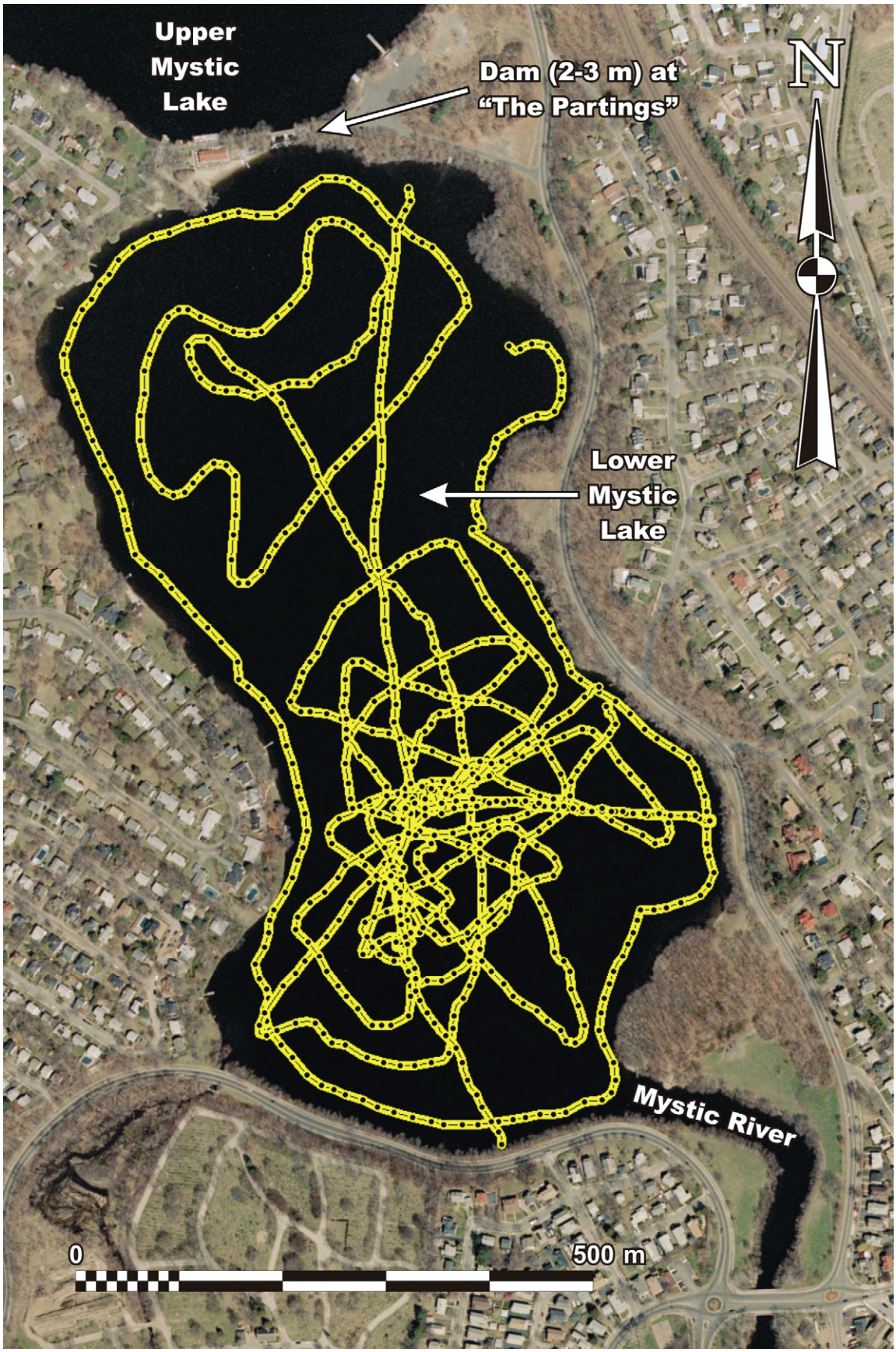
Upper
Mystic
Lake
Dam (2-3 m) at
"The Partings"
N
Lower
Mystic
Lake
Mystic River
0
500 m

3.1.2 Bathymetric survey and morphometric observations (LML only)

Water depths in the lake were collected at a limited number of point locations between 1996 and 2000. In September 2001, a Garmin GPSMAP 168 Sounder (a combination GPS/depth sounder unit) was used to automatically record 10.3 km of GPS track logs (latitude/longitude coordinates) with associated depth readings around the entire lake. The same instrument was used in December 2001 and January 2002 to collect another ~2.7 km of similar measurements for approximate total of 13 km (Figure 25).

3.1.3 Standard naming convention for sediment cores (LML and BIM)

Multiple sediment cores were retrieved from the LML and BIM (see below), and a standard naming convention is used to identify each of the cores. The naming convention is composed of a four part code to reference 1.) core location, 2.) date of core retrieval, 3.) core style, and 4.) core number. For example, sediment core "LML-01MAY2002-HMR-2" refers to the second slide-hammer percussion core taken from the Lower Mystic Lake on 1 May 2002. Specific details of this system are summarized in Table 3 below.

Two special cases exist. In the case of Livingstone-style square-rod piston cores that were obtained in multiple, consecutive drives, a drive number designation is also appended. For two-sided freeze cores retrieved prior to 2001, a "side" designation of either "A" or "B" is appended if necessary.

Table 3—Summary of standard core naming convention.

Code	***Value***
core location	*LML* or *BIM* (i.e. Lower Mystic Lake or Belle Isle Marsh)
date of core retrieval	*DDMMMYYYY* format (e.g. 23NOV1996)
core style	1.) *GLW*--for gravity-driven Glew minicores [lacustrine] (Glew, 1991) 2.) *FRZ*--for freeze cores [lacustrine] (Renberg, 1981 and Hughen et al., 1996) 3.) *LIV*--for modified, Livingstone-style, square-rod piston cores [lacustrine](Wright et al., 1983) 4.) *EKM*--for Ekman dredge cores [lacustrine] 5.) *HMR*--for Aquatic Research Instruments slide-hammer percussion cores [lacustrine] (http://www.aquaticresearch.com) 6.) *PVC4*--for cores retrieved by a custom 10 cm diameter Schedule 40 PVC coring system [terrestrial]
core number	*N* (refers to the N^{th} core of a particular type collected during a visit)

3.1.4 Sediment core retrieval

Several sediment coring technologies were employed to retrieve portions of the sedimentary record from the LML and BIM. All lacustrine sediment core retrieval was performed from either anchored boats or floating platforms because ice cover on the lake during the winter does not generally reach comfortable thicknesses. Marsh coring was coordinated with low tides.

3.1.4.1 Glew minicorer (LML only)

A gravity-driven Glew minicorer with adjustable weights was used to retrieve sediment cores up to 1 m long on multiple occasions between 1996 and 2000. This corer uses 4 cm diameter core tubes of variable length. After sediment cores were brought to the surface and capped, they were transported in their natural vertical position back to the

laboratory. For sediment cores retrieved by this device in 1998 and 2000, an extra step of carefully siphoning excess water off of the core tops was also performed.

3.1.4.2 Simple wedge style and oversized wedge-box style freeze corers (LML only)

A simple, gravity-driven, hollow, aluminum wedge style freeze corer (Renberg, 1981) was built, and used between 1996 and 2000 to obtain frozen sediment cores (i.e. "freeze cores") of the upper portion of the sedimentary record from the deep southern basin of the lake. This corer has the form of a symmetrical wedge 75 cm long, ~13 cm wide, and ~10 cm deep, and generally retrieves two thin (<1 cm) slabs of frozen sediment up to about 55 cm long from the larger faces of the wedge.

To accommodate the excessive thickness of the soft, gas-charged upper layer[31], a second, oversized, hollow, aluminum wedge-box style freeze corer (Figure 26) was constructed. A design supplied in Figure 5 of Hughen et al. (1996) served as a basic template for this corer, but some changes and modifications were made according to our needs. This corer has a flat freezing surface 125 cm long with the upper 95 cm of the corer in the form of a box (20 cm wide by 13 cm deep), and the lower 30 cm tapered in as an asymmetrical wedge. To concentrate freezing action on the 125 cm long freezing surface, the other three sides of the corer are insulated. This corer retrieves a single large (up to 110 cm long) and thick slab of frozen sediment per use.

[31] An explanation and discussion of this gas-charged upper layer is present in Chapter 4 below.

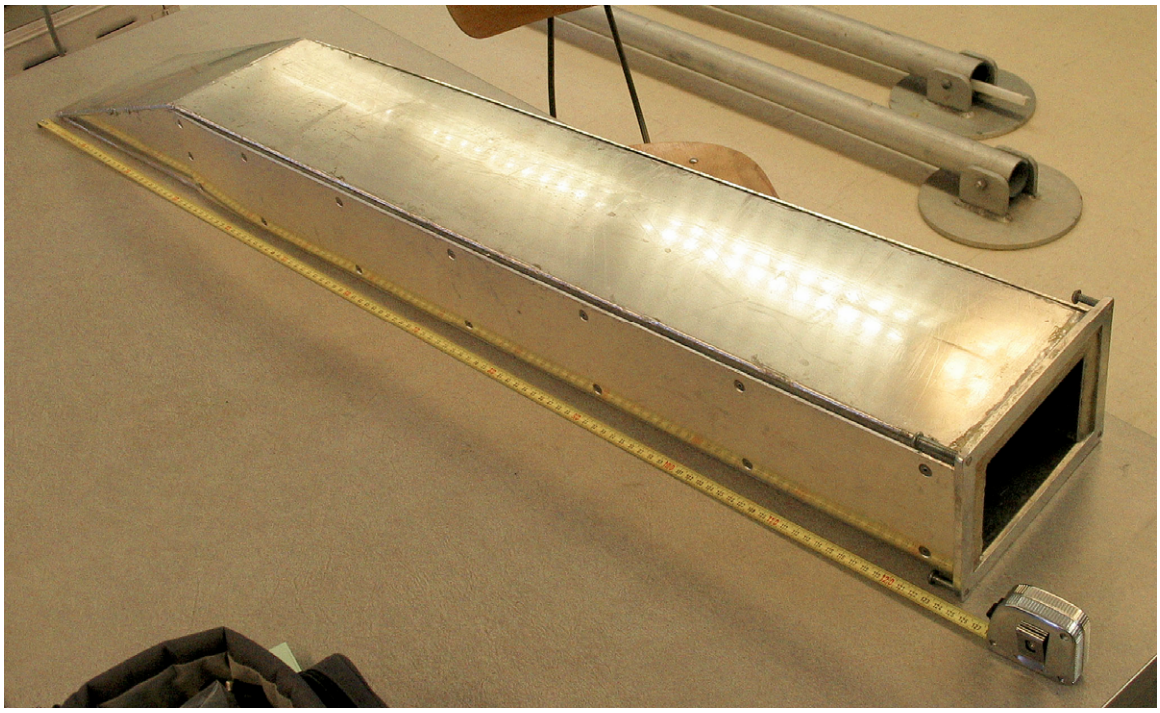
Figure 26—Photo of oversized, wedge-box style freeze corer.

For both corers, a mixture of dry ice and 200 proof ethanol was employed as the freezant. Pellet-style dry ice was employed with the first corer. For the second corer, the dry ice was first crushed into a fine powder so it would form a very thick slurry when the ethanol was mixed in. For both cores, in-sediment freeze times were generally 15 minutes, and occasionally extended to 20 minutes.

Freeze cores were maintained frozen in a custom built locker box packed with dry ice on their return to the laboratory.

3.1.4.3 Livingstone-style square rod piston corer (LML only)

A Livingstone-style square rod piston corer mounted on magnesium alloys rods was used to retrieve two long, sediment cores composed of multiple, meter-long drives from close, but separate spots (~10 m apart) in the deep southern basin of the lake in November 1996. The stainless steel coring tube on this corer has an inner diameter of 5

cm. Following retrieval of the uppermost drive for each core, a 10 cm diameter PVC casing was extended from the lake surface down into the sediment pile to guide subsequent drives. To insure the recovery of a complete sedimentary record, the starting depth between the two cores was offset by 50 cm such that the drives of one core would cover the gaps between drives of the second core. Core drives were extruded in the field, wrapped, and returned to the laboratory in PVC half-tubes.

3.1.4.4 Ekman dredge sediment sampler (LML only)

A gravity-driven, 15 cm x 15 cm x 15 cm Ekman dredge surface sampler was used to obtain two samples in October 1998 from the deep southern basin of the lake. The samples were gently covered with paper towels on return to the surface in an attempt to wick off excess water and to minimize the destruction of stratigraphy by gas exsolution.

3.1.4.5 Slide-hammer percussion corer (LML only)

An Aquatic Research Instruments slide-hammer percussion corer was used in May 2002 to retrieve several long sediment cores from the deep southern basin of the lake. This corer uses 7.0 cm O.D./6.4 cm I.D. core tubes, and with 250 cm core tubes can retrieve cores up to 237 cm in length. Sediment core tops were packed with absorbent, green floral foam before the cores were capped. Transport back to the laboratory occurred in a horizontal orientation given the core lengths.

3.1.4.6 Custom 10 cm diameter Schedule 40 PVC coring system (BIM only)

A custom, percussion-driven, terrestrial coring system using 10 cm diameter Schedule 40 PVC tubing was designed to obtain large sample volumes up to 3 m long from the Belle Isle Marsh. Core recovery for the system is provided by a steel core catcher in conjunction with an expandable piston for suction.

3.2 Laboratory work and analyses

This section provides an explanation of the lab methods used related to this dissertation.

3.2.1 Processing of bathymetric data (LML only)

To visualize the ~13 km of automated GPS track/depth logs recorded with the Garmin GPSMAP 168 Sounder (>1500 data points), latitude/longitude coordinates were converted to the UTM coordinate system and exported with the associated depth data to a Microsoft Excel spreadsheet. Golden Software Surfer was then used to grid the data via the krigging method. To avoid bathymetric/elevational "artefacts" outside of the lake basin proper where depth data was not collected, a zero depth value was manually assigned every 20 m along the shoreline of the lake. The gridded data was then contoured, and Surfer was used to calculate a variety of morphometric parameters including surface area and depth range volumes for a hypsometric curve. Finally, the bathymetric contours were overlaid on to 1m resolution color air photos of the lake and surrounding area.

3.2.2 Discarded sediment cores (LML only)

All ten Glew minicores and two Ekman dredge sediment samples obtained on various occasions between 1996 and 2000 were destroyed by the expansion of dissolved gases when brought to the surface[32]. No laboratory analyses were performed on these sediment cores, and they were discarded.

3.2.3 Non-frozen sediment core splitting, logging, and archiving (LML and BIM)

Sediment cores retrieved by the Livingstone-style square rod piston corer and slide-hammer percussion corer were split lengthwise into halves, and carefully cleaned with a piece of aluminum flashing. Core stratigraphy was logged after allowing the halves to slightly oxidize for several hours to better expose the stratigraphy. One half of each core was dedicated for subsequent sampling and analyses, and the other half was generally maintained as an archive when possible. Sediment cores were tightly wrapped in plastic wrap, placed in plastic D-tubes, and archived in a walk-in refrigerator throughout their existence.

3.2.4 Frozen sediment core preparation, logging, and archiving (LML only)

Frozen sediment cores were maintained frozen during their entire life cycle in a chest freezer, and worked on in increments of 2-3 minutes in a regular (i.e. unfrozen) laboratory environment. Occasionally, extremely cold, dry New England winter days

[32] An explanation and discussion of the dissolved gas problem is found in the "Results—general description of LML sedimentary record" section in the next chapter.

provided opportunities for longer working periods by working outside[33]. Select cores were prepared by first shaving them down to a flat, smooth surface using a frozen carpenter's wood plane. To enhance the visibility of core stratigraphy, a thin surface layer of ice was sublimated away, and the liberated sediment was allowed to oxidize. This was accomplished by positioning a small, low RPM fan within the chest freezer to blow a gentle stream of air over the prepared core surface for 24-48 hours. The cores were then logged and returned to the chest freezer for storage. Frozen sediment cores obtained between 1996 and 2000 were wrapped in plastic wrap and aluminum foil. Subsequent frozen cores were similarly wrapped, but additionally covered with two independently sealed layers of plastic to retard sublimation.

3.2.5 Sediment core photography (LML and BIM)

Select non-frozen and frozen sediment cores were photographed with a variety of setups that improved with time. Low ambient humidity days were chosen for photographing the frozen sediment cores to prevent rapid frost-over.

Earlier attempts at photography occurred using a light table with standard fluorescent illumination. Photographs were taken using a manual focus, 35 mm SLR camera, and regular photographic film. A standard exposure setting was not used, and no attempts at color calibration were undertaken. Using this technique, the two long sediment cores obtained by the Livingstone-style square rod piston corer were photographed in early 1997, and freeze core LML-18OCT1998-FRZ-1 was photographed

[33] To make this worthwhile, simple cold/freezing temperatures are not sufficient, and frigid temperatures (< -10°C) are necessary. The pore water in the sediment cores is partially saline, and has a significantly lower freezing/melting point than fresh water.

in late 1998. Film negative images were later converted to digital format by scanning them on a Polaroid SprintScan film scanner at 2700 dpi.

Later photography efforts used a light table illuminated with natural light, full spectrum, high frequency, fluorescent light bulbs. A FujiFilm HC-300Z video camera with a 1280x1000 pixel capture resolution was used to capture electronic images, and a standard exposure setting was made based on a gray card. Using this setup, the two long piston cores were rephotographed in 2001[34], and freeze core LML-19JAN2002-FRZ-1 was photographed in early 2002.

Subsequent photography efforts improved on the above setup by replacing the FujiFilm video camera with a high resolution Canon PowerShot G3 still camera with a 2272x1704 pixel capture resolution. The three sediment cores obtained by the slide-hammer percussion corer and all Belle Isle Marsh cores were photographed using this setup in early 2003.

Digital images were mosaicked by hand in Adobe Photoshop to create high-resolution whole core images. The images were stored in Adobe Photoshop PSD file format because of its ability to manage multiple layers of images and markups.

3.2.6 Magnetic susceptibility analysis (LML and BIM)

Select unfrozen sediment cores from the LML and all BIM cores underwent magnetic susceptibility analysis using two different systems. All cores were allowed to

[34] Unfortunately, this photography occurred after subsampling for basic sedimentary analyses and thin-sections had already occurred.

adjust to room temperature before analysis began to prevent temperature-dependent variation of susceptibility.

A Sapphire Instruments SI-2 system attached to a PC was used to measure whole core susceptibility on the LML Livingstone-style square rod piston core drives before they were split. Measurements were made at 1 cm resolution using an 11 cm inductance loop.

A Bartington MS2 magnetic susceptibility meter and MS2E high resolution surface scanner coupled with a TamiScan automated track and interfaced with a PC was the second system used to measure the magnetic susceptibility. Split cores from LML slide-hammer percussion core series and all of the BIM custom 10 cm diameter Schedule 40 PVC coring system series cores were measured at 0.3 cm resolution using this system.

The TamiScan automated track system is limited to approximately 150 cm of run in the normal, forward direction. For smaller diameter, lighter weight cores such as the slide-hammer percussion core series, it was possible to simply slide the > 150 cm cores up along the track to measure subsequently deeper portions of the stratigraphy in the normal, forward direction. For larger diameter, heavy weight cores like the 10 cm diameter marsh cores, however, such adjustment was not possible. For those cores, it was necessary to measure the stratigraphy deeper than ~150 cm in the reverse direction, and then splice it into the base of the regular forward direction data. This is indicated in the results by the use of curves of two different colors.

3.2.7 Bulk density and loss on ignition analysis (LML and BIM):

Select sediment cores were subsampled to characterize their basic sedimentology via analysis of wet bulk density, dry bulk density, organic carbon content, and inorganic carbon content. Using a 1 cc constant volume sampler, subsamples were extracted from the two LML Livingstone-style square rod piston cores at 10 cm resolution, and all of the BIM custom 10 cm diameter Schedule 40 PVC cores at 1 cm resolution.

Wet/dry bulk density was determined for the 1 cc samples first, and then organic/inorganic carbon content was estimated via loss on ignition following Dean (1974) and Heiri et al. (2001). Extracted samples were stored in tightly capped 15 cm plastic scintillation vials, and were generally processed within 24-48 hours of extraction. Samples were processed in batches of 50 (two trays of 25 crucibles each). In lieu of a large sized desiccator to prevent samples from absorbing ambient humidity between weighing steps, the samples were instead maintained in a 100°C drying oven, and were immediately weighed once removed from the oven.

3.2.8 Subsampling and resin impregnation of the LML varved section (LML only)

The uppermost 2.5 m of the sedimentary pile in the LML is laminated, and serves as the focus of this dissertation. The laminae are organized as siliciclastic-biogenic sedimentary couplets, and are true varves (i.e. the couplets are deposited on an annual basis). A detailed discussion of this portion of the record is presented in the Results chapter, and is not treated further here. All of the sediment cores retrieved for this dissertation recovered some portion of the laminated section, but complete coverage was provided by three cores—piston core LML-NOV1996-LIV-1 (drives 2 and 3), freeze

cores LML-19JAN02-FRZ-1 and LML-18OCT1998-FRZ-1. Therefore, these cores were subsampled and impregnated with resin for further detailed study.

Subsampling and impregnating used techniques modified from Merkt (1971) and Lamoureux (1994). Sediment subsampling trays (2.5 cm wide, 1.0 cm deep, and of variable length between 6 and 18 cm) were prepared from aluminum sheeting, and sample labels were physically scribed onto them. Abundant drill holes were made in the base of these subsampling trays to promote impregnation.

For the piston core drives, the aluminum subsampling trays were pushed flush into the split cores, and then liberated with the enclosed sediment by use of a "cheese-cutter" like tool. Tray subsample locations were staggered down the length of the core to provide a minimum overlap of at least 1 cm between subsampled sections. To provide this overlap, use of the archive core halves was necessary. Following extraction the subsamples were flash-frozen in liquid nitrogen.

For the freeze core, it was first inscribed with a needle to delineate a series of overlapping subsamples that would fit into the aluminum subsampling trays described above. The frozen subsample blocks were then cut out using a carpenter's coping saw fitted with a coarse-toothed blade. Excessively thick subsamples were thinned as necessary using a frozen carpenter's wood plane or a Dremel™ tool with cutting blade.

The frozen subsamples were then freeze-dried in a Virtis FreezeMobile 10 until a constant vacuum was reached (generally 30-40 mT after 24-36 hours). The dried subsamples were impregnated in disposable aluminum pans with Polysciences, Inc. Spurr

Low-Viscosity Epoxy Resin[35] under vacuum for 24-36 hours, and then cured for 24 hours in a drying oven at 50°C.

To promote excellent impregnation of the samples, two additional considerations were taken. First, resin circulation underneath the subsamples was encouraged by using miniature "railroad ties" to suspend the subsamples above the base of the disposable aluminum impregnation pans. Second, resin was added in two steps—during the first step, special care was taken to develop a wicking or chimney effect to draw resin up into the sample from below, and prevent the trapping of air bubbles.

3.2.9 Preparation of X-ray thin slabs and petrographic thin sections

A rock trim saw was used to cut the impregnated sediment subsamples from the surrounding matrix. In general, impregnated subsamples from the freeze core did not undergo further preparation with the exception of a few blocks which were polished down to show the stratigraphy because of poor visibility through the resin[36]. The subsamples from the piston cores, however, provided material for both continuous thin slabs (2 mm thick) for X-ray analysis and petrographic thin sections (see Figure 27 below). The thin slabs were produced by using a slab saw to cut an approximately 2.5 mm thick slab from

[35] Information about this product is available online at "http://www.polysciences.com/shop/assets/datasheets/127.pdf".

[36] Experimental work with thin sections of impregnated freeze core sediments showed that they are essentially useless for microscopic work. Though stratigraphy is visible with the naked eye, on the microscopic scale it is totally disrupted because of pervasive ice crystal casts. For this reason, preparation of freeze core sediments beyond simply impregnation was not carried out. Details about this problem are discussed in the Results chapter, in particular, Figure 38 which illustrates the issue.

the edge of each impregnated block down its length[37]. From the remaining blocks, individual billets for oversized petrographic thin sections (7.5 cm x 2.5 cm) were cut along diagonal paths to allow the correlation of stratigraphy between billets. Thin sections were commercially produced from the billets at Texas Petrographic Services Inc. (Houston, TX). The 2.5 mm thin slabs were later hand polished down to a uniform 2.0 mm thickness and 5 micron finish before X-ray analysis.

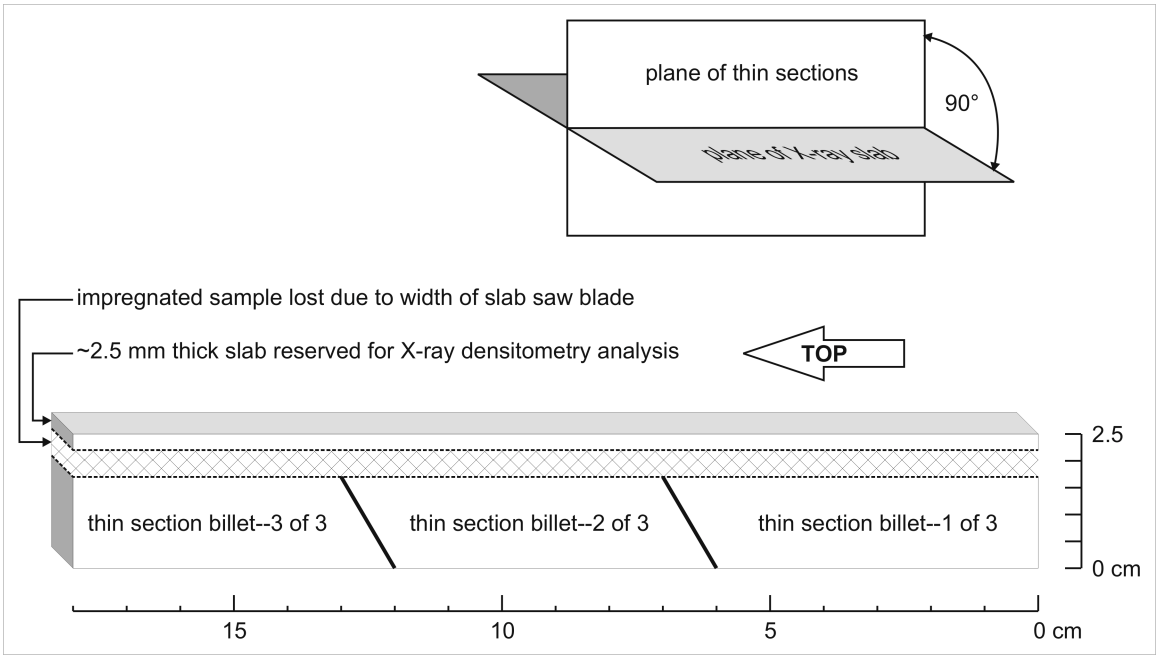

Figure 27—Diagram showing how an impregnated sediment block was used for both petrographic thin sections, and X-ray thin slabs. The X-ray thin slab was cut off of the side of the main block perpendicular to the orientation of the plane of thin sectioning.

3.2.10 Petrographic microscope thin section examination and imagery: (LML only)

Thin sections were examined with a petrographic microscope under both plane- and cross-polarized illumination to distinguish the stratigraphy and composition of the sediments. To facilitate construction of a varve chronology and provide a permanent

[37] These long, 2mm thick, thin slabs resemble popsicle sticks, and are cut perpendicular to the plane of the

record for easy referral later on, electronic images of the full thin sections were captured under both plane- and cross-polarized illumination. This was accomplished using a Zeiss petrographic macroscope coupled with a FujiFilm HC-300Z video camera (1280x1000 pixel capture resolution). Images were captured at the macroscope's lowest magnification where the field of view is 1.64 cm x 1.28 cm so multiple overlapping panels were captured to cover an entire thin section. The panels were later mosaicked by hand in Adobe Photoshop to create high-resolution whole thin section images, and stored in Adobe Photoshop PSD file format.

3.2.11 X-ray imagery of thin slabs: (LML only)

The thin slabs of impregnated sediment underwent X-ray imaging in the Department of Radiology at the University of Massachusetts Medical School in early 2001[38]. Using a late model X-ray machine designed for detailed biopsy imagery, the thin slabs were laid directly onto Kodak X-0mat TL film, and were imaged using a 30 kV beam strength and 60 second exposure time.

The X-ray exposures were later moved to digital format by scanning them in at 2000 dpi on an Agfa DuoScan scanner. To facilitate subsequent evaluation and varve thickness measurements, stratigraphic defects such as cracks, gaps, faults, and folds in the stratigraphy were carefully evaluated using the petrographic thin sections as a cross

---

thin sections. See the Figure 27 diagram for a visual explanation.

[38] Special thanks is owed to Dr. Andrew Karellas, Professor of Radiology and Director of Radiologic Physics Research Laboratory at the UMass Medical School, for making this work possible. He provided access to the facilities, but more importantly to his assistant, Dr. Patricia L. Belanger, a specialist in high detail radiography. Dr. Belanger worked with the author to quickly determine optimal exposure conditions, and provide highly detailed X-ray images of the impregnated thin slabs.

reference[39]. The defects were then meticulously repaired by hand in Adobe Photoshop to provide a master palinspastic reconstruction of the stratigraphy[40]. Images were stored in Adobe Photoshop PSD file format.

3.2.12 Back scattered electron microscope (BSEM) examination and imagery: (LML only)

Within the lowest meter of the LML laminated section, the laminae are thin and less pronounced. To better understand this portion of the record, petrographic thin sections were examined via back scattered electron imagery on a JEOL JSM-5410 scanning electron microscope with analog controls. A 4Pi image acquisition system attached to the SEM allowed for high resolution digital image capture directly from the SEM raster scanner.

Prior to imagery, the thin sections were hand polished down to a semi-gloss finish using a progressively finer 5, 1, then 0.3 micron grit sequence, and then sputter-coated with carbon.

Given the analog nature of the JEOL JSM-5410 SEM, it was generally impossible to accurately reproduce imaging conditions between sessions. A 20 kV beam strength was used exclusively; however, the spot size and working distance parameters were

---

[39] See the "4.1.4 Completeness and quality of the sedimentary record" section in Chapter 4 for a detailed explanation about such defects including examples.

[40] The X-ray images displayed at various spots within the main body of this dissertation are palinspastically reconstructed images, not the raw X-ray images with stratigraphic defects. Appendix A provides both types of imagery (i.e. the raw and palinspastically reconstructed imagery) side-by-side for comparison. We chose to build palinspastic reconstructions for the sake of an eventual X-ray grayscale densitometry analysis to be performed over the entire laminated section of the record. This analysis has not yet been performed. With many tiny cracks and small defects in the raw imagery, such a densitometry analysis would be not only laborious, but also extremely error-prone as one would be forced to work with hundreds of tiny segments

occasionally varied to produce the best quality images possible. In general, the spot size was set between 17-20, and the working distance between 10-12.

All imaging was done at 100x magnification which resulted in a field of view of 1.28 mm x 0.96 mm in size. Image captures by the 4Pi system were done at 2560x1920 pixel resolution yielding a theoretical 0.5 micron resolution. To fully cover the stratigraphy present within a thin section, multiple transects down each thin section were needed. Adjacent capture frames were generally overlapped between 10-20 percent to facilitate mosaicking.

The images outputted from the JEOL/4Pi system generally suffered from a significantly uneven illumination because of a permanent equipment problem with the JEOL SEM. In general, this unequal illumination was essentially linear, and thus could be described as a simple plane or gradient. An automated/scripted routine was built using ImageJ (Rasband, 2006) to assess the unequal illumination based on all the images in an individual transect. The routine then builds a compensatory gradient image to correct for the unequal illumination, and produces a new directory of illumination-corrected images for subsequent mosaicking.

The mosaicking was done by hand in Adobe Photoshop to produce long, high resolution, master BSEM image transects. These images were stored in Adobe Photoshop PSD file format.

In a final step, the BSEM image transects were then overlaid on to the petrographic scope thin section imagery for cross correlation. To exactly orient and

---

that could be easily mixed up. With the palinspastic reconstructions, a single long transect down an X-ray thin slab is possible, and this significantly helps to reduce possible errors.

downscale the BSEM image transects, distinct objects (sand grains, plant fragments, etc.) towards the ends of the transects were identified in both the BSEM and thin section imagery (cross-polarized exposure). A vector (distance and angular orientation) was determined for the distinct objects in each type of imagery. From the vector distance, a downscaling factor was calculated, and from the angular orientation trigonometric relationships were used to calculate the necessary angle of rotation. Finally, the BSEM image transects were overlaid on to the thin section imagery using the calculated values.

3.2.13 ^{14}C, ^{210}Pb, and ^{137}Cs analyses (LML and BIM)

Multiple samples were taken from different sediment cores for radiometric age analysis.

Samples for ^{14}C age analysis were picked with stainless steel tweezers, and included only macroscopic vegetation fragments of terrestrial plants (leaves or twigs). After picking samples, they were washed with distilled, deionized water. Earlier samples were placed in glass scintillation vials with foil-lined lids, and preserved in a refrigerator. Later samples were dried in a 95°C drying oven or via freeze drier, and stored in glass scintillation vials with foil-lined lids within a dessicator. Prior to submission, samples underwent pretreatment with an acid/base wash to remove possible post-depositional contamination, in particular, possible precipitated carbonate and mobile humic acid from other sources (Abbott and Stafford, 1996). Samples were analyzed at either Lawrence Livermore National Labs or at the University of California Riverside. Results were calibrated into their 2 sigma, calibrated calendar year equivalents using the PC client version of the Calib v5.0.1 program (Stuiver and Reimer, 1993).

Samples for ^{137}Cs and ^{210}Pb analysis were either cut from a freeze core for the LML samples, or extracted from a peaty marsh core for the BIM samples. The samples were placed in preweighed test tubes, freeze-dried in a Virtis FreezeMobile 10 until a constant vacuum was reached (generally 30-40 mT after 24-36 hours), and then submitted to the EAWAG-SURF Laboratory for analysis under the guidance of Dr. Michael Sturm.

CHAPTER 4

RESULTS

In this section, results for both laboratory and field work are presented first for the Lower Mystic Lake, and second for Belle Isle Marsh.

4.1 Results for the Lower Mystic Lake

4.1.1 Sediment core recovery

The following section provides an inventory of the sediment cores retrieved for the LML portion of this project, and brief comments about their disposition. Figure 28 shows coring locations for each of the cores.

4.1.1.1 Glew minicores

The following Glew minicores were retrieved from the LML for this project.

Table 4—Inventory of Glew minicores retrieved from the LML.

Sediment core	***Comments***
LML-02MAY1996-GLW-1	10 m water depth; overpenetrated; exploratory core taken while looking for deep sub-basin
LML-02MAY1996-GLW-2	10 m water depth; captured active sed/water interface; exploratory core taken while looking for deep sub-basin
LML-02MAY1996-GLW-3	23.2 m water depth; captured active sed/water interface; destroyed by expansion of dissolved gases so discarded
LML-02MAY1996-GLW-4	23.2 m water depth; overpenetrated; destroyed by expansion of dissolved gases so discarded
LML-23NOV1996-GLW-1	20.3 m water depth; captured active sed/water interface, but later destroyed by expansion of dissolved gases so discarded
LML-23NOV1996-GLW-2	20.3 m water depth; overpenetrated; destroyed by expansion of dissolved gases so discarded

LML-24NOV1996-GLW-3	19.5 m water depth; overpenetrated as only short tubes available; destroyed by expansion of dissolved gases so discarded
LML-24NOV1996-GLW-4	19.5 m water depth; overpenetrated as only short tubes available; destroyed by expansion of dissolved gases so discarded
LML-18OCT1998-GLW-1	23.4 m water depth; overpenetrated; ~70 cm sediment recovery; destroyed by expansion of dissolved gases so discarded
LML-18OCT1998-GLW-2	23.4 m water depth; overpenetrated; ~100 cm sediment recovery; destroyed by expansion of dissolved gases so discarded
LML-29APR2000-GLW-1	22 m water depth; destroyed by expansion of dissolved gases so discarded
LML-29APR2000-GLW-2	22 m water depth; destroyed by expansion of dissolved gases so discarded

Expansion of dissolved gases destroyed all of the Glew minicores retrieved from the deep southern sub-basin of the lake. An explanation of this issue is not presented here, but is discussed below in the "4.1.3.1 Textural description" section of this chapter.

Figure 28—Locations of sediment cores retrieved from the Lower Mystic Lake. When multiple sediment cores are listed for a location, the boat or coring platform was moved a few meters between cores. Sediment cores retrieved prior to 2001 were located by orientation with respect to objects around the lake, and from 2001 onwards via GPS.

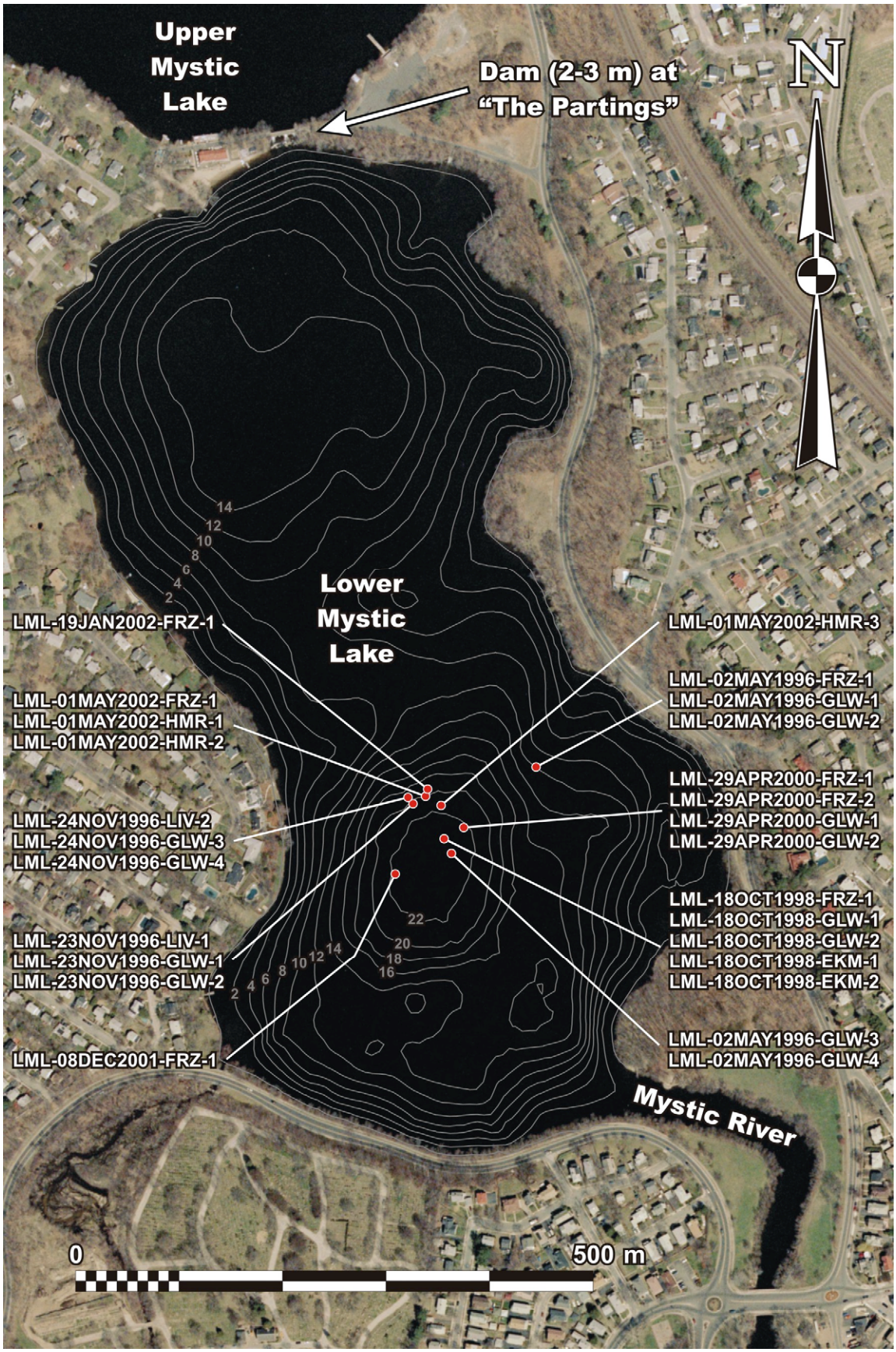
Upper
Mystic
Lake
Dam (2-3 m) at
"The Partings"
N
Lower
Mystic
Lake
LML-19JAN2002-FRZ-1
LML-01MAY2002-FRZ-1
LML-01MAY2002-HMR-1
LML-01MAY2002-HMR-2
LML-24NOV1996-LIV-2
LML-24NOV1996-GLW-3
LML-24NOV1996-GLW-4
LML-23NOV1996-LIV-1
LML-23NOV1996-GLW-1
LML-23NOV1996-GLW-2
LML-08DEC2001-FRZ-1
LML-01MAY2002-HMR-3
LML-02MAY1996-FRZ-1
LML-02MAY1996-GLW-1
LML-02MAY1996-GLW-2
LML-29APR2000-FRZ-1
LML-29APR2000-FRZ-2
LML-29APR2000-GLW-1
LML-29APR2000-GLW-2
LML-18OCT1998-FRZ-1
LML-18OCT1998-GLW-1
LML-18OCT1998-GLW-2
LML-18OCT1998-EKM-1
LML-18OCT1998-EKM-2
LML-02MAY1996-GLW-3
LML-02MAY1996-GLW-4
Mystic River
0
500 m

4.1.1.2 Frozen sediment cores

The following freeze cores were retrieved from the LML for this project.

Table 5—Inventory of frozen sediment cores retrieved from the LML.

Sediment core	***Comments***
LML-02MAY1996-FRZ-1, [side A]	10 m water depth; overpenetrated; exploratory core taken while looking for deep sub-basin; ~40 cm sediment recovery; slab very thin
LML-18OCT1998-FRZ-1, [sides A & B]	23.4 m water depth; captured intact sed/water interface; 64 cm sediment recovery; for Frog series impregnations
LML-29APR2000-FRZ-1, [sides A & B]	22 m water depth; overpenetrated; ~28 cm sediment recovery; for Rana series impregnations
LML-29APR2000-FRZ-2, [sides A & B (incomplete)]	22 m water depth; overpenetrated; stratigraphy disturbed—corer appears to have fallen over
LML-08DEC2001-FRZ-1	22.5 m water depth; overpenetrated; 45 cm recovery; oversized corer malfunction (maiden voyage), so slab thin
LML-19JAN2002-FRZ-1	19.7 m water depth; overpenetrated; 106 cm recovery; beautiful, thick slab
LML-01MAY2002-FRZ-1	20.4 m water depth; possibly captured sed/water interface; recovery quantity unspecified; beautiful, thick slab

4.1.1.3 Livingstone-style square rod piston cores

The following Livingstone-style square rod piston cores were retrieved from the LML for this project.

Table 6—Inventory of square rod piston cores retrieved from the LML.

Sediment core	***Comments***
LML-23NOV1996-LIV-1, 10 drives	20.3 m water depth; overpenetrated; 9.75 m total length; drives 2 and 3 contain laminated sequence, and serve as source for Bird series impregnations
LML-24NOV1996-LIV-2, 11 drives	19.5 m water depth; overpenetrated; 11.0 m total length; drives 1 and 2 contain laminated sequence

4.1.1.4 Ekman dredge samples

The following Ekman dredge samples were retrieved from the LML for this project.

Table 7—Inventory of Ekman dredge samples retrieved from the LML.

Sediment core	*Comments*
LML-18OCT1998-EKM-1	23.4 m water depth; destroyed by expansion of dissolved gases so discarded
LML-18OCT1998-EKM-2	23.4 m water depth; possibly captured sed/water interface, but destroyed by expansion of dissolved gases so discarded

As mentioned above, an explanation of the issue with dissolved gases is presented below in the "4.1.3.1 Textural description" section of this chapter.

4.1.1.5 Slide-hammer percussion cores

The following slide-hammer percussion cores were retrieved from the LML for this project.

Table 8—Inventory of slide-hammer percussion cores retrieved from the LML.

Sediment core	*Comments*
LML-01MAY2002-HMR-1	20.4 m water depth; overpenetrated; 101 cm total length
LML-01MAY2002-HMR-2	20.4 m water depth; overpenetrated; 228 cm total length
LML-01MAY2002-HMR-3	21.5 m water depth; overpenetrated; 220 cm total length

4.1.2 Sediment core logs and photography

Brief log sheets for all sediment cores, and core photography if available, were archived in electronic format for future reference.

4.1.3 General description of LML sedimentary record

The different sediment coring technologies discussed in the Methods chapter retrieved different portions of the LML sedimentary record. When all the recovered sediment cores are arranged and overlapped, they compose an approximately 12.3 m

thickness of sediments up to the active sediment/water interface[41]. The base of the lacustrine sequence was not reached by 12.3 m depth, and probably continues at least several meters deeper[42].

A general textural and stratigraphic/structural description of the sedimentary record follows below.

4.1.3.1 Textural description

The LML sedimentary record shows a marked variation in simple texture—the lower portion of the record is well-consolidated, and the upper portion is very soft. The change in texture is relatively abrupt, and occurs at about 1.25 m depth in the sedimentary pile (Figure 29). This variation has significant implications for sediment core retrieval, and the types of laboratory analyses performed on the retrieved sediments.

The well-consolidated portion of the record extends from the base of the recovered material (e.g. 12.3 m depth) up to about 1.25 m depth in the sediment pile (Figure 29). The texture of this portion of the record allows it to be retrieved with traditional lacustrine coring technologies. In November 1996, this portion of the record was recovered in the two long Livingstone-style square rod piston cores mentioned above (i.e. LML-23NOV1996-LIV-1 and -2). The uppermost part of this well-consolidated

---

[41] The active sediment/water interface refers to its estimated position in 2005. Most coring attempts overpenetrated past the sediment/water interface because of the very soft nature of the uppermost sediments. However, a freeze core in October 1998 successfully captured it, and from extrapolation, an estimated position for the interface in 2005 was determined.

[42] An AMS radiocarbon date on a terrestrial macrofossil taken from 54 cm depth in Drive 11 of core LML-24NOV1996-LIV-2 yielded a 2 sigma, calibrated, calendar year age of BC 11732-10938 with a relative probability of 1.000. Specific details about the date can be found in the "4.1.14.1 ^{14}C age results vs. the varve chronology" section below.

portion of the record was also recovered again in May 2002 via the three slide-hammer percussion sediment cores (i.e. LML-01MAY2002-HMR-1, -2, and –3).

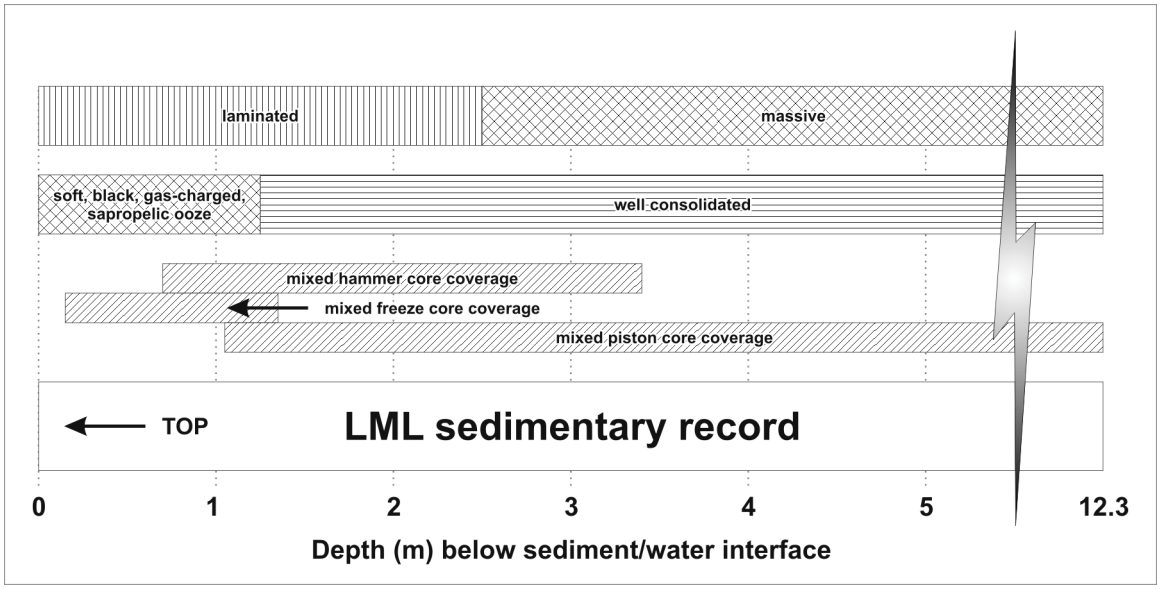

Figure 29—Summary diagram of the LML sedimentary record from the maximum coring depth (12.3 m) up to the estimated sediment/water interface in 2005. A break in the depth axis (jump from 5.0 to 12.3 m depth) is indicated by the lightning bolt at the right. Top/up direction is to the left. Sedimentary structure, texture, and the type of sediment core coverage are indicated by the range bars with different hatch patterns.

Above the zone of well-consolidated sediment, the LML record is essentially a black, sapropelic ooze. It varies in consistency upwards from a soft, loose mud at the base to a nepheloid layer at the sediment/water interface (Figure 29). This zone is also charged with dissolved gases such as CH_4, H_2S, and CO_2 similar to the overlying monimolimnion (Ludlam and Duval, 2001; Duval and Ludlam, 2001). The gases are stable in the pressure and temperature regime at the lake bottom, but quickly come out of solution when brought to the surface. This exsolution process generally obliterates the

stratigraphy, and makes it impossible to retrieve this portion of the LML record with traditional coring technologies[43].

To overcome the issue of exsolving gases, this portion of the record was retrieved by freeze coring (Figure 29). Seven different freeze cores were obtained, and are briefly inventoried in the "4.1.1.2 Frozen sediment cores" section above. The cores obtained between 1996 and 2000 were captured using the shorter 75 cm hollow wedge style freeze corer described in Chapter 3. These cores were up to ~1.0 cm thick and 65 cm long, and thus, did not overlap with the well-consolidated portion of the record. An additional three extra long freeze cores up to ~2.0 cm thick and ~110 cm long were obtained with the oversized wedge-box style freeze corer between December 2001 and May 2002. One of these extra long freeze cores, LML-19JAN2002-FRZ-1, did overlap with the well-consolidated portion of the record.

Only one of the seven freeze cores, LML-18OCT1998-FRZ-1, captured the active sediment/water interface. The others overpenetrated and passed it because their simple weight allowed them to settle down into this excessively soft, sapropelic zone.

---

[43] As an example, within minutes of bringing a Glew minicore to the surface, gas bubbles begin to expand, and quickly become visible to the naked eye. Over the next several hours, the bubbles grow and coalesce, and carry clumps of sediment upwards to form a floating mass. The floating mass is then slowly redeposited over the next few days. Even when excess water is carefully siphoned off of core tops to prevent floating sediment masses, expanding gases still cause close to total disruption of the stratigraphy. All ten Glew minicores and two Ekman dredge samples retrieved from the deep, southern sub-basin of the lake between 1996 and 2000 suffered this fate. Duval and Ludlam (2001) encountered the same issue in the Lower Mystic Lake, and reported that expanding gases caused sediment to overflow from Ekman dredges when they were brought to the surface. On rare occasions, it appears that the quantity of dissolved gases actually diminishes to such an extent that retrieval of sediments by traditional coring technologies becomes feasible. For example, while Duval and Ludlam (2001) normally experienced overflowing dredge samples as described above, they also reported that during the summer of 1993 they were able to obtain samples that did not overflow. This degassing phenomenon is probably limited to just the shallow surface sediments (maybe 20-30 cm depth), and does not extend deep into the sedimentary pile (S. Ludlam, 2006, personal communication).

4.1.3.2 Stratigraphic/structural description

While the LML sedimentary record shows a marked variation in simple texture, it can also be divided into two sections with a strikingly different stratigraphic/structural contrast. The major stratigraphic/structural change occurs at about 2.5 m depth in the sediment pile—it is not coincident with the textural change at 1.25 m depth which is discussed above.

The first section extends from the base of the recovered material (approximately 12.3 m depth) up to 2.5 m depth in the sediment pile (Figure 29). It is composed of a massive, brown gyttja. A few sand layers and some laminae occur within the gyttja from about 8-10 m depth, and occasional color banding is noticeable, but otherwise the material is structureless to the naked eye.

The second section extends from 2.5 m depth in the sediment pile up to the present sediment/water interface (Figure 29). It is composed of exquisite, rhythmically laminated, dark/light sedimentary couplets (Figure 30). The couplets are rather subtle on a fresh core surface, but become readily apparent as the material oxidizes. This is particularly true for the uppermost 1.25 m of stratigraphy (e.g. the soft, sapropelic, gas-charged zone discussed in the "4.1.3.1 Textural description"section above) which is essentially completely black on retrieval.

In general, the couplets are simple, and range from 1.0-2.5 mm in thickness in the lower half of the section. At about 1.25 m depth—the same depth as the marked textural change—the couplets become significantly more complex. They are not strictly couplets, but include multiple light/dark components. They also begin an exponential thickening

upward towards the modern sediment/water interface such that the uppermost couplets reach 20+ mm thickness.

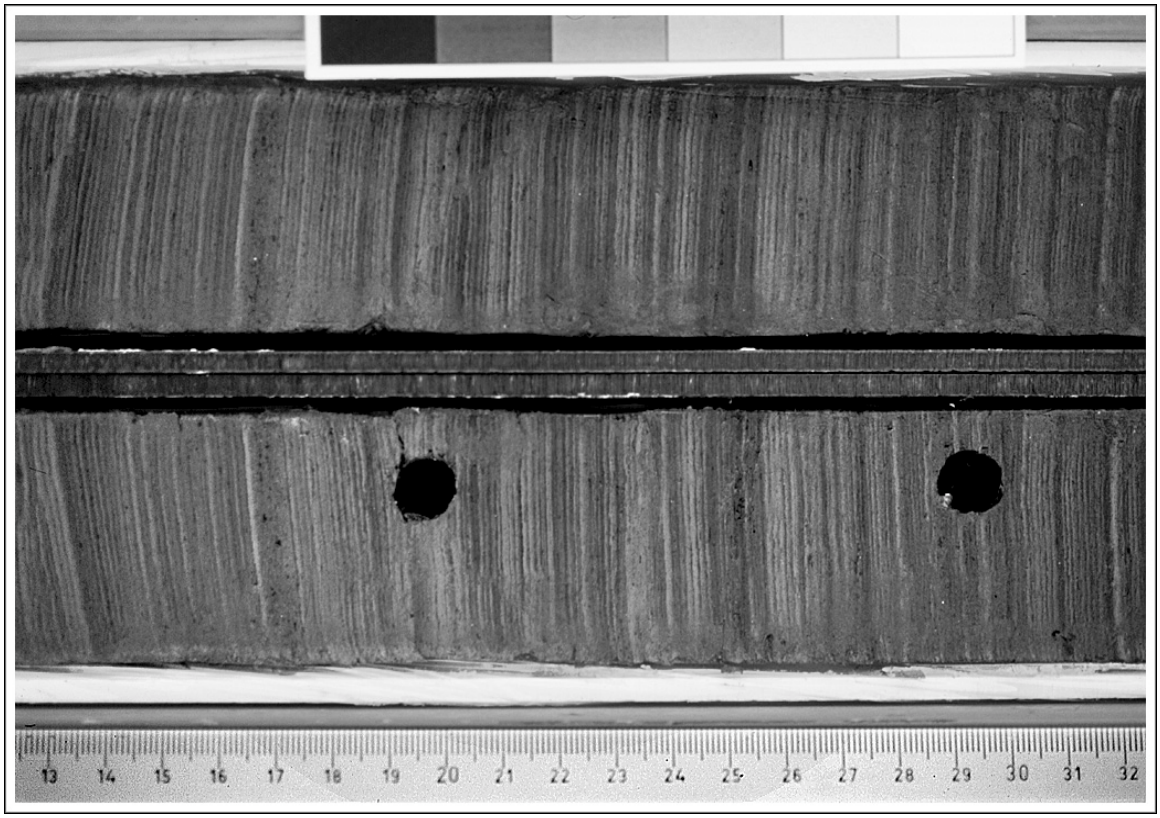

Figure 30—An example of the exquisite, rhythmically laminated, dark/light sediment couplets from the LML sedimentary record. This example come from drive 3 of piston core LML-23NOV1996-LIV-1 (top/up is to the left). A large, graded bed with organic detritus can be seen at about 17 cm depth.

Occasional, anomalous graded beds with organic detritus can be observed with the naked eye throughout this 2.5 m section. This sequence of laminated sedimentary couplets is the section of the LML record on which this dissertation is based. It is more thoroughly discussed in the "4.1.9 The LML sedimentary couplets are true varves" section below.

4.1.4 Completeness and quality of the sedimentary record

Based on simple visual observation, it is difficult to evaluate the completeness and quality of the massive portion of the LML sedimentary record (i.e. below 2.5 m depth in the sediment pile). Stratigraphic defects such as faults, folds, and mixed/homogenized zones are, if they exist, essentially unrecognizable. In turn, the stratigraphic defects that exist in the laminated portion of the record (i.e. < 2.5 m depth in sediment pile) are easily identifiable because they stand out in obvious contrast to the otherwise well-behaved laminae. The lower (2.50-~1.25 m depth) and upper (~1.25-0 cm depth) halves of the laminated portion of the record will be addressed separately because of their significant difference in texture.

4.1.4.1 Lower half of the laminated portion of record

The lower half of the laminated portion of the record (2.50-~1.25 m depth) was retrieved by multiple non-frozen sediment cores including the two long piston cores, and all three of the slide-hammer percussion cores. In all of these cores with the exception of LML-23NOV1996-LIV-1, significant stratigraphic defects are visible.

One significant type of defect visible in LML-24NOV1996-LIV-2 and all three of the slide hammer piston cores (LML-01MAY2002-HMR-1, -2, and -3) is a zone of homogeneous sediment within the normal laminated sediments (Figure 31). When such homogenized zones are not concordant with bedding, they may represent shear zones which have accommodated mass movement events. When the zones are concordant, they may represent gas expansion/escape events that destroy stratigraphy, or selective preservation of laminae related to fluctuations in the depth of the monimolimnion.

Unfortunately, the only solution to reconstructing the stratigraphy lost in one of these homogenized zones is to compare it with another sediment core.

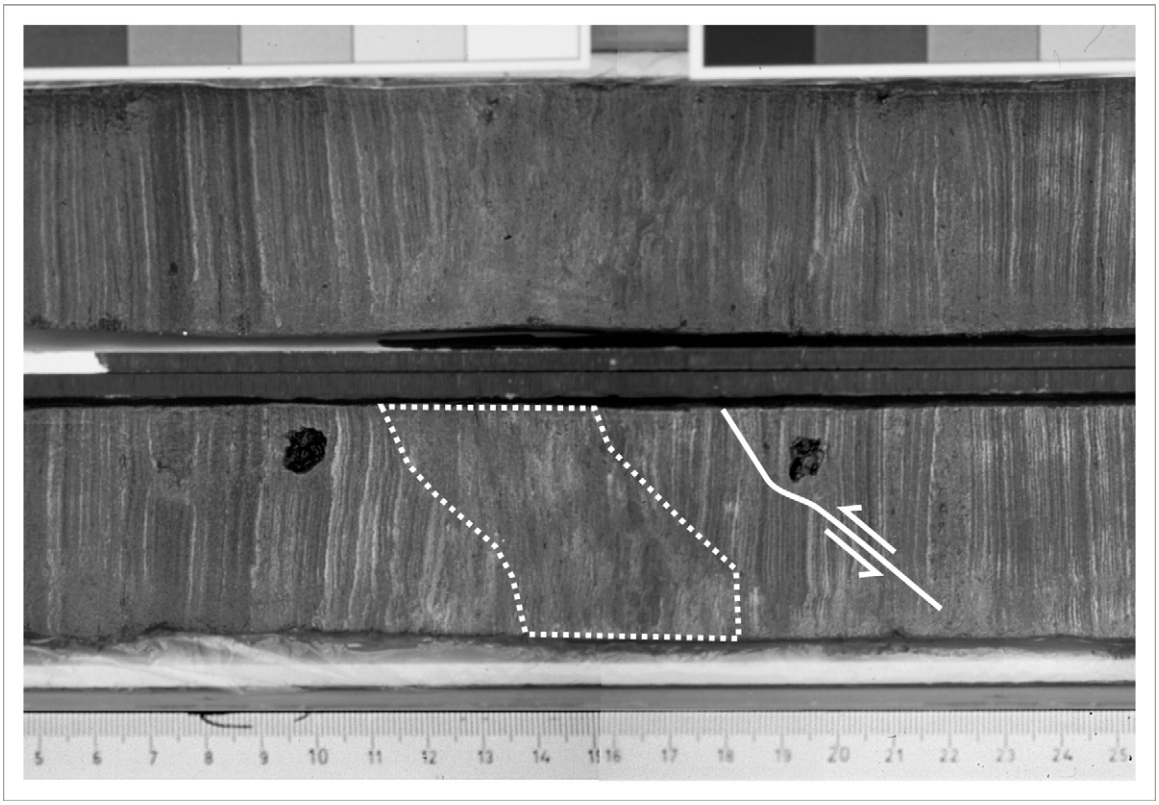

Figure 31—Stratigraphic defects in Drive 2 of core LML-24NOV1996-LIV-2. Top/up is to the left. This figure shows both sides of the split core from about 5-25 cm depth. The dotted white line (~11-18 cm) delineates an area where beautifully laminated sediments are abruptly interrupted by a zone of homogenized sediments, possibly the result of a mass movement event. The solid white line and shear arrows (~18-22 cm) indicate a fault with the sense of relative motion. In this case, displacement along the fault is so great that a reconstruction of the stratigraphy is not possible with just this core. The same homogenized zone and fault are also present on the upper core half in a symmetric, mirror image orientation, but they are not delineated by white lines so the reader has an unimpeded view.

A second type of very common defect seen in all of the cores is faulting at various scales. In general, the relative displacement along these faults is small, and equivalent stratigraphy can often be identified on either side of the fault within the same core (or thin section). Thus, the offset can be accounted for, and corrected easily. In a few cases, the relative displacement is large enough that consultation with another core is necessary.

Another important consideration with faulting is that when one's observations are based on a single plane of section, the existence of a fault may be virtually unrecognizable if its trace parallels stratigraphy (Figure 32).

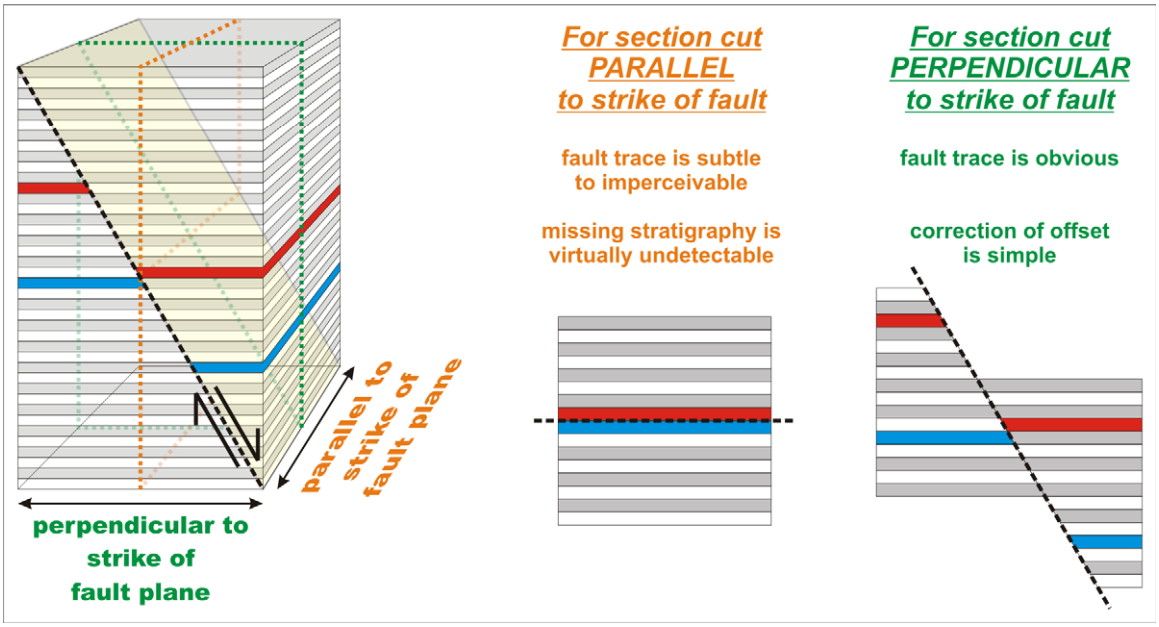

Figure 32—The recognition of a fault surface in a sediment core (or thin section) is highly dependent on the orientation of the section cut through the fault. In the 3-D block (left), a fault plane (light yellow) has offset the laminated stratigraphy (white and gray couplets) which includes red and blue marker beds for reference by the reader. If the 3-D block is sectioned by a plane whose strike is perpendicular to the strike of the fault plane (dotted green line on 3-D block), the resulting diagonal orientation of the fault trace makes it easy to identify (right). Furthermore, although it is offset, there is no apparent loss of stratigraphy. In turn, if the 3-D block is sectioned by a plane whose strike is parallel to the strike of the fault plane (dotted orange line on 3-D block), the resulting orientation of the fault trace is horizontal (middle). As a result, the existence of the fault may be virtually unrecognizable since its trace parallels the normal stratigraphy. Furthermore, the perspective would result in an apparent loss of stratigraphy (note how the four couplets which exist between the marker beds essentially disappear to the observer). If the stratigraphy in question provides some type of chronologic control (e.g. the couplets are deposited on an annual basis), this apparent loss of stratigraphy will result in an incomplete chronology, and, even worse, leave no clue to the investigator that this is the case. A simple solution to this problem is to examine all stratigraphy from two orthogonal planes of section. We have accomplished this for the LML stratigraphy by cutting X-ray thin slabs from the same impregnated blocks as the thin sections, but in a vertically perpendicular orientation (see Figure 27 in Chapter 3).

Given that all of the non-frozen sediment cores that retrieved the lower half of the laminated portion suffer from small scale faulting, the lack of a homogenized zone in sediment core LML-23NOV1996-LIV-1 means it holds the most complete record.

4.1.4.2 Upper half of the laminated portion of record

The excessive thickness of the soft, sapropelic, gas charged upper half of the laminated portion of the record (~1.25-0 m depth) made it difficult to retrieve this section in its entirety. All freeze cores with the exception of LML-18OCT1998-FRZ-1 overpenetrated and passed the active sediment/water interface. Also, despite the multiple attempts made with the regular sized freeze corer between 1996 and 2000, a combined total of only about 70 cm of the section was captured. Not until 2002 with the retrieval of the first successful oversized freeze core, LML-19JAN2002-FRZ-1, was the complete section obtained, and its true thickness actually known for the first time. LML-19JAN2002-FRZ-1 was long enough to overlap with the uppermost sediments retrieved by piston coring, yet still also overlap with the base of LML-18OCT1998-FRZ-1[44].

Unlike the non-frozen cores from the lower half of the laminated portion of the record, none of the freeze cores have homogenized zones—they consist entirely of laminated sediments. Small scale faulting is present, but is less common than observed in the laminated sediments retrieved in the non-frozen sediment cores. This difference in the quantity of small scale faulting may be related to the fact that the deeper sediments are

[44] A second, extra long freeze core obtained in May 2002 (i.e. LML-01MAY2002-FRZ-1) probably also covers the same gap as LML-19JAN2002-FRZ-1. However, after it was confirmed that the January 2002 freeze corer completed the missing stratigraphy, LML-01MAY2002-FRZ-1 was not worked up.

more compacted, and/or it may be related to the different coring methods which were employed.

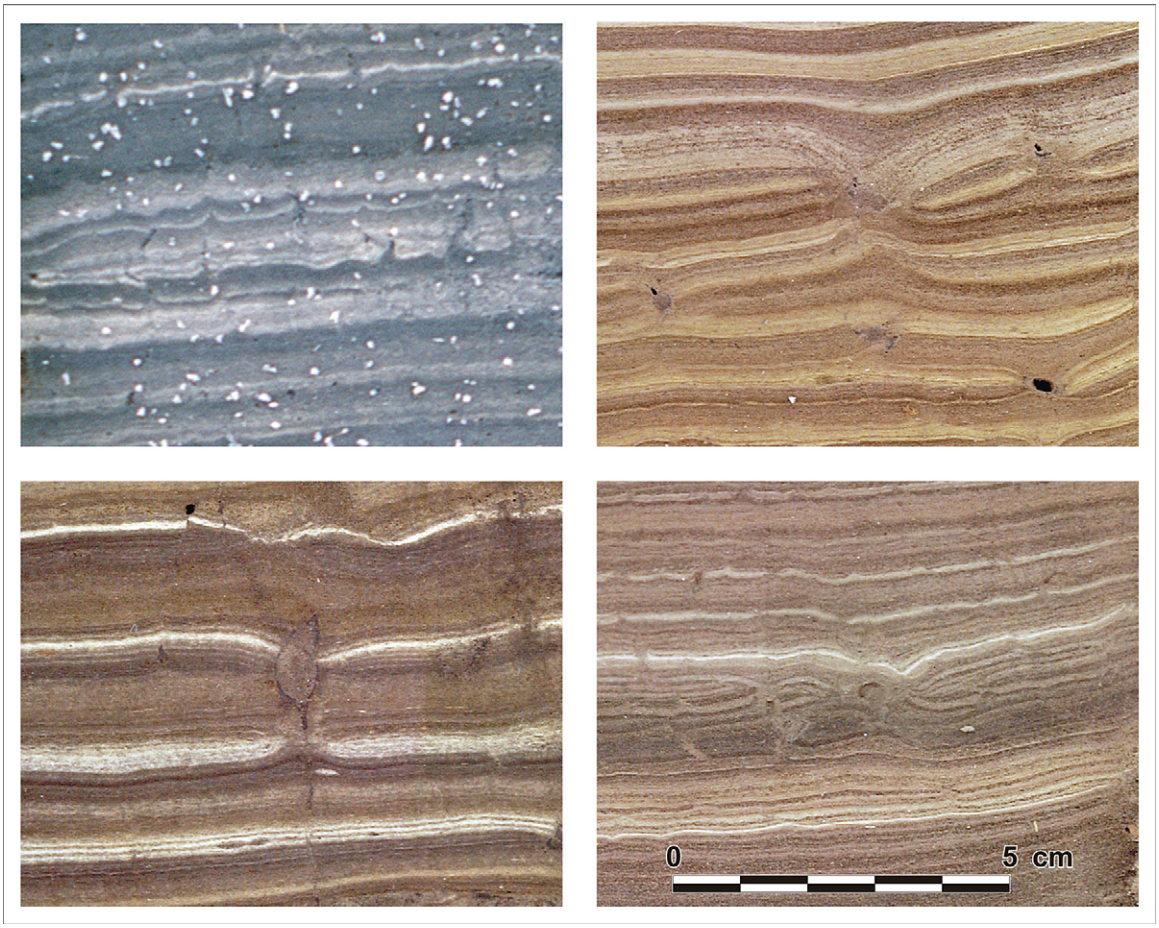

Figure 33—Examples of common, small scale, stratigraphic defects present in the stratigraphy captured by freeze cores. The upper left image is from core LML-18OCT1998-FRZ-1. Towards the middle of that image, the many cusp- and flame-like features pointing upwards are gas escape structures. The white grains on top of the core are ice crystals. The other three images are from core LML-19JAN2002-FRZ-1, and illustrate the pinch and swell structures of unknown origin at different sizes and grades of completion. All four images share the same scale which is illustrated in the lower right hand corner of the diagram.

Two other types of small-scale stratigraphic defects commonly appear in the stratigraphy captured by freeze core. These include gas escape structures, and a pinch and swell structure of unknown origin (Figure 33). In general, it is easy to correct for such defects given the broad field of view provided by the freeze core slabs. Similar defects

are not found in the deeper laminated sediments retrieved in non-frozen cores. For the gas escape structures this makes obvious sense as the dissolved gases are concentrated in this portion of the record.

4.1.5 Sediment cores used to complete the laminated portion of the record

As mentioned above, this dissertation is based on study of the laminated portion of the LML record. Coverage is provided by two piston core drives and two freeze cores that exhibit significant overlap to ensure the continuity between sections. Details of the coverage are provided here, and graphically in Figure 34.

Drive 3 of piston core LML-23NOV1996-LIV-1 covers about 70 cm of laminated sedimentation from the very base of the laminated sequence upwards. Despite the fact that it should be end-to-end with Drive 2 from the same core, those two drives actually overlap by about 9.3 cm, and appear to provide a continuous sequence.

Drive 2 of piston core LML-23NOV1996-LIV-1 contains more than 80 cm of laminated sedimentation. Its upper portion overlaps with the base of oversized freeze core LML-19JAN2002-FRZ-1 by about 26 cm.

Oversized freeze core LML-19JAN2002-FRZ-1 covers about 106 cm of laminated sedimentation. Its upper portion overlaps with the base of regular sized freeze core LML-18OCT1998-FRZ-1 for about 45 cm.

Regular sized freeze core LML-18OCT1998-FRZ-1 covers about 65 cm of laminated sedimentation. Importantly, it extends up to, and clearly captures the active sediment/water interface in October 1998 when the core was retrieved.

Figure 34—Sediment cores used to provide overlapping coverage of the laminated stratigraphy in the LML. Complete coverage of the sequence is provided by overlap between two piston core drives and two freeze cores. Note that the 0 cm depth datum is the estimated position of the sediment/water interface in 2005 which was extrapolated from the known position in October 1998. The category bars at the right show the extent of the textural and stratigraphic/structural characteristics of the sequence. The 1990 and 1980 varve tags indicate the sedimentary couplets deposited in those years. See "4.1.9.4 Robust, internal proof that the couplets are actually varves" section in the text for an explanation of why the couplets are considered varves.

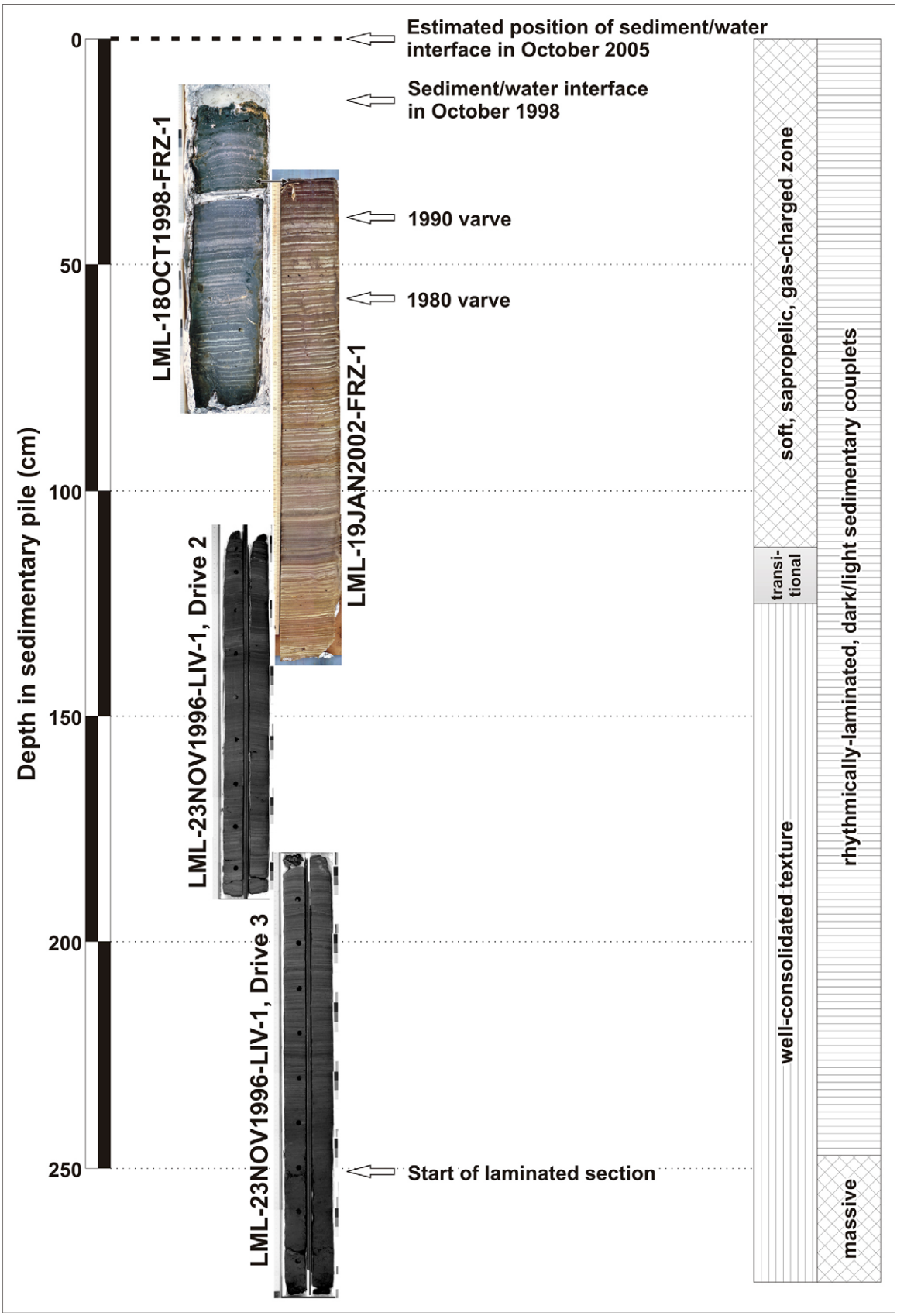
Depth in sedimentary pile (cm)
0
50
100
150
200
250
Estimated position of sediment/water interface in October 2005
Sediment/water interface in October 1998
1990 varve
1980 varve
Start of laminated section
LML-18OCT1998-FRZ-1
LML-19JAN2002-FRZ-1
LML-23NOV1996-LIV-1, Drive 2
LML-23NOV1996-LIV-1, Drive 3
soft, sapropelic, gas-charged zone
transi-tional
well-consolidated texture
massive
rhythmically-laminated, dark/light sedimentary couplets

4.1.6 Magnetic susceptibility analysis results

Magnetic susceptibility analysis was only possible on non-frozen sediment cores. Thus, no results for the uppermost 1.0-1.25 m of the stratigraphy exist as this was exclusively retrieved by freeze coring. The non-frozen cores which underwent this analysis include the two long piston cores from November 1996 (i.e. LML-23NOV1996-LIV-1 and -2), and the three slide-hammer percussion cores from May 2002 (LML-01MAY2002-HMR-1, -2, and -3). Figure 35 shows plots of the results for these sediment cores. In general, biogenic/organic-rich sediments produce a susceptibility signal with a low value, and clastic sediments return higher values. Given that the sediments are composed of these two end members in differing proportions, the susceptibility curves essentially serve as an index of the relative percentages of these two components.

In Figure 35, a set of tie lines links up common stratigraphy between the cores. The transition from massive to laminated sediments in each core is indicated by the tie line around 1.6-1.7 m depth. Based on the tie lines, the second piston core appears to have penetrated about 3 m deeper than the first piston core.

4.1.6.1 Massive portion of record

In general, the piston cores show a long, gradual decrease in magnetic susceptibility values up through the massive-textured portion of the record. From the base of the second piston core (e.g. LML-24NOV1996-LIV-2), values fluctuate around a high value of 2.0E-4 units, but they decrease progressively upward such that by the top of the massive stratigraphy they are about an order of magnitude lower (e.g. ~2.0E-5 units). Despite the general trend of the curves, higher frequency variability is common. In

particular, a series of spikes in the susceptibility value curves towards the base of the cores are obvious—these represent the few sand layers mentioned in the "4.1.3.2 Stratigraphic/structural description" section above.

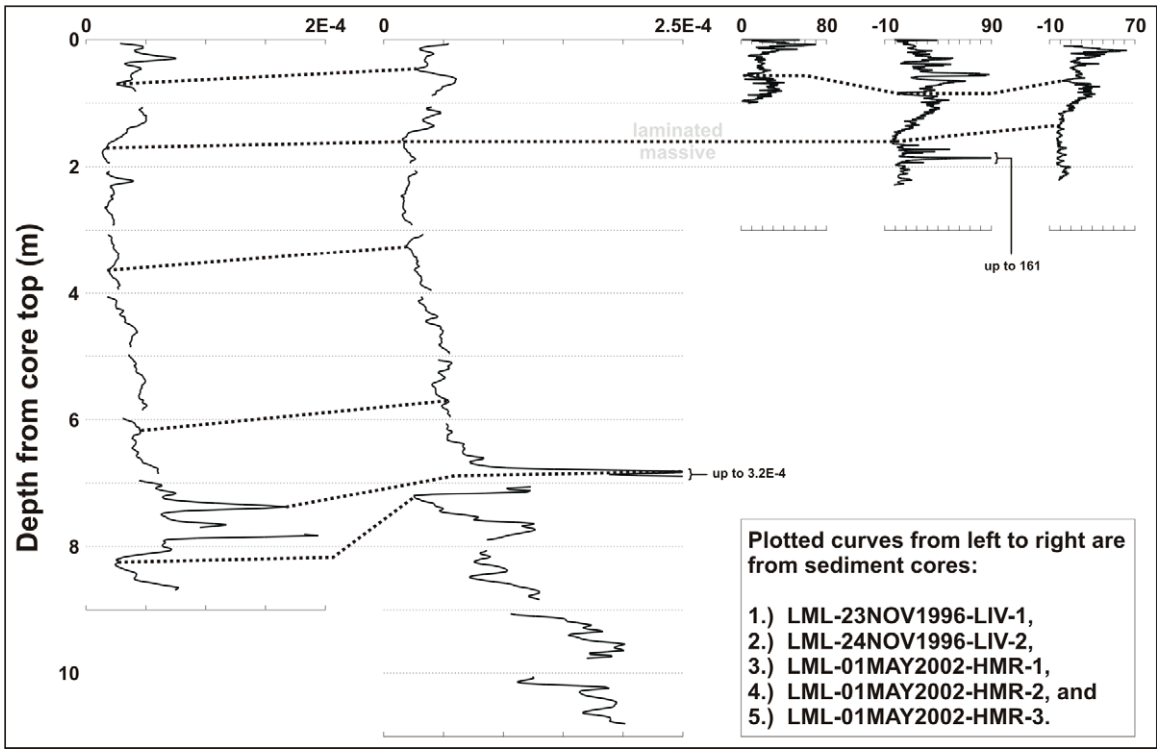

Figure 35—Results of magnetic susceptibility analyses from non-frozen LML sediment cores. Piston core analyses were performed at 2 cm resolution using one system, and slide-hammer percussion core analyses at 0.3 cm resolution using a second system. The absolute value of results between the two systems is not directly comparable; however, the relative values and shape of the resulting curves are comparable. The small gaps in the piston core curves are breaks between the individual core drives. Note that for sediment core LML-23NOV1996-LIV-1, Drive 1 did not undergo analysis because it was volumetrically deficient; thus, the core top datum for that core in this figure only is the top of Drive 2, and not Drive 1. Consequently, the apparent depth for any point in that core in this figure only is about a 1 m too shallow because Drive 1 is not present. The large spikes seen towards the base of core LML-23NOV1996-LIV-1 are the sand layers discussed in the "4.1.3.2 Stratigraphic/structural description" section above. Peaks in the curves for LML-24NOV1996-LIV-2 and LML-01MAY2002 are truncated because of the plot scale, but the peak values are indicated. The dense dashed lines are proposed tie lines that link up common features (e.g. common stratigraphy) between the curves. The tie line at 1.6-1.7 m depth represents the transition from massive texture to laminated stratigraphy.

4.1.6.2 Laminated portion of record

Within the laminated section, susceptibility values first start off low in the range of 2.0E-5 units as a result of the long term decreasing trend within the massive section. They rapidly increase to approximately 5.0E-5 units, and then fluctuate around that value till the end of the sediment cores. Recall that the end of the sediment cores is not the end of the laminated sequence. The uppermost 1.0-1.25 m of the record was retrieved by freeze coring (see Figure 29), and therefore did not undergo magnetic susceptibility analysis.

4.1.7 Bulk density and loss on ignition analysis results

Analysis of wet and dry bulk density, and organic and inorganic carbon content via loss on ignition was only possible for non-frozen sediment cores. Only the two long piston cores from November 1996 (i.e. LML-23NOV1996-LIV-1 and -2) underwent these analyses. The results are illustrated in Figure 36. In general, wet and dry bulk density show lower values for biogenic/organic-rich sediments, and higher values for clastic sediments. Organic carbon content is a direct measure of the combustible organic matter in a sample, and is generally a mirror opposite of the wet and dry bulk density curves. Inorganic carbon content provides an approximation of the quantity of mixed carbonate minerals present in a sample, but may also be influenced by clay content (Dean, 1974).

4.1.7.1 Massive portion of record

Within the massive section of the record, wet bulk density values generally range from 0.95 to 1.25 g/cc, and dry bulk density values from 0.15 to 0.35 g/cc. For both

Figure 36—Results of bulk density and LOI analyses on sediment cores LML-23NOV1996-LIV-1 (upper set in red) and LML-24NOV1996-LIV-2 (lower set in blue). The analysis was performed at 10 cm resolution. The small gaps in the curves are breaks between the individual core drives. The peak in the dry bulk density curve for core LML-24NOV1996-LIV-2 is truncated because of the plot scale, but the peak value is indicated. The dense dashed line for each core marks the transition from massive texture to laminated stratigraphy.

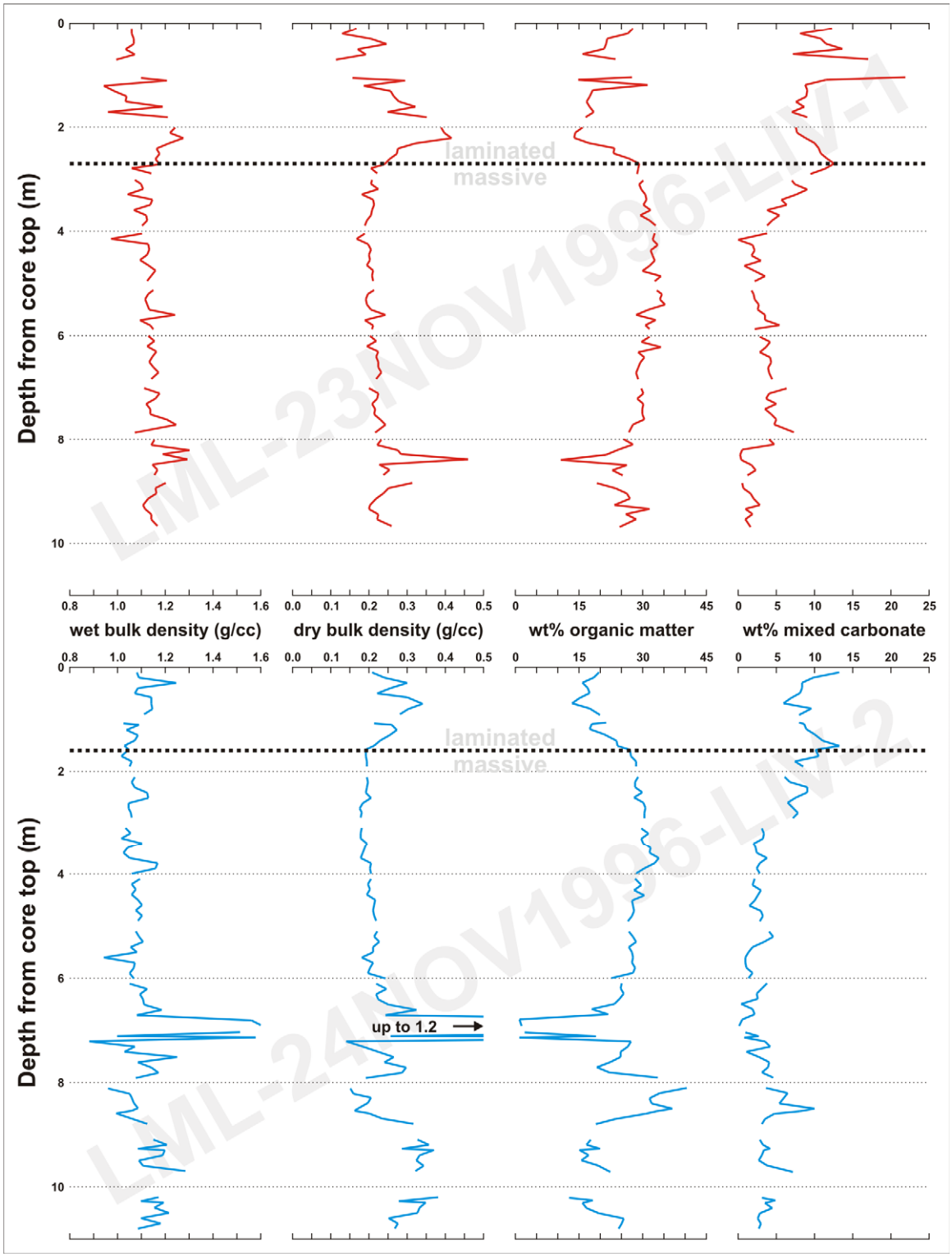
Depth from core top (m)
laminated
massive
wet bulk density (g/cc)
dry bulk density (g/cc)
wt% organic matter
wt% mixed carbonate
up to 1.2
LML-23NOV1996-LIV-1
LML-24NOV1996-LIV-2

parameters, a subtle trend towards progressively lower values from the base upwards is observable. Positive value spikes in both parameters within the lower part of the section are related to the few sand layers mentioned in the "4.1.3.2 Stratigraphic/structural description" section above.

Organic matter generally comprises from 15-35 weight percent of the samples within the massive section of the record. This parameter also shows a trend—there is a gradual increase in values from the base upwards, and then a subtle decrease within the last few meters of the section. The few sand layers which occur towards the base of the section as mentioned above are manifested by abrupt negative spikes in the record.

Inorganic carbon as mixed carbonate generally composes less than five weight percent of the samples from the massive portion of the record, but in the last few meters of that section rises up to values in the range of 10-12 weight percent. The sand layers towards the base of the section do not result in spikes in the inorganic carbon curves unlike as seen in the wet/dry bulk density and organic carbon results.

4.1.7.2 Laminated portion of record

Within the laminated portion of the record, wet bulk density values generally range from 0.95 to 1.25 g/cc, and dry bulk density values range from 0.1 to 0.4 g/cc. These ranges are the same, or very close, to the ranges for the massive portion of the record. Regarding a trend for the results, within the first 70-90 cm of this section, the values show a sharp rise from low values in the preceding massive-textured material.

The values then decline for the remaining portion of the record, but with significant swings of variability[45].

Organic matter generally ranges from 15-30 weight percent in the laminated section which is similar to the range in the massive-textured section. Opposite to the trend of bulk density values, there is a sharp drop from high values in the first 70-90 cm of the section as the sedimentation transitions from massive to laminated. Subsequently, there is an increase in values over the remaining part of the record, but also with significant swings of variability.

Finally, inorganic carbon content values show a general range between 7-14 weight percent with one large peak in core LML-23NOV1996-LIV-1 that reaches about 22 weight percent. Regarding a trend for this parameter, it shows a sharp decline at the beginning of the section followed by a significant recovery and peak of values, followed by a second decrease in values till the end of the sequence.

4.1.8 Sediment core impregnation and thin section results

In January 2000, five subsample blocks from freeze core LML-18OCT1998-FRZ-1 underwent resin impregnation. The subsamples were labeled from A (top) to E (base), and the series was referred to as the "Frog" series to facilitate labeling[46]. Figure 37

---

[45] This trend is most obvious in core LML-23NOV1996-LIV-1 because it contains a thicker sequence of laminated sediments, and because it contains a more complete record of the stratigraphy than the second long piston core as explained in the "4.1.4 Completeness and quality of the sedimentary record" section above.

[46] The point of this short code word, "Frog", and similar short series names was to avoid writing out the regular, long core name and/or drive number as necessary. While the regular, long core name (i.e. "LML-23NOV1996-LIV-1, Drive 2") is very descriptive, it is difficult to scribe onto a small thin section or 2 mm thin X-ray slab; hence, the need for a short code word for each series.

shows the location of subsample blocks within the core. Impregnation was extremely poor, and the uppermost four blocks were directly discarded. Impregnation of block Frog E was marginal, and was reserved for subsequent thin sectioning.

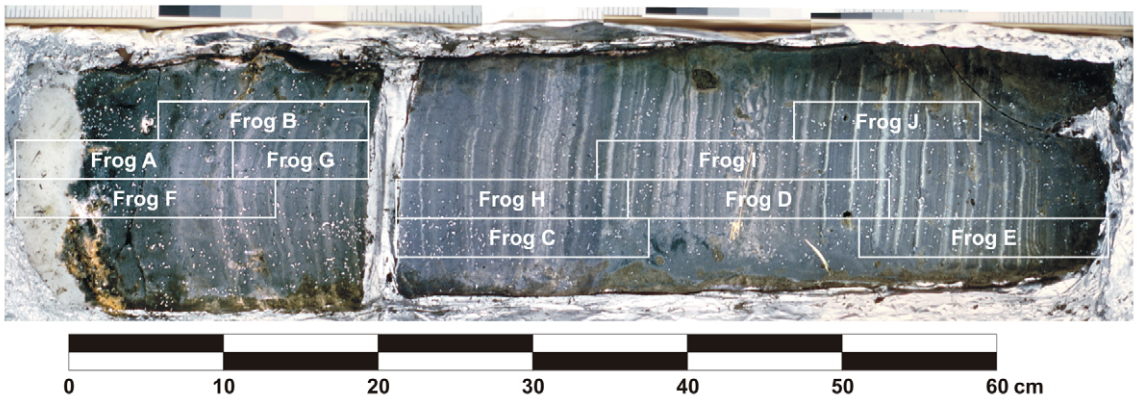

Figure 37—Location of "Frog" series impregnation subsample blocks in freeze core LML-18OCT1998-FRZ-1. Top/up is to the left. This freeze core clearly captured the active sediment/water interface as confirmed by >4 cm of sediment-free ice visible at the top of the core.

Freeze core LML-18OCT1998-FRZ-1 was resampled again in February 2000, and subsample blocks Frog F (top) to Frog J (base) were impregnated well. The blocks produced five full-block, 2 mm thick, X-ray thin slabs, and 12 partial-block thin sections. Figure 37 shows the location of subsample blocks and thin-sections within the core. The thin sections displayed a pervasive honeycomb texture as a result of massive ice crystal casts, and they were unsatisfactory for microscopic examination (Figure 38).

In March 2000, 14 impregnated sediment blocks were produced from drives 2 and 3 of piston core LML-23NOV1996-LIV-1. To facilitate labeling, this series of blocks was referred to as the "Bird" series. From the 14 impregnated blocks, 14 full-block, 2 mm thick, X-ray thin slabs, and 31 partial-block thin sections were produced. Figure 39 shows the placement of the blocks and thin-sections. Thin section quality was excellent, and they served well for both optical and electron microscope examination.

Figure 38—Example of ice crystal casts caused by freeze coring. This transmitted light image is of thin section Bird E-1 from freeze core LML-18OCT1998-FRZ-1. The two outlined rectangles are 3x expanded views of the underlying areas, and show the pervasive, honeycomb-like structure resulting from the ice crystal casts. Some of the ice crystals reached very large sizes, for example, at the very right of the image some casts can be seen to approach 0.5 cm in length. The stratigraphy is generally visible when examining the thin section as a whole, but microscopic examination is frustrated by the ice crystal casts.

In May 2000, another freeze core, LML-29APR2000-FRZ-1, was subsampled and impregnated to evaluate whether a freshly retrieved freeze core would show fewer ice crystal casts, and provide suitable thin sections for microscopic examination. Four subsample blocks were labeled from A (top) to D (base), and the series was referred to as the "Rana" series to facilitate labeling. Four full-block, 2 mm thick, X-ray thin slabs, and 11 partial-block thin section were produced from the subsamples. Like the thin sections produced from freeze core LML-18OCT1998-FRZ-1, the thin sections from the freshly retrieved freeze core still displayed ice crystal casts, though smaller, and were unsatisfactory for microscopic examination (Figure 38).

In February 2002, seven impregnated sediment blocks were produced from the extra long freeze core LML-19JAN2002-FRZ-1. Thin sections were not produced from these blocks because prior experience with impregnating freeze core sediments showed that ice crystal casts would make microscopic examination unfeasible. Instead, the impregnated blocks were produced for simple visual examination. The stratigraphy in the lower four blocks was obscured by surface smearing so the blocks were polished down to

Figure 39—Location of "Bird" series impregnation subsamples in Drives 2 and 3 of piston core LML-23NOV1996-LIV-1. Note that to provide a minimum overlap of at least 1 cm between subsample blocks, it was necessary to use both the work and archive halves of the core. X-ray thin slabs were cut from the full length of each impregnated block before thin section billets were cut. Note that while the location of all the X-ray thin slabs illustrated above is on the left side of each block, they were actually cut from the side that was most convenient on a block by block basis. Thus, the left side position of the X-ray thin slabs above is just for illustrative purposes. The thin section billets were cut along diagonal lines, and are labeled as illustrated.

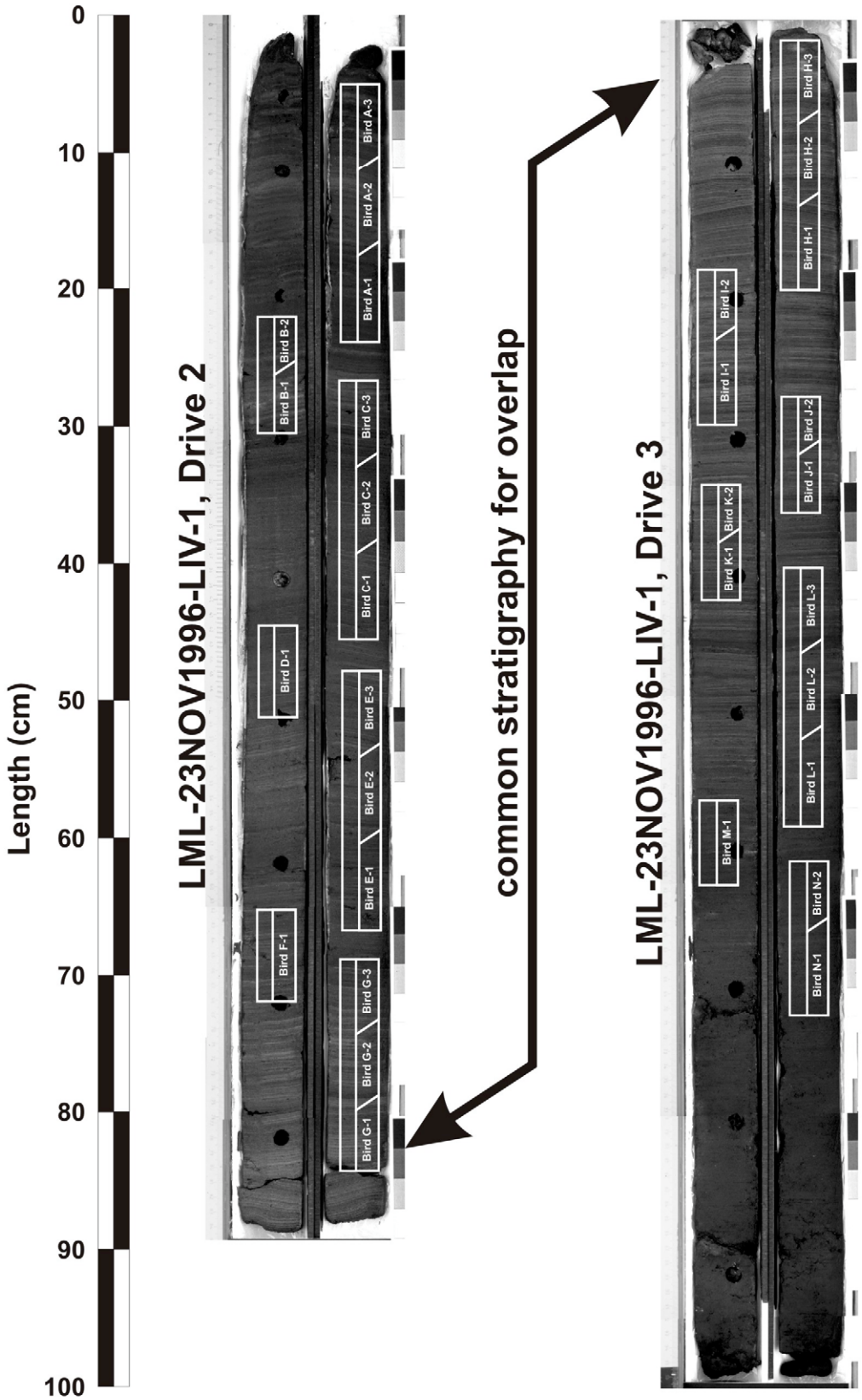
Length (cm)
0
10
20
30
40
50
60
70
80
90
100
LML-23NOV1996-LIV-1, Drive 2
Bird F-1
Bird G-1
Bird G-2
Bird G-3
Bird E-1
Bird E-2
Bird E-3
Bird D-1
Bird C-1
Bird C-2
Bird C-3
Bird B-1
Bird B-2
Bird A-1
Bird A-2
Bird A-3
common stratigraphy for overlap
LML-23NOV1996-LIV-1, Drive 3
Bird N-1
Bird N-2
Bird M-1
Bird L-1
Bird L-2
Bird L-3
Bird K-1
Bird K-2
Bird J-1
Bird J-2
Bird I-1
Bird I-2
Bird H-1
Bird H-2
Bird H-3

clarify it. The stratigraphy in the upper three blocks was clear so the blocks were left as is. This series was not given a short code name as no thin sections were produced, and the original large subsample blocks were left intact.

4.1.9 The LML sedimentary couplets are true varves

The 2.5 m of exquisitely laminated sedimentary couplets in the LML record are actually varves (i.e. the couplets are deposited on an annual basis). This section provides a detailed description of the couplets, relates them to the annual sedimentary cycle in the lake, and then provides robust internal proof that the couplets are indeed varves, and not simply couplets deposited on a random or non-annual basis.

4.1.9.1 General composition and structure of the sedimentary couplets

The laminated portion of the LML record is composed primarily of simple siliciclastic-biogenic sedimentary couplets. As mentioned earlier, the couplets generally range from 1.0-2.5 mm thickness in the lower half of the section. At about 1.25 m depth—the same depth as the marked textural change—the couplets become significantly more complex. They are not strictly couplets, but include multiple light/dark components. They also begin an exponential thickening upward towards the modern sediment/water interface such that the uppermost couplets reach 25+ mm thickness.

When thin sections of the couplets are observed with the naked eye, or plane-polarized light on a petrographic microscope, the siliciclastic-rich layers are generally

darker in color, and the biogenic-rich layers are generally lighter[47]. However, under cross-polarized light, in X-ray exposures, and via back-scattered electron microscope imagery the relationship is reversed—layers rich in siliciclastic material are light/bright, and layers rich in biogenic components are darker. Figure 40 shows multiple views of a sample section of couplets.

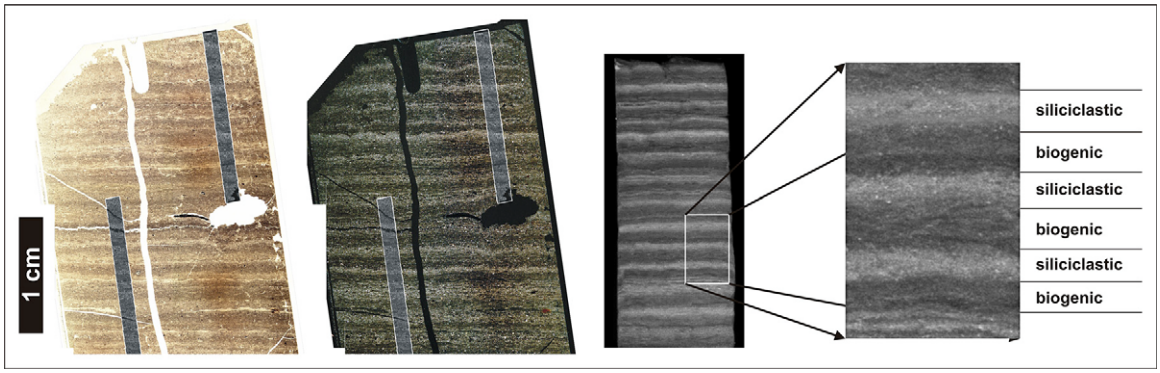

Figure 40—Multiple views of the same set of couplets under different types of illumination. The images at the left and left-middle are plane-polarized and cross-polarized light images, respectively, from the upper half of thin section Bird E-3. The image at right-middle is the same set of couplets, but from X-ray illumination of the Bird series X-ray thin slab. The first three images share the same scale as indicated by the scale bar at the left of the figure. The image at the right is a 4x enlargement of the area indicated on the X-ray thin slab image. The gray strips overlaid on top of the thin section images are ultra high-resolution BSEM transect mosaic images. The upper right strip, for example, is actually composed of 18 overlapping 2560x1920 pixel BSE images that allow us to resolve sedimentary components as small as individual diatoms. Under plane-polarized light, siliciclastic-rich layers generally have a darker color while the biogenic-rich layers are generally lighter in color. The relationship is exactly the reverse for the cross-polarized, X-ray, and BSE images. In these types of images, the siliciclastic materials are generally lighter/brighter, and the biogenic-rich sediments are darker.

An important observation about the structure of the couplets is that the transition from biogenic to siliciclastic sedimentation is often gradual. In turn, the transition from siliciclastic to biogenic sedimentation is generally more pronounced. As a result, the

[47] On a fresh sediment core surface, the laminae are rather subtle, but after the surface has been allowed to oxidize for a period of time, the laminae become readily visible.

pronounced siliciclastic to biogenic transition is an obvious natural splitting point to separate the couplets up from one another.

In general, the couplets are prominent and easy to identify from about 1.75 m depth in the sediment pile up to the active sediment/water interface. They do exhibit changes in character at different ranges within this span, however. In turn, the older/deeper couplets from 2.5 m up to 1.75 m depth are generally thinner, and in some zones slightly more diffuse. As a result, they are somewhat less prominent.

4.1.9.2 Possible controls on siliciclastic and biogenic sedimentation, and their annual cycle

Given the siliciclastic-biogenic composition of the LML couplets, what are the possible environmental parameters that control sedimentation of one type or the other? Deposition of siliciclastic material is presumably related to either runoff from precipitation and/or stream flow in the Aberjona River. Deposition of biogenic material is presumably related to the abundance of diatoms and/or other photosynthetic organisms. Figure 41 shows annual plots for these parameters, and each is briefly discussed below.

Average monthly precipitation for Boston is plotted in blue in Figure 41, and is based on records from 1818-1989 (source NOAA NCDC). While average precipitation does exhibit some small monthly peaks (March, August, and November), there is not a large amount of variability, and all monthly values fall in the small range of between 80-100 millimeters.

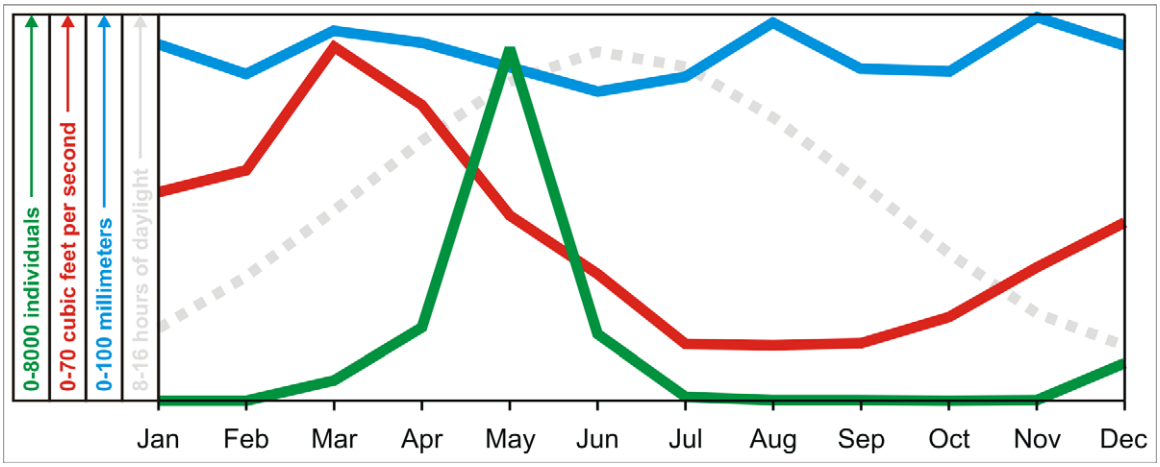

Figure 41—Plot of monthly values for parameters which may control the composition and timing of sedimentation in the LML. Scales for each of the parameters are listed at the left. The blue line represents average monthly precipitation for Boston. The red line represents stream flow of the Aberjona River. The green line represents abundance of five planktic diatom species collected in phytoplankton tows. The gray line represents average monthly number of daylight hours in Boston, and hence, a general gauge of photosynthetic activity.

Monthly values for stream flow in the Aberjona River, the main input for the UML, and hence the LML, are plotted in red in Figure 41. Data is based on the period from 1944 to 1999 (source: USGS stream gauge network station number 01102500). There is a pronounced peak in flow during the month of March that is related to spring rains and snow melt (we will refer to this as the "spring flush"). Monthly values of stream discharge drop to minimum values in July, August, and September, and then begin a slow gradual rise through the fall and winter until the spring flush peak is reached again during the next calendar year.

Monthly values for planktic diatom abundances are plotted in green in Figure 41. The values are based on phytoplankton tows in the UML collected between April 1974

and March 1975 (Chesebrough and Screpetis, 1975)[48]. Planktic diatom genera included in the analysis include *Asterionella*, *Fragilaria*, *Synedra*, *Cyclotella*, and *Tabellaria* with the first two genera dominating the counts. There is a very pronounced peak in abundances during the month of May as the spring flush is waning. This strong peak is related to the increased number of daylight hours (see below), and a fresh supply of silica and nutrients following spring overturn (Chesebrough and Screpetis, 1975). Of importance to several discussions below, the genus *Cyclotella* appeared in small quantities, but only once per year during the months of July, August, and September.

Average monthly values for the number of daylight hours in Boston are plotted by the dotted gray line in Figure 41. The values were calculated as the difference between daily sunrise and sunset times for 2006 obtained from the U.S. Naval Observatory website (source: http://aa.usno.navy.mil/data/docs/RS_OneYear.html). The number of daylight hours serves as a general gauge of photosynthetic activity. There is a broad peak in this parameter during the months of May, June, July, and August.

4.1.9.3 Couplet architecture related to the annual sedimentary cycle

The regular, rhythmic nature of the LML couplets, and their quantity (2.5 m thickness) suggests their deposition is not simply random, but guided by a well-established pacemaker. An obvious choice for the pacemaker would be the annual sedimentary cycle in the lake. Given the four possible controls on sedimentation

[48] While this diatom abundance data is actually from the UML, we make the assumption that it is also representative for the LML because they are adjacent (formerly confluent until the dam at "The Partings" was built in AD 1864), and the LML actually receives the outflow from the UML.

discussed above, can all or a subset of them explain the observed architecture (i.e. composition and structure) of the LML couplets?

As mentioned above, runoff from precipitation and/or stream flow in the Aberjona River are presumably the controls on siliciclastic sedimentation. The monthly values of precipitation are relatively constant, and do not show much variability throughout the year. The Aberjona stream flow, however, does show significant variability with a single strong annual pulse related to the spring flush in March. Importantly, it slowly ramps up in the months prior to reaching its peak, and then as it is waning, it is punctuated by a strong pulse of biogenic sediment (i.e. the planktic diatom abundance peak in May followed by high photosynthetic activity through the summer months). This annual pattern of stream flow closely mimics the architecture of the siliciclastic component within the couplets—there is a gradual ramp up, a strong peak, and then pronounced termination. We therefore conclude that if the couplets are indeed deposited on an annual basis, stream flow in the Aberjona River is undoubtedly the most important control on siliciclastic sedimentation because its annual cycle closely mimics the architecture of the siliciclastic component within the couplets.

Photosynthesizing organisms, including planktic diatoms specifically, or other photosynthesizers in general, are the source of biogenic sediment in the LML. While there is some level of photosynthetic activity in the lake at all times of the year, it peaks during the late spring and summer in response to the increased daylight hours and nutrient availability. Importantly, as siliciclastic deposition wanes following its March peak, the strong pulse of planktic diatoms in May followed by several months of generally high photosynthetic activity results in a pronounced transition from siliciclastic to biogenic

sedimentation. This annual cycle of biogenic sediment production clearly parallels the distribution of biogenic component within the couplets, in particular, the pronounced transition from siliciclastic to biogenic sedimentation.

4.1.9.4 Robust, internal proof that the couplets are actually varves

The regular, rhythmic nature of the LML couplets, their quantity, and the apparent coordination between couplet architecture and the annual sedimentary cycle provides strong circumstantial evidence that the couplets are deposited on an annual basis; i.e. the couplets are actually varves. But since other processes that occur on a random temporal basis could also produce a simple, alternating sequence of siliciclastic and biogenic laminae, additional proof that the couplets are indeed true varves is needed. Robust and compelling internal evidence comes from the couplets themselves via high resolution BSEM and thin section imagery[49].

In particular, the evidence is provided by the distribution of frustules of the diatom *Cyclotella* within the biogenic component of the couplets in high resolution BSEM imagery (Figure 42). As briefly mentioned above, Chesebrough and Screpetis (1975) recognized a bloom of *Cyclotella* (albeit in small quantities) once per year during the months of July, August, and September. On select BSEM image transects, the location of every visible *Cyclotella* frustule was laboriously mapped out by hand at full resolution, and the results were overlaid onto the thin section images under cross-polarized illumination. In general, the *Cyclotella* blooms fall right within the biogenic

[49] Robust external (vs. internal) evidence that the couplets are true varves is provided in the "4.1.14 Validation of the LML varve chronology" section below.

component of each couplet. This distribution unequivocally demonstrates that the couplets are deposited on an annual basis, and not at random intervals[50]. Hence, the couplets can be classified as true varves.

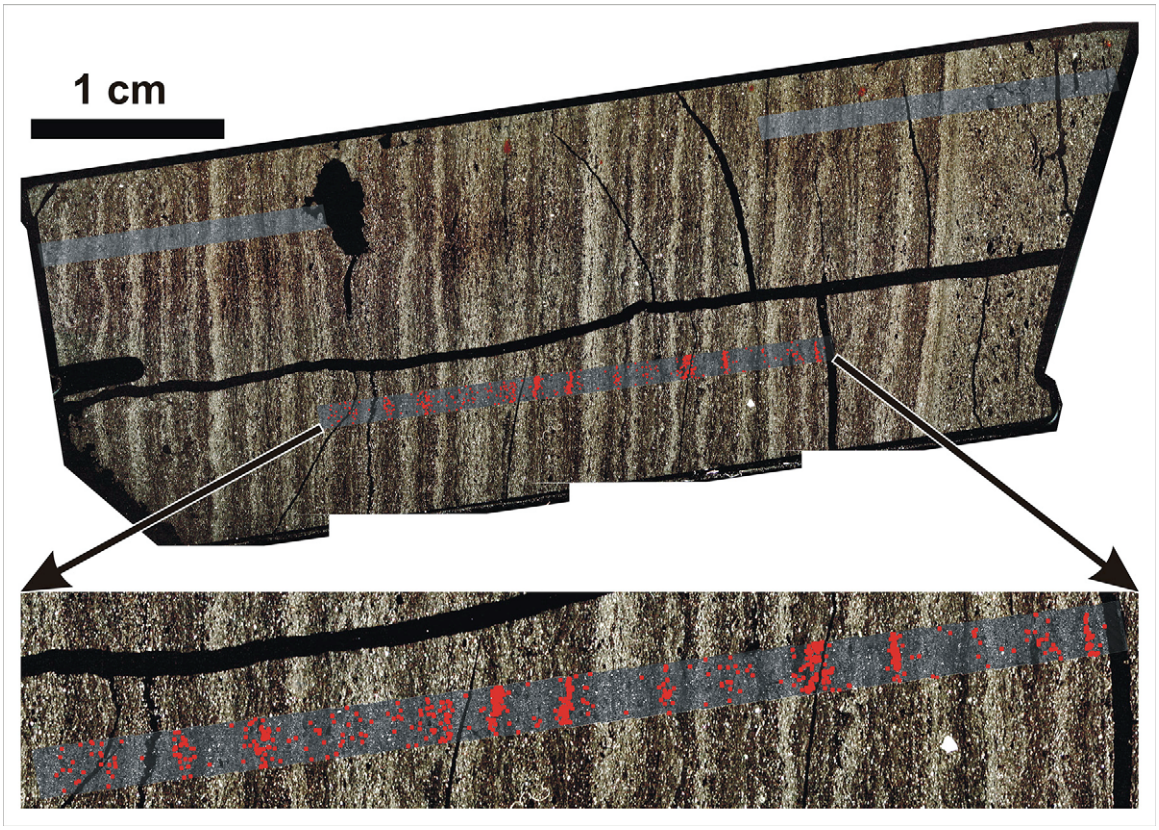

Figure 42—Figure showing the distribution of *Cyclotella* frustules that unequivocally demonstrates the LML couplets are deposited on an annual basis, and thus are true varves. This image of the Bird E-3 thin section under cross-polarized light (top/up is to the left) shows the dark/light (i.e. biogenic/siliciclastic) sedimentary couplets. The three gray strips parallel to the length of the thin section are BSEM image transect mosaics. The red dots on the middle BSEM image transect mark the locations of *Cyclotella* frustules that were mapped by hand. An expanded version of the middle BSEM image transect to show more detail is indicated by the arrows. The distribution of the *Cyclotella* blooms within the biogenic portion of each couplet unequivocally demonstrates that the couplets are true varves.

[50] An extremely important corollary of this BSEM image mapping technique is that it can also be used to provide persuasive evidence that certain laminae may, in fact, not be deposited on an annual basis. An example of this is provided in the "4.1.11.2 Zone of massive diatom blooms and siliciclastic pulses" section below when the technique is used to examine a small, anomalous zone of fibrous diatom blooms that is unique throughout the entire record.

As true annual varves, the couplets provide an exact, robust, annual chronometer for the sequence that is independent of the vagaries of radiocarbon dating, the prime tool used to date sediments of Holocene age.

4.1.9.5 Offset between varve year and calendar year

As mentioned above, the best way to define the limits of a couplet is by using the pronounced transition from siliciclastic to biogenic sedimentation following the spring flush. This transition occurs during the late spring, or approximately April-May of the calendar year. An important consequence is that the interpreted varve/sediment year is offset from the actual calendar year. For example, while calendar year 2004 runs from January through December 2004, varve year 2004 runs from April-May 2004 through April-May 2005.

4.1.9.6 A few exceptions to the accumulation of simple clastic-biogenic varves

While the majority of the laminated portion of the LML record is composed of the simple clastic-biogenic varves as described above, a few anomalous zones of sedimentation exist. In particular, over two short intervals of the record, the normal sedimentary couplets are replaced with distinct annual quadruplets (a biogenic-siliciclastic-biogenic-siliciclastic sequence). And during one short unique interval of the record, the laminated sediments appear to lose their annual significance, and several siliciclastic pulses and massive diatom blooms are deposited during single calendar years. Finally, within another anomalous zone deposited recently, the distinct varve stratigraphy breaks down, and the annual couplets become unresolvable. Each of these exceptions can

be related to a strong disruption of the normal environmental conditions, and this interpretation is backed by straight-forward physical sedimentary and/or historical evidence. Each of these exceptions is discussed in detail in the "4.1.11 Anomalous zones within the varve record" section below.

4.1.10 Construction of the LML varve chronology

A master chronology of the LML varves extending from AD 1998 back to AD 1060 was constructed and revised in several stages. Several small gaps exist in the record, but their existence is obvious and well-controlled. Included in the chronology are the occasional, anomalous graded beds with organic detritus mentioned earlier.

4.1.10.1 Initial varve chronology

An initial chronology was completed in early 2001. It was based strictly on petrographic microscope observations of the thin sections produced from drives 2 and 3 of piston core LML-23NOV1996-LIV-1[51]. The varves were split from one another based on their appearance under cross-polarized illumination, and markups recorded as paths within the Adobe Photoshop PSD file imagery. The chronology was not extended to the deepest varves (Bird L, M, and N series thin sections) as the varves from that portion of the record are generally thinner, and in some zones slightly more diffuse (see "4.1.9.1 General composition and structure of the sedimentary couplets" section above).

When the initial chronology was constructed, a gap of unknown size existed in the varve record. The uppermost piston core sediments (Bird A series) did not overlap with

any of the existing freeze cores despite repeated attempts to bridge the gap. Thus, the initial varve chronology could not be connected to the active sediment/water interface, and was left floating.

Attempts to anchor the chronology were made using five AMS ^{14}C dates, and the horizon related to European settlement from around AD 1630. The location of the European settlement horizon was inferred from preliminary pollen assemblage analysis that tightly bracketed it to a 30 cm range in the stratigraphy (this analysis was performed by T. Parshall, see the "4.1.14.4 Preliminary pollen age data vs. the varve chronology" section below for more details). Unfortunately, the ^{14}C and pollen age data did not agree—the ^{14}C results suggested the inferred pollen age was too young by about 150 calendar years. Given that four of the five radiocarbon dates showed good internal correspondence, they were adopted over the pollen data as the working model for anchoring the floating chronology at that time.

4.1.10.2 Revised varve chronology

The chronology underwent a major reexamination in late 2001 and early 2002 as high resolution, grayscale imagery of the 2 mm thick, X-ray thin slabs became available, and more importantly, the physical gap in the record was finally patched with an oversized freeze core.

In a side-by-side comparison between the X-ray thin slab and thin section imagery, it was noted that the former provided superior image quality. This was

[51] Drive 2 was the source for the Bird A-G series of impregnated blocks and thin sections. Drive 3 was the source for the Bird H-N series. See Figure 39 above for the locations of individual thin sections.

especially true for lowest 75 cm of the varves which are generally thinner, and in some zones slightly more diffuse. The X-ray thin slabs offered the additional advantage of providing continuous coverage over the length of an impregnated sediment subsample block whereas the same coverage was provided by up to three different thin sections. For these reasons, the X-ray imagery was used as the base for the chronology despite the fact that a thin section-based version already existed.

As the revised chronology was built, a laborious varve-by-varve cross-check against the thin section imagery was performed to identify and account for any stratigraphic defects present in the sequence, and produce palinspastic reconstructions of the X-ray imagery. This task was greatly simplified by the perpendicular orientation of the samples as explained in the "4.1.4 Completeness and quality of the sedimentary record" section, and Figures 31-32 above. Markups were recorded as paths within the Adobe Photoshop PSD file imagery. Appendix A contains both the X-ray and thin-section imagery for the "Bird" series of impregnations.

The most important element of the revised chronology was the retrieval of freeze core LML-19JAN2002-FRZ-1. That oversized freeze core bridged the gap from the uppermost piston core sediments (i.e. Bird A series) up to freeze core LML-18OCT1998-FRZ-1 which captured the active sediment/water interface in 1998. For the first time, the chronology was physically linked to the active sediment/water interface, and the true thickness of the entire laminated sequence became known. Using these two freeze cores, the varve chronology was extended up to the active sediment/water interface in 1998. Markups were recorded as paths within Adobe Photoshop PSD file imagery of these cores

Figure 43—Part 1 of 4 of the LML master varve chronology. This figure shows the overlap between freeze cores LML-18OCT1998-FRZ-1 (left) and LML-19JAN2002-FRZ-1 (right). The 4-5 cm of sediment-free frozen water at the top of the first freeze core indicate that it captured the active sediment/water interface at the bottom of the lake when it was retrieved (i.e. October 1998).

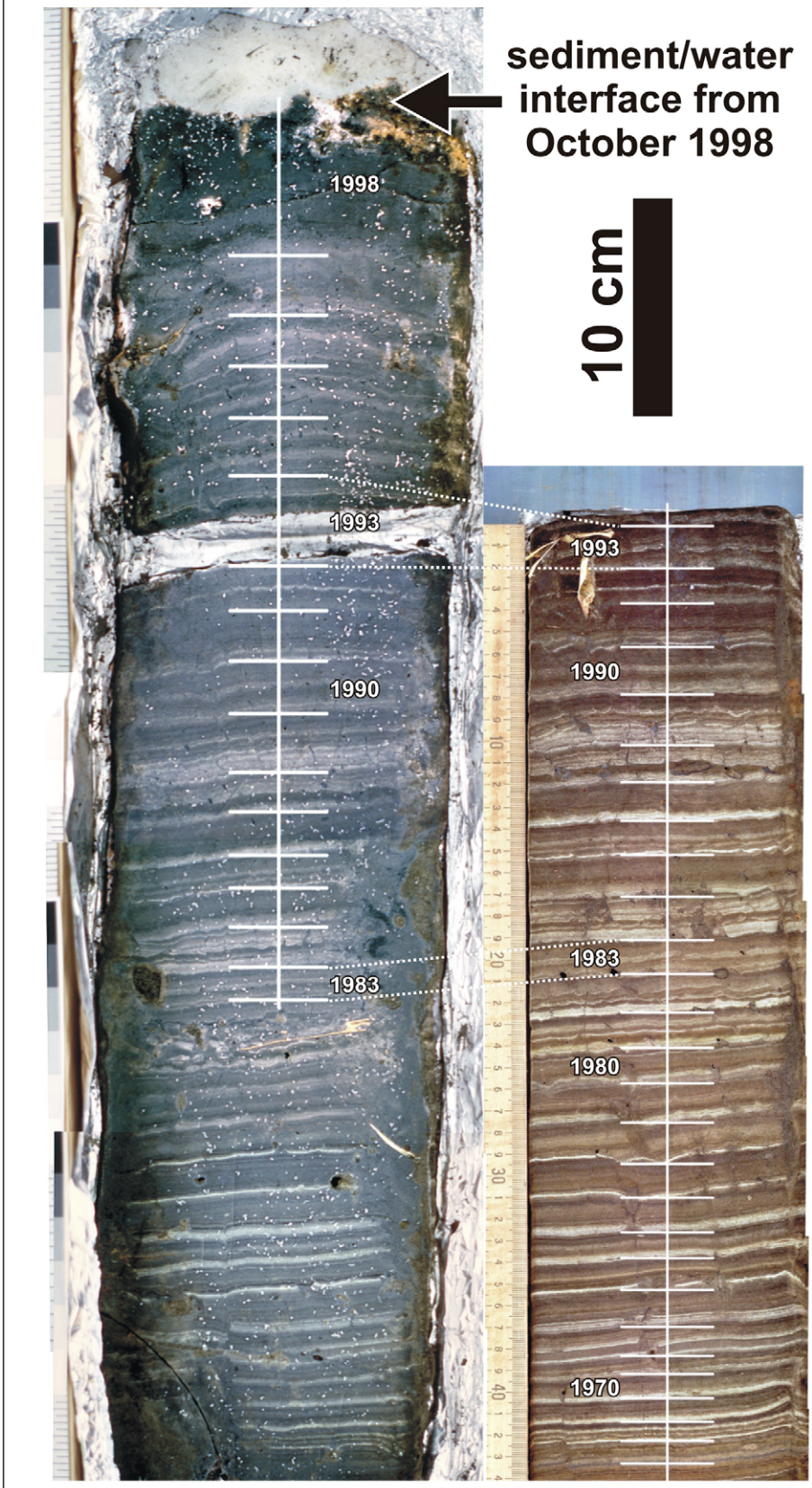
sediment/water
interface from
October 1998
10 cm
1998
1993
1990
1983
1993
1990
1983
1980
1970

Figure 44—Part 2 of 4 of the LML master varve chronology. This figure shows the very base of freeze core LML-18OCT1998-FRZ-1 (left) and the basal 66 cm of freeze core LML-19JAN2002-FRZ-1 (right). An arrow indicates the highest stratigraphic level reached by the piston core sediments (Bird A series impregnation), and thus shows the significant overlap between the cores. The blackish zone running from 1896-1930, inclusive, is discussed in the "4.1.11.3 Black/dark zone at base of sapropelic layer" section below.

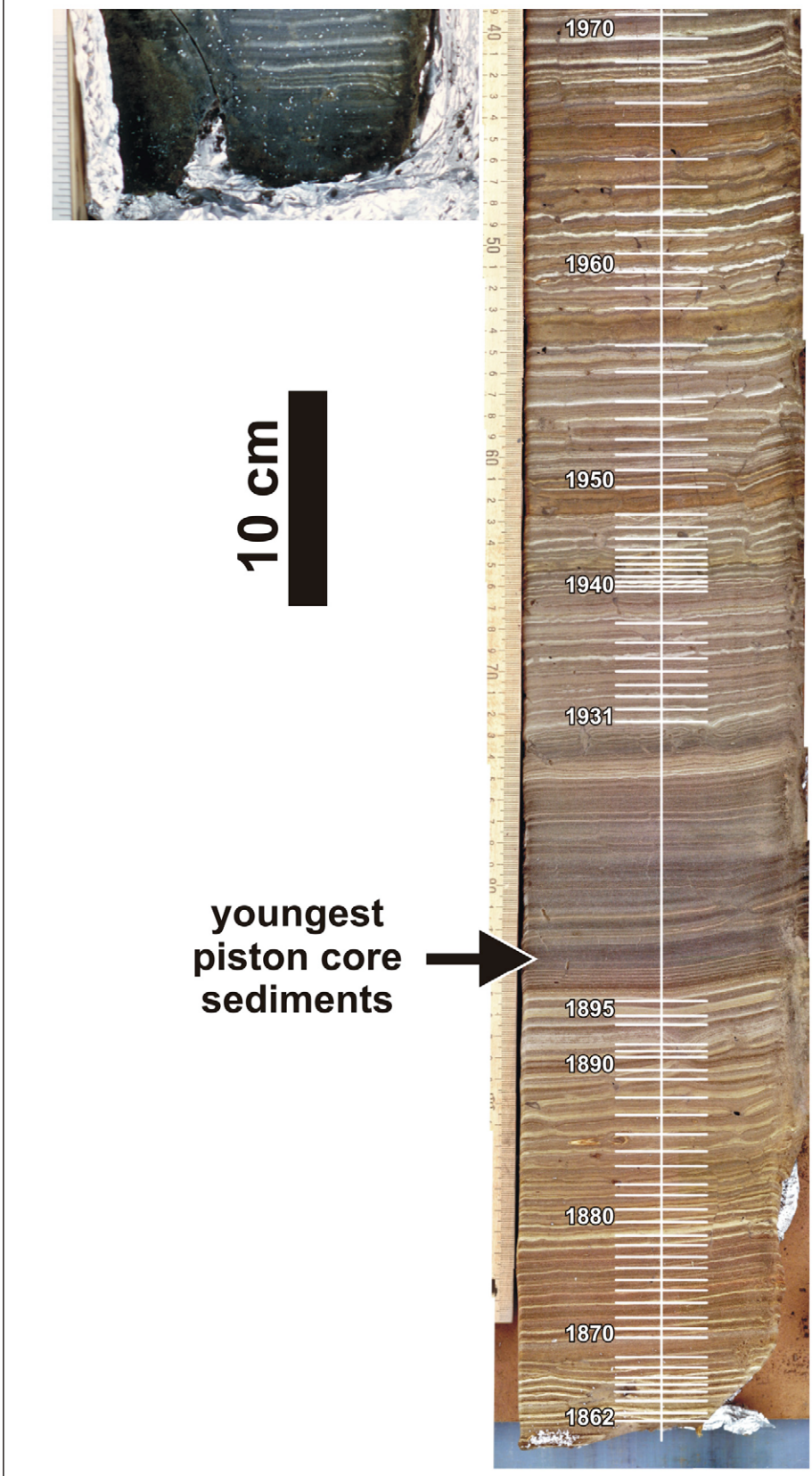
1970
1960
1950
1940
1931
10 cm
youngest
piston core
sediments
1895
1890
1880
1870
1862

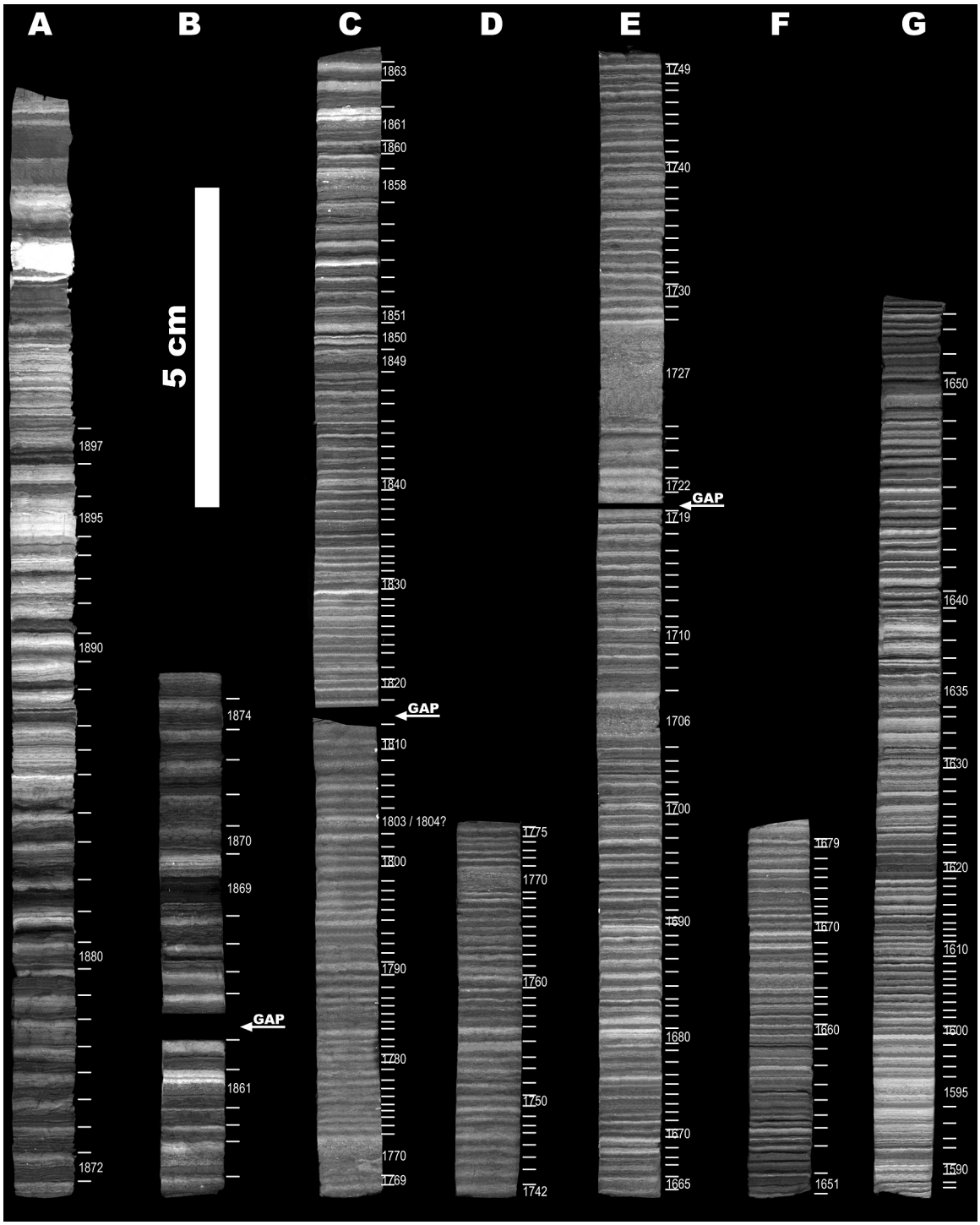

Figure 45—Part 3 of 4 of the LML master varve chronology. This figure shows the palinspastically reconstructed X-ray thin slab imagery of the Bird A (left) through Bird G (right) series impregnations. The larger occasional, anomalous graded beds with organic detritus are clearly visible within the normal varved stratigraphy at this scale. Several small gaps are visible in the sequence, and were identified by a detailed cross-examination between the orthogonally cut thin section and X-ray imagery.

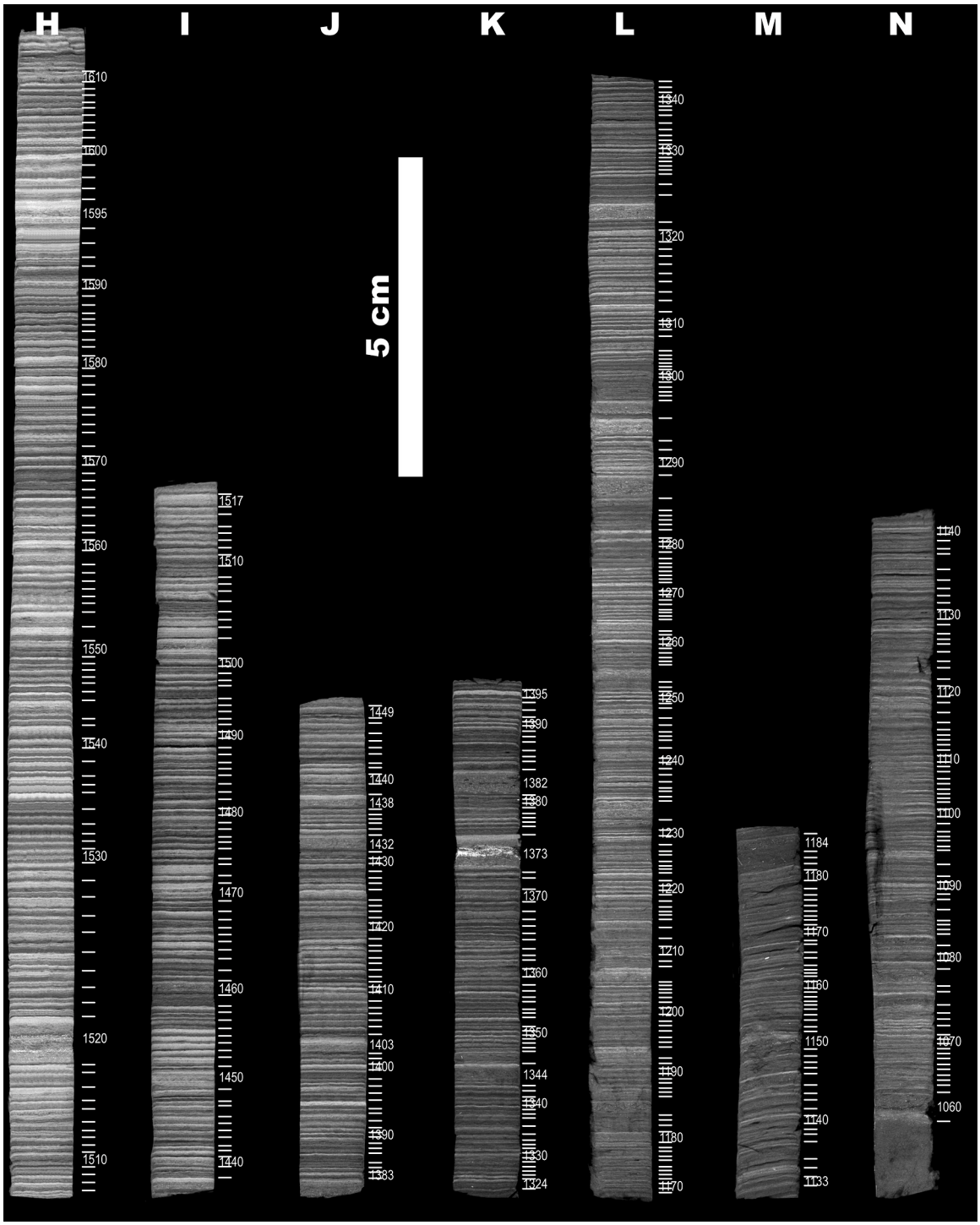

Figure 46—Part 4 of 4 of the LML master varve chronology. This figure shows the palinspastically reconstructed X-ray thin slab imagery of the Bird H (left) through Bird N (right) series impregnations. The larger occasional, anomalous graded beds with organic detritus are clearly visible within the normal varved stratigraphy at this scale.

as was done for the X-ray based portion. The complete varve chronology is illustrated in the Figures 43-46.

4.1.11 Anomalous zones within the varve record

There are three zones in the varve record where the composition and/or structure of the couplets is distinctly different from the majority of the rest of the record. In each case, it appears that the exceptions can be related to a strong disruption of the normal environmental conditions, and this interpretation is backed by straight-forward physical sedimentary and/or historical evidence. These three sections are inventoried below.

4.1.11.1 Zones of quadruplet architecture varves

As mentioned earlier, the varves from about 1.25-2.5 m depth are generally simple, siliciclastic-biogenic couplets. Occasionally, a varve with an extra siliciclastic layer is encountered, but these occur with no regular frequency. However, at two spots within the chronology, the varves appear to take on a quadruplet architecture that repeats year after year for a period of one to two decades. The first occurrence is within the Bird L series sample block impregnation (varves from AD 1311-1324[52]), and the second occurrence is within the Bird H series sample block impregnation (varves from AD 1521-1539). The quadruplet architecture is less pronounced in the Bird L series sediments, but quite obvious in the Bird H series sediments. These quadruplet varves are composed of a biogenic-siliciclastic-biogenic-siliciclastic sequence. The distinguishing and conspicuous

Figure 47—Quadruplet-style varves from thin section Bird H-1 as observed under cross-polarized light. The whole Bird H-1 thin section (top/up direction to left) is presented at the bottom of the figure with the section of interest marked by a white rectangle. An expanded view of the section within the white rectangle is presented at the top of the figure. The black scale bar at the lower right of both images indicates 1 cm. The thin, horizontal, grayscale strips are high resolution BSEM image mosaic transects. The red dots on the upper transect indicate the location of *Cyclotella* diatom frustules. Quadruplet varves are divided from one another by the vertical tick marks along the horizontal, white line towards the top of the expanded view image. Pictured are varves from AD 1521 (right) through AD 1528 (left) which are immediately preceded by a thick graded bed with organic detritus. Each quadruplet varve is composed of a biogenic-siliciclastic-biogenic-siliciclastic sequence. Importantly, the first siliciclastic layer deposited in each quadruplet varve is thin, and the second siliciclastic layer is thick.

[52] This range may actually extend back to AD 1298 as similar quadruplet style varves appear in the varves dated to AD 1289-1292.

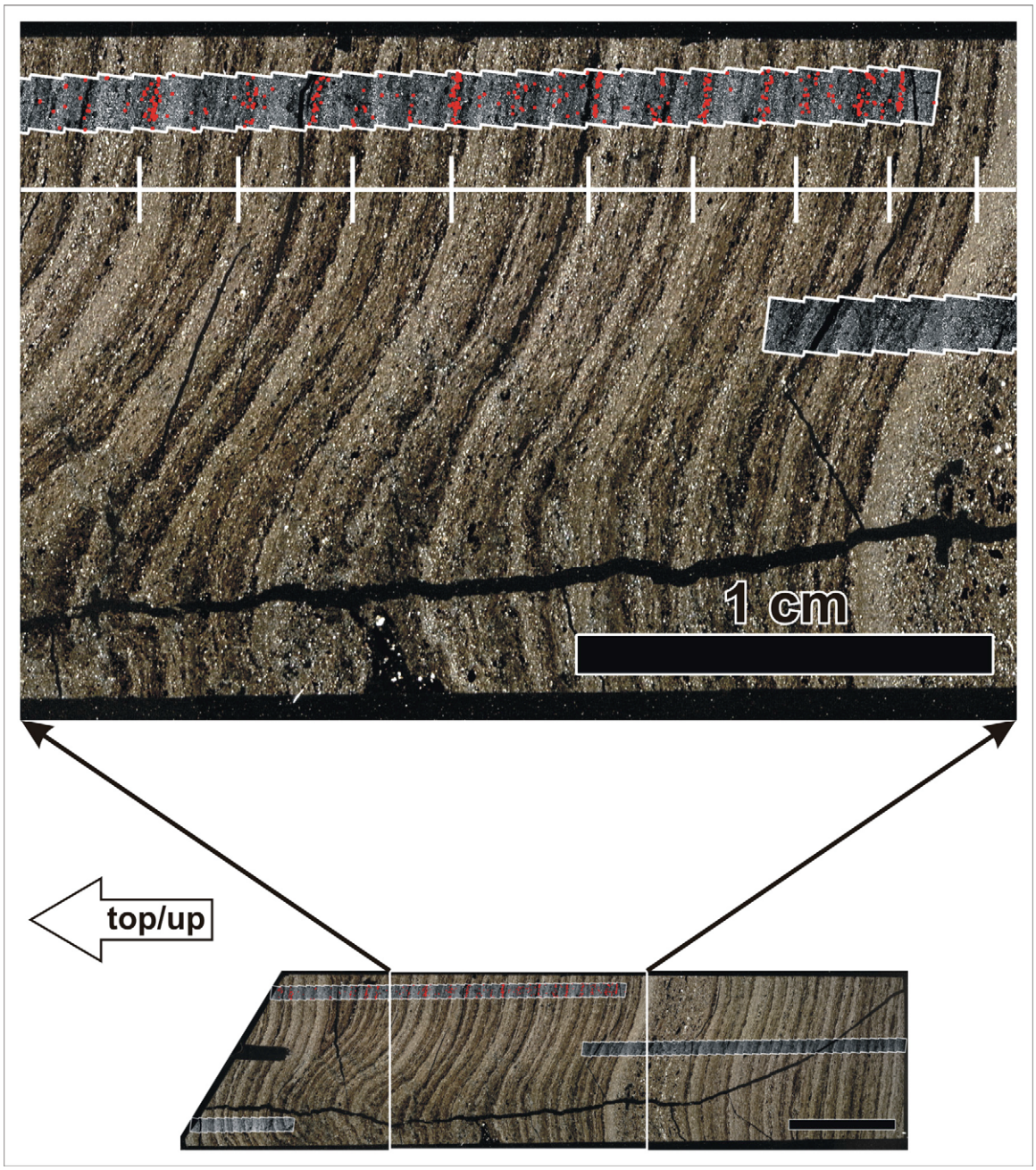
1 cm
top/up

factor which makes these quadruplets varves stand out is that within each varve the first siliciclastic layer is thin, and the second one is thicker (Figure 47).

The distribution of *Cyclotella* frustules was hand mapped on a BSEM image mosaic transect covering one of these zones of quadruplet varve (Figure 47). It was expected that the annual *Cyclotella* bloom would fall within just one of the two biogenic layers of each quadruplet thus confirming the annual nature of the quadruplet varves. However, *Cyclotella* frustules were noted in both biogenic components of the quadruplet varves.

A discussion of the possible significance and origin of these quadruplet architecture varves, as well as a justification for their annual origin, is presented in the "5.5 Significance of the three anomalous zones in the LML varve record" section of Chapter 5.

4.1.11.2 Zone of massive diatom blooms and siliciclastic pulses

The second anomalous zone within the varve record is a zone of massive diatom blooms separated by siliciclastic pulses. This zone includes the varves deposited from AD 1636-1659 (Bird F and G series impregnations). On a freshly split sediment core, the lighter colored diatom blooms have a gelatinous appearance to the naked eye. Under cross-polarized light at higher magnifications, they take on a fibrous appearance indicating that they are composed of elongate diatoms. High resolution BSEM imagery of individual blooms demonstrates the elongate nature of the diatoms (Figure 48 upper part), and from cleaned, Naphrax-mounted samples a tentative identification of the

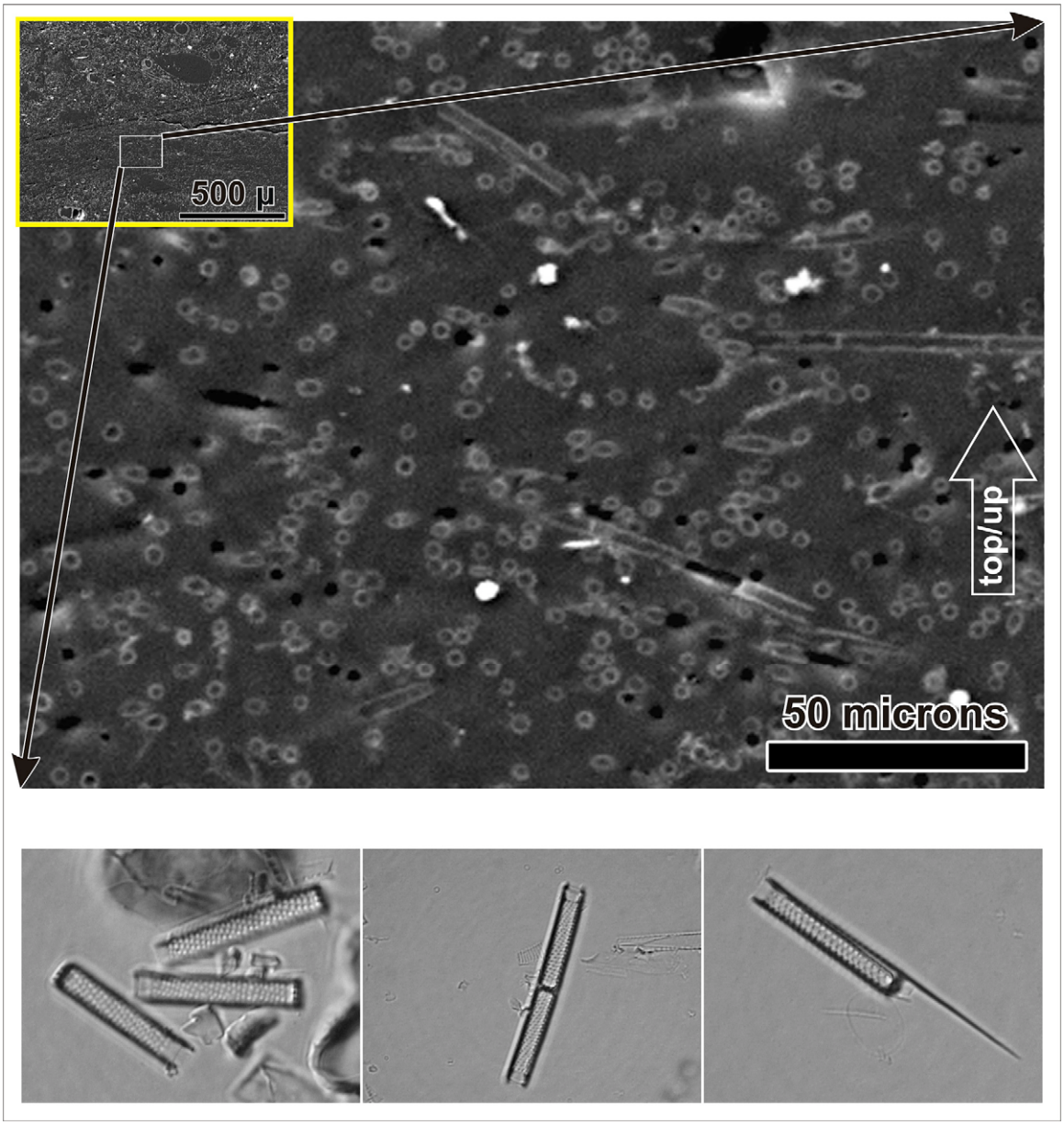

Figure 48—BSEM imagery of a massive diatom bloom (upper part) and optical microscope imagery of individual diatoms (lower part). In the upper part of this figure, the yellow-bounded inset image is a single BSEM frame from thin section Bird G-3 captured at 2560x1920 pixel resolution. Note that the actual location of the capture is indicated by a similar yellow rectangle in the next figure (Figure 49). A white rectangle within the inset image indicates the section of interest that is expanded to form the main image in the upper part of this figure. Scale bars in microns are included in the lower right corner for both images. The expanded image shows a massive, monospecific bloom of elongate, tube-like diatoms. The many small circles and ovals are cross sections through these diatoms (i.e. the length of the diatom frustule is not parallel to the plane of section, but extends out of the page towards the viewer). The lower part of this figure shows three optical microscope images of individual diatom frustules from one of these blooms after being cleaned and mounted in Naphrax.

diatoms as the genus *Aulacoseira* (Figure 48 lower part) is suggested based on their general morphology.

During the deposition of these varves, the normal annual sedimentary cycle responsible for depositing the simple, biogenic-siliciclastic couplets appears to break down. Evidence for the breakdown comes from the distribution of *Cyclotella* frustules which were manually mapped on the high resolution BSEM image mosaic transects from the Bird G-2 and G-3 thin sections (Figure 49). A few discrete pulses of *Cyclotella* frustules are visible, but otherwise the frustules are somewhat randomly distributed throughout the laminae. Importantly, they do not occur only within the biogenic components, but are also found within the siliciclastic portion.

The distribution of the few discrete *Cyclotella* pulses and some prominent/less prominent siliciclastic layers in this anomalous zone suggests each varve contains two, and occasionally three, siliciclastic laminae. Where this limited visual guidance is available, the varves are divided up appropriately. Where no such guidance is available, for example, the expanded view portion of Figure 49, it is assumed each varve contains two siliciclastic laminae.

A discussion of the possible significance and origin of this zone of massive diatom blooms and siliciclastic pulses is presented in the "5.5 Significance of the three anomalous zones in the LML varve record" section of Chapter 5.

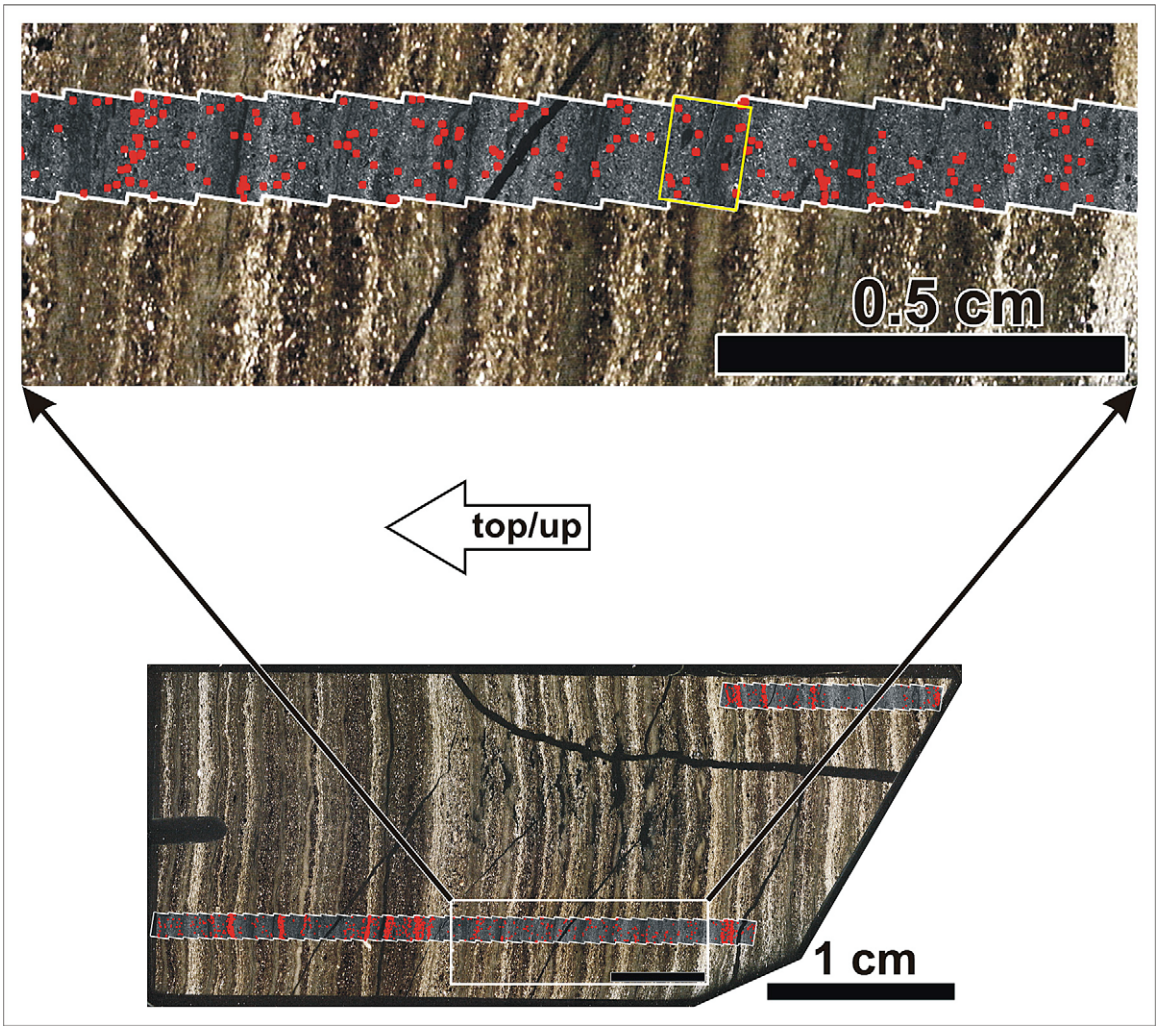

Figure 49—Cross-polarized light view of thin section Bird G-3 showing massive diatom blooms separated by siliciclastic pulses. The whole Bird G-3 thin section (top/up direction to left) is presented at the bottom of the figure with the section of interest marked by a white rectangle. An expanded view of the section within the white rectangle is presented at the top of the figure. The yellow rectangle there marks the single BSEM frame capture examined in Figure 48 above. The black scale bar at the lower right of each image indicates the appropriate scale for each image. The massive diatom blooms are best seen in the upper image as the homogeneous greenish gray zones separated by the siliciclastic layers. The thin, horizontal, grayscale strips are high resolution BSEM image mosaic transects. The red dots on these transects indicate the location of *Cyclotella* diatom frustules. Some discrete pulses of *Cyclotella* frustules are seen in the lower image. However, throughout the rest of this anomalous zone (thin sections Bird G-2 and F-1 included), their distribution is somewhat random including within the siliciclastic laminae as seen in the upper image of this figure.

4.1.11.3 Black/dark zone at base of sapropelic layer

The third anomalous zone in the varve record is a 13 cm thick black/dark zone that forms the base of the soft, sapropelic, gas-charged zone described in the "4.1.3.1 Textural description" section above (also see Figure 29 and Figure 34). This anomalous zone was completely captured by oversized freeze core LML-19JAN2002-FRZ-1, and runs from 72-85 cm depth in that core (Figure 44). The very uppermost LML-23NOV1996-LIV-1 piston core sediments also captured a few centimeters of the base of the zone, and they are visible in the Bird A-3 thin section (Figure 50).

During deposition of this interval, the normal, annual sedimentary cycle appears to break down, and the distinct biogenic-siliciclastic couplets which both precede and follow the interval become unresolvable. The varve chronology brackets this interval to AD 1896-1930. The sediment in this zone has properties unique to the entire record. For example, whereas the other stratigraphy oxidizes and changes color after being freely exposed to the atmosphere for several hours, this anomalous zone maintains a dark gray to black color. Additionally, the sediment presents a curious characteristic when an attempt is made to impregnate it with resin after freeze drying—the material splits, and clumps together in blocks. This characteristic was noted in both the piston core and freeze core sediments, and is illustrated in Figure 50 below.

A discussion of the possible significance and origin of this black/dark anomalous zone is presented in the "5.5 Significance of the three anomalous zones in the LML varve record" section of Chapter 5.

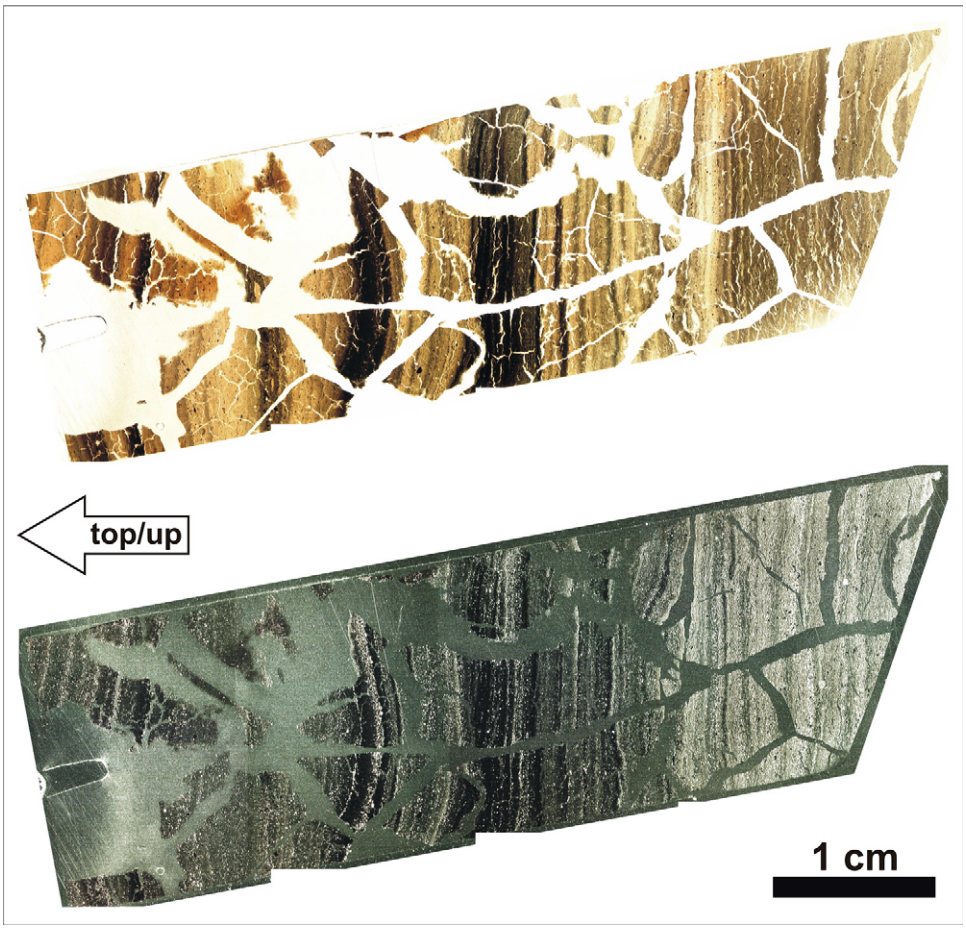

Figure 50—Plane-polarized (upper) and cross-polarized (lower) light images of the Bird A-3 thin section. This thin section, the stratigraphically highest sample available from piston core LML-23NOV1996-LIV-1, captured a few centimeters at the base of the anomalous black/dark zone described in the text. As seen in this figure, the sediment in this anomalous zone displays the curious characteristic of splitting and clumping into blocks when freeze-dried and impregnated with resin.

4.1.12 Graded beds in the LML varve chronology

The existence of a series of occasional, anomalous graded beds within the normal varved stratigraphy has been mentioned several times. The thickness of these graded beds is quite variable. The smaller graded beds generally have a thickness about the same magnitude as the surrounding stratigraphy, but the larger ones can be many times thicker. A more thorough analysis of thickness is presented in Chapter 5.

Based on visual examination of the petrographic thin sections and X-ray imagery, a complete list of the graded beds has been prepared, and is listed in Table 9. In general, quite a few of the graded beds from the historic period were deposited during years in which known historical hurricanes have struck the New England area. This relationship is fully explored in Chapter 5.

Table 9—List of graded beds found within the stratigraphy of the LML varve record. The "Bird series" column identifies the Bird series impregnated sample block and thin section in which each graded bed is found. The most recent four graded beds listed here (i.e. 1934, 1938, 1954, and 1955) are not part of the Bird series impregnations. Instead, they come from polished, impregnated blocks from freeze core LML-19JAN2002-FRZ-1.

Year AD	***Bird series***	***Year AD***	***Bird series***	***Year AD***	***Bird series***
1955	n/a	1552	H-2	1254	L-2
1954	n/a	1543	H-2	1247	L-2
1938	n/a	1520	H-1	1246	L-2
1934	n/a	1501	I-2	1241	L-2
1895	A-2	1470	I-1	1232	L-1/L-2
1869	B-1/B-2	1460	I-1	1231	L-1/L-2
1861	C-3/B-1	1450	I-1	1213	L-1
1858	C-3/B-1	1440	J-2/I-1	1207	L-1
1857	C-3	1438	J-2/I-1	1193	L-1
1850	C-3	1432	J-2	1184	M-1/L-1
1849	C-3	1425	J-2	1150	M-1
1804	C-1	1403	J-1	1145	M-1
1770	D-1/C-1	1382	K-2/J-1	1136	N-2/M-1
1727	E-2/E-3	1373	K-2	1093	N-1
1706	E-2	1344	K-1	1086	N-1
1649	G-3	1322	L-3	1082	N-1
1635	G-2	1307	L-3	1081	N-1
1626	G-2	1294	L-2/L-3	1078	N-1
1610	H-3/G-1	1293	L-2/L-3	1076	N-1
1595	H-3/G-1	1288	L-2	1060	N-1
1559	H-2	1263	L-2		

4.1.13 The LML varve thickness record

Based on the X-ray imagery of the piston core sediments, and regular core photography for the two freeze cores, the thickness of each and every varve was

calculated[53] in order to construct a varve thickness record. The complete time series for those thickness values are presented in Figure 51 below. Given the nature of the record, it is convenient to discuss it in two sections; the first running from AD 1060 up to 1865, and the second from AD 1865 up to the present.

4.1.13.1 Thickness from AD 1060-1865

In general, from the beginning of the record (AD 1060) up to about AD 1865, the varves range from 1-2.5 mm thick. A subtle sigmoidal trend in the thickness values can be identified, and details are presented in the next chapter when this varve thickness record is analyzed in detail. Many smaller spikes in thickness are present in the record up to about AD 1500. After that the spikes become fewer, but more prominent. These spikes in thickness are almost exclusively related to varves which contain the occasional, anomalous graded beds which exist in the stratigraphy.

Two zones of increased thickness are also visible, and both are preceded by spikes in thickness. The first zone runs from about AD 1520-1540, and corresponds with one of the anomalous zones of quadruplet varves discussed in the "4.1.11 Anomalous zones within the varve record" section above. The second zone runs from about AD 1635-1660, and corresponds with the anomalous zone of massive diatom blooms separated by

[53] As mentioned earlier in the "4.1.10.2 Revised varve chronology" section, varve boundary markups were recorded on path layers in the Adobe Photoshop imagery. The author discovered that when these paths are exported from Adobe Photoshop ("File→Export→Paths to Illustrator" function), the result is a PostScript-like text file that contains the exact coordinates of the varve boundaries given in "points" units (72 points/inch). With some simple manual parsing, and a trivial conversion from points to metric units, the exact thicknesses for each and every varve are quickly calculated. Later, Francus et al. (2002) used this information to construct a semi-automated utility to simplify the manual parsing step.

siliciclastic pulses also discussed in the "4.1.11 Anomalous zones within the varve record" section above.

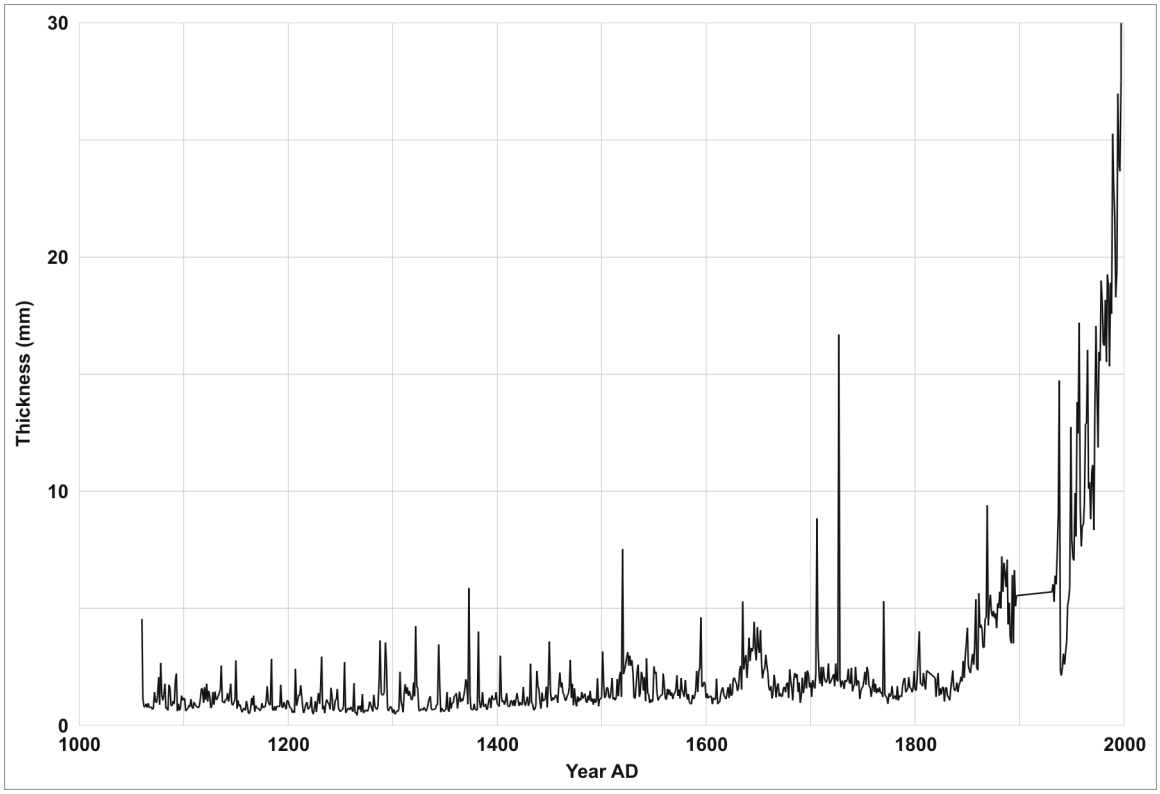

Figure 51—Thickness record for the LML varve chronology. The thickness value for the 1998 varve (66 mm), the last varve in the record, has been truncated because of the chosen vertical scale in this plot.

4.1.13.2 Thickness from AD 1865 to present

The LML varves shows a massive, exponential increase in thickness beginning around AD 1865 and heading up to the present. Thicknesses for individual varves are not available for the period from AD 1896-1930 as this corresponds with the anomalous, 13 cm thick black/dark zone in which the biogenic-siliciclastic couplets become unresolvable (see "4.1.11 Anomalous zones within the varve record" section above). However, assuming a consistent rate of sedimentation during this interval, each varve

should be about 3.7 mm thick (130 mm ÷ 35 varves) which seems appropriate for that part of the chronology..

The increased thickness of the varves in this section is partially related to less compaction, but more importantly related to a significant hydrographic change in the lake system (construction of the dam at "The Partings"), and massive changes in the watershed related to increasing population. A more detailed discussion about this portion of the record is presented in the next chapter when this varve thickness record is analyzed in detail.

4.1.14 Validation of the LML varve chronology

Multiple lines of evidence provide a strong verification of the historic portion of the LML varve chronology, and these are presented below. The same degree of validation is simply not possible for the prehistoric portion of the record as the only available check is that of ^{14}C dating.

4.1.14.1 ^{14}C age results vs. the varve chronology

AMS ^{14}C dates were obtained on 16 macrofossils from the LML stratigraphy. Calibrated, calendar year, 2 sigma age ranges for the results are presented in Table 10 below as well as graphically in Figure 52. Given that drives 2 and 3 of piston core LML-23NOV1996-LIV-1 were used as the basis for the varve chronology because of their completeness, the multiple samples from the other LML cores are referenced according to their stratigraphic equivalence in that piston core. The varve chronology determined age for each of the samples is provided as well.

Table 10—Calibrated results of ^{14}C age analyses from the LML. Samples from multiple cores were referenced to their equivalent depth in drives 2 and 3 of core LML-24NOV1996-LIV-1 given that those drives serve as the basis for the varve chronology because of their completeness. These equivalent depths are presented in brackets beneath the actual core drive and depth from which the samples were retrieved. The varve chronology determined ages for each of those depths is also specified. The four del ^{13}C values of –25 within parentheses represent estimated values. The calibrated, calendar year, 2 sigma age ranges with relative probabilities were obtained from the Calib v5.01 computer program (Stuiver and Reimer, 1993).

Lab Code + Core + Drive and Depth + [LIV-1 Strat. Equiv.] Varve chronology age	***Material***	***del ^{13}C***	***Fraction Modern***	***^{14}C Age***	***Calibrated 2s age ranges with relative probability***
CAMS73198 LML-23NOV1996-LIV-1 Drive 2, 51.6 cm [Drive 2, 51.6 cm] AD 1730	leaf	(-25)	0.9627 ± 0.0046	310 ± 40	AD 1472-1653 @ 1.000
CAMS73199 LML-23NOV1996-LIV-1 Drive 2, 60.5 cm [Drive 2, 60.5 cm] AD 1694	leaf	(-25)	0.9746 ± 0.0046	210 ± 40	AD 1530-1537 @ 0.005 AD 1635-1696 @ 0.308 AD 1725-1814 @ 0.498 AD 1835-1847 @ 0.008 AD 1850-1877 @ 0.021 AD 1917-1952* @ 0.160
UCI7514 LML-01MAY2002-HMR-1 53.3 cm [Drive 2, 66.8 cm] AD 1661	leaf	-25.9	0.9519 ± 0.0026	395 ± 25	AD 1440-1521 @ 0.835 AD 1578-1581 @ 0.006 AD 1591-1620 @ 0.159
UCI7529 LML-01MAY2002-HMR-1 63.2 cm [Drive 2, 76.1 cm] AD 1630	leaf	-29.3	0.9620 ± 0.0022	310 ± 20	AD 1495-1506 @ 0.023 AD 1511-1601 @ 0.747 AD 1616-1646 @ 0.230
CAMS73200 LML-24NOV1996-LIV-2 Drive 1, 59.75 cm [Drive 2, 81.0 cm] AD 1600	leaf	(-25)	0.9423 ± 0.0045	480 ± 40	AD 1327-1342 @ 0.025 AD 1394-1475 @ 0.975
UCI7534 LML-23NOV1996-LIV-1 Drive 3, 8.5 cm [Drive 3, 8.5 cm] AD 1567	beetle	-27.2	0.9660 ± 0.0032	280 ± 30	AD 1497-1504 @ 0.010 AD 1512-1601 @ 0.563 AD 1616-1666 @ 0.404 AD 1784-1795 @ 0.023
UCI7515 LML-01MAY2002-HMR-3 86.6 cm [Drive 3, 19.9 cm] AD 1504	leaf fragments	-26.0	0.9289 ± 0.0024	590 ± 25	AD 1301-1367 @ 0.723 AD 1382-1411 @ 0.277
UCI7516 LML-01MAY2002-HMR-1 80.9 cm [Drive 3, 20.2 cm] AD 1502	pine needle	-25.0	0.9243 ± 0.0022	630 ± 20	AD 1290-1326 @ 0.399 AD 1343-1394 @ 0.601

CAMS73201 LML-24NOV1996-LIV-2 Drive 1, 80.25 cm [Drive 3, 25.9 cm] AD 1458	leaf	(-25)	0.9162 ± 0.0035	700 ± 40	AD 1229-1231 @ 0.004 AD 1240-1247 @ 0.009 AD 1251-1321 @ 0.716 AD 1349-1391 @ 0.271
UCI7530 LML-01MAY2002-HMR-3 97.75 cm [Drive 3, 34.7 cm] AD 1386	two twigs	-31.2	0.9357 ± 0.0021	535 ± 20	AD 1326-1343 @ 0.114 AD 1394-1433 @ 0.886
UCI7532 LML-23NOV1996-LIV-1 Drive 3, 35.2 cm [Drive 3, 35.2 cm] AD 1383	stick	-32.0	0.9265 ± 0.0021	615 ± 20	AD 1296-1332 @ 0.392 AD 1337-1398 @ 0.608
UCI7533 LML-24NOV1996-LIV-2 Drive 1, 89 cm [Drive 3, 35.2 cm] AD 1383	leaf	-31.1	0.9299 ± 0.0021	585 ± 20	AD 1307-1363 @ 0.709 AD 1385-1410 @ 0.291
UCI7528 LML-01MAY2002-HMR-2 130.5 cm [Drive 3, 42.3 cm] AD 1322	mixed organic fragments	-27.8	0.8854 ± 0.0020	975 ± 20	AD 1017-1052 @ 0.510 AD 1081-1128 @ 0.377 AD 1135-1152 @ 0.113
AA23999 LML-24NOV1996-LIV-2 Drive 2, 38 cm [Drive 3, 54.3 cm] AD 1210	wood	-30.4	0.8833 ± 0.0049	995 ± 45	AD 906-911 @ 0.006 AD 971-1159 @ 0.994
UCI7531 LML-01MAY2002-HMR-3 126.9 cm [Drive 3, 69.5 cm] AD 1074	large twig	-31.6	0.8655 ± 0.0020	1160 ± 20	AD 779-792 @ 0.058 AD 803-900 @ 0.694 AD 917-964 @ 0.247
AA24000 LML-24NOV1996-LIV-2 Drive 11, 54 cm [~12.1 m depth from extrapolation]	macros	-23.2	0.2428 ± 0.0068	11370 ± 225	BC 11732-10938 @ 1.000

Figure 52 is a graphic summary of the above data. It plots the calibrated, calendar year, 2 sigma age range results for each ^{14}C sample vs. the varve chronology determined age for the sample based on its stratigraphic position. Ideally, the results should fall along the 1:1 line between the two axes. Instead, several of the calibrated age ranges plot above that line which suggest those ^{14}C dates are systematically too old, perhaps reworked. Nonetheless, that the samples parallel the 1:1 line provides strong external evidence that what we have interpreted and counted as varves are, in fact, true varves.

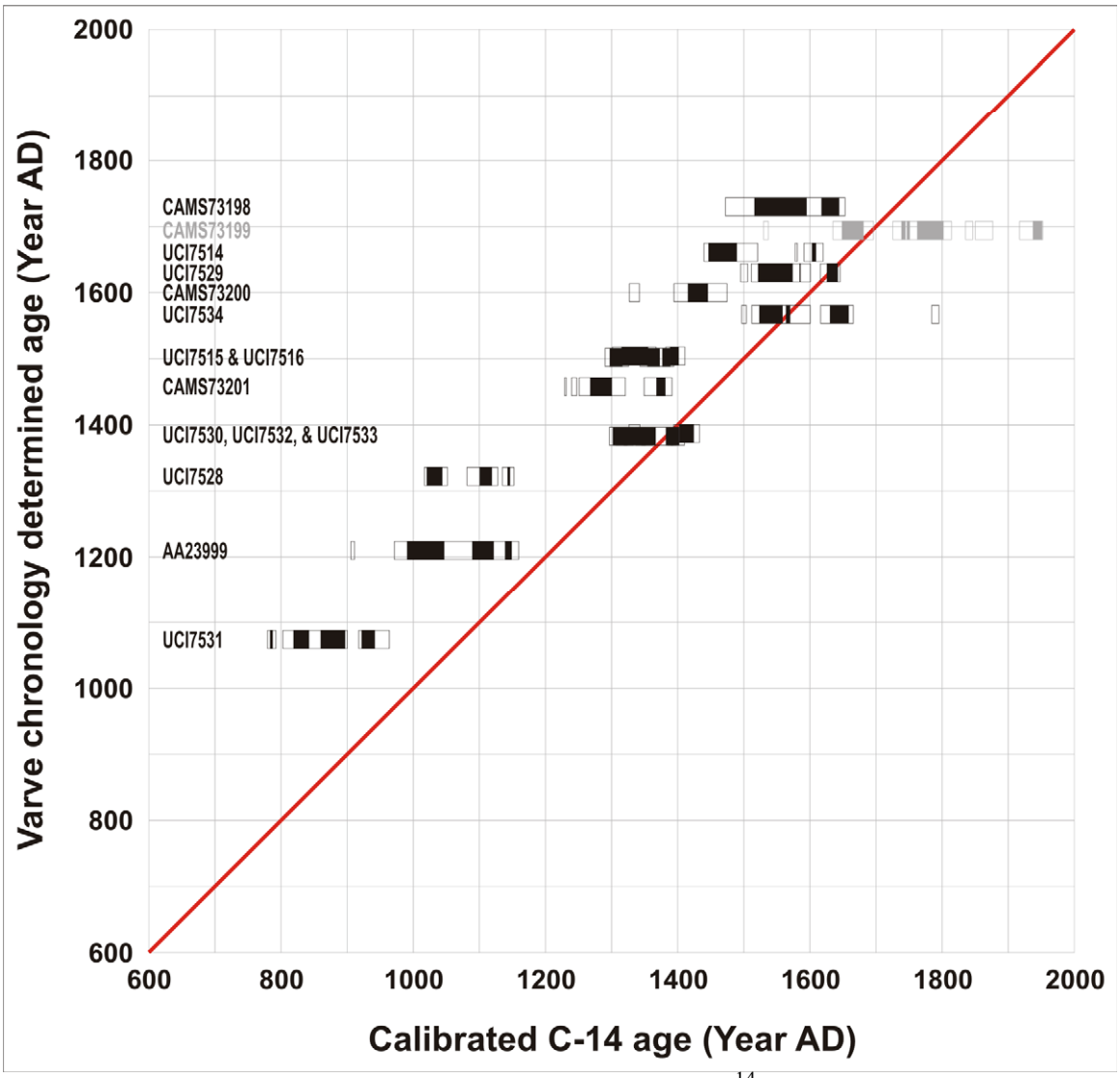

Figure 52—Plot of calibrated, calendar year age ranges for ^{14}C samples from LML versus their varve chronology determined ages. The block plots indicate the calibrated, calendar year, 1 sigma (black-filled boxes) and 2 sigma (white-filled boxes) age ranges for each ^{14}C sample as determined by the Calib v5.01 computer program (Stuiver and Reimer, 1993). Lab code labels to identify the sample for each of the block plots are provided at the left edge of the graph. Note that in two cases, multiple samples fall at essentially the same stratigraphic level (i.e. same varve age), so their block plots overlap significantly. Results for the CAMS73199 sample are illustrated in gray because they may be invalid, and the result of contamination from above. See the text for an explanation.

The results for sample CAMS73199 are presented for the sake of completeness, but that sample appears to be invalid, and the result of contamination from above. When it (a leaf) was sampled from the sediment core, it was essentially horizontal, and no

problem with the stratigraphy was obvious to the naked eye. However, during the varve-by-varve cross-check performed between the petrographic thin sections and X-ray thin slabs (see the "4.1.10.2 Revised varve chronology" section above), a small fault was noted in the stratigraphy at that location. Though the fault seems small in the X-ray imagery, that the sample was pulled from it suggests that it (the sample) should be viewed with caution.

4.1.14.2 ^{137}Cs age results vs. the varve chronology

The analysis of ^{137}Cs activity down freeze core LML-19JAN2002-FRZ-1 core returned excellent results showing a prominent peak in ^{137}Cs activity related to the 1963 peak in nuclear arms testing (Pennington et al., 1973; Krishnaswami and Lal, 1978). A second, very subtle peak is visible slightly higher in the stratigraphy, and may represents deposition related to the 1986 Russian Chernobyl disaster (Appleby, 2001).

Figure 53 shows a plot of ^{137}Cs activity results (red curve) against freeze core LML-19JAN2002-FRZ-1 from which the joint ^{137}Cs/^{210}Pb samples were obtained. The annual dates on the freeze core were assigned based on the varve chronology. Note that these annual dates were assigned *prior* to sending out samples for ^{137}Cs and ^{210}Pb analysis. As can be seen, the peaks in the ^{137}Cs activity curve exactly confirm the varve chronology derived ages.

Figure 53—Results of ^{137}Cs (red) and ^{210}Pb (green) activity analysis down freeze core LML-19JAN2002-FRZ-1. The labeled ages on the freeze core were assigned based on the LML varve chronology *before* samples were sent out for analysis of ^{137}Cs and ^{210}Pb activity. The 1963 ^{137}Cs arms testing peak exactly confirms the varve chronology derived age. The 1986 ^{137}Cs Chernobyl peak is very subtle, but it does appear at the appropriate stratigraphic level. The ^{210}Pb results also provide a stunning confirmation of the accuracy of the varve chronology. The green, dotted tie lines indicate calculated activities of ^{210}Pb at one to five half-lives assuming an initial activity value of ~500 Bq/kg. Given the half-life of ^{210}Pb as 22.3 years, five half-lives is equivalent to 111.5 years. Over the same period, the varve chronology suggests a start age of 1993, and an end age of 1881. The difference between those two dates is 112 years which is essentially exactly equivalent to the 111.5 year difference as determined by ^{210}Pb activity. The superb coordination between the sediment ages as determined by the varve chronology, and these two independent radiometric age analyses provides very strong support for the accuracy of the varve chronology.

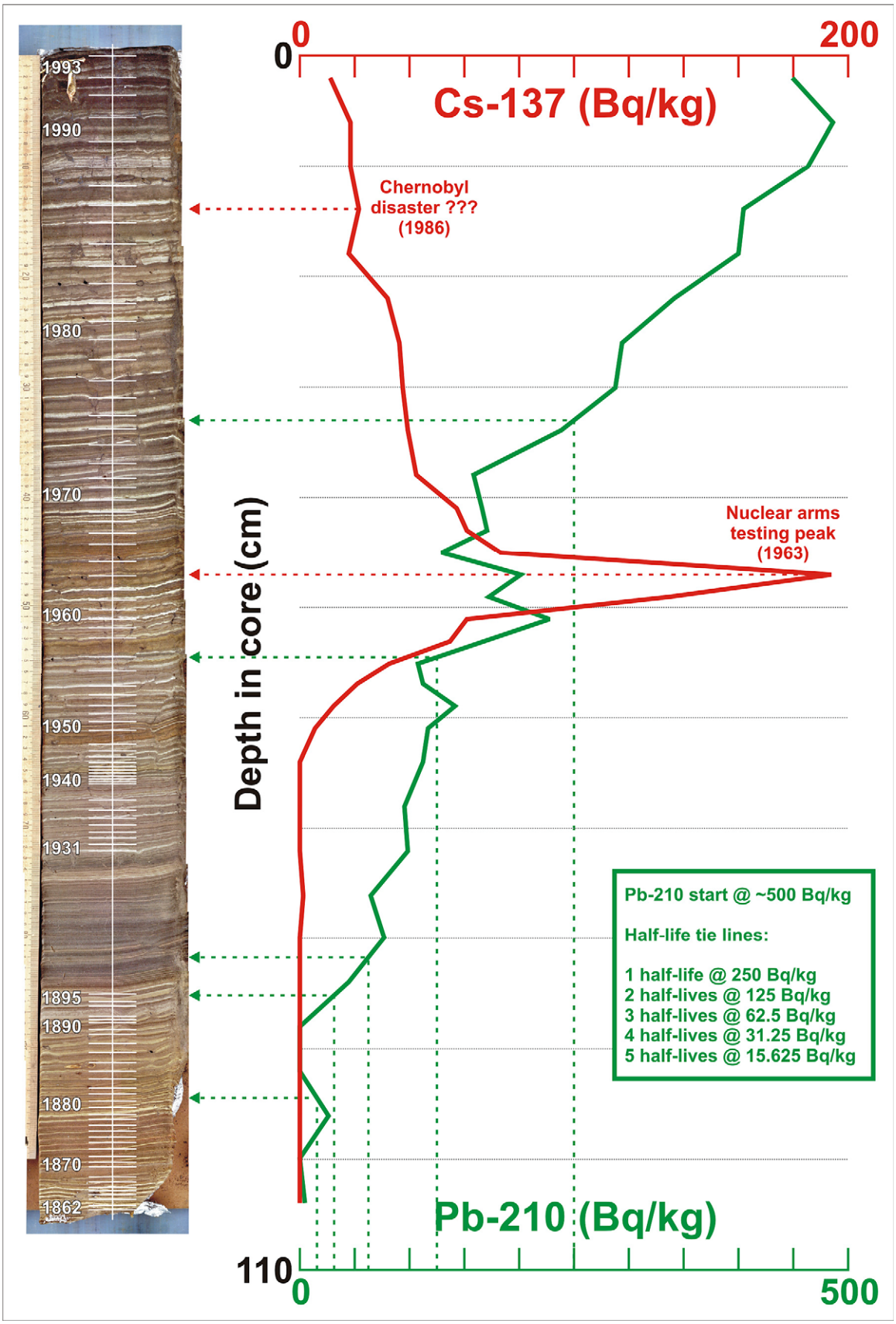
0
200
Cs-137 (Bq/kg)
Chernobyl
disaster ???
(1986)
Nuclear arms
testing peak
(1963)
Depth in core (cm)
1993
1990
1980
1970
1960
1950
1940
1931
1895
1890
1880
1870
1862
Pb-210 start @ ~500 Bq/kg
Half-life tie lines:
1 half-life @ 250 Bq/kg
2 half-lives @ 125 Bq/kg
3 half-lives @ 62.5 Bq/kg
4 half-lives @ 31.25 Bq/kg
5 half-lives @ 15.625 Bq/kg
Pb-210 (Bq/kg)
110
0
500

4.1.14.3 ^{210}Pb results vs. the varve chronology

Results of the ^{210}Pb activity analysis (green curve) are plotted together with the ^{137}Cs data in Figure 53. While the ^{210}Pb activity shows a general decrease down core, the activity keeps decreasing all the way to zero, and does not stop at a stable, positive, supported background level. This frustrates some of the typical methods for calculating ages using this isotope (Appleby and Oldfield, 1978; Appleby, 2001). Nonetheless, a simple analysis of the raw activity curve over five ^{210}Pb half-lives provides another very strong confirmation about the accuracy of the varve chronology.

The top of the freeze core was dated to 1993 according to the varve chronology. In fact, all of these ages assigned to the freeze core seen in Figure 53 were made strictly based on the varve chronology *prior* to sending out samples for ^{137}Cs and ^{210}Pb analysis. ^{210}Pb activity at the top of the core had a starting value of ~500 Bq/kg. Given this initial activity, the first five half-life activity values for down core sediments were calculated as 250, 125, 62.5, 31.25, and finally15.625 Bq/kg. Tie lines were extended from the values up to the actual activity curve, and then over to the freeze core image.

At the point of five ^{210}Pb half-lives, the varve chronology determined age for the core was 1881, or a difference of 112 years from the initial 1993 starting age. ^{210}Pb has a half-life of 22.3 years; thus, five half-lives are equivalent to 111.5 years. Thus, the varve chronology and ^{210}Pb activity curves essentially exactly agree as to the elapsed age of the sediments (112 years vs. 111.5 years). This provides another very strong confirmation about the accuracy of the varve chronology.

4.1.14.4 Preliminary pollen age data vs. the varve chronology

While the varve chronology was floating, the age significance of the preliminary pollen assemblage analyses by T. Parshall was initially downplayed because it conflicted with the results of five initial radiocarbon dates (see the "4.1.10.1 Initial varve chronology" section above). However, after the varve chronology was physically linked to the active sediment/water interface with the retrieval of freeze core LML-19JAN2002-FRZ-1 core, it became apparent that the pollen results were, in fact, correct, and show excellent correspondence with the varve chronology derived ages for the stratigraphy. Pollen samples A, B, and C were obtained from an approximately 30 cm range within piston core LML-23NOV1996-LIV-1.

Sample A contained mostly oak (*Quercus*) pollen and no agricultural weed pollen. This was interpreted as a pre-European settlement assemblage. According to the varve chronology, the sample was extracted from the varves deposited from AD 1595-1599.

Sample B contained a small amount of rye (*Secale*) pollen, but otherwise was similar to sample A. This was interpreted as a very early Colonial Period assemblage. The first European settlers (i.e. the Pilgrims) arrived to Plymouth, MA, and founded the Massachusetts Bay Colony in AD 1620. However, they did not arrive to the Medford area (about 65 km northwest of Plymouth) until about a decade later in AD 1630 when the first land claim was staked out on the north side of the Mystic River downstream from the Lower Mystic Lake (Seaburg and Seaburg, 1980)[54]. According to the varve chronology, the sample was extracted from the varves deposited between AD 1643-1646.

[54] This first land claim was for the plantation of Matthew Cradock, the governor of the Massachusetts Bay Colony.

Sample C showed the first appearance of European weed (*Rumex*), ragweed (*Ambrosia*), and grass pollen. This was interpreted as indicating open landscape related to European settlement. According to the varve chronology, the sample was extracted from the varves deposited from AD 1730-1735.

The excellent correspondence between the preliminary pollen analysis data and varve chronology provides strong support for the validity of the varve chronology.

4.1.14.5 Freeze core yellow zones vs. drought years

During preparation and analysis of freeze core LML-19JAN2002-FRZ-1, a series of conspicuous, yellowish-brown colored varves were observed in the stratigraphy. These yellowish-brown colored varves are only present in the stratigraphy up to and including 1966, the year in which the Amelia Earhart Dam was built downstream of the LML. Lack of thin sections produced from this freeze core has prevented further analysis of what might produce this conspicuous color difference. Nonetheless, it was noted that these varves show excellent correspondence with years of low precipitation or drought suggesting a strong cause/effect relationship.

Figure 54 below shows the total annual precipitation in Boston from AD 1818-1990. Several periods (even single years) of low precipitation which fall within the age range of freeze core LML-19JAN2002-FRZ-1 are circled in red. Those periods include the early 1940s, 1949-1950, 1957, and 1963-1966.

Figure 55 below shows a high resolution image of the freeze core which includes the low precipitation periods mentioned above indicated by red bars. The obvious yellowish-brown colored varves show a striking correspondence with these periods of

low precipitation. The actual mechanism which produces this anomalous color difference is not known at present. However, these anomalously-colored varves occur in the stratigraphy only up to and including 1966—the year in which the Amelia Earhart Dam was built, and the point at which all estuarine circulation on the river ceased. Thus, a working hypothesis is that the color difference may be related to changes in physical sedimentation and/or water chemistry related to sea water backing up the Mystic River due to decreased flow conditions. This working hypothesis will be tested with further investigation.

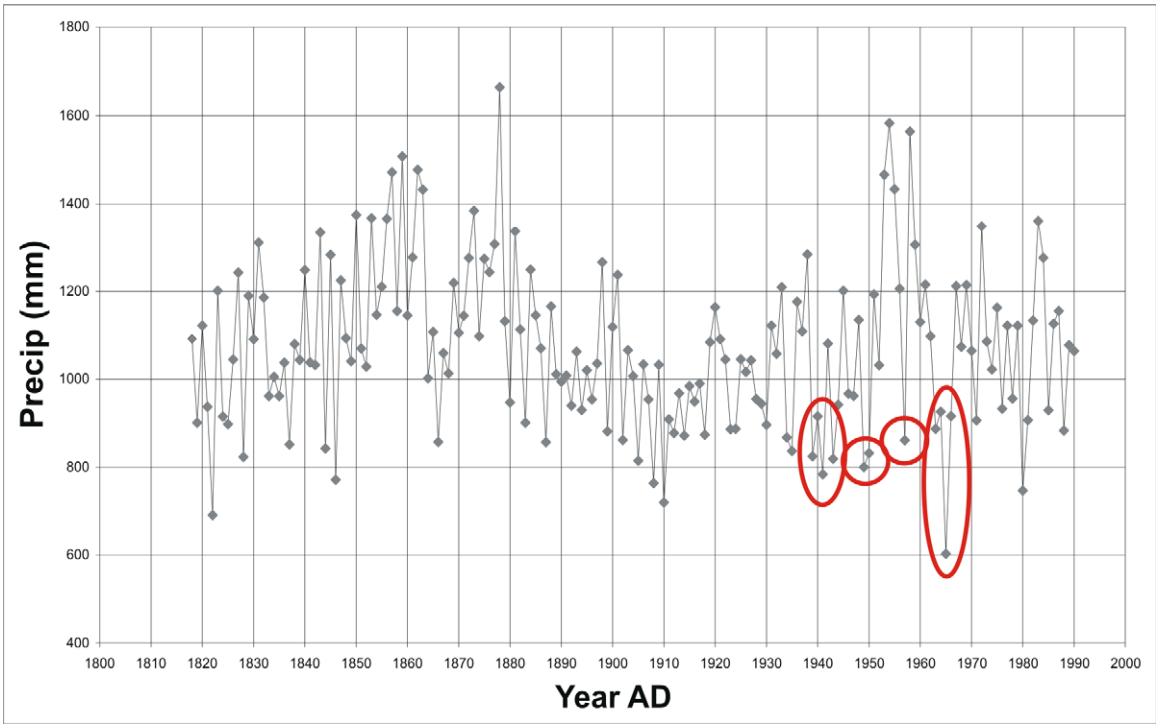

Figure 54—Plot of total annual precipitation in Boston from AD 1818-1990. The red circles indicate either single years or periods of years with low values of total precipitation. The low precipitation 1980 year is not included because the yellowish-brown colored varves only occur up to and including 1966, the year in which the Amelia Earhart Dam was completed.

Irrespective of the actual mechanism responsible for the color change, the striking correspondence between these yellowish-brown varves and low precipitation years

strongly suggests that they are linked. Thus, this serves as another chronologic control to support the validity of the varve chronology.

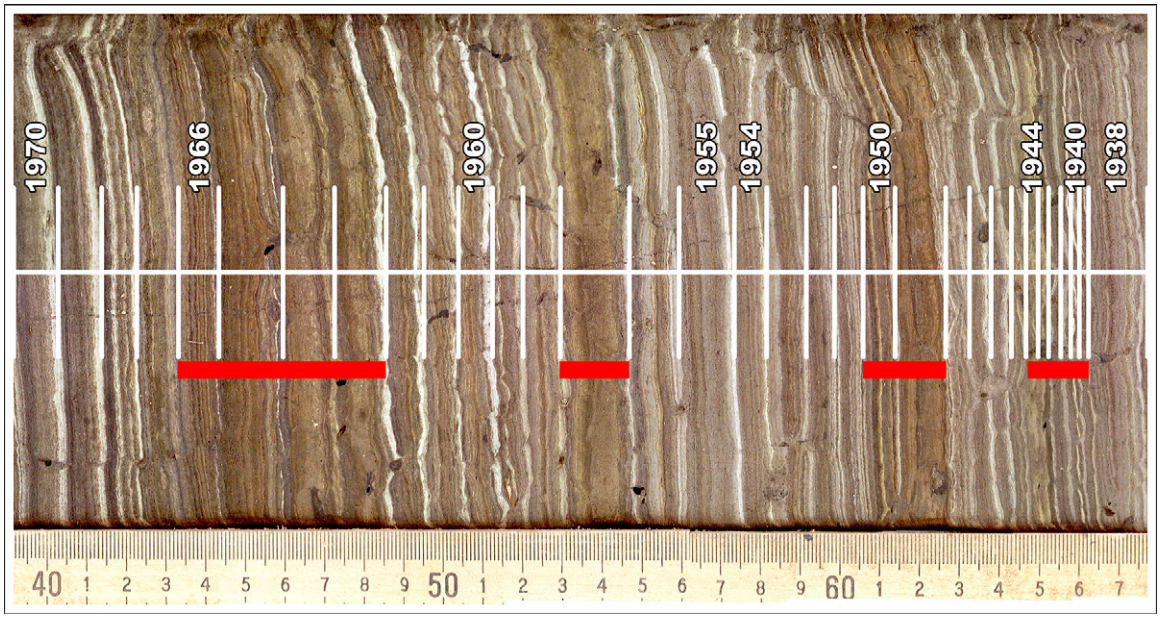

Figure 55—Close up showing the conspicuous, yellowish-brown colored varves in freeze core LML-19JAN2002-FRZ-1. Top/up is to the left. The red boxes mark these anomalously-colored varves which show excellent correlation with years of low precipitation.

4.1.14.6 Significant change in varve composition/thickness related to dam building and eutrophication

The Upper and Lower Mystic Lakes were confluent until AD 1864 at which point dam construction was completed at "The Partings", the natural narrow constriction between the lakes. This dam construction resulted in a significant change to the LML's hydrographic regime as any inflowing sea water or sewage was now strictly confined to the lower lake. This resulted in a more lagoonal or stagnant situation which favored increased eutrophic conditions. A second consequence of dam construction was a direct reduction of siliciclastic input. While the lakes were confluent, sediment transport from the UML to the LML was possible as both traction load and suspended load. But

following dam construction, only finer suspended loads could pass from the UML to the LML.

During the middle to late 19th century, the human population in the LML watershed also began an explosive growth trend. Concomitant with this growth was land clearing, manure and phosphate use, road construction, and the development of upstream industry among other factors. As a result of such activities, the LML experienced a steadily increasing supply of nutrients and sediments leading towards eutrophic conditions.

An apparent consequence of this combined dam building and population growth was a tremendous increase in biogenic sedimentation in the lake which caused the average varve thickness to increase abruptly. This increase in biogenic vs. siliciclastic sedimentation is visible in the varves themselves, for example, in the X-ray imagery. Figure 56 shows the varves deposited prior to dam construction, and those deposited immediately after.

The increase in sedimentation is also reflected in the varve thickness record (Figure 51). In the 700 years from the beginning of the record up to the early 1860's, the varves generally fluctuated between 1-2.5 mm thickness. But starting in the 1860's, the average varve thickness quickly jumped up to the ~4 mm range.

This prominent change in sedimentation tied to well-documented historical events in the lake and watershed provides additional strong evidence to support the validity of the LML varve chronology.

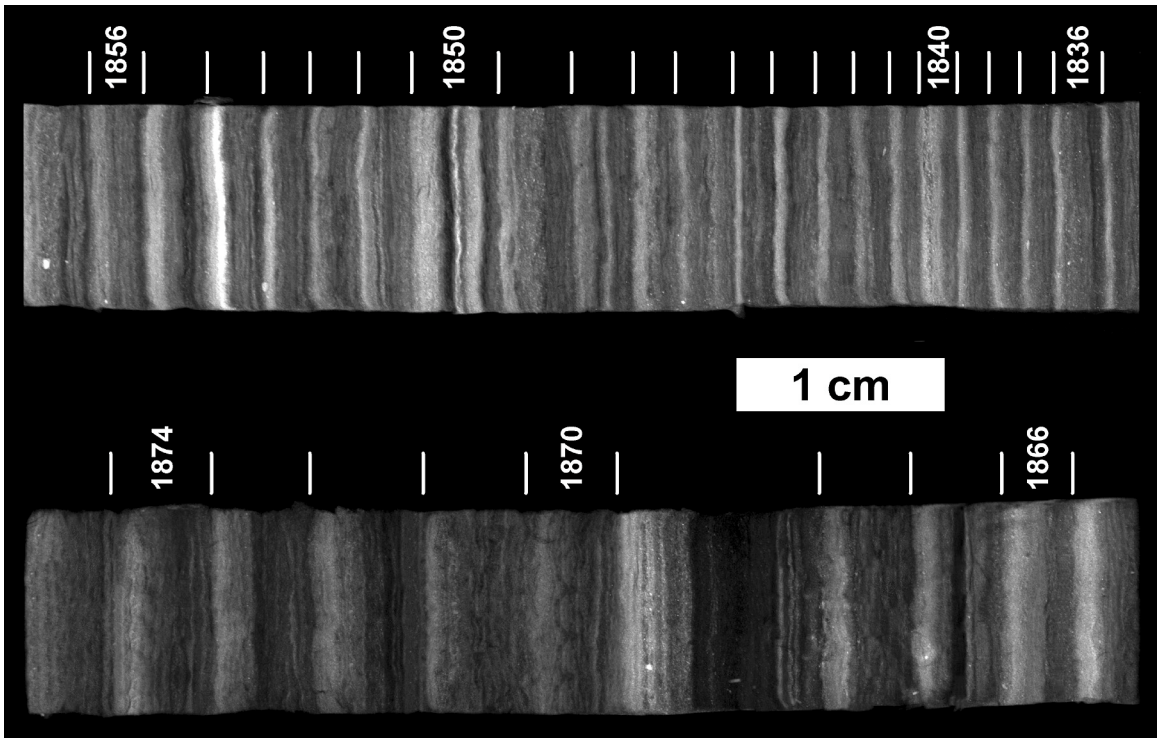

Figure 56—X-ray exposure images showing the pre- and post-1860's varves in the LML varve chronology. The massive increase in biogenic sedimentation resulting from the construction of the dam at "The Partings", and eutrophication driven by the human population increase is obvious. The AD 1836-1856 segment is overall much lighter in color indicating an increased proportion of siliciclastic material. The AD 1866-1874 segment is overall significantly darker indicating these varves are composed of a much larger proportion of biogenic sediment.

4.2 Results for the Belle Isle Marsh

4.2.1 Sediment core recovery

Eight custom, 10 cm diameter, Schedule 40 PVC sediment cores were retrieved from Belle Isle Marsh for this project. The names of the cores, and their lengths are provided below.

Table 11—Inventory of 10 cm diameter, PVC sediment cores retrieved from the BIM.

Sediment core	***Comments***
BIM-14SEP2002-PVC4-1	168 cm total length
BIM-14SEP2002-PVC4-2	hit rejection at ~30-35 cm depth, so core abandoned
BIM-14SEP2002-PVC4-3	107 cm total length
BIM-14SEP2002-PVC4-4	185 cm total length
BIM-14SEP2002-PVC4-5	192 cm total length
BIM-14SEP2002-PVC4-6	189 cm total length
BIM-14SEP2002-PVC4-7	180 cm total length
BIM-14SEP2002-PVC4-8	186.6 cm total length
BIM-14SEP2002-PVC4-9	179 cm total length

The sediment cores were retrieved from a rough 3x3 grid with an approximately 50 m cell spacing, and their locations are illustrated in Figure 57 below.

4.2.2 Sediment core logs and photography

Brief log sheets and core photography for all BIM sediment cores were archived in electronic format for future reference.

4.2.3 General description of BIM sedimentary record

In general, sediment cores retrieved from the middle and eastern side of the marsh are dominated by peaty sediments, and reflect deposition in a high marsh environment according to the floral assemblages. Occasional sand layers are encountered in the stratigraphy, and presumably represent deposition from storm surge overwash events. This is supported by the fact that the largest number of sand layers are encountered in the cores closest to the causeway (BIM-14SEP2002-PVC4-7 and -8), the point from which overwash enters the marsh (Figure 57).

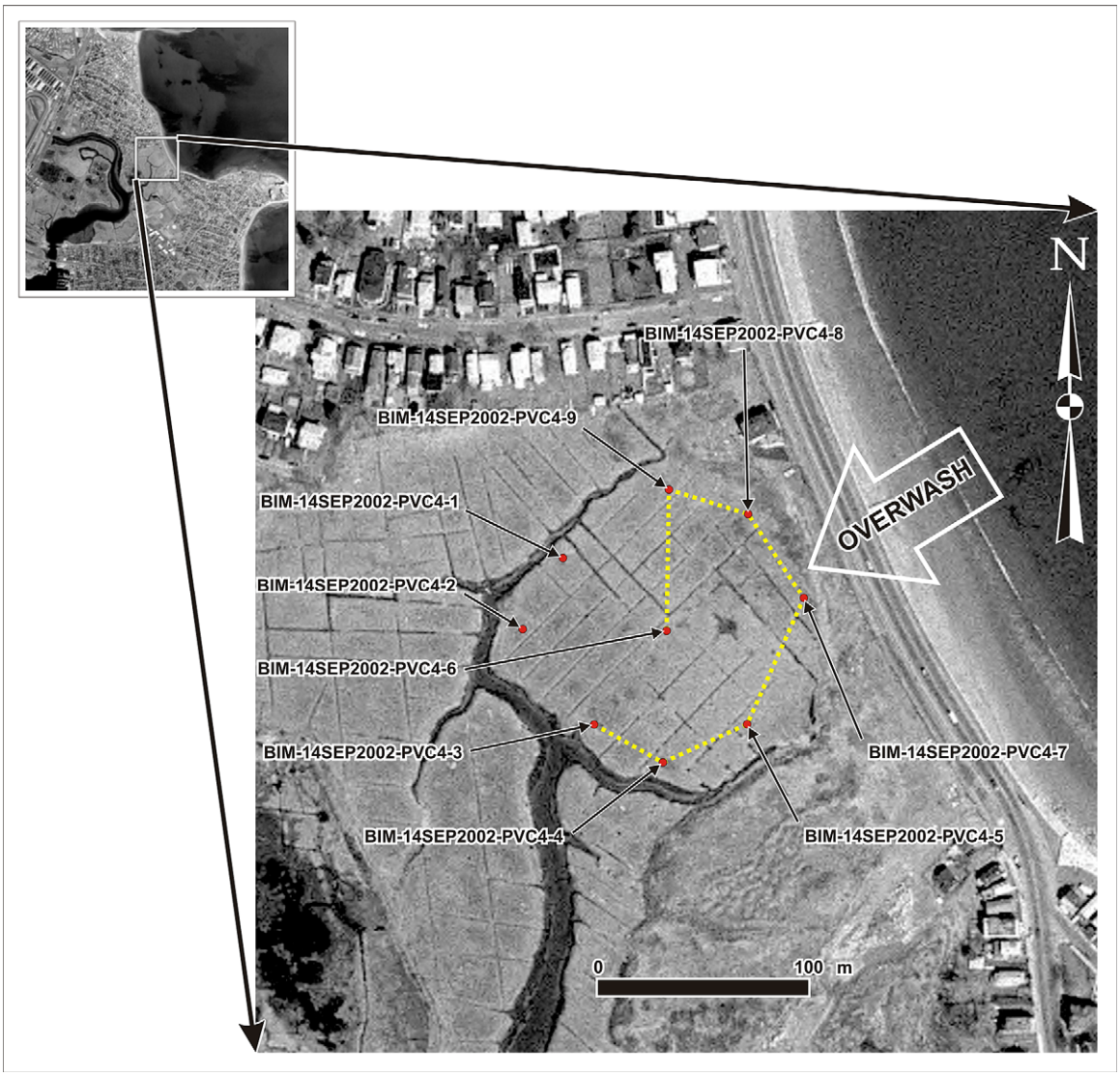

Figure 57—Sediment coring locations at Belle Isle Marsh. The principal path for storm surge overwash is from the northeast across the causeway, and into the marsh. The dotted yellow line indicates the cross section transect which is illustrated in Figure 58. The inlet for the tidal Belle Isle Creek is shown in the very lower left corner of the thumbnail image. The large NNE/SSW trending runways at Logan International Airport are found just 500 m from the mouth of the creek (just beyond the coverage of the thumbnail image). Figure 2 in Chapter 1 (the area map image) provides a wider field of view to show their proximity of the marsh and the airport.

The western side of the marsh (cores BIM-14SEP2002-PVC4-1 and -3) is more dominated by siliciclastic sediments, and probably reflects deposition in a low marsh or tidal channel environment. The presence of sand layers in such environments may be related to storm surge overwash events, but the link is more tenuous given that sandy sediments are typically found in the channels anyway.

Cores BIM-14SEP2002-PVC4-4 and -9 are less peaty than expected. BIM-14SEP2002-PVC4-9 may have penetrated an old tidal channel (J. Ridge, personal communication), and the same may be true for BIM-14SEP2002-PVC4-4 given its location close to a modern channel.

Belle Isle Marsh has been the subject of several undergraduate projects undertaken at Tufts University under the guidance of J. Ridge. The general stratigraphic framework is known (Gillette, 1996), but this has never been formally published[55]. Gillette (1996) recognized seven stratigraphic units in the marsh. That basic framework is followed here, but two of the units are consolidated into a single entity, and generic unit names are used. Based on the eight sediment cores retrieved from the marsh, a brief description of each unit in regular stratigraphic order is provided below.

Unit I (> 70-80 cm depth in Figure 58, and equivalent to the combination of Gillette's (1996) "Prehistoric Red Peat II" and "Prehistoric Red Peat I") consists of a brown to reddish brown peat with interspersed peaty mud and mud beds in the eastern portion of the marsh (cores BIM-14SEP2002-PVC4-5, -7, and -8). The amount of mud increases westward—cores in the center of the marsh (BIM-14SEP2002-PVC4-4, -6, and -9) show in increasing amount of peaty mud vs. peat, and cores retrieved from the western part of the marsh (BIM-14SEP2002-PVC4-1, -3, and presumably -2[56]) are dominated by peaty mud to mud. The muds throughout the unit range from gray to brownish with the color presumably related to the amount of organic matter. Occasional,

[55] Special thanks are extended to J. Ridge for making a summary of this work available for guidance.

[56] As indicated earlier, core BIM-14SEP2002-PVC4-2 was abandoned because rejection during the coring processes occurred at just 30-35 cm depth. Presumably, it is even more dominated by siliciclastic sediments than the neighboring BIM-14SEP2002-PVC4-1 and -3 cores, and this fact caused the rejection.

Figure 58—A cross section transect through Belle Isle Marsh linking up stratigraphy in seven of the eight sediment cores retrieved there. Standard, long core names such as "BIM-14SEP2002-PVC4-7" have been abbreviated to shorter counterparts (i.e. "BIM7") in this figure to facilitate readability of the diagram. The lateral spacing between cores is proportional to their spacing in real life with the total length of the transect being 300 m. Vertical exaggeration in the diagram is approximately 94x. The BIM-14SEP2002-PVC4-1 core was not included in the cross section because it is dominated by siliciclastic sediment like the BIM-14SEP2002-PVC4-3 core. The labels for the stratigraphic units as discussed in the text are included at the left. Dark and light green pointer arrows around each core indicate sand layers. In some cases, sand layers can be correlated between cores. Boldly dashed lines and dark green arrow pointers indicate sand layers that are continuous across at least half of the marsh in an E-W direction. Light dashed lines and light green arrow pointers indicate sand layers that are only of local extent.

BIM3
BIM4
BIM5
BIM7
BIM8
BIM9
BIM6
Unit VI
Unit V
Unit IV
Unit III
Unit II
Unit I
0
50 m
Depth in core (cm)
0
20
40
60
80
100
120
140
160
180

very dark gray to black horizons from several millimeters up to ~1 cm thick are noticeable, and may represent fires which affected the marsh. Besides these thin, dark horizons possibly related to fires, other portions of the stratigraphy appear to have taken on a dark gray color. Such bands range from 1 cm thick up to 10+ cm thick, and affect the stratigraphy irrespective of its composition. Often, these darker bands are encountered underneath mud layers, and may be related to a microenvironment of diagenetic activity beneath such layers (J. Ridge, personal communication). Within this unit, several discontinuous sand layers are visible in the stratigraphy, but one layer (89.4 cm depth in BIM-14SEP2002-PVC4-7) is apparently continuous across at least half of the marsh (from BIM-14SEP2002-PVC4-7 to the -5 and then -4 cores).

Unit II (between 55-80 cm depth in Figure 58, and equivalent to Gillette's (1996) "Prehistoric Clay Beds") consists of two tan to gray mud bands separated by a brown peat to muddy peat. A single sand layer is present in this unit, but is only present in two cores (BIM-14SEP2002-PVC4-8 and -9) towards the eastern edge of the marsh where the influence of overwash events is most likely.

Unit III (between 45-60 cm depth in Figure 58, and equivalent to Gillette's (1996) "Prehistoric Black Peat") consists of peat to peaty clay that has been discolored to a dark gray. The dark gray discoloration is less prominent in the cores from the southern half of the marsh (BIM-14SEP2002-PVC4-3, -4, -5, and -7) where the peat is brown to reddish brown. No sand layers were recognized in this unit.

Unit IV (between 15-55 cm depth in Figure 58, and equivalent to Gillette's (1996) "Historic Clayey Peat") consists of a gray to tan peaty mud which grades upward into a gray to brown to reddish brown muddy peat which in turn grades up into a dark gray

muddy peat. Several sand layers are present in the lower half of this unit, in particular, in two of the cores at the eastern edge of the marsh (BIM-14SEP2002-PVC4-7 and -8) where the effect of overwash events is most likely. Three of the sand layers (41.2 cm, 47.6 cm, and 54.7 cm depth in BIM-14SEP2002-PVC4-7) appear to be continuous across at least half or more of the marsh.

Unit V (between 10-24 cm depth in Figure 58, and equivalent Gillette's (1996) "Airport Clay Bed") is a prominent gray to blue gray peaty mud to peaty clay which extends across the entire marsh. Gillette (1996) attributes deposition of this unit to construction/expansion of Logan International Airport from about 1945-1950. No sand layers are present in the unit.

Unit VI (< 10-20 cm depth in Figure 58, and equivalent to Gillette's (1996) "Post-1950 peat") is a brown to reddish brown peat to muddy peat which caps the stratigraphy. The base of the unit is gradually transitional with the underlying mud/clay units, and this is most obvious in cores BIM-14SEP2002-PVC4-4 and -9. Core BIM-14SEP2002-PVC4-7 records several sand layers within this unit as its position places it close to the source of overwash events. One of the sand layer is actually continuous marsh-wide in nearly all of the cores except BIM-14SEP2002-PVC4-3.

4.2.4 Magnetic susceptibility analysis results

Results of magnetic susceptibility analysis performed at 3 mm resolution on the BIM sediment cores are presented in Figure 59 below. In general, the peaty, organic-rich horizons show low, and sometimes negative susceptibility values while muddy, clay- and siliciclastic-rich horizons show higher values. The occasional sand layers also generally

show some type of positive expression in the susceptibility curve, but because of their limited thickness they often simply result in blips, not in massive spikes like the thicker clay and mud beds.

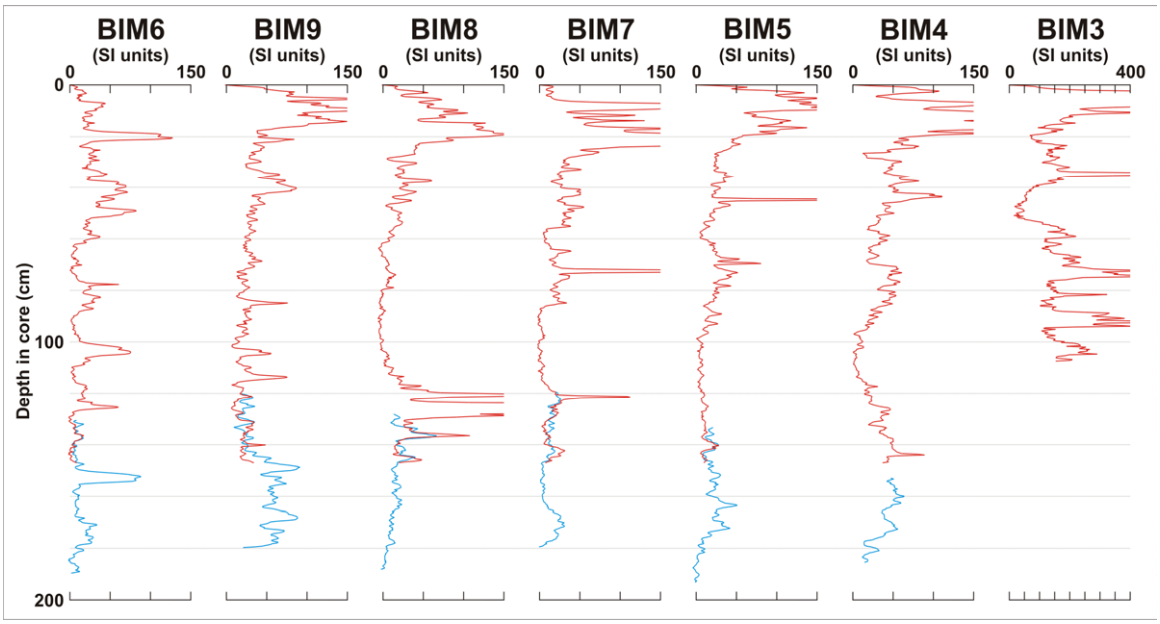

Figure 59—Results of magnetic susceptibility analyses for Belle Isle Marsh sediment cores. Standard, long core names such as "BIM-14SEP2002-PVC4-7" have been abbreviated to shorter counterparts (i.e. "BIM7") in this figure to facilitate readability of the diagram. Note that the results are not plotted in simple order according to the core names, but instead are presented in the same order in which the sediment cores appear in cross section (see Figure 58). All results share a common scale for susceptibility values with the exception of those from core BIM-14SEP2002-PVC4-3. The dominance of siliciclastic material in that core (and also BIM-14SEP2002-PVC4-1, see text for explanation) forced the use of a different scale. Many peaks in the curves are truncated because of the chosen plot scale. Some of the analyses returned negative values so when the result curves dip below zero, it is not a mistake, and the results are correctly plotted. The blue segment at the base of each curve represents data measured in the reverse direction that was spliced into the regular forward direction data (see the "3.2.6 Magnetic susceptibility analysis (LML and BIM)" section in Chapter 3 for a explanation).

4.2.5 Bulk density analysis results

Results from wet/dry bulk density analyses at 1 cm resolution on the Belle Isle Marsh sediment cores are presented in Figure 60 below. This analysis was not performed

on cores BIM-14SEP2002-PVC4-1 and -3 because those cores do not represent a high marsh environment.

In general, wet and dry bulk density show lower values for peaty sediments, and higher values for clastic sediments. Whole core wet bulk density values average between about 0.8 g/cc and 1.2 g/cc, and similar whole core averages values for dry bulk density range between 0.4 g/cc and 0.8 g/cc. The occasional sand layers are generally reflected by positive peaks in the curves, but the expression is not large because of the limited thickness of the layers.

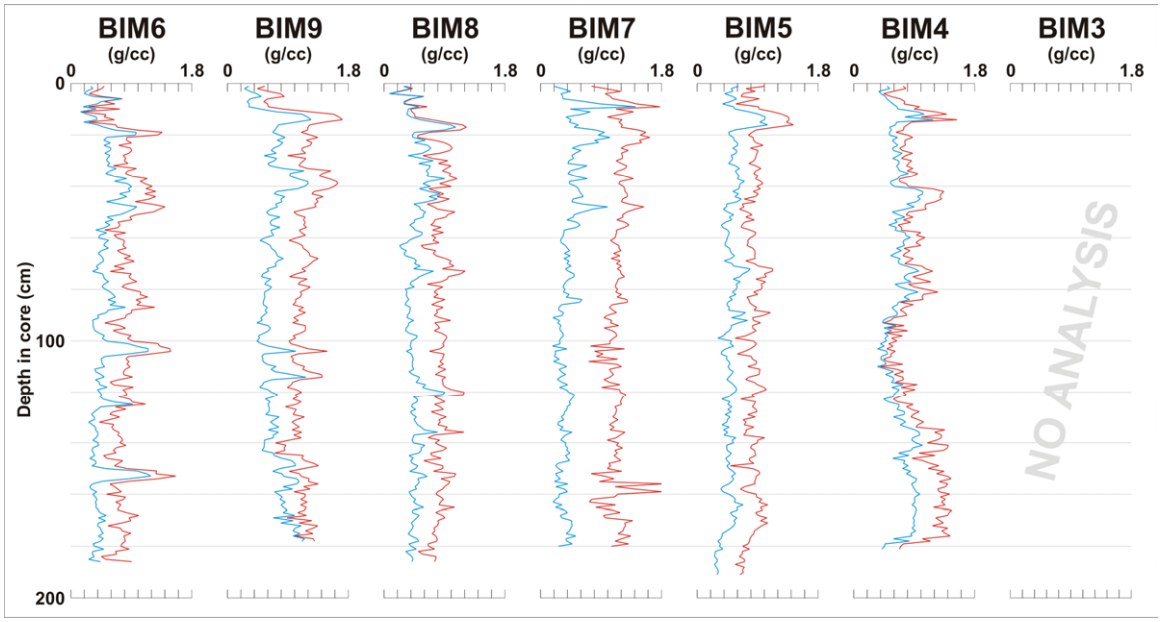

Figure 60—Results of wet (red curve) and dry (blue curve) bulk density analyses of Belle Isle Marsh sediment cores. Standard, long core names such as "BIM-14SEP2002-PVC4-7" have been abbreviated to shorter counterparts (i.e. "BIM7") in this figure to facilitate readability of the diagram. Note that the results are not plotted in simple order according to the core names, but instead are presented in the same order in which the sediment cores appear in cross section (see Figure 58).

4.2.6 Loss on ignition analysis results

Results from loss on ignition analysis at 1 cm resolution on the Belle Isle Marsh sediment cores are presented in Figure 61 below. This analysis was not performed on

cores BIM-14SEP2002-PVC4-1 and -3 because those cores do not represent a high marsh environment.

In general, values for organic carbon content are high in peaty sediments, and lower for samples dominated by siliciclastic sediment. Values for inorganic carbon content should provide an approximation of the quantity of mixed carbonate minerals present in a sample, but this parameter is also influenced by clay content.

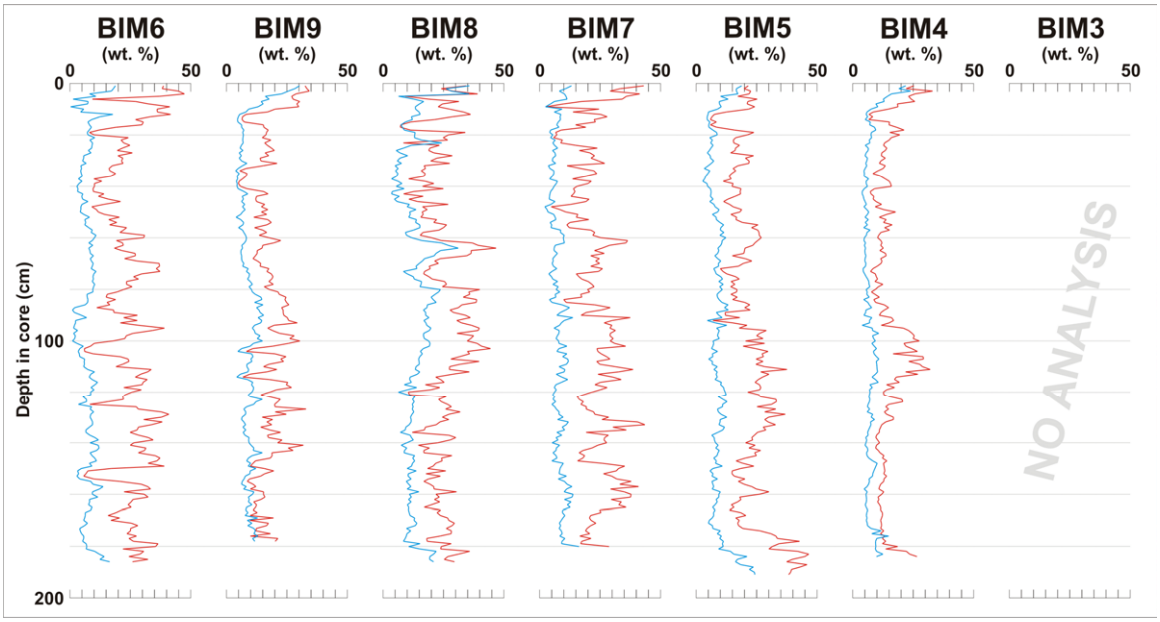

Figure 61—Results of organic (red curve) and inorganic/carbonate (blue curve) carbon content via loss on ignition analysis of Belle Isle Marsh sediment cores. Standard, long core names such as "BIM-14SEP2002-PVC4-7" have been abbreviated to shorter counterparts (i.e. "BIM7") in this figure to facilitate readability of the diagram. Note that the results are not plotted in simple order according to the core names, but instead are presented in the same order in which the sediment cores appear in cross section (see Figure 58).

Whole core average values for organic carbon content generally fall in the range of 23-25 weight percent for peat-rich cores, but range down to 15-17 weight percent for BIM-14SEP2002-PVC4-4 and -9 because of possible influence by tidal channels. Whole core averages for inorganic carbon content generally range between 5-15 weight percent for all cores. The occasional sand layers do generally produce negative peaks in the

organic carbon content curve though the limited thickness of the layers means their expression is not as prominent as the thicker mud layers.

4.2.7 Results of radiometric and other chronologic control

A chronologic framework for the Belle Isle Marsh stratigraphy was established using core BIM-14SEP2002-PVC4-7, and the results of seven ^{14}C dates, a ^{137}Cs activity curve, and a prominent cultural/anthropogenic marker bed (Figure 62). An analysis of ^{210}Pb activity down core was also performed, but the results were not useful. Results are discussed by category below.

4.2.7.1 ^{14}C results

AMS ^{14}C dates ("UCI" series) were obtained on marsh peat samples from three stratigraphic horizons in core BIM-14SEP2002-PVC4-7. Gillette (1996) obtained several conventional ^{14}C dates ("GX" series) on larger peat blocks from her core SB-I/J-1, and based on correlation between stratigraphic units and marker beds, four of those dates have been applied to the equivalent stratigraphic level in BIM-14SEP2002-PVC4-7. Results from these analyses and their calibrated, calendar year, 2 sigma age ranges are presented in the Table 12 below, and plotted graphically alongside core BIM-14SEP2002-PVC4-7 in Figure 62. For the four Gillette (1996) samples, the equivalent stratigraphic depth in BIM-14SEP2002-PVC4-7 is also specified in Table 12 below.

Figure 62—Chronologic framework and age-depth curve for sediment core BIM-14SEP2002-PVC4-7. Results from ^{14}C, ^{137}Cs, and ^{210}Pb analyses, and a prominent anthropogenic layer provide chronologic control for this core, and in turn, the marsh. The "UCI" series ^{14}C samples were directly extracted from this core. The "GX" series sample dates are from Gillette (1986), but the results were applied to this core (see explanation in "4.2.7.1 ^{14}C results" section below). Each radiocarbon date is accompanied by a black and white box plot that shows the calibrated, calendar year, 1 sigma (black-filled boxes) and 2 sigma (white-filled boxes) age ranges for each date as determined by the Calib v5.01 computer program (Stuiver and Reimer, 1993). The height of the box plots and the semi-transparent white zones over the actual sediment core represent the sampling interval over which the material for ^{14}C dating was collected. Two of the ^{14}C dates (GX22396 and UCI7510) appear to be too old, and are illustrated in a gray shade (see text for discussion). Results from the analysis of ^{137}Cs (red curve) and ^{210}Pb (green curve) activity down the upper part of the core are presented in the light yellow shaded box towards the top of the diagram. A prominent clay bed related to the expansion of Logan International Airport between 1945 and 1950 also provides two dated horizons. The red line provides an age-depth curve for the core by joining the median values of the full 2 sigma calibrated age ranges for the ^{14}C dates, and the five known dates towards the top of the core. Lightly dotted lines join the 2 sigma age ranges for each of the ^{14}C dates forming an error envelope for the actual ages. The five dark green arrow pointers which surround the core indicate the position of continuous sand layers which extend across at least half of the marsh in an E-W direction. The similar light green pointers indicate sand layers of only local extent.

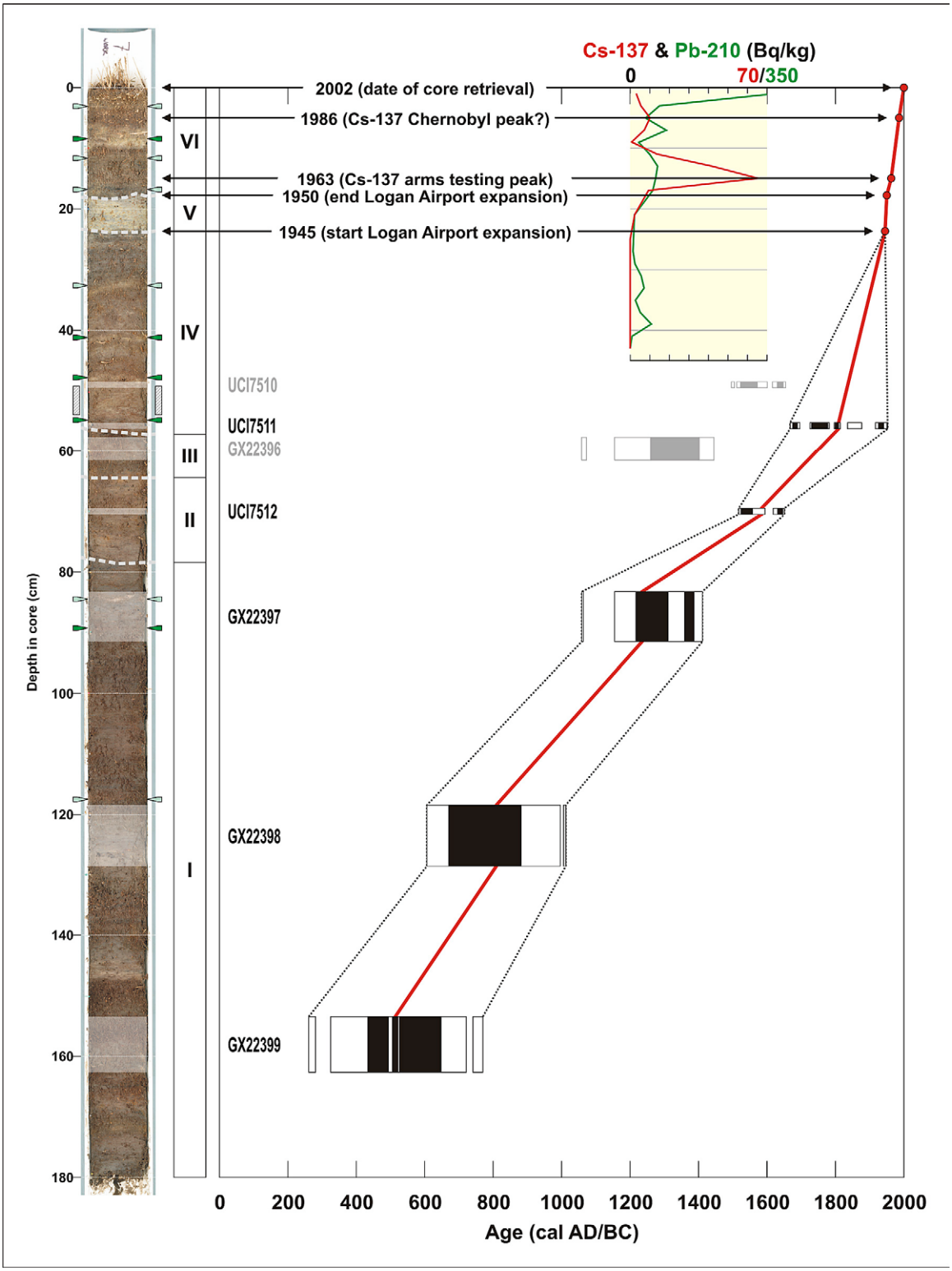
Cs-137 & Pb-210 (Bq/kg)
0
70/350
2002 (date of core retrieval)
1986 (Cs-137 Chernobyl peak?)
1963 (Cs-137 arms testing peak)
1950 (end Logan Airport expansion)
1945 (start Logan Airport expansion)
VI
V
IV
III
II
I
UCI7510
UCI7511
GX22396
UCI7512
GX22397
GX22398
GX22399
Depth in core (cm)
0
20
40
60
80
100
120
140
160
180
0
200
400
600
800
1000
1200
1400
1600
1800
2000
Age (cal AD/BC)

Table 12—Calibrated results of ^{14}C age analyses from the BIM. The first three listed samples (the "UCI" series) were directly extracted from core BIM-14SEP2002-PVC4-7 (i.e. BIM7). The last four listed samples (the "GX" series) are from Gillette's (1996) SB-I/J-1 core, but their equivalent stratigraphic depth in BIM7 is also given. The calibrated, calendar year, 2 sigma age ranges with relative probabilities were obtained from the Calib v5.01 computer program (Stuiver and Reimer, 1993).

Lab Code + Core + Drive and Depth	***Material***	***del ^{13}C***	***Fraction Modern***	***^{14}C Age***	***Calibrated 2s age ranges with relative probability***
UCI7510 BIM-14SEP2002-PVC4-7 49 cm [not applicable]	marsh peat	-10.3	0.9641 ± 0.0026	295 ± 25	AD 1496-1505 @ 0.016 AD 1512-1601 @ 0.685 AD 1616-1655 @ 0.299
UCI7511 BIM-14SEP2002-PVC4-7 55.75 cm [not applicable]	marsh peat	-9.4	0.9808 ± 0.0024	155 ± 20	AD 1668-1696 @ 0.167 AD 1725-1782 @ 0.427 AD 1797-1814 @ 0.111 AD 1835-1877 @ 0.088 AD 1917-1952* @ 0.207
UCI7512 BIM-14SEP2002-PVC4-7 70 cm [not applicable]	marsh peat	-13.4	0.9637 ± 0.0021	295 ± 20	AD 1517-1594 @ 0.691 AD 1618-1651 @ 0.309
GX22396 SB-I/J-1 47-55 cm BIM7 equiv. 57.7-61.5 cm	marsh peat	-15.1		675 ± 105	AD 1058-1073 @ 0.006 AD 1155-1445 @ 0.994
GX22397 SB-I/J-1 80-88 cm BIM7 equiv. 83.3-91.5 cm	marsh peat	-17.2		725 ± 80	AD 1059-1063 @ 0.003 AD 1155-1411 @ 0.997
GX22398 SB-I/J-1 115-125 cm BIM7 equiv. 118.4-128.6 cm	marsh peat	-13.8		1250 ± 110	AD 606-996 @ 0.996 AD 1005-1012 @ 0.004
GX22399 SB-I/J-1 151-160 cm BIM7 equiv. 153.5-162.7 cm	marsh peat	-14.3		1495 ± 110	AD 261-281 @ 0.010 AD 325-721 @ 0.973 AD 741-770 @ 0.017

Two of the seven radiocarbon dates appear to be too old. Those are samples GX22396 and UCI7510.

Sample GX22396 was retrieved more than 20 cm higher in the stratigraphy than the next conventional ^{14}C date below it (i.e. GX22397), and more than 8 cm higher than AMS sample UCI7512. But it returned an age value almost equivalent to the lower

sample (675 vs. 725 ^{14}C years), and older than the intermediate sample (675 vs. 295 ^{14}C years).

A similar problem exists for AMS sample UCI7510. It was sampled from the stratigraphy more than 20 cm higher than sample UCI7512, and about 7 cm higher than sample UCI7511, but it returned an age value equivalent to the lowest sample (295 ^{14}C years), and older than the intermediate sample (295 vs. 155 ^{14}C years).

4.2.7.2 ^{137}Cs results

Analysis of ^{137}Cs activity down core BIM-14SEP2002-PVC4-7 rendered excellent results which show a prominent peak in ^{137}Cs activity related to the 1963 peak in nuclear arms testing (Pennington et al., 1973; Krishnaswami and Lal, 1978). A second, more subtle peak in ^{137}Cs is visible slightly higher in the activity curve, and probably represents deposition related to the 1986 Russian Chernobyl disaster (Appleby, 2001). The results are graphically illustrated in Figure 62 (red curve in inset graph)

4.2.7.3 ^{210}Pb results

Analysis of ^{210}Pb activity down core BIM-14SEP2002-PVC4-7 was also performed, but the results are unsuitable for interpretation. The activity does not decrease monotonically down core, but decreases rapidly in the upper 5 cm of the core, and then exhibits several increases and decreases down the remainder of the samples. The results of this analysis are graphically illustrated in Figure 62 (green curve in inset graph).

4.2.7.4 Logan International Airport expansion marker bed

A prominent anthropogenic marker bed related to the expansion of Logan International Airport between 1945 and 1950 (Gillette, 1996 and J. Ridge, personal communication) provides two additional known dates to control the chronology of core BIM-14SEP2002-PVC4-7. The large NNE/SSW trending runways of the airport are just 500 m from the mouth of tidal Belle Isle Creek. Massive infilling of Boston Harbor for these runways and other portions of the airport generated large amounts of suspended sediment that form a prominent clayey bed throughout the marsh.

4.2.8 Chronology of marsh sand layers

Sediment core BIM-14SEP2002-PVC4-7 contains 11 sand layers. Five of the sand layers, indicated by the dark green arrow pointers in Figure 58 and Figure 62, are continuous across at least half of the marsh in an E-W direction. Six of the sand layers, indicated by the similar light green arrow pointers in the same figures, are sand layers of only local extent. Presumably, the continuous layers reflect overwash events of greater intensity while layers of only local extent reflect less intense events.

Using the age-depth curve established in Figure 62 for sediment core BIM-14SEP2002-PVC4-7, the age of deposition for each of these sand layers was estimated. To do so, horizontal tie lines were drawn from the sand layers over to the age-depth curve. The ages were determined by the intersection of the horizontal tie lines with the median age value and error envelope for the full, 2 sigma age range. For sand layers deposited more recently than AD 1945, no error envelope is present as the age control in

that part of the core is based on five absolutely dated horizons. Table 13 provides the results in a compiled form.

Table 13—Estimated age of deposition for sand layers in sediment core BIM-14SEP2002-PVC4-7. The year AD is given with a "+/-" error, if applicable. Continuous sand layers are listed in the left column, and sand layers of only local extent in the right column.

Continuous sand layers	**Sand layers of only local extent**
1978	1991
1870 +/- 40	1971
1840 +/- 54	1954
1812 +/- 70	1906 +/- 20
1235 +/- 88	1235 +/- 88
	824 +/- 101

CHAPTER 5

DISCUSSION AND INTERPRETATION

5.1 Graded beds in LML varve record are deposited by hurricanes

As briefly mentioned in the "Graded beds in the LML varve chronology" section of Chapter 4, many of the graded beds from the historic period of the varve chronology correspond with years in which known historical hurricanes have struck the New England area. In fact, this is the case for 13 out of the 17 graded beds (see Table 14 below). For the remaining 4 out of 17 graded beds, one occurs during a year in which a tremendous and legendary nor'easter storm occurs (Minot's Lighthouse Gale of 1851[57]), and one may correspond with a known historical event operating right at the edge of the LML[58].

[57] The Minot's Lighthouse Gale of 1851 occurred on 16-17 April of that year. Recall from the discussion in the "4.1.9.5 Offset between varve year and calendar year" section of Chapter 4 that a varve year from the LML is offset from the calendar year because the varves are divided from one another at the prominent siliciclastic-biogenic transition which occurs in the April-May timeframe (i.e. end of April). Thus, while the Minot's Lighthouse Gale took place in mid-April of 1851, any sedimentary expression of it should occur in the varve from the year earlier (i.e. 1850). In fact, this is exactly what is seen in the LML record—the regular siliciclastic cap for the 1850 varve is followed by a very thin biogenic layer which is immediately followed by another thick siliciclastic cap. In essence, the 1850 varve has a double siliciclastic cap which is not normal. We interpret the second siliciclastic cap from the 1850 varve to have actually been deposited in mid-April 1851 related to the legendary Minot's Lighthouse Gale.

[58] Construction of the Mystic Valley Parkway, the main road which snugly hugs the eastern edge of the LML just meters from the shore, began in 1895 and finished in 1897. Preparations for laying the road would have left large quantities of sediment openly exposed. There is a graded bed in the 1895 varve which is actually more like an episodic accumulation of siliciclastic material as internally it can be seen to be composed of multiple layers. We suggest this episodic accumulation of siliciclastic material is related to having abundant, openly exposed sediment sitting right next to the lake, and not a product of hurricane deposition like the other graded beds.

Table 14—Varve years which contain graded bed from the historical portion of the LML varve chronology. Thirteen out of the seventeen years (shown in bold text) are years in which a hurricane is known to have struck the New England area. The remaining four out of the seventeen years (shown in non-bold text) are not associated with hurricane strikes.

Year AD	*Bird series*
1955	**n/a**
1954	**n/a**
1938	**n/a**
1934	**n/a**
1895	A-2
1869	**B-1/B-2**
1861	**C-3/B-1**
1858	**C-3/B-1**
1857	C-3
1850	C-3
1849	**C-3**
1804	**C-1**
1770	**D-1/C-1**
1727	**E-2/E-3**
1706	**E-2**
1649	G-3
1635	**G-2**

This strong coordination suggests that the graded beds are deposited in the basin as the result of a passing hurricane. In fact, this is not surprising—in the discussion of paleotempestology in Chapter 1, anomalous sand layers, whether they be in a coastal marsh or pond or elsewhere, have been previously recognized as just that—a sedimentary signature that reflects the passage of a hurricane.

This observation just scratches the surface of the relationship between the graded beds and hurricane events. What is the mechanism and source that delivers these sand layers to the lake? Does the thickness of the graded bed have any significance? Is there a graded bed for every known storm, and vice versa?

To begin to answer these questions, a thorough review of the known historical hurricanes that have affected the Boston area is in order, and we use the next section to provide that review.

5.2 Brief history of historical Boston hurricanes

Information about hurricanes which have affected the Boston area during historical times comes from a variety of sources.

For pre-20th century hurricanes, the most useful and comprehensive resource is the *Early American Hurricanes 1492-1870* volume produced by Ludlum (1963). The volume brings together information from many different preexisting works, but also incorporates a large amount of additional research from news reports, diaries, and other historical documents. Importantly, the volume takes a decidedly meteorological tack, and is keenly focused on attempting to piece together details about the development, intensity, trajectory, and outcome of each storm.

For hurricanes from AD 1851 onwards, a primary resource for data is the Atlantic Hurricane Database Re-analysis Project[59]. This ongoing project is run by the Hurricane Research Division (HRD)[60], and its goal is to extend and revise the National Hurricane Center's North Atlantic hurricane database of tropical cyclone tracks and intensities. Additional resources are provided by historical documentation and other printed materials

[59] The URL for the project including all the data is "http://www.aoml.noaa.gov/hrd/data_sub/re_anal.html".

[60] The HRD is a part of the Atlantic Oceanographic and Meteorological Laboratory (AOML) which is, in turn, an Oceanic and Atmospheric Research (OAR) facility which is, in turn, part of the National Oceanic and Atmospheric Administration (NOAA).

which become available in ever-increasing quantities especially throughout the 20th century.

5.2.1 Regarding trajectories and intensities of pre-20th century hurricanes

Modern technology allows us to observe, monitor, and track tropical storms in great detail. For historical storms occurring before such technology, storm trajectories and intensities are reconstructed based on network of observations from both ocean bound vessels and from land. Provided that the network of observations is distributed appropriately, storm trajectories can be reconstructed with a fair degree of accuracy. However, because of the way we measure the intensity of modern hurricanes, it is really only possible to estimate the intensity of these older storms.

The intensity of a modern hurricane is based on its sustained wind speed which is then classified according to the five-category Saffir-Simpson Hurricane Scale. Sustained wind speed measurements are essentially non-existent for pre-20th century hurricanes. But in general, certain levels of wind damage and storm surge heights can be expected for each Saffir-Simpson intensity category. Thus, reports of wind damage and storm surge can be used to provide an estimate of the probable Saffir-Simpson intensity of these older storms. NOAA's National Hurricane Center provides an excellent description of the wind damage and storm surge heights expected for each Saffir-Simpson category, and that is reproduced below in Table 15.

Table 15—Saffir-Simpson hurricane intensity categories according to sustained wind speeds, and the expected wind damage and storm surge levels that would result. This table has been reproduced from NOAA's National Hurricane Center website. The URL for the website is "http://www.nhc.noaa.gov/aboutsshs.shtml".

Saffir-Simpson category	Sustained wind speed, and expected wind damage and storm surge levels
1	Winds 74-95 mph (64-82 kt or 119-153 km/hr). Storm surge generally 4-5 ft above normal. No real damage to building structures. Damage primarily to unanchored mobile homes, shrubbery, and trees. Some damage to poorly constructed signs. Also, some coastal road flooding and minor pier damage.
2	Winds 96-110 mph (83-95 kt or 154-177 km/hr). Storm surge generally 6-8 feet above normal. Some roofing material, door, and window damage of buildings. Considerable damage to shrubbery and trees with some trees blown down. Considerable damage to mobile homes, poorly constructed signs, and piers. Coastal and low-lying escape routes flood 2-4 hours before arrival of the hurricane center. Small craft in unprotected anchorages break moorings.
3	Winds 111-130 mph (96-113 kt or 178-209 km/hr). Storm surge generally 9-12 ft above normal. Some structural damage to small residences and utility buildings with a minor amount of curtainwall failures. Damage to shrubbery and trees with foliage blown off trees and large trees blown down. Mobile homes and poorly constructed signs are destroyed. Low-lying escape routes are cut by rising water 3-5 hours before arrival of the center of the hurricane. Flooding near the coast destroys smaller structures with larger structures damaged by battering from floating debris. Terrain continuously lower than 5 ft above mean sea level may be flooded inland 8 miles (13 km) or more.
4	Winds 131-155 mph (114-135 kt or 210-249 km/hr). Storm surge generally 13-18 ft above normal. More extensive curtainwall failures with some complete roof structure failures on small residences. Shrubs, trees, and all signs are blown down. Complete destruction of mobile homes. Extensive damage to doors and windows. Low-lying escape routes may be cut by rising water 3-5 hours before arrival of the center of the hurricane. Major damage to lower floors of structures near the shore. Terrain lower than 10 ft above sea level may be flooded requiring massive evacuation of residential areas as far inland as 6 miles (10 km).
5	Winds greater than 155 mph (135 kt or 249 km/hr). Storm surge generally greater than 18 ft above normal. Complete roof failure on many residences and industrial buildings. Some complete building failures with small utility buildings blown over or away. All shrubs, trees, and signs blown down. Complete destruction of mobile homes. Severe and extensive window and door damage. Low-lying escape routes are cut by rising water 3-5 hours before arrival of the center of the hurricane. Major damage to lower floors of all structures located less than 15 ft above sea level and within 500 yards of the shoreline. Massive evacuation of residential areas on low ground within 5-10 miles (8-16 km) of the shoreline may be required.

For tropical disturbances that do not reach the minimum of 74 mph to be classified as a hurricane, two other non-hurricane categories exist. A system with wind speeds < 39 mph would be classified as a "tropical depression", and one with wind speeds from 39-73 mph would be classified as a "tropical storm".

While the generalizations about expected wind damage and storm surge levels in Table 15 are useful, the results of a natural process do not always end up like expected. Importantly, historical records are often incomplete, and of a geographically spotty nature; thus, damage accounts might come from areas that were not subjected to maximum wind damage. Combined with the fact that many historical accounts are written from a human-interest perspective (diaries, etc.), or from just a single source, it should be clear why the intensity of these pre-20th century storms can only be estimated.

5.2.2 Storm summaries

Many hurricanes have affected the greater New England area to various degrees during historical times. But given the location of the LML and BIM, it is only the storms that have had a significant effect on the immediate Boston area that are of interest to us. We use this section to summarize those storms whether their significant effects were related to wind, rain, or storm surge. A compilation of estimated storm trajectories is illustrated in Figure 63. Within this section, information on the pre-1870 storms is almost exclusively supplied by the authoritative Ludlum (1963) volume.

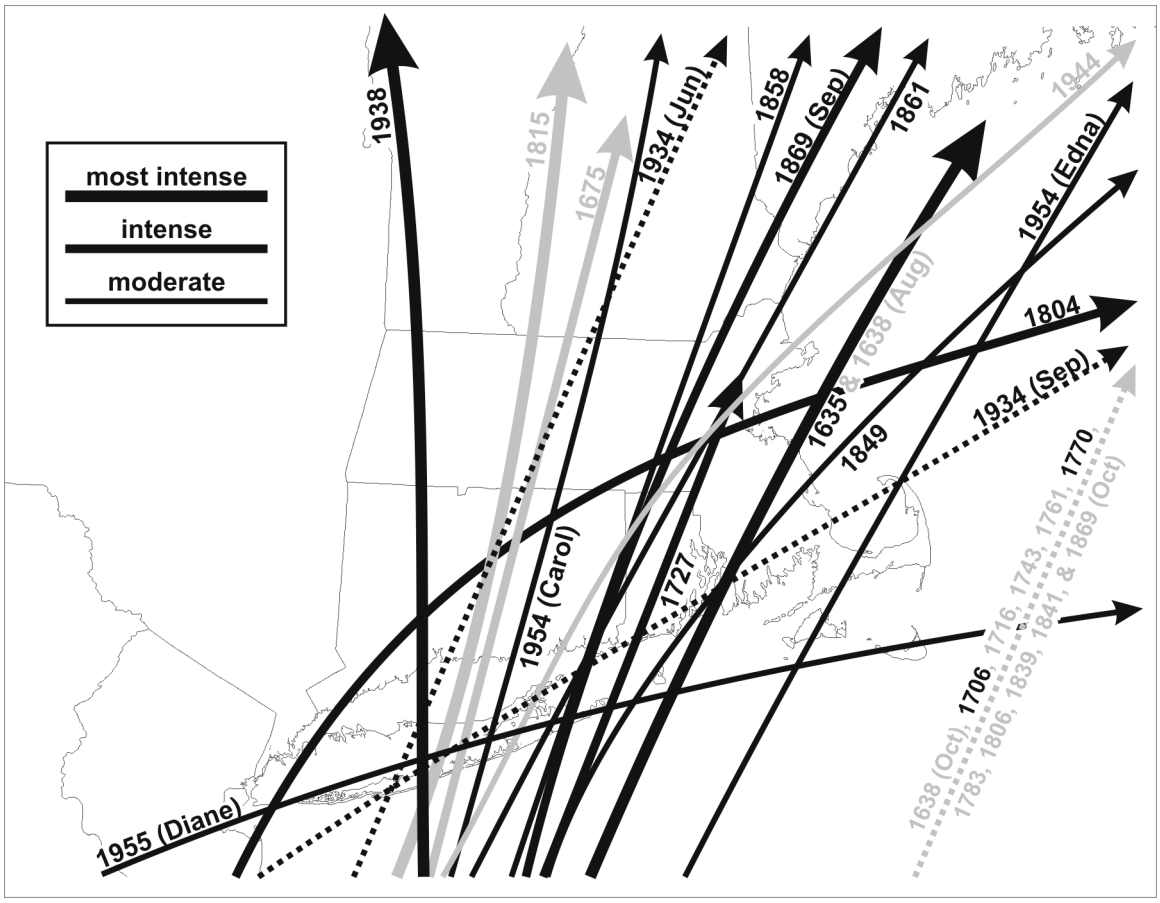

Figure 63—Trajectories of historical hurricanes that have struck the New England area. For the storm tracks illustrated in black (versus gray), an anomalous sedimentary layer, in particular, a graded bed, is found in the LML varve chronology for that year. The dashed arrow at the right indicates various storms that passed off shore, and therefore their precise trajectories are unknown. As intensity for the pre-20th century storms can only be estimated, the three different widths of the trajectory arrows provide a qualitative expression of a particular storm's intensity. Storms categorized as "most intense" probably reached modern Category 3-4 intensity, "intense" storms probably reached modern Category 2-3 intensity, and "moderate" storms probably reached modern Category 1-2 intensity. For the 20th century hurricanes where the actual sustained wind speeds are known, they also use the same qualitative expression of intensity in this diagram, but in the text the actual Saffir-Simpson category is cited. The two dotted 1934 trajectories represent a special case because one of the two storms, probably the September one, left a graded bed in the LML varve record, but both of the storms probably did not ever reach "moderate" intensity as described above.

5.2.2.1 The Great Colonial Hurricane of 1635

Ludlum (1963) provides an excellent summary of the Great Colonial Hurricane, a very intense storm that struck the Boston area on 25 August 1635, only 15 years after the Pilgrims landed at Plymouth, and just five years after the first land claim was made in the vicinity of the LML. The path of this hurricane brought it directly between Boston and Plymouth (Figure 63), and the result was catastrophic.

It is perhaps best described by the observers of the day. One account comes from John Winthrop, governor of the Massachusetts Bay Colony, who Ludlum (1963) describes as a very conscientious observer of weather-related matters.

> "Aug. 16 The wind having blown hard at S. and S.W. a week before, about midnight it came up at N.E. and blew with such violence, with abundance of rain, that it blew down many hundreds of trees, near the towns, overthrew some houses, and drove the ships from their anchors…About eight of the clock the wind came about to N.W. very strong, and, it being then about high water, by nine the tide had fallen three feet. Then it began to flow again about one hour, and rose about two or three feet, which was conceived to be, that the sea was grown so high abroad with a N.E. wind, that, meeting with the ebb, it forced it back again…This tempest was not so far as Cape Sable, but to the south more violent, and made a double tide all that coast…The tide rose at Naragansett [sic] fourteen feet higher than ordinary, and drowned eight Indians flying from their wigwams."

Another important contemporary account comes from William Bradford in his history about the early years of the Plymouth Plantation. Bradford wrote:

> "This year, the 14th or 15th of August (being Saturday) was such a mighty storm of wind and rain as none living in these parts, either English or Indians, ever saw…It began in the morning a little before day, and grew not by degrees but came with violence in the beginning, to the great amazement of many. It blew down sundry houses and uncovered others. Divers vessels were lost at sea and many more in extreme danger. It caused the sea to swell to the south wind of this place above 20 foot right up and down, and made many of the Indians to climb into trees for their safety…It blew down many hundred thousands of trees, turning up the

> stronger by the roots and breaking the higher pine trees off in the middle…The signs and marks of it will remain this hundred years in these parts where it was sorest."

These accounts identify an impressive storm surge along the southern New England coast, somewhere between 14-20 feet. But these extreme values were only reached because of the configuration and orientation of Narragansett Bay which acts as a funnel—on a straight coastline the water level heights would have probably not reached such extreme values. Nonetheless, together with the reports of massive wind damage, this suggests the storm was of great intensity, probably of at least Category 3, and possibly up to Category 4 intensity given expected damage descriptions in Table 15 above. Only two other hurricanes of similar size and intensity (AD 1815 and 1938) have struck the New England area since the arrival of European settlers.

While the storm surge along the southern coast of New England was quite severe, according to Winthrop's account, it was not nearly as significant within the Bay of Massachusetts. In fact, during high tide, winds from the NW actually lowered the tide by about three feet[61].

---

[61] There is one contradictory account about the level of storm surge in the Boston area by Perley (1891) in his *Historic Storms of New England* book. In his account of this storm, he wrote, "The wind caused the tide to rise to a height unknown before. At Boston it measured twenty feet, and was brought in twice in twelve hours. The Narragansett Indians were obliged to climb into the tops of trees to save themselves from the great tide in the region." First of all, Perley was not a contemporary of the event, and wrote his volume some 260 years later based on New England folklore, legends, and his own research. Second, it appears he might have mixed up some of his references during research which would have been easy to do in the late 19th century without the benefit of modern technology. In particular, he mentioned a surge of 20 feet in Boston. Recall it was William Bradford of Plymouth Plantation that mentioned a storm surge of 20 feet (Governor Winthrop reported 14 feet). But Bradford mentioned that the surge was "to the south wind of this place." As Bradford was located at Plymouth, the water body directly to the south of that location is Buzzard's Bay, a SW-facing bay directly to the east of Narragansett Bay. Given the report of a 14 foot storm surge in Narragansett Bay, it is very probable that the likewise situated Buzzard's Bay would have experienced something similar. Therefore, we conclude that Perley's account of a 20 foot storm surge in Boston is probably not correct given that the two contemporary accounts place the major surge as being along the southern New England coast.

5.2.2.2 The Triple Storms of 1638

Ludlum (1963) mentions that three storms of probable tropical origin that passed by the New England area during 1638 (Figure 63), but only the first two appear to be of any significance and will be discussed here. The primary reference for these storms again comes from John Winthrop.

Regarding the first storm which passed on 13 August 1638, Winthrop wrote that,

> "…in the night was a very great tempest, or hiracano at S.W. which drave a ship on the ground at Charlestown, and brake down the windmill there, and did much other harm. It flowed twice in six hours, and about Naragansett, it raised the tide fourteen to fifteen foot above the ordinary spring tides, upright."

The storm appears to have generated a significant storm surge along the southern New England coast, in fact, about the same magnitude as that raised by the Great Colonial Hurricane just three years earlier. But the overall intensity of the storm appears to be nothing like that of the 1635 storm given that there is nowhere near the same degree of wind damage. For certain, when the next moderately intense hurricane passed in 1675, comparisons of it were made not with this 1638 storm, but directly back to the 1635 hurricane. So despite the rather large storm surge along the southern New England coast, our conclusion is that this storm was not very intense.

Regarding the second storm which passed by on 5 October 1638, Winthrop wrote that,

> "Being the third day of the week and two days before the change [equinox?], the wind having blown at N.E. all day, and rainy in the night, was a mighty tempest, and withal the highest tide, which has been since our coming into this country; but through the good providence of God, it did little harm."

This second storm also apparently generated a storm surge, and since Winthrop did not mention it was focused on the southern New England coast, we assume that it occurred within the Bay of Massachusetts. That said, given his comment about "little harm", it seems obvious that this was not a very intense storm.

5.2.2.3 The New England Hurricane of 1675

Several sources document a hurricane that passed through central New England (Figure 63) on 2 September 1675 according to Ludlum's (1963) analysis. Simon Bradstreet reported a "dreadful storm of wind and rain at East" from New London, CT, and just 16 km to the east in Stonington there were reports of blow down of crops and "multitudes" of trees. Ludlum (1963) also reported that further east in Rhode Island, Peter Easton made a comparison of the storm to the Great Colonial Hurricane of 1635, and mentioned that it had knocked down his windmill. Ludlum (1963) also mentions an account from the Boston area by John Hull who wrote in his diary that,

> "a very violent storm, that exceedingly blew down the Indian corn and the fruit of trees; did much spoil on the warves, and among the ships and vessels in Boston, to value supposed a thousand pounds."

Ludlum (1963) concluded that this hurricane was one of the most destructive hurricanes that has hit the New England area during historic times, and that it should fall, "just a notch below the great storms of 1635, 1815, 1938, and 1944." We are not entirely in agreement with this interpretation because the contemporary reports of wind damage show it to be significantly less than that produced by the earlier 1635 hurricane (and several other storms we summarize below). For example, the "multitudes" of trees blown down at one spot in Connecticut seems quite different than the reports of whole forests

being blown down by the earlier storm. For certain, in the immediate Boston area the wind damage is significantly less—it only succeeded in blowing down crops and shaking fruit from trees. Part of the difference for the Boston area may be explained by the fact that this 1675 hurricane followed a track through central New England at least 100 km to the west of the 1635 hurricane. Another consideration is that this 1675 hurricane did not even make it into Perley's (1891) account of historic New England storms partially based on folklore and legend. Overall, we are cautious about Ludlum's (1963) assessment of the intensity of this storm, and think it is probably too high except for limited areas. With regard to the Boston area itself, based on the reported wind damage, we suggest the storm would have been perceived there as of moderate intensity.

5.2.2.4 The Stormy Season of 1706

Ludlum (1963) suggests that several storms of tropical origin appear to have passed by the New England area in late 1706 (Figure 63), but very limited information is available. In particular, the Boston News Letter[62] reported that New Haven, CT received excessive rains from 14-16 October 1706, so much so that it produced an unusual flood on the Connecticut River that carried away 1000 bales of hay. From the same source, there is a report from New York from 14 October which reads,

> "We have great rains here and mighty Floods; They write from Albany, that the late great Rains has caused the greatest Flood there that

[62] The Boston News Letter was published from 1704-1776, and passed through the hands of several owners during its lifetime. The name of the paper also changed a couple of times, and was later known as the Weekly News Letter, and finally as the Massachusetts Gazette (source: http://www.aejmc.net/newspaper/WDSloan-BostonNews.html). We mention this now as Ludlum (1963) used this newspaper in one of its several incarnations as a primary source for information about storms during its 72 year existence.

> ever was known; they say that Renslaers[sic] Island was 6-foot under water, and that it drowned their low lands."

Ludlum (1963) provides no accounts of this storm directly from the Boston area, but again, he specifically mentions that the sources for this mid-October storm are "meager".

A second, severe storm apparently passed offshore between Virginia and New England just a few weeks later on or about 6 November 1706. According to Ludlum (1963), a fleet of ships bound for England was scattered by great winds when it was just two days from port in New England. Similarly, he reports that another fleet from Virginia saw 14 of its ships sink, gave up on several others as lost, and had to send many of the ships back to Virginia to repair extensive wind damage to masts and sails (Ludlum, 1963).

It is somewhat difficult to assign estimates of intensity to these storms because documentary sources are so minimal. An obvious characteristic of the first storm mentioned above is that it was a prodigious rain producer. Unfortunately, there are no accounts directly from the Boston area. Regarding the intensity of the second storm mentioned above, the information that is available seems to suggest that the storm may not have significantly affected land, but was certainly significant at sea.

5.2.2.5 The 1716 Hurricane

Ludlum (1963) identified a violent storm of wind and rain in eastern Massachusetts on 24-25 October 1716, and related it to the passage of a hurricane off shore of New England (Figure 63). The only reference to the storm from the Boston area

comes from Samuel Sewall (Ludlum, 1963). He briefly noted in his diary that, "many trees, fences, etc. blown down." In fact, Ludlum (1963) notes that the local newspaper, the Boston News Letter, made no mention of the storm after its passage.

Apparently, the more severe effects of the storm were felt on outer Cape Cod, Martha's Vineyard, and further off shore. An account from the Cape, for example, mentions that the Sunday mass in Eastham was cancelled because of the excessive wind, and from Martha's Vineyard a diarist reported a violent wind and rain storm (Ludlum, 1963). Though the Boston News Letter did not mention the storm after its passage, as ships that met the storm at sea arrived to port, it did publish some reports about what they experienced. For example, one ship bound for Europe reported high winds about 30 leagues (equivalent to about 170 km) off shore, and it was also reported that 6 or 7 ships that made port in New Hampshire had lost their masts in the storm while at sea (Ludlum, 1963).

Ludlum (1963) did not attempt to categorize the intensity of this storm, but we interpret it to be one of the less significant hurricanes that affected the Boston area. While there is the single, brief Sewall account, it is exceedingly curious that the Boston News Letter did not mention the storm after its occurrence. In fact, this newspaper proved itself to be a keen observer of other extreme weather events throughout its 72 year history (see Footnote 62). For example, it did mention other hurricanes which affected the Boston area including those in 1727, 1743, 1761, and 1770. That this storm was not even cursorily mentioned in the pages of that publication suggests that it was not very memorable at least for the Boston area.

5.2.2.6 The Hurricane of 1727

The Hurricane of 1727 was a compact, but intense storm that literally cut a path of destruction through Rhode Island, the Boston area, and northeastern Massachusetts before finally makings its way out to sea once again (Figure 63). The passage of the storm on 27 September was impressive and memorable, so much so that when a hurricane of similar intensity and characteristics passed through the same area 77 years later in 1804, some of the older residents made comparisons directly back to the earlier 1727 storm (Ludlum, 1963). The intensity of the 1727 hurricane was significant—it literally ripped up hundreds of trees by their roots along its entire path over land.

Thanks to the ever increasing population and availability of printed materials such as newspapers, Ludlum (1963) was able to provide a thorough summary of this hurricane. For example, from the coastal Connecticut and Rhode Island area where the storm made landfall come reports of wind, rain, and many uprooted trees. From Swansea, RI in Narragansett Bay, another account mentioned that the storm "blew up trees by the roots in abundance; blew down several chimneys, and blew off the roof of a house, and blew sundry vessels on shore," (Ludlum, 1963).

From further northeast along the path of the hurricane, Ludlum (1963) points out the Weekly New Letter of Boston which published the following excerpt:

> "On Saturday last…we had here a violent storm of wind and rain, which lasted till about midnight, whereby great damage was done to the wharfs and shipping in the harbor, as also to the fruits of the earth, and to many buildings: Many trees blown up by the roots, and chimnies blown down: a kitchen chimney of Mr. Jacob Sheaf's at the bottom of the Common, blew down and beat on the roof, which killed a child of about 7 years of age, wounded two others, and broke the bone of Mrs. Sheaf's leg."

Ludlum (1963) points out that many ports northeast of Boston suffered great damage. For example, from coastal Marblehead about 20 km northeast of Boston, the following account was given:

> "The last Saturday we had a most terrible storm of wind and rain, such as has not been known among us, which began about noon and continued to about twelve at night. The wind was at N.E. and N.E. by N. which brought in a very high tide… It blew up many trees by the roots."

And from further north in the area of Newbury, Ludlum (1963) identifies the diary account of Stephen Jacques who wrote that:

> "In the month of September on Saturday in the afternoon the wind began to be strong and increased more in the night. It blew down and brake six trees in my old orchard and trees all over the woods. There never was the like known. It twisted young walnut trees in the midst. It raised a great tide, which swept away near two hundred loads of hay that was in swath."

In summary, the Hurricane of 1727 was a storm of very significant intensity as evidenced by the fact that it ripped up trees by their roots over its entire track across land. Telling also, are some of the quotes which suggest people had never experienced a storm of such intensity. According the verbal descriptions of storm damage presented in Table 15, it seems that this storm would have been ranked as at least a Category 3 storm on the Saffir-Simpson intensity scale.

5.2.2.7 Benjamin Franklin's Eclipse Hurricane of 1743

Though the Hurricane of 1743 passed off shore of New England (Figure 63), it is remembered for the very large storm surge it raised from the Boston area northwards into

New Hampshire[63]. Several accounts about the storm are available from Boston area sources.

Ludlum (1963) points out the 2 November 1743 entry in a meteorological register kept by John Winthrop[64] of Harvard College in Cambridge. Winthrop wrote:

> "NE by N. worst in years—great damage on land as well as at sea. Barometer 29.35". Tide within 4" of 20 years ago[65]. Storm abated about 7 P.M. Barometer lowest at 2 P.M."

Ludlum (1963) also points out three additional accounts by the Boston press. The Boston Evening Post provides the first account which also helps constrain the duration of the storm to about 22 hours[66]:

> "Last Friday night, soon after a total and visible eclipse of the Moon (which began about nine and ended past one o'clock) came on a storm of wind and rain, which continued all the following day with great violence, and the wind being at N.E, the tide was raised as high within a few inches, as that remarkable one about 20 years ago…the greatest damage by far has been done here, that was ever known to be done by a storm in the memory of man."

A second account comes from the Boston Post Boy:

---

[63] An interesting point explains why Ludlum (1963) chose the name he applied to this storm. The track and timing of this hurricane brought it from the Philadelphia area up past Boston during the evening on which a total lunar eclipse was occurring. The position of the storm prevented the eclipse from being seen in the Philadelphia area where Benjamin Franklin was resident. But his brother in the Boston area was able to see the eclipse because the storm did not arrive to that area till later. Franklin used the time difference between the storm at both locations to infer its southwest to northeast movement which, according to Ludlum (1963), was the first tangible step in the scientific process of understanding storm motion.

[64] This "John Winthrop" is obviously different from the earlier John Winthrop, governor of the Massachusetts Bay Colony, who commented on the Great Colonial Hurricane of 1635 as discussed in the "5.2.2.1 The Great Colonial Hurricane of 1635" section above.

[65] Undoubtedly, Winthrop is referring to the legendary flooding of Boston Harbor that occurred in February 1723 with this comment about "Tide within 4" of 20 years ago." That 1723 flood was not related to the passage of a tropical system, but a nor'easter storm. According to Perley (1891), the 1723 flood level reached 20" higher than any previous storm, and that level was only ever exceeded once again in April 1851 by a similar nor'easter storm.

> "The wind being excessive high vast damage was done to the wharves and shipping, some vessels that got loose were drove ashore higher up than was ever known before, and several small vessels were cast upon the wharves and boats floated into the streets… Tis impossible to enumerate all the particulars the terrible effects of this storm or estimate the damage sustained by it."

The third account comes from the Boston News-Letter:

> "At noon the wind seemed to blow in prodigous[sic] gusts, and with the greatest fierceness and brought in an exceeding high tide, which overflowed most of our wharves, and came up into several streets higher than has been known for these twenty years past."

It is somewhat difficult to assign an intensity to this storm because it followed an unknown trajectory off shore. For certain, its obvious notable characteristic is the water level reached by the storm surge. While the wind associated with this storm was also fierce, it seems to have really only affected the immediate coastal zone and ports. For example, the various accounts are almost exclusively focused on the damage at the ports, and make essentially no mention of trees blown down further inland. This is in great contrast to the damage reports following the 1635 and 1727 hurricanes where inland wind damage was severe. If the path of this 1743 hurricane had brought it closer to land, certainly the wind damage would have been more severe. But its off shore track left its relative intensity on land greatly diminished where it reached only a moderate intensity.

5.2.2.8 The Southeastern New England Hurricane of 1761

Ludlum (1963) documented another strong hurricane which passed off shore of New England on 23-24 October 1761 (Figure 63). The storm wreaked its greatest havoc

---

[66] The storm began soon after the eclipse started which was at 9:00 pm according to the Boston Evening Post. And according to Winthrop's account, it ended about 7:00 pm the next day.

in Rhode Island and southeastern Massachusetts. For example, Ludlum (1963) cites the following account from the area of Providence, RI:

> "…on both roads east and west so far as we have heard, the roofs of houses, tops of barns, and fences have been blown down, and it is said thousands of trees have been torn up by the roots by the violence of the above storm."

Damage was not just produced by the wind—a storm surge of unspecified height combined with the wind to destroy the Weybosset Bridge in Providence at the head of Narragansett Bay (Ludlum, 1963).

Though Boston did not lie within the zone of greatest destruction, it also experienced winds of great intensity according to accounts from that area pointed out by Ludlum (1963). For example, Edward Holyoke, the President of Harvard College in Cambridge, called it, "as great a storm as I have ever known," and another account from Dedham also mentioned whole trees that had been pulled up with their roots. According to Ludlum (1963), the Boston News Letter reported the event as "the severest NE storm of wind and rain that has been known here for 30 years past," probably in reference to the severe 1727 hurricane.

Accounts from the Boston area also provide a reference for the duration of the storm as well as brief meteorological details (Ludlum, 1963). In particular, John Winthrop, the same fellow who provided information about the 1743 storm, mentioned that the severe part of this storm began about 9:00 pm on 23 October, and ended by 2:00 am the following day. This seems relatively brief given that the effects of other storms such as the 1770 hurricane discussed below lasted about a day. Given that the greatest destruction was centered to the southeast of Boston and in Rhode Island, it's possible that

the severe portion of the storm lasted longer in those areas. Winthrop also recorded a barometer reading taken at the height of the storm reporting it as 29.57", and classified the wind as coming from the northeast at his force 4[67], the highest rating he used (Ludlum, 1963).

Despite its off shore trajectory, the 1761 hurricane appears to have been a storm of significant intensity. Overall, it would probably be classified a notch below the 1727 hurricane from about a quarter of a century earlier, in particular, in the areas where it was most destructive (Rhode Island and southeastern Massachusetts).

5.2.2.9 The Late Season Storm of October 1770

Another hurricane of great intensity passed by the New England coast on 19-20 October 1770, and despite its off shore track (Figure 63), it raised an impressive storm surge that slightly surpassed the tremendous surge raised by the 1743 hurricane[68] just 27 years earlier (Ludlum, 1963). Accounts of the storm are available in locations that stretch from coastal Connecticut all the way up to coastal Maine.

---

[67] Ludlum (1963) does not provide details about what this "force 4" means except that it was the highest rating Winthrop had available. We interpret this to mean it was probably based on a qualitative scale that Winthrop used personally, or that may have been in general use at the time.

[68] Determining the absolute level reached by a historical tide or storm surge is sometimes difficult because references are often given as relative to the water levels reached by other storms. For example, the water level associated with the 1743 hurricane was said to have reached just 4" below the level that occurred during the 1723 harbor flood. But then the water level associated with the later 1770 hurricane was said to have been only surpassed by the 1723 harbor flood level itself. So this means that the 1770 water level fell within the 4" range between the 1743 and 1723 levels. What then was the water level for the 1723 harbor flood? According to Perley (1891), "it was twenty inches higher than any had been known to rise before." But that was in 1743—in another spot we hear from Perley (1891) that the 1723 level was actually exceeded in just one instance that being 1851. Thus, all the relative relationships allow us to conclude the following sequence of increasing water levels: 1743, 1770, 1723, and finally 1851. The good part about knowing at least the relative relationships is that when one absolute value is determined, an absolute value can be computed for each of the other levels.

From the Connecticut area, Ludlum (1963) points out the meteorological account of Ezra Stiles who wrote that the storm was “a violent hurricane. Wind N or NE. Rain violent—hail—vane of church steeple blown off—cleared up after 1500.” Ludlum (1963) notes that, “the mention of hail (probably actually ice pellets or modern sleet) would indicate that a very cold air mass lay to the west of the storm track over western and northern New England, a situation that would certainly intensify the storm circulation.”

According to Ludlum (1963), the Boston area lay within a track of high winds. He pointed out several accounts from the Boston area to support this. For example, the Massachusetts Gazette wrote that:

> "…a most violent storm came on the wind about NNE, attended with rain and hail. The tide rose about noon to such a height that it overflowed most of the wharves in this town…it is said that the tide rose higher than has ever been known, excepting once about 47 years ago, it rose a foot higher."

The veteran weather observer in Cambridge, John Winthrop, also provides some useful observations as usual (Ludlum, 1963). He recorded a very low barometer reading of 28.96” at 3:00 pm on 20 October, and at that point he classified the wind as blowing at force 3, his second to highest rating (see Footnote 67 above for more information). Commenting that, "a great storm does a vast damage," he noted that the rain and hail continued into the evening for a total precipitation figure of 2.48 inches (Ludlum, 1963). Interestingly, this account also allows us to conclude that the storm lasted for about 24 hours as it started on the evening of the previous day.

More reports are available from New Hampshire and Maine to the north showing the large extent of this storm. For example, the Massachusetts Gazette published

accounts from Portsmouth, NH where some buildings and many fences were blown down, and the storm surge caused damage to the wharves (Ludlum, 1963). From Bedford, NH, about 60 km inland, Ludlum (1963) points out the account of Matthew Patten who described the event as a very great storm of rain and hail, and who mentioned it rained steadily there for 24 hours[69]. Finally, as far north as Portland, ME, Rev. Thomas Smith wrote that it was "an exceeding great N.E. storm."

Regarding the intensity of this storm, on first glance it seems similar to the 1743 hurricane, in particular, because both raised very high storm surges. Neither of the storms appear to have caused large amounts of tree blow down so they were obviously less powerful than other storms such as the Hurricane of 1727. One significant difference between the 1743 and 1770 hurricanes, however, is that the 1770 hurricane seems to have affected a much larger area from southern New England all the way up to northern New England. Importantly, the account from Bedford, NH about 60 km inland shows that the effects of this hurricane such as significant precipitation were not just confined to the coast, but extended inland. Like the 1743 hurricane, if the track of this storm had brought it closer to land, certainly the wind damage would have been more severe. Thus, we conclude that the 1770 hurricane should probably be classified as a moderate intensity storm, but one that had a significant effect over a very large area.

[69] This supports our interpretation in the paragraph above that the storm lasted about 24 hours according to material from John Winthrop.

5.2.2.10 The Stormy October of 1783

Ludlum (1963) identified two storms of probable tropical origin that passed off shore of New England in October 1783 (Figure 63). In general, their effects on the Boston area seem rather limited, but they are covered here for the sake of completeness.

The first storm arrived on 9 October 1783, and was mentioned in short accounts from Connecticut to Massachusetts according to Ludlum's (1963) research. A report from the New Haven area, for example, mentioned "a severe northeast storm; and the fullest tide that has been known these forty years[70], which has done considerable damage along shore by carrying off fences, lumber, etc." From the Boston area, Ludlum (1963) points out comments from two different sources, "Last Thursday night we had the severest north east storm that has been felt for a number of years," and, "a very severe storm of rain."

Ludlum (1963) reports that the second storm passed by on 18-19 October, and short accounts of its passage are available from Connecticut all the way up through New Hampshire and Vermont. The intensity of this storm was apparently less than the first storm that month, and the storm surge was unremarkable, but this second hurricane produced a significant amount of precipitation at least in Bedford, NH (Ludlum, 1963). From New Haven, CT comes the following account:

> "Saturday evening last there came on a violent storm of wind and rain, which continued for 24 hours; but happily the tide not being very high, there was little damage done in our harbor."

From the Boston area, Ludlum (1963) notes that the residents there considered this second storm more severe than the first one, but reported very little damage from

storm surge. From Ipswich in northeastern Massachusetts, Ludlum (1963) quotes Manasseh Cutler as reporting, "a very severe storm of rain attended with excessive winds from the northeast…towards the close of the storm on the 19th a considerable quantity of snow fell, but soon melted."

According to Ludlum (1963), Matthew Patten of Bedford, NH reported the following:

> "18th Was a great rain all day and the whole night following.
>
> 19th Rained all the fore part of the day. Hard in the afternoon. It snowed until some time in the night. It fell two inches deep or more. The wind at NE. All this storm was violent and tedious.
>
> 20th The rain made a good freshet."

Regarding the intensity of these storms, the nature of the historical accounts does not seem to suggest they were very extraordinary in the Boston area. In fact, the effects seem rather insignificant when compared against the other storms which have been discussed. Thus, for the Boston area in particular, we interpret the effect of these two storms as insignificant.

5.2.2.11 New England's Snow Hurricane of 1804

Based on more than 20 contemporary documentary sources, Ludlum (1963) provides a lengthy summary of a compact, but intense hurricane that moved up the Atlantic coast, cut across southern New England, and then passed directly over Boston and Salem, MA on 8 October 1804 (Figure 63). The storm caused a tremendous amount of damage, and according to Ludlum (1963) was widely considered to be "the severest

[70] Ludlum (1963) suggests this is a reference to the high water levels produced by the 1743 hurricane.

blow on record," at the time. But within a decade this storm was almost all but forgotten because it was eclipsed by the Great September Gale of 1815, one of just three large, extremely intense hurricanes that have affected the New England area since the arrival of European settlers (Ludlum, 1963).

From the Yale University campus in New Haven, CT there are reports of the storm which began about 6:00 am and provided a very heavy rain till about midday according to Ludlum (1963). In the early afternoon, there was a lull in the storm, but by 6:00 pm, a driving rain had returned, and violent, gale-force winds continued throughout the night. The observers measured a total of 3.66" of precipitation for the event (Ludlum, 1963).

An account of the event from New London is very similar—a violent gale beginning in the morning, followed by a lull in the early afternoon, followed by a return to gale-like condition until late in the evening (Ludlum, 1963). From Providence, RI further to the east, Ludlum (1963) cited an account which said, "during the course of the night, this town experienced the heaviest gale within the recollection of any of its inhabitants."

Moving up the coast to the Boston area, another very similar report is provided. Wind picked up to gale conditions from the south-southeast during the morning later shifting to the east and gaining strength till about 3:00 pm. There was then a lull for a few minutes, followed by resumed winds from the northeast, "with a violence and fury unprecedented in the annals of this town." It was strong enough to topple the steeple of the North Church, and send the tower roof from another church sailing 200 feet through the air (Ludlum, 1963).

Continuing further up the coast, the reports from Salem, MA show that it had been dealt a severe blow (Ludlum, 1963). From that town, Edward Holyoke provided an account of how the storm began about 9:00 am, brought rain and thunder the whole day, and then in the evening the wind became violent again, and raged the rest of the night (Ludlum, 1963).

Continuing northward, the next account Ludlum (1963) points out comes from Portsmouth, NH. The damage there was surprisingly light; in fact, they reported that, "in the town no damage was done, except blowing down some trees and fences—nor was any material injury to vessels in the harbor." Fortunately, Portsmouth and areas further north were spared the brunt of the high intensity winds seen to the south because of the compact nature of the hurricane.

Ludlum (1963) also pointed out an absolutely stunning diary account of the event and its results by Rev. William Bentley who also lived in Salem. According to Ludlum (1963), Bentley was an experienced weatherman, and kept a meteorological register of local events. Following Ludlum's (1963) example, we quote Bentley's diary entry in full given its extraordinary nature and usefulness for understanding the 1804 hurricane:

> "This morning the wind was in the South and the weather uncertain. About 7 it shut down and it began to rain at S.E. and soon the wind rose and the wind changed to N.E. Its violence increased till sundown and continued all night. The barn belonging to Perkins on the Neck, was blown down and one horse killed. Beckets barn down, all vessels drove from their anchors. Chimnies were blown down, roofs and windows injured and trees destroyed in great number. The fences suffered so much that in the eastern part of the Town which I visited it was easy to pass over any lot in that part of the Town. The damage is so equally divided that few have special cause to complain. It was the heaviest blow ever known in Salem and it will be remembered as the Violent Storm of 9 Oct. 1804. We had thunder and lightning all day. We lost the Railing from the top of the house in which I live. It was totally destroyed.

We are every moment receiving accounts of the injuries done by the Storm. The Vessels in Cape Ann and Marblehead that were at anchor are ashore. The damage done in Boston is great. The celebrated Steeple of the North Church is blown down. Mr. Atwater Phippen who for many years has noticed the fall of rain, distinguished the rain of yesterday as the greatest he ever knew, four inches fell in the day and three inches in the night.

Continued account of the Storm. From the Coast, accounts general only as yet. Roads everywhere much obstructed by the fall of trees, etc. Revere's Buildings over his furnace destroyed. Not of great value. Covering of Chapel Church tower blown down. Mr. Eaton at Boston, new brick walls tumbled upon his old house from which he had just time to escape. The woman who lived with him killed, servants wounded. The spire of Charleston steeple bent down. The top of Beverly steeple blown off. The dome of the Tabernacle in this town uncapped, and shattered the Lantern. A vessel from Cape Ann harbour, belonging to Kennebunk, lost her anchor and split her sails and drove up over our Bar into the Cove within the Beacon upon Ram Horn rock. This is the only Vessel ashore on our coast not in the Harbour. The Boston account is an almost total destruction of all small boats at the wharves. The damage to Houses, buildings, trees, fences, etc. is incalculable, but such losses not heavy to individuals, but a distressing loss to the public.

This day I rode through south fields and Marblehead farms to Nahant. Every where trees are blown down and barns unroofed and the road in several places would have been impassable had it not been cleared. Even at Nahant Great head, Wood lost part of the roof of his new Barn erected this year. The reports are endless, but we cannot distinguish truth from falsehood at any distance from home at present. But the reports shew[sic] the state of the public mind. The quantity of seaweed driven up is beyond any former example. I had a good opportunity of examining a rich variety on every part of Nahant. The most common there in deep water is the Kelp, the seagrass and the wrack as they are called. The Dulce Conpici, etc. were in less abundance. It would not have been imagined that the beaches over which we passed had ever been used for pleasure had they been seen only after the late storm.

I cannot refuse to adopt the belief that the late storm was the most severe ever felt in this part of America. All the accounts which I have seen represent nothing like it. In Boston, the old people are said to represent that a storm like it happened 16 September 1727. As yet I have found no tradition of such a storm among our old people or upon record or any report of its consequences. I suspect as our winters have less horrour we partake more of a southern climate from the great quantity of heat and consequently have more stormy weather of this kind and therefore may

> expect more of it in future years. I can find no history of wharves, ships, trees, houses, fences, out houses which lead to suspect great calamities from high winds. From Cape Ann we learn that many of their boats were lost entirely and some greatly injuried by the storm. But we have hopes from the news from Plymouth and Portland, that the storm was much more limited than we have expected from its great severity here and near Boston."

One of the curious characteristics of this storm which led to the name Ludlum (1963) applied to it is that it resulted in significant snowfalls in many areas as it met a high pressure, cold air mass descending from Canada. Ludlum (1963) concluded that this would have increased the pressure gradient and overall intensity of the system. As far west as the Rochester, NY area, heavy rains gave way to snow which essentially melted as it fell (Ludlum, 1963), and by the day after the storm accumulating snow stretched from the hills of southern Connecticut up into Canada. Significant amounts accumulated in some localities; for example, up to 18" was reported in the Catskill Mountains of New York, 24-30" of snow was reported in the Berkshire Mountains of western Massachusetts, and 3-4 feet was reported from some of the higher areas of Vermont's Green Mountains (Ludlum, 1963).

Regarding the intensity of this storm, it is clear from the contemporary accounts of damage and devastation that it was of at least a very intense nature perhaps even edging towards the most intense class. Quite telling was the fact that it was considered by many to be the severest blow on record, that is until the arrival of the Great September Gale of 1815 about a decade later. Ludlum (1963) opined that the 1804 storm might have packed the same wallop as its 1815 brethren, but at a much reduced scale on the local level. One other consideration regarding the intensity is that because of its interaction with the descending air mass from Canada, the hurricane may have been intensified. But at that

point it would not have been a truly tropical system anymore, so it may be inappropriate to fit it into a class meant for tropical systems.

5.2.2.12 The Great Coastal Hurricane of 1806—II

Ludlum (1963) documented a hurricane that passed by the New England area on 23-24 August 1806. The storm followed an unknown track offshore (Figure 63), and apparently dealt Cape Cod and the Massachusetts islands a significant blow, especially flooding rains. The storm's effect on the Boston area was essentially inconsequential, but nonetheless it is covered here for the sake of completeness.

Ludlum (1963) provides an account from Edgartown on Martha's Vineyard where the storm was accompanied by torrents of rain on 23 August. By the evening it had stopped, but picked up again in the night to a very severe gale. Importantly, Ludlum (1963) identified an observer who noted that a previously empty barrel was now filled by 30" of rain thanks to the storm. The observer suggested the barrel actually missed another 6" for a grand total of 36" of rain that fell during the storm[71]. Agricultural crops apparently suffered great damage during the storm.

Ludlum (1963) provides another account that comes from the town of Brewster on Cape Cod where the winds and rains apparently caused a huge destruction of crops, and a salt works. According to Ludlum (1963), the quantity of rain there was also apparently exceptional as an observer noted that, "It is supposed there is 18 inches of water on the level."

---

[71] The figure of 30" of rain seems rather exceptional and perhaps unbelievable. To keep things in perspective, the maximum precipitation recorded in Boston during any 24 hour period of "modern"

The Boston area was hardly affected by the storm because it was too far to the west of the heavy rain belt. In fact, no accounts of extraordinary weather were published. The only obvious clue that would indicate the passage of the storm was a rain gauge measurement that recorded a 0.40" rain fall between noon and 1:00 pm on 24 August.

5.2.2.13 The Great September Gale of 1815

Ludlum (1963) identifies the Great September Gale of 1815 as the second of just three massively-sized, intense hurricanes that have struck the New England area since the arrival of European settlers (the other two storms include the Great Colonial Hurricane of 1635 and the New England Hurricane of 1938). The path of this storm brought it across Long Island and then up through central New England on the morning of 23 September 1815 (Figure 63). A wealth of written material is available to document this storm partially because of the ever increasing quantity of written records, but more importantly because the storm was extraordinary, and it forced people to take note.

According to Ludlum (1963), the storm itself had a significant forward velocity of about 50 mph when it made landfall close to Saybrook, CT at the mouth of the Connecticut River at about 9:00 am. Ludlum (1963) carefully traced its path, and suggests it followed a path connecting Saybrook and Willimantic in Connecticut, then through Southbridge and Gardner in Massachusetts, and finally up to Jaffrey and Hillsboro in New Hampshire.

---

recorded history was related to the passage of Hurricane Diane on 18-19 August 1955. The total for that 24 hour period was 8.40" of rain. Over its 3 day traverse, however, it dropped up to 20" in some areas.

Ludlum (1963) points to an interesting account showing the effects of the storm at its strongest point where it made landfall. The account comes from Mr. V. Utley who lived in River Head at Lyme in Connecticut:

> "…a cool wind and very heavy rain from N.E. which continued till 8 A.M. and then abated a little, when the wind veered to the S.E. and a much warmer wind was sensibly felt by most people who stood in the open air.
>
> The violence of the wind increased gradually till 9 o'clock, at which time it blew a perfect hurricane, and continued with the utmost fury until 11 A.M.
>
> In its course it tore down barns, unroofed dwelling-houses, upset cider mills, carried away carriage houses, &c. &c. It tore up the largest trees by the roots; some orchards are nearly destroyed, the trees lay level with the ground; the heart sickens at the sight. The forest from New London to Connecticut River, (which is as far as I have heard) exhibits to the eye the most dreadful destruction ever made by a tornado in this part of the country; whole forests of trees are either broken down, or torn up by the roots and crossing each other; fences level with the ground. At River Head the tide rose 6 feet higher than ever it was known to rise before, carrying away bridges, &c. I have not heard of any lives being lost.
>
> P.S. The leaves and exterior parts of limbs of trees taste salt by water taken up from the ocean and probably carried into the country."

In general, the greatest damage befell the communities on the eastern side of the hurricane where the rapid forward momentum of the storm itself combined with the forward velocity of the hurricane circulation. Thus, a 75 mile wide swath east of the hurricane's center track was the zone of greatest wind damage, and included eastern Connecticut, all of Rhode Island, east-central Massachusetts, and southeastern New Hampshire (Ludlum, 1963). Ludlum (1963) notes that the line separating zones of light vs. heavy destruction was so obvious that it was noted by an Albany-Boston post rider:

> "From Brimfield to this place (Boston), there appeared to be one continued scene of devastation, in the unroofing of houses, upsetting of

barns, sheds, and other buildings, and in the general prostration of fences, trees, grain, and every description of vegetation."

Another gauge of the strength of the storm comes from Concord, NH where after traveling over land almost 200 km, the hurricane was still strong enough to produce devastation that led to this account, pointed out by Ludlum (1963):

> "Last Saturday was experienced in this vicinity the most severe gale of wind, or rather hurricane, known by the oldest inhabitants. The wind commenced in the morning at N.E.—about noon it changed to S.E. and for two hours it seemed to threaten everything with ruin. The sturdy oak, the stately elm, and the pliant popular, were alike victims to its fury. The destruction of orchards and buildings has been great; there is scarcely an apple left on the standing trees. Many cattle have been killed by the falling trees. Had this violent wind taken place in the season of vegetation, there is no calculating its effects; it might have produced famine."

On the west side of the storm track, wind damage was much less severe, but the rainfall was more intense (Ludlum, 1963). Reports of such heavy rains come from Connecticut, and from western Massachusetts and Vermont where the accounts are more concerned with post-storm flooding than the amount of wind damage they suffered (Ludlum, 1963).

Given this project's interest in the immediate Boston area, an important account pointed out by Ludlum (1963) comes from veteran weather observer Prof. John Farrar of Harvard University:

> "This storm was very severely felt throughout a greater part of New England. It was most violent on and near the coast, but does not appear to have extended far out at sea. It was preceded by rain, which continued to fall for about twenty four hours with a moderate wind from the N.E. Early in the morning of the 23d the wind shifted to the east, and began to blow in gusts accompanied with showers. It continued to change toward the south and to increase in violence while the rain abated. Between 9 and 10 o'clock A.M. it began to excite alarm. Chimneys and trees were blown over both to the west and north, but shingles and slates, that were torn from the roofs of buildings, were carried to the greatest distance in the

> direction of about three points west of north. The greatest destruction took place between half past 10 and half past 11. The rain ceased about the time the wind shifted from southeast to south; a clear sky was visible in many places during the utmost violence of the tempest, and clouds were seen flying with great rapidity in the direction of the wind. The air had an unusual appearance. It was considerably darkened by the excessive agitation and filled with the leaves of trees and other light substances, which were raised to a great height and whirled about in eddies, instead of being driven directly forward as in a common storm. Charles river raged and foamed like the sea in a storm, and the spray was raised to the height of 60 or 100 feet in the form of thin white clouds, which were drifted along in a kind of waves like snow in a violent snow storm. I attempted with several others to reach the river, but we were frequently driven back by the force of the wind, and were obliged to screen ourselves behind fences and trees or to advance obliquely. It was impossible to stand firm in a place exposed to the full force of the wind. While abroad, we found it necessary to keep moving about, and in passing from one place to another, we inclined our bodies toward the wind, as if we were ascending a steep hill. It was with great difficulty that we could hear each other speak at the distance of two or three yards. The pressure of the wind was like that of a rapid current of water, and we moved about almost as awkwardly as those do who attempt to wade in a strong tide."

Regarding storm surge associated with this hurricane, Ludlum (1963) does not point out any resources that specifically talk about the conditions in the Bay of Massachusetts, but abundant material is available for the southern coast of New England and Narragansett Bay. In this regard, the 1815 hurricane seems to be very similar to the 1635 and later 1938 hurricanes. Narragansett Bay is susceptible to massive storm surges from northward-traveling hurricanes because of its N-S orientation. The peak of storm surge in the 1815 also coincided with the regular astronomical high tide leading to astonishing water levels (Ludlum, 1963). The result, according to Perley (1891), is that, "the wind brought in the tide ten or twelve feet above the height of the usual spring tides, and seven and a half feet higher than ever known before, overflowing and inundating streets and wharves."

Though the Great September Gale of 1815 arrived before the development of the Saffir-Simpson intensity scale for hurricanes, it was obviously of great intensity. Given the historical documentation cited by Ludlum (1963) and the descriptions of expected damage in Table 15 above, we suggest that it was of at least Category 3, and possibly up to Category 4 intensity.

5.2.2.14 The Atlantic Coast Hurricane of Late August 1839

The Atlantic Coast Hurricane of Late August 1839 was identified by Ludlum (1963) as a "vigorous" hurricane that passed up along the Atlantic coast in late August 1839 (Figure 63). He points to one account from Cape Cod that identified this off shore hurricane as one of the most severe storms in years, and a second by William Mitchell of Nantucket which made the same conclusion for that island (Ludlum, 1963). The wind damage on Nantucket was also notable according to the Nantucket Inquirer which commented that, "on land the trees, shrubbery, corn, and other vegetable have suffered greatly."

Ludlum (1963) did not identify any accounts that would suggest this storm was very significant in the Boston area, in fact, he noted that damage at Boston Harbor was negligible. However, it appears that the intensity of the storm increased rapidly heading northwards. For example, just 22 km to the northeast in coastal Salem, Ludlum (1963) pointed out that historian J.B. Felt recorded the event as "a more violent northeast storm than has been experienced for a considerable period. It was destructive to trees, fences, and shipping." And in coastal Maine the result was even worse—it was suggested that

the storm caused more damage than the gigantic, and memorable Great September Gale of 1815 which had passed just a quarter of a century earlier (Ludlum, 1963).

In summary, for the Boston area, historical documentation indicates this storm was relatively insignificant, though for the outer Cape Cod and Islands it was quite damaging. This somewhat mimics the hurricanes of 1806 and 1841 where Cape Cod and the Islands were strongly affected, but the protected port of Boston was hardly affected.

5.2.2.15 The Memorable October Gale of 1841

The Memorable October Gale of 1841 was a significant hurricane that passed off shore of New England (Figure 63) on 3 October 1841 (Ludlum, 1963). For outer Cape Cod and the Islands, and the ships that happened to be at sea at the time, the storm was a terrible disaster, and is still remembered in those communities as "The October Gale" (Ludlum, 1963). While the storm was noted as a strong gale in the Boston area, Ludlum (1963) cites an account which mentions that Boston Harbor did not suffer any notable damage. Given the distribution of the storm's intensity and resulting damage, it is very similar to the 1806 and 1839 hurricanes discussed above, and we mention it for the sake of completeness.

Apparently, the storm wound up to hurricane strength very quickly (Ludlum, 1963), which indicates a strong pressure gradient. The rapidity caught many vessels off guard, and hundreds of fisherman lost their lives as a result (Ludlum, 1963).

Ludlum (1963) points out an account from the Nantucket Inquirer which shows the intensity of the storm there:

> "A great number of chimneys, some of them from buildings nearly new, were thrown down by force of the wind. The walks upon the roofs of

> some thirty dwelling houses in various quarters of the town were blown off. Trees of large dimensions, flag-staffs, fences, and other exposed objects, were prostrated. The tide rose to a height almost unprecedented reaching from two to three feet above the surface of the wharves, and extending into most of the lower streets, strewing in various directions quantities of lumber, cord wood, and other buoyant objects."

According to Ludlum (1963) similar destruction was noted at Martha's Vineyard and in the communities along the outer Cape.

From the above description, it is obvious that the Memorable October Gale of 1841 was a very intense and damaging storm at least along outer Cape Cod and the Islands. But for the Boston area, it was essentially insignificant.

5.2.2.16 The October Hurricane of 1849

Ludlum (1963) identified a hurricane that passed by New England on the evening of 6 October 1849(Figure 63). From New York City to New Haven to Providence to Boston come reports of a severe northeasterly winds accompanied by very heavy rains (Ludlum, 1963).

Ludlum's (1963) analysis of the storm's trajectory suggests the center passed close to the eastern tip of Long Island, and also close to Fort Trumbull near New London, CT. But northeasterly winds registered at Providence and Boston means the track had to fall to the southeast of those cities.

Regarding the heavy rains produced by the storm, during its 33 hour track across Long Island it dropped a total of 6.5", and at Fort Trumbull 6.15" were registered for the event (Ludlum, 1963). Rain totals for Providence and Boston may exist, but they were not cited by Ludlum (1963) who was obviously intimately familiar with available

resources. Nonetheless, both cities reported heavy rains, and it is reasonable to expect they might have received similar quantities in the 6" range.

Additional information about wind damage comes from the Boston area where, according to Ludlum (1963), trees were uprooted, and chimneys blown over. The wind damage was not strictly local because all telegraph lines towards the south ceased operation as they were downed by the storm.

Regarding an estimated intensity for this storm, wind damage in the Boston area appears to be light to moderate. Based on the descriptions of expected wind damage in Table 15 above, we suggest this storm may have had a Saffir-Simpson equivalent intensity of Category 1 or 2. For certain, while the wind damage was not so severe, it appears the rainfall associated with this storm was significant, probably on the order of 6" for the whole event.

5.2.2.17 The New England Tropical Storm of 1858

Ludlum (1963) identifies a moderately intense hurricane that after moving up the Atlantic coast off shore finally passed over eastern New England on 16 September 1858 (Figure 63). According to Ludlum's (1963) analysis, after passing over Long Island somewhere east of the center, but west of Sag Harbor, the storm made landfall on the New England mainland, passed closed to Providence, RI, and then moved across eastern Massachusetts.

Heavy, gusty winds and rain were reported from Providence throughout the event, but in the Boston area, the heaviest winds only accompanied the first several hours of the storm (Ludlum, 1963). Wind damage in the Boston area was light. Besides the blow

down of a single, uncompleted house in Chelsea, the damage consisted mostly of fruit blown from trees with only minor problems noted in Boston Harbor (Ludlum, 1963). Unfortunately, Ludlum (1963) does not provide any information about rain fall amounts, but it was reported to last for about 22 hours on Long Island, so it can be expected to have lasted about the same amount of time for the Boston area.

Ludlum's (1963) analysis of this storm is not as complete as the analyses he prepared for many of the other storms. But in general, the wind damage in the Boston area seems light, so it probably would have been ranked with a Saffir-Simpson Category 1 equivalence.

Fortunately, the date of this storm places it within the temporal boundaries of the Atlantic Hurricane Database Re-analysis Project, thus, extensive work has been done to generate best estimates of the storm's trajectory and intensity. Regarding an estimated intensity for the storm, while over the ocean it actually reached a Category 2 Saffir-Simpson intensity. But by the time it made landfall in New England, it had weakened to Category 1 intensity. This confirms our interpretation of the storm's intensity based on the resulting wind damage.

5.2.2.18 The "Expedition" Hurricane of November 1861

The "Expedition" Hurricane of November 1861 (Figure 63) was so named because it coincided with a military plan by President Lincoln (the "Expedition") to capture a set of strategic harbors, forts, and other coastal localities to enforce the blockade against sea-based commerce by the Confederacy (Ludlum, 1963). While this storm only reached moderate intensity while over land, it was remarkable for producing impressive

storm surges all the way up the eastern seaboard from about Cape Hatteras northward (Ludlum, 1963). For example, Ludlum (1963) indicates the Narragansett Bay area experienced the highest water levels noted since the devastating storm surge produced by the Great September Gale of 1815, and in Boston the water levels approached those produced during the legendary Minot's Lighthouse Gale of 1851.

According to Ludlum (1963), the storm arrived to the Boston area on the evening of 2 November as a strong gale with the winds increasing to a very strong intensity in the early morning hours of 3 November. While heavy rains had been falling, it increased to a particularly heavy deluge between 8:00-9:00 am before ending about 10:00 am (Ludlum, 1963). The impressive storm surge did not actually arrive until about noon time that day, a couple of hours after the most intense rain ended, and even longer after the strongest winds had blown in the early morning (Ludlum, 1963).

Despite the strong winds, Ludlum (1963) did not provide any accounts of significant wind damage in the Boston area. We interpret this to mean that despite the massive storm surge this storm raised up and down the eastern seaboard, in fact, it was only a storm of moderate strength at least when it passed through the Boston area. This analysis of intensity based on resulting wind damage is again perfectly complemented by the results of the Atlantic Hurricane Database Re-analysis Project. That project determined that the storm did reach Category 1 while over the ocean, but by the time it made landfall in New England, its intensity had degraded to that of a tropical storm.

5.2.2.19 The September Gale of 1869 in Eastern New England

The September Gale of 1869 was an intense hurricane, the strength of which New England had not experienced in more than half a century since the passage of the Great September Gale of 1815 (Ludlum, 1963). Though the storm had an intensity perhaps approaching that of the 1815 hurricane, it was very different by virtue of being much more compact (the zone of greatest destruction it produced was only 40-50 miles wide) whereas the 1815 hurricane was much larger (Ludlum, 1963).

According to Ludlum's (1963) analysis of the storm's trajectory, it made landfall on the southern coast of New England around the Connecticut/Rhode Island border, cut northeastward up through Rhode Island, passed through Massachusetts probably between Worcester and Boston, cut across the southeastern corner of New Hampshire, and finally made it into Maine (Figure 63). This trajectory was reconfirmed by the Atlantic Hurricane Database Re-analysis Project.

The intensity of the storm was impressive, and unlike some storms that quickly weaken over land, this storm maintained its full hurricane strength as it crossed through Massachusetts roughly between Milford and Lawrence. This path left much of Boston and its modern surrounding metro area within the narrow zone of greatest destruction. Wind damage was extraordinary—thousands of trees were blown up by their roots, and major structural damage was done to many buildings in the Boston area (Ludlum, 1963).

According to Ludlum (1963), the passage of the storm was accompanied by heavy rain squalls which started about 3:00 pm, continued throughout the passage of the storm. When the storm finally exited the Boston area about 7:00-7:30 pm, the squalls were still

going strong, but they ended soon thereafter. Ludlum (1963) mentions that according to one account, the total amount of rain that fell in those few hours was 1.22".

Ludlum (1963) presents an interesting comment about water levels in Boston Harbor related to the storm. The astronomical high tide for that day was scheduled for 2:00 pm, so by the time the strongest winds arrived in Boston the tide had already well-receded. Thus, damage in the harbor was significantly lessened by this fact (Ludlum, 1963).

Regarding the intensity of this storm, the significant tree blow-down and structural damage is reminiscent of that wrought by the Great September Gale of 1815, but just on a much smaller scale. Based on the description of expected damage in Table 15, we estimated the intensity of that storm as Category 3 and possibly up to Category 4. Given the reduced size of the 1869 hurricane, we estimate that it should fall squarely within the range of Category 3 intensity. This estimate is reconfirmed by results from the Atlantic Hurricane Database Re-analysis Project which suggests the storm made landfall as Category 3, and maintained that same intensity until exiting Massachusetts at which point the intensity quickly dropped to tropical storm levels.

5.2.2.20 Unnamed tropical storms of 1934

Two unnamed tropical storms of apparently low intensity passed through Massachusetts in 1934 (Figure 63). The first storm passed by on 19 June, and followed a trajectory that skimmed across Long Island, then over the southern portion of Rhode Island, then across Buzzard's Bay, and finally out across southeast Massachusetts. The second storm followed a more NNE trajectory first cutting across central Long Island,

then up across central Connecticut, central Massachusetts, and finally over the SE corner of New Hampshire.

Meteorological data for these two storms is not readily available, but we assume that they were probably only of low intensity by the time they passed over Massachusetts. Another indication that the storms were not so intense is that neither did they make it into the annals of storm folklore like other more severe storms. Nonetheless, because of their trajectories, if these storms did produce significant amounts of precipitation, there is a good chance it would have been registered in the LML watershed. According to the hour water level data available for Boston Harbor, neither of these storms produced any significant storm surge.

5.2.2.21 The New England Hurricane of 1938

One of the most memorable hurricanes to pass though New England in historical times was the great storm of 1938. The storm was of legendary stature--only two other storms of generally equivalent strength and size had affected New England since the arrival of European settlers—the great hurricanes of 1635 and 1815. One significant difference, however, was that the 1938 storm followed a track significantly further to the west than those other two storms (Figure 63). Nonetheless, because of the massive size of this storm, the effects felt in Boston were still severe. For example, at the Blue Hill Observatory, gusts of wind up to 186 mph were recorded with sustained speeds up to 121 mph (Scotti, 2003). The actual speeds reached were probably faster—the values cited above were what the instruments recorded before actually failing. Even in the immediate Boston area the winds were exceptional—enough so to pick up a DC-2 airliner at the

airport, and fling it a half mile away (Scotti, 2003). Nonetheless, with sustained wind speeds of 121 mph, the hurricane would be characterized as only a modern Category 3 status.

Specific values for precipitation in the Boston area are somewhat difficult to encounter. However, in general, New England had been trapped in a low pressure trough for the preceding week, so by the time the hurricane precipitation arrived, the ground was already saturated in many areas. Combined with precipitation rates of about 6"-8" in just four hours, flooding in central Connecticut and western Massachusetts was catastrophic. For example, the Connecticut River ended up cresting at its second highest height ever, about 20 feet over the regular flood stage. Flooding on the Merrimack River north of Boston was also severe, so presumably Boston also received significant precipitation.

The storm surge produced by this storm along the southern New England coast was exceptional. However, storm surge in the Boston area was essentially negligible according to the hourly water level data available for Boston Harbour.

5.2.2.22 The Great Atlantic Hurricane of 1944

Another significant 20th century hurricane that passed by the Boston-area was the Great Atlantic Hurricane of 1944 (Figure 63). The sustained windspeeds for this storm while it was at sea clearly placed it within Category 4 intensity. But by the time this storm made landfall, the winds quickly dropped to Category 1 intensity, and continued to rapidly decelerate after that. There are no obvious reports of wind damage from the Boston area related to the storm, but the storm did dump about 6" of rain in the Boston area.

5.2.2.23 Hurricanes Carol and Edna of 1954

Two hurricanes of significant intensity passed by the New England area in 1954 (Figure 63). On 31 August, Hurricane Carol, a Category 2 storm, made initial landfall in eastern-central Long Island. It then continued north-northeast through the eastern half of Connecticut, up through Massachusetts, and into middle New Hampshire. Hurricane Carol produced sustained winds between 80-100 mph in most of eastern Massachusetts, and was responsible for a significant amount of tree and utility pole blow down. Rainfall amounts averaging between 2"-5" depending on location. Storm surge along the southern New England coast was significant, but negligible in the Boston area.

Just two weeks later, Hurricane Edna made landfall further to the east first at Martha's Vineyard, and then over lower Cape Cod. Edna had reached Category 3 intensity at sea, but like Hurricane Carol, it weakened to Category 1 intensity at landfall,. Importantly, Edna dropped a record 5.64" of rain in just 24 hours which lead to significant inland flooding.

5.2.2.24 Hurricanes Connie and Diane of 1955

Like the preceding year, 1955 saw two back-to-back hurricanes of significant intensity that together produced massive flooding in New England (Figure 63). Hurricane Connie reached Category 4 intensity while at sea, but never actually made landfall in New England. Nonetheless, Connie blanketed New England with torrential rains that saturated the ground. In Massachusetts; in particular, up to about 7"-8" was received in the western part of the state where the flooding quickly turned disastrous. The quantity of

precipitation decreased eastward towards the Boston area where they received about 2” of rain.

Hurricane Diane appeared at the southern New England shores about a week later, and began a slow, 3 day traverse that dropped record amounts of rain on ground that was already saturated by Connie. The zone of highest precipitation extended from northern Connecticut to the Boston area where upwards of 15”, and in some areas closer to 20”, of rain was received. Catastrophic flooding ensued making Diane the first hurricane to cause $1 billion in damage.

Wind damage from Connie and Diane not extraordinary given that the first storm did not make a landfall in New England, and the second had weakened to tropical storm intensity by the time it made landfall.

5.2.3 Synopsis of historical hurricane impacts on the Boston area

Given the large number of storms summarized above, a simple summary categorization for the overall impact of each storm on the Boston area would be useful. We do this in Table 16 below where a five-bin categorization of impact level for the Boston area is defined. Note that the level that each storm has been placed into is partially subjective because it is based on our interpretation of the historical details presented for each storm, but also because there is progressively less information about events going further back in time.

Table 16—Summary of interpreted impact levels for historical storms on Boston.

Hurricane date	***Interpreted level of impact for Boston area***
1635, 1815[72], and 1938	severe impact—these storms had a severe impact due to their very intense nature, but also large size
1727, 1804, and 1869	very strong impact—these storms were also very intense, in some cases perhaps as strong as their "severe" brethren, but they were also smaller in size, so their effect was delivered over a much reduced area
1743, 1770, 1849, 1861, 1954, and 1955	strong impact—these were generally storms of lower intensity, but they produced excessive amounts of precipitation and/or storm surge which raised their effective level of impact
1638, 1675, 1706, 1761, and 1858	moderate impact—these storms had a moderate impact; there was nothing particularly notable about them except that they were hurricane-strength storms of wind and rain
1716, 1783, 1806, 1839, and 1841	negligible impact—these storms had a negligible impact on the Boston area because their tracks were simply too far away to have a significant effect there

5.3 One if by land, and two if by sea[73]—source of the graded beds

What is the source of the occasional, anomalous graded beds in the LML varve record? Do they come from the downstream, seaward side of the system, or do they come from the landward side of the system, specifically, the lake watershed?

[72] One of the small gaps that exists in the LML varve record is from 1812-1818 inclusive. This is due to a obvious angular unconformity, possibly fault, that is clearly visible in the X-ray thin slab imagery. Thus, in the current varve record, no varve exists for the year 1815 which is unfortunate given the storm's great intensity. It is expected that this small gap (along with the few other small gaps that exist in the record) could be bridged with new cores from the LML.

[73] "One if by land, and two if by sea"—these words come from the poem Paul Revere's Ride by Henry Wadsworth Longfellow, and were used to describe the number of lanterns to be held in the tower of the Old North Church in Boston to advise Paul Revere about whether the British would take a landward or seaward route to begin their reprisal raids against the colonists. The famous midnight ride, in fact, followed several miles along the Mystic River, and had Revere cross it close to the outlet of the Lower Mystic Lake. The words are also appropriate regarding our understanding about the source of the graded beds in the LML varve record. Our initial expectation attributed them to a seaward source, but as our understanding of the system grew, a landward source was implicated.

5.3.1 Initial expectation—graded beds a product of storm surge

When this project was initiated, our working hypothesis was that occasional, anomalous graded beds (and resulting anomalous varve thicknesses) that we observed in the stratigraphy were related to storm surge deposition, like the majority of hurricane record studies since Liu and Fearn's (1993) pioneering work from Lake Shelby along the Alabama coast. The difference was that we expected to use an ultra high-resolution medium—an annually-laminated sedimentary record. Part of this expectation was based on our understanding that marine water migrated up the Mystic River, and reached the Lower Mystic Lake on only rare and infrequent occasions. This was almost exclusively based on the elaborate civil engineering study documented by Totten et al. (1861), in which a report by Horsford (1860) concluded that flow of marine water into the lake was, "occasional and rare, rather than frequent." Thus, following that scenario, the graded beds would have originated from the seaward side of the system.

5.3.2 Current understanding—graded beds from intense precipitation and erosive flow

Subsequently, we have come to understand that sea water reaching the LML was not actually a rare and infrequent event, but, in fact, it was rather common (R. Duffy, personal communication, and Ludlam and Duval, 2001). In fact, based on Ludlam and Duval's (2001) analysis which documents the rapidly changing depth of the chemocline in the LML from the mid-1960's to the mid-1990's, it seems certain that marine water must have reached the lake frequently since it has maintained its meromictic condition for close to a millennium according to the varve chronology.

We have now reached a different conclusion about the source of the graded beds—their source must be the lake watershed. By what mechanism? We now hypothesize that intense, hurricane-strength rains saturate the watershed, resulting in erosive overland flow that entrains sediment, which is then carried into the lake where it is deposited as a graded bed. This is enhanced if the hurricane-strength winds disturb vegetation, and uproot trees which would expose fresh, loose sediment. Importantly, this link between intense precipitation (not necessarily from hurricanes), erosive overland flow, and lacustrine deposition is not unique, and has been reported or proposed in other studies. Some of those studies include Desloges (1994), Page et al. (1994), Hammer and Stoermer (1997), Campbell (1998), Eden and Page (1998), Thorndycraft et al. (1998), Rodbell et al. (1999), Brown et al. (2000), Brown et al. (2002), and Noren et al. (2002).

5.3.3 Evidence for intense precipitation and erosive flow as source

Several lines of evidence have converged to convince us that the graded beds are not the result of storm surge or overwash as originally expected.

First, the occasional, anomalous graded beds that correspond with years of known historical hurricanes exist throughout the varved stratigraphy. In particular, this includes at least four graded beds within the period from 1931-1968 (see Table 14; includes years 1934, 1938, 1954, and 1955). This portion of the stratigraphy is represented by two polished impregnated blocks from freeze core LML-19JAN2002-FRZ-1. The critical aspect of this period is that it is post-1908. In 1908, the Cradock Dam was built downstream of the LML near Medford Square. After this point, marine water no longer

made it up the river easily[74]. Thus, the graded beds seen in the post-1908 stratigraphy must have been generated within the lake watershed.

A second reason that rules against storm surge as the probable source for the graded beds is that some record high water events do not leave an expression in the stratigraphy. Yet hurricanes which produce only a small surge do apparently leave a graded bed. For example, in February 1723, a nor'easter storm of great intensity produced a storm surge in Boston Harbor, and the water reached a record level that was 20" higher than was ever known before. None of the 13 hurricanes during the historical period that are associated with graded beds produced a storm surge that reached the level of the 1723 harbor flood, though some came close. Nonetheless, all those 13 hurricanes resulted in the deposition of graded beds.

Another interesting comparison to help demonstrate the insignificance that storm surge plays in depositing a graded bed is illustrated by comparing the 5.2.2.7 Benjamin Franklin's Eclipse Hurricane of 1743 with the 5.2.2.9 The Late Season Storm of October 1770. As mentioned above, the 1723 harbor flood reached a record water level that was only once again exceeded in the history of Boston by the Minot's Lighthouse Gale in April 1851. Both the 1743 and 1770 hurricanes produced storm surges that apparently rose to within four inches of the water level reached during the 1723 harbor flood. But only the 1770 hurricane resulted in the deposition of a graded bed—the 1743 hurricane left no anomalous record whatsoever.

---

[74] It is our understanding that the Cradock Dam locks were occasionally left open on purpose, but not as a matter of regularity. According to R. Duffy (personal communication), for example, there was formerly a bathing beach on the Arlington side of the Mystic River in the 1930's. He suggested that on a few occasions when bacteria counts got very high, authorities left the Cradock Dam locks open on purpose to help flush out the system. But again, this apparently only occurred on exceptional occasions.

What was the difference between these 1743 and 1770 hurricanes such that one would leave a graded bed, and the other nothing? The storm summaries for each of these hurricanes produces the probable answer. Almost all the accounts of the 1743 hurricane mention the impressive storm surge that it raised, but there is very little talk of precipitation. For the most part, the havoc wreaked by this storm was confined to the coast as a result of the storm surge and violent winds there. In contrast, the accounts of the 1770 hurricane talk about the massive storm surge it raised, but there are also significant comments about precipitation including both rain and hail. John Winthrop, of Harvard University, wrote accounts about both the 1743 and 1770 hurricanes. He does not provide any value for the amount of precipitation that fell during the 1743 storm, but he explicitly gives a total precipitation figure of 2.48" for the 1770 storm. Finally, for the 1770 hurricane there are reports of significant precipitation up to 60 km inland, but again, nothing similar for the 1743 storm. Given that both of these hurricanes produced massive storm surges of almost exactly the same magnitude, the only essential difference is that of precipitation. Very little mention of precipitation is made for the 1743 hurricane, and it did not produce a graded bed. In turn, precipitation was one of the notable characteristics of the 1770 hurricane, and that storm did produce a prominent graded bed.

5.3.4 Summary

In summary, the evidence seems clear. Though we originally expected the occasional, anomalous graded beds to come from the seaward side of the system essentially as a function of storm surge, this is not the case. The graded beds come from the landward side of the system, in particular the lake watershed. They appear to be

intimately tied to hurricane strength precipitation which saturates the watershed, and results in erosive overland flow that entrains sediment, and carries it into the lake where it is deposited as a graded bed. This is greatly enhanced by hurricane-strength winds that disturb vegetation, and uproot trees exposing fresh, loose sediment.

5.4 Analysis of the LML varve thickness record

In the "4.1.9 The LML sedimentary couplets are true varves" section of Chapter 4, the architecture of the biogenic-siliciclastic LML varves was intimately linked to the normal, annual sedimentary cycle in the lake. On visual inspection, the varves are generally uniform and sedimentation is not anomalous. Taken together, these suggest that the thickness of a typical varve should fall within some "normal" range of values. For example, a "normal" range of thickness values could be defined as within two standard deviations of the average varve thickness.

5.4.1 Varve thickness and anomalous sedimentation events

Presumably, if the lake were to experience an anomalous sedimentation event related to a natural event such as the passage of a hurricane, the result of such an event could push that year's varve thickness outside of the normal range of values. A first indication supporting this was made in the "4.1.13 The LML varve thickness record" section of Chapter 4 when it was observed that the spikes in the varve thickness record were almost exclusively related to the occasional, anomalous graded beds present within the stratigraphy.

An important caveat when interpreting a thickness signal in such a manner is that the system must be in a close to natural state. If not, it may be difficult or simply impossible to link a change in varve thickness to a natural event. For example, the direct and indirect impact of anthropogenic activity can easily alter the magnitude and composition of material delivered to a lake, or the quantity of biogenic sediment produced therein. Via both scenarios the thickness of a varve would be affected. So in a system with significant anthropogenic activity, there may simply be too many competing factors to unequivocally relate an anomalous varve thickness to some natural event.

Other non-anthropogenic controls may play a role in moderating the thickness of anomalous sedimentation events like graded beds. An obvious control that comes to mind is storm trajectory which is discussed in more detail in the "5.4.7 Does varve thickness have any relationship to storm intensity?" section below

5.4.2 Usefulness of LML varve thicknesses pre- and post-AD 1865

When the LML varve thickness record was originally presented in Chapter 4, it was split into two portions; one from AD 1060-1865, and the other from AD 1865 to the present. Within the AD 1060-1865 section, the varve thicknesses show variation, but in general stay within the 1-2.5 mm range. As mentioned earlier, European settlers began to arrive to the area around the LML in about AD 1630. Certainly, their presence altered the environment, especially in the immediate colonization period of the early 17th century (~1630-1680). But the relative stability of the varve thickness record suggests that their presence and actions did not cause a radical shift in the magnitude of sedimentation until about AD 1865.

In the mid-1860's, a significant change in the LML's hydrography was abruptly realized. The Upper and Lower Mystic Lakes, confluent since their formation, were separated by the dam at "The Partings" which was completed in AD 1864. At the same time, the lake watershed also saw a tremendous increase in population and industrialization that resulted in immense changes in water quality and sediment delivery patterns. The result was a massive, exponential increase in varve thickness upwards to the present day. Certainly, a portion of the increased thickness can be explained by compaction (or lack of it). But nonetheless, from at least the mid-1860's onward, the anthropogenic forcing on the system is tremendous, and only increasing. For example, in 1908, the Cradock Dam was built downstream of the LML, and that immediately altered the estuarine dynamics of the river. The Amelia Earhart Dam, constructed further downstream in 1966, altered the dynamics even further, and is now responsible for actually controlling the water level within the lake.

As mentioned above, the use of variations in varve thickness to infer anomalous sedimentation events or patterns can only provide meaningful results if the system is in a close to natural state. The LML appears to be in such a state during the period from AD 1060-1865 given the apparent long term stability of the varve thicknesses during this interval. However, by 1865, the anthropogenic footprint is simply too large, and varve thickness is no longer primarily driven by natural forces.

While an examination of simple varve thickness in the post-AD 1865 portion of the record may not result in anything useful because so many direct or indirect anthropogenic forces could be moderating factors which control thickness, this does not preclude this portion of the record from being useful. For example, it has been

demonstrated above that the occasional, anomalous graded beds are typically deposited during the passage of a hurricane. So the presence of such graded beds in the post-AD 1865 portion of the record is still useful for tracking the passage of hurricanes. The difference is that in the early part of the record, the presence of such a graded bed would be clearly anomalous, whereas in the later part of the record, different threshold criteria may be required to identify hurricane-related anomalies because so many direct and indirect anthropogenic factors also affect varve thickness.

5.4.3 Long term trend of the LML varve thickness record from AD 1060-1865

An in-depth analysis of varve thicknesses in the AD 1060-1865 portion of the record was undertaken to identify varves of unusual thickness. As mentioned in the "4.1.13 The LML varve thickness record" section of Chapter 4, a subtle sigmoidal trend is present in the thicknesses values from this portion of the record. The trend, however, was not obvious in the varve thickness plot (Figure 51 in Chapter 4) because a scale necessary to accommodate the excessively thick varves towards the end of the record left the earlier portion of the record compressed. This AD 1060-1865 thickness data is replotted here (lower part of Figure 64), but at a scale where the subtle sigmoidal trend becomes more obvious.

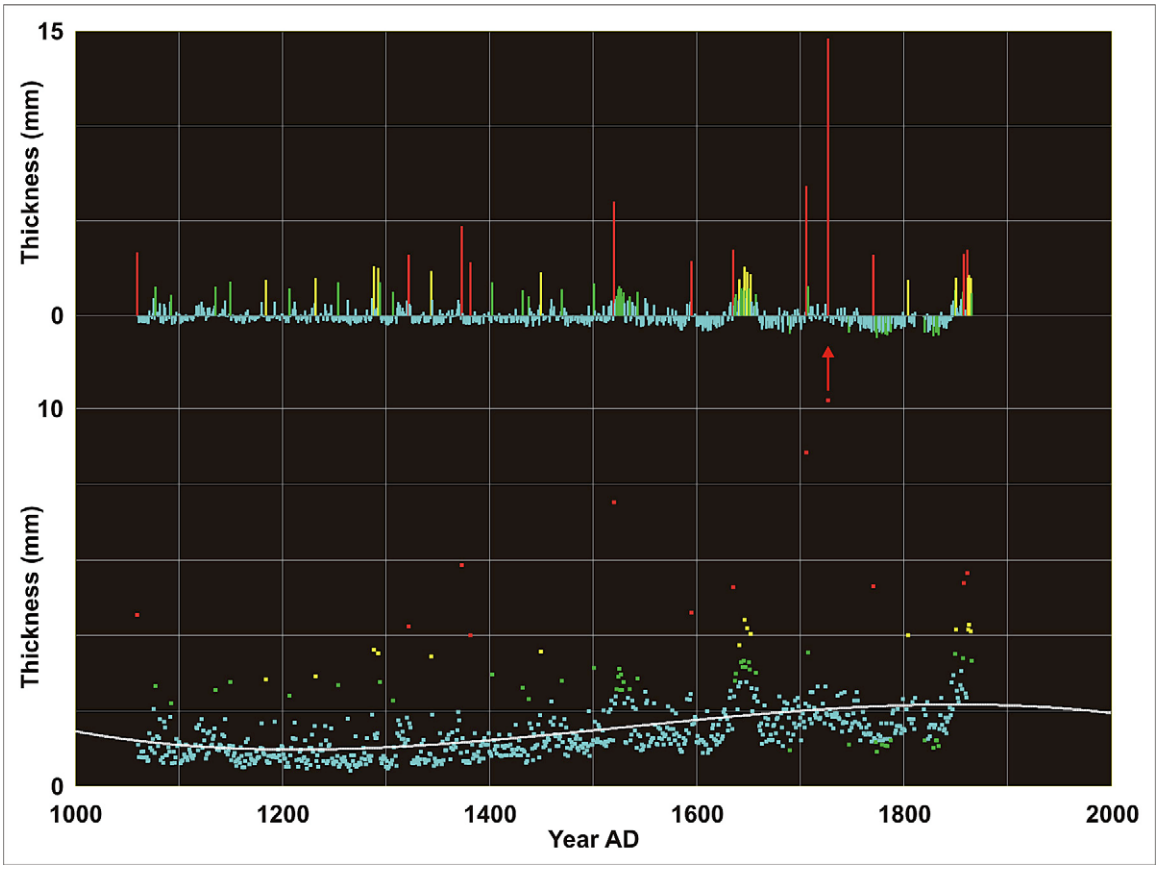

Figure 64—LML varve thickness record for the AD 1060-1865 period (lower part of plot). A third order polynomial curve (white sigmoidal curve) has been fit to the general trend of this thickness data. The thickness data point for AD 1727 had to be illustrated with a thickness of about 10 mm because of the scale of the lower plot, but in reality it should fall at about 16.7 mm thickness, hence the accompanying red arrow pointing upwards. Residual thicknesses from the curve fit are presented in the upper part of this plot. Both the native thickness values and residuals values are color-coded to easily identify values which fall at certain distances from the average. In particular, blue indicates residual thicknesses which fall within one standard deviation of the average, green indicates a range of 1-2 standard deviations, yellow indicates a range of 2-3 standard deviations, and red indicates a range of greater than 3 standard deviations.

This sigmoidal trend represents a long term, low frequency variation in sedimentation. The cause of the trend is unknown, but it should be subtracted out before a statistical analysis of the varve thicknesses is performed. Microsoft Excel was used to

estimate the equation for a third order polynomial curve[75] that fits the trend (white curve in Figure 64 above), and then to manually calculate residuals from the curve fit, as well as provide basic descriptive statistics for those residuals. Subsequently, the data set and polynomial equation were imported into the SYSTAT TableCurve 2D program which is specialized in manipulating and visualizing data sets with fitted curves and residuals.

5.4.4 LML varves of anomalous thickness deposited from AD 1060-1865

A total of 35 positive residuals between 1-2 standard deviations, 15 residuals between 2-3 standard deviations, and 12 residuals >3 standard deviations were identified. These residual thicknesses are listed in Table 17 below.

Table 17—LML varves deposited between AD 1060-1865 with positive, residual thickness values of at least one standard deviation. The color-coding corresponds to that used in Figure 64 (i.e. green indicates residual thicknesses which fall within 1-2 standard deviations of the average, yellow indicates a range of 2-3 standard deviations, and red indicates a range of greater than 3 standard deviations. Years marked by an asterisk (*) are varves which include graded beds. Years marked by the percentage sign (%) belong to one of the three zones of anomalous sedimentation discussed in Chapter 4, in particular, a zone of quadruplet architecture varves. Years marked by a tilde (~) also belong to one of the three zones of anomalous sedimentation discussed in Chapter 4, in particular, the zone of massive diatom blooms and siliciclastic pulses. Years marked by a plus symbol (+) include those at the very end of the sequence when the dam at "The Partings" was being built, and anthropogenic impacts like eutrophication were rapidly increasing.

1-2 standard deviations		2-3 standard deviations		>3 standard deviations	
Year AD	Residual (mm)	Year AD	Residual (mm)	Year AD	Residual (mm)
1865 +	1.163391818	1864 +	1.95093491	1861 *	3.46487425
1857 *	1.229048186	1863 +	2.11999638	1858 *	3.21037757
1849 *	1.330256401	1862 +	1.99417618	1770 *	3.17932372
1707	1.534786175	1850 *	1.99064335	1727 *	14.6293481
1657 ~	1.09755672	1804 *	1.85617506	1706 *	6.81994871
1651 ~	1.194324465	1652 ~	2.15721298	1635 *	3.42467041
1650 ~	1.406442566	1649 *	2.29786723	1595 *	2.84980973

[75] The resulting equation was $y = -9.20864272693094E\text{-}09x^3 + 4.23025355069709E\text{-}05x^2 - 6.19653867070431E\text{-}02x + 30.3361667921192$.

1647 ~	1.274036013	1646 ~	2.53378003	1520 *	5.98552816
1645 ~	1.452930377	1641 ~	1.87299407	1382 *	2.81222012
1644 ~	1.272487012	1450 *	2.22766146	1373 *	4.69843799
1643 ~	1.423549877	1344 *	2.34298562	1322 *	3.16841034
1638 ~	1.131155701	1293 *	2.49855649	1060 *	3.33015505
1637 ~	0.93045478	1288 *	2.59350373		
1543 *	1.247305956	1232 *	1.95087187		
1535 %	1.003078589	1184 *	1.84537007		
1529 %	1.210443286				
1528 %	0.984653954				
1527 %	1.406564441				
1526 %	0.990274693				
1525 %	1.564584654				
1524 %	1.351494269				
1523 %	1.036803483				
1501 *	1.657192845				
1470 *	1.386868111				
1438 *	1.001563706				
1432 *	1.321692539				
1403 *	1.735683579				
1307 *	1.235295388				
1294 *	1.735307326				
1254 *	1.698259698				
1207 *	1.433279964				
1150 *	1.75271922				
1136 *	1.517861708				
1093 *	1.089316875				
1078 *	1.506331658				

Not surprisingly, these positive residuals show excellent correspondence with varve years which contain the occasional, anomalous graded beds found in the stratigraphy. This is particularly true for the larger residuals. Every single one of the 12 residuals of >3 standard deviations (indicated by red in Figure 64 and Table 17) corresponds with a varve with a graded bed.

Of the 15 residuals between 2-3 standard deviations (indicated by yellow in Figure 64 and Table 17), 9 of them also correspond with varves which contain a graded bed. The remaining 6 residuals in this class include those for AD 1641, 1646, 1652, and 1862-1864. The first three of those (i.e. AD 1641, 1646, and 1652) are varves from one of the three anomalous zones discussed in Chapter 4. In particular, these varves come from the

zone of massive diatom blooms separated by siliciclastic pulses. The last three residuals (i.e. AD 1862-1864) correspond with varves right at the AD 1865 transition point when the dam at "The Partings" was being built, and the impacts of anthropogenic activity were becoming significant. In retrospect, it may have been wise to truncate this thickness analysis a few years earlier than AD 1865 which was chosen.

Of the 35 residuals between 1-2 standard deviations (indicated by green in Figure 64 and Table 17), 16 of these residuals also correspond with varves which contain some of the thinner graded beds. This leaves 19 remaining residuals in this class. Eight of those (AD 1523-1529, and 1535) correspond with varves which come from one of the three anomalous zones discussed in Chapter 4. In particular, they come from a zone of quadruplet architecture varves. An additional nine of the residuals (AD 1637-1638, 1643-1645, 1647, 1650-1651, and 1657) also correspond with varves which come from one of the three anomalous zones discussed in Chapter 4. In particular, they come from the anomalous zone of massive diatom blooms separated by siliciclastic pulses. Finally, regarding the remaining two residuals, AD 1707 and 1865, there are no special considerations for the AD 1707 varve, but the 1865 one is right at the transition point when the dam at "The Partings" was being built, and the impacts of anthropogenic activity were becoming significant.

5.4.5 Conclusions drawn from this varve thickness analysis

Overall, this thickness analysis did a good job of identifying the varves with graded beds. A total of 56 varves with graded beds of all sizes were *visually* identified in the interval from AD 1060-1865 (see the "4.1.12 Graded beds in the LML varve

chronology" section in Chapter 4). This thickness analysis identified 37 of those 56 varves (66%) based simply on the fact that their thicknesses were at least one standard deviation greater than the average varve thickness. This means 19 of those 56 varves (34%) with graded beds do not show thicknesses that are significantly different than the average varve thickness. However, those 19 varves were re-examined visually following this thickness analysis, and the graded beds they contain are certainly the most subtle of the series.

An important conclusion from this analysis is that all 12 of the excessively thick varves (>3 standard deviations from average) contain graded beds. And 9 out of 15 (60%) of the very thick varves (2-3 standard deviations from average) also contain graded beds. The remaining 6 out of 15 very thick varves are also not "normal" varves. Three are from one of the anomalous zones discussed in Chapter 4, in particular, the zone of massive diatom blooms separated by siliciclastic pulses where the annual sedimentary cycle appears to break down, and multiple biogenic and siliciclastic layers are deposited in a single year. And the final three varves come from the transition point when the dam at "The Partings" was being built, and the impacts of anthropogenic activity were becoming significant.

The point of this conclusion is that within the 795 varve years present in the AD 1060-1865 portion of the record[76], never once did a simple biogenic-siliciclastic varve produced by the normal, annual sedimentary cycle ever reach an atypical thickness. Thus,

[76] There are some small gaps in the record for a total of 10 missing varve years throughout this entire interval.

the only way to produce a very thick, or excessively thick varve is by including the result of an anomalous sedimentation event (i.e. a graded bed) or pattern within a varve.

5.4.6 Can anomalous thickness be used to unequivocally identify a hurricane signal?

Regarding the varves with excessive thicknesses of >3 standard deviations from the average, and which fall during the historical period, every single one of those varves corresponds to a year with a known historical hurricane[77]. These include years 1635, 1706, 1727, 1770, 1858, and 1861 as seen in the list below (Table 18). Presumably, all of the prehistoric varves with a similar thickness of >3 standard deviations from the average also represent years whose thickness was augmented by a hurricane-related sedimentation event.

Table 18—Excessively thick (>3 standard deviations from the average) varves from the LML record. Following the system established in Table 17, the asterisk (*) indicates that the varves contain graded beds.

>3 standard deviations	
Year AD	**Residual (mm)**
1861 *	3.46487425
1858 *	3.21037757
1770 *	3.17932372
1727 *	14.6293481
1706 *	6.81994871
1635 *	3.42467041
1595 *	2.84980973
1520 *	5.98552816
1382 *	2.81222012
1373 *	4.69843799
1322 *	3.16841034
1060 *	3.33015505

[77] It is obvious that during this same period of time, there were undoubtedly other exceptional rainfall events that must have occurred, but that were not associated with the passage of a hurricane. But only the hurricane-related events produced excessively thick (>3 standard deviations from the average) varves indicating that another mechanism such as vegetation disturbance enhances sediment delivery to the lake during such an event.

There are nine varves that have a thickness of 2-3 standard deviations from the average, and which fall during the historical period. Those include years 1641, 1646, 1649, 1652, 1804, 1850, 1862, 1863, and 1864 as seen in Table 19 below. Of those nine, only three of them have graded beds (1649, 1804, and 1850). Of those three varves with graded beds, two of them (1804 and 1850) correspond with years of known storms (a hurricane and a nor'easter[78], respectively). Regarding the remaining six of nine varves that have a thickness of 2-3 standard deviations from the average, and fall during the historical period, but do not contain graded beds, these varves also represent periods of anomalous sedimentation. For example, the 1641, 1646, and 1652 varves fall within the anomalous zone of massive diatom blooms and siliciclastic pulses that is discussed below in the "5.5 Significance of the three anomalous zones in the LML varve record" section below, and the 1862-1864 varves fall right at the end of the sequence when the dam at "The Partings" was being built, and anthropogenic impacts were rapidly increasing.

Returning to the original question, "Can anomalous thickness be used to unequivocally identify a hurricane signal?", it appears that for the varves with thicknesses of >3 standard deviations from the average, yes, varves of such thickness are almost unquestionably the result of a hurricane-related sedimentation event. However, for those varves just 2-3 standard deviations (or less) from the average, the presence of a graded bed may indicate a hurricane-related sedimentation event, but it is not certain.

[78] The graded bed in the 1850 varve year actually corresponds with the 1851 calendar year given the offset between varve years and calendar years. The exceptional and legendary nor'easter storm this corresponds with is the Minot's Lighthouse Gale of 1851. See Footnote 57 at the beginning of this chapter for a more in-depth explanation of the 1850 varve year/1851 calendar year correspondence.

Table 19—Very thick (2-3 standard deviations from the average) varves from the LML record. Following the system established in Table 17, years marked by an asterisk (*) are varves which include graded beds. Years marked by a tilde (~) belong to one of the three zones of anomalous sedimentation discussed in Chapter 4, in particular, the zone of massive diatom blooms and siliciclastic pulses. Years marked by a plus symbol (+) include those at the very end of the sequence when the dam at "The Partings" was being built, and anthropogenic impacts like eutrophication were rapidly increasing.

2-3 standard deviations	
Year AD	**Residual (mm)**
1864 +	1.95093491
1863 +	2.11999638
1862 +	1.99417618
1850 *	1.99064335
1804 *	1.85617506
1652 ~	2.15721298
1649 *	2.29786723
1646 ~	2.53378003
1641 ~	1.87299407
1450 *	2.22766146
1344 *	2.34298562
1293 *	2.49855649
1288 *	2.59350373
1232 *	1.95087187
1184 *	1.84537007

5.4.7 Does varve thickness have any relationship to storm intensity?

In this section, the relationship between anomalous varve thickness and the overall impact level of a storm is explored. Table 20 below is essentially a simplified reproduction of Table 16 which was presented above, but all post-AD 1865 storms are removed because they were not part of the statistical varve thickness analysis. The varve years in this table are colored according the scheme presented in Figure 64 and Table 17 above (i.e. red for >3 standard deviations, yellow for 2-3 standard deviations, and green for 1-2 standard deviations).

Table 20—Comparison of anomalously thick varves versus their interpreted level of impact for the Boston area.

Hurricane date	***Interpreted level of impact for Boston area***
1635 and 1815[79]	severe impact
1727, and 1804	very strong impact
1743, 1770, 1849, and 1861	strong impact
1638, 1675, 1706, 1761, and 1858	moderate impact
1716, 1783, 1806, 1839, and 1841	negligible impact

Note that as the interpreted level of impact increases, there is a progressively higher chance that the hurricanes for a particular level resulted in graded beds. For example, at the lowest impact category, 0 of out 5 storms (i.e. 0%) produced a graded bed, but at the next higher impact level it increases to 2 out of 5 storms (i.e. 40%), and for the next higher level it increases to 3 out of 4 (i.e. 75%), and for the next higher level 2 out of 2 (100%), and for the highest impact level 1 out of 1 (i.e. 100% when excluding the 1815 date as it is missing from the record). Thus, as a storm increases in intensity, the likelihood that it leaves a clue about itself increases.

But do the thickness anomalies correspond with the interpreted levels of impact, for example, a more intense storm producing a thicker varve? Given the distribution of the data points that are available, there does not seem to be a straightforward correlation between thickness and storm intensity. For example, the six varves of thickness >3 standard deviations from the average fall over the upper four levels of intensity. This is somewhat unintuitive because for many relationships, as one increases the magnitude of force applied to a situation, the magnitude of the result varies as well.

[79] We have no varve for the year 1815 because a small gap exists in the LML varve record at this point. Please see Footnote 72 above for a longer explanation.

There are several factors which may account for this lack of a straightforward relationship between storm intensity and varve thickness. For example, during the historic period many direct and indirect anthropogenic effects may moderate the effectiveness of intense hurricane-strength precipitation in entraining/eroding sediment. This is different from the effect that forced us to confine our statistical thickness analysis to pre-AD 1865 data. In particular, since the colonists were actively engaged in agriculture, they may have significantly altered the effectiveness of a storm to entrain sediment and deliver it to the lake as a graded bed. If a certain set of fields close to the lake were actively tilled one year, but left fallow the next year, this could have created a bias, and may explain why there is not a straightforward intensity/thickness relationship for all storms during historical times.

If this is true, it suggests that for the period prior to European settlement, the thickness of a particular storm event layer may indeed vary more directly according to the strength of the storm that produced it. Native Americans were obviously present on the landscape prior to the arrival of European settlers, and used the land for purposes such as agriculture. But their effect was significantly less intense as they did not undertake the massive land clearing for agriculture and animal husbandry practiced by the European settlers. Thus, prior to European settlement, there were fewer anthropogenic effects to directly or indirectly moderate the effectiveness of the storm in entraining sediment.

Another important natural/non-anthropogenic consideration to keep in mind is that of storm trajectory. For example, a very severe storm that passes directly over the lake should produce a thick graded bed. But if a storm of the very same intensity were to follow a different trajectory further away from the lake, the resulting graded bed would

probably not be as thick. Thus, when using the results from only one site, it is difficult to use the simple thickness of an anomalous deposit as a gauge of the true/absolute intensity of a storm. However, the relative intensity of that storm as experienced at the location of the record seems feasible.

5.5 Significance of the three anomalous zones in the LML varve record

As mentioned in Chapter 4, three zones of anomalous sedimentation were encountered in the LML varve record. Brief interpretations and suggested explanations for these zones are presented below.

5.5.1 Zones of quadruplet architecture varves

As mentioned in the "4.1.11 Anomalous zones within the varve record" section of Chapter 4, two anomalous zones of quadruplet architecture varves are present in the varve record. An example of these varves from the Bird H impregnation series is illustrated in Figure 47 of that same chapter. These quadruplet architecture varves comprise a biogenic-siliciclastic-biogenic-siliciclastic sequence with a conspicuous feature being that the first siliciclastic layer is thin, and the second one thicker. These varves were deposited year after year over the period of one to two decades. The location of *Cyclotella* frustules was hand mapped out on BSEM imagery of one of these sections with the expectation that a single *Cyclotella* bloom would appear just once each year. Unexpectedly, *Cyclotella* blooms were found in each of the biogenic layers.

It appears that the extra siliciclastic and *Cyclotella*-bearing biogenic layers are actual components of the annual sedimentary cycle for a decade or two while these

quadruplet varves are being deposited. At present, the actual mechanism that produces this variation is unknown; however, the following provisional scenario is proposed. It is suggested that such quadruplet architecture varve zones result from a very strong disturbance of vegetation around the lake, in particular, related to the passage of an intense hurricane. Following a strong vegetation disturbance, late summer and fall precipitation events are able to entrain siliciclastic material via overland flow, and carry it into the lake to produce a thin siliciclastic layer. Then, during the winter when nutrients are less abundant, *Cyclotella* blooms for a second time that year[80].

In fact, there is strong sedimentological evidence to support this scenario. Both zones of quadruplet varves are initiated abruptly, and are immediately or closely preceded by a prominent graded bed. As documented earlier, such graded beds are interpreted to be deposited during the passage of a hurricane, in particular, from sediment entrainment and overland flow related to hurricane-strength precipitation and vegetation disturbance. After a decade or two, the vegetation would recover enough to prevent the November precipitation peak from making a difference.

Other explanations regarding the distribution of the *Cyclotella* frustules exist, but are improbable especially since these quadruplet varves are contiguous and occur as a zone. For example, the "quadruplet" interpretation could simply be incorrect, and the supposed "quadruplet" varves could actually be just two regular couplets varves that were lumped together inappropriately. But this seems very unlikely as it would require a

[80] S. Ludlam (personal correspondence) has suggested that while *Cyclotella* generally likes high nutrients, in the case of the LML, it is actually a low nutrient indicator. Presumably, this is because the diatom biomass in the lake is already dominated by other diatoms which are indicative of more eutrophic conditions. Thus, by comparison, *Cyclotella* only appears during periods of relatively lower nutrient availability.

regular, repeating alternation of the thin-thick siliciclastic component every other year over the period of two to four decades. Another possibility to explain the frustule distribution is that the thin siliciclastic layer could perfectly split the annual *Cyclotella* bloom by being deposited *after* the bloom begins, but *before* it ends. But this also seems very unlikely as it would require this perfect timing to occur year after year over a couple of decades.

A future, in-depth examination of these anomalous varves to provide more clues about their formation and development is planned, and the provisional scenario cited above will be revised as necessary.

5.5.2 Zone of massive diatom blooms and siliciclastic pulses

As mentioned in the "4.1.11 Anomalous zones within the varve record" section of Chapter 4, a second zone of atypical sedimentation found in the LML varve record is composed of massive diatom blooms and siliciclastic pulses. The massive diatom blooms are composed of an elongate diatom tentatively identified by a non-expert as of the genus *Aulacoseira* based on the simple morphology of the frustule. Manual mapping of *Cyclotella* frustules over the varves in that section (Figure 49 in Chapter 4) showed that the frustules were somewhat randomly distributed throughout the laminae, and did not generally occur as discrete pulses. This was interpreted to suggest that the normal annual sedimentary cycle for depositing simple, biogenic-siliciclastic varves had broken down, and multiple biogenic and siliciclastic pulses were being deposited in a single year.

Like for the quadruplet architecture varves, it is suggested that this change may be due to a strong disturbance of the vegetation around the lake. It is suggested that a natural

source produced the main, initial disturbance which was then partially sustained by anthropogenic activity.

In particular, these massive diatom blooms begin immediately following the AD 1635 varve which contains a graded bed. As mentioned above, such graded beds are interpreted to be deposited during the passage of a hurricane. The particular hurricane probably responsible for this graded bed was the Great Colonial Hurricane of 1635, a large, intense hurricane that blew down a massive number of trees and disturbed vegetation on its traverse through southeastern New England[81].

Coincident with this natural mechanism was an anthropogenic contribution that sustained and contributed to the initial disturbance. The very first land claims by European settlers were staked out in the area immediately around the lake and vicinity in 1630. Thus, the period subsequent to the 1635 hurricane was probably also coincident with actual deforestation, land clearing, and manure usage by the European settlers.

A very close analogy to the massive tree blow-down and vegetation disturbance caused by the 1635 hurricane and sustained by anthropogenic activity can be found in some of the work done on the Hubbard Brook Experimental Forest in New Hampshire (Merrens and Pearl, 1992; Pu and others, 1993; Ulrich and others, 1993; Hughes and Fahey, 1994; Martin and Hornbeck, 1994; Pardo and others, 1995; Hornbeck and others, 1997). Following clear-cutting of the forest, watershed-derived materials and nutrients increased dramatically (nutrients by up to 1200%) until new vegetation was established. This caused large phytoplankton blooms and eutrophication of the streams which drained

[81] A summary of this storm is available in the "5.2.2.1 The Great Colonial Hurricane of 1635" section above.

the area, as well as in the standing water bodies where the drainage collected. Such conditions would be excellent for *Aulacoseira* sp. because its heavy, silicified frustule requires abundant silica and nutrient-rich waters.

Thus, we suggest that heavy vegetation damage in the LML watershed which was initially produced by the 1635 hurricane and later sustained by anthropogenic activity resulted in a situation analogous to the Hubbard Brook clear-cutting experiment. Until vegetation could recover (about 23 years according to the varve chronology), sediment was easily entrained and carried into the lake to form the multiple siliciclastic bands seen per year. These multi-annual siliciclastic sediment delivery events would then fertilize the lake, and allow for the prominent *Aulacoseira* sp. blooms.

5.5.3 Black/dark zone at base of sapropelic layer

As mentioned in the "4.1.11 Anomalous zones within the varve record" section of Chapter 4, a third, anomalous, 13 cm thick black/dark zone exists within the LML varve record at the base of the soft, sapropelic zone. During deposition of this interval, the normal, annual sedimentary cycle appears to break down, and the distinct biogenic-siliciclastic couplets which both precede and follow the interval become unresolvable. This anomalous zone is unique in the record, and has several curious properties such as it does not oxidize and change color when left out like other portions of the stratigraphy, and it splits and clumps together in blocks during resin impregnation. According to the varve chronology, it spans the period from about 1895-1930.

We suggest that this black/dark anomalous zone may correspond with a period of massive, poisonous pollution, a sad chapter in the history of the Aberjona River/Mystic Lakes/Mystic River system.

While pollution of the Mystic Lakes and River system probably paralleled the Industrial Revolution which started about 1850, it was not really a problem at that point. But the pollution picked up continuously, and by the 1890's reached excessive and poisonous levels. Chapman (1936) mentions a Fish Committee appointed by the town of Winchester in 1861 to protect fishing resources when the supply of fish was still good. But by the 1890's, this Fishing Committee ceased to exist because, "increasing pollution of the Aberjona and Mystic waters left it with no fish to protect," (Chapman, 1936). He also mentions that pollution of the lake by upstream industry sources such as tanneries, dye houses, and gelatin factories began in the 1880's and 1890's.

Valeriani (1979) provides a similar chronology of increasing pollution suggesting the Mystic Lakes and River became polluted by late 1890's. It began in the 1870's when pollution from tanneries upstream in Woburn started to affect the lake (Valeriani, 1979). He points out an 11 October 1879 Medford Chronicle newspaper article in which a petition to harness some of the tidal flow on the Mystic River was denied—"The selectmen of Medford appeared and opposed the petition because the plan would obstruct navigation, and now that Boston had turned a sewer into Mystic Pond it was especially desirable to have free flow of water up and down the river." By the 1880's, the pollution had reached such a significant level that Charlestown, which had been using the Upper Mystic Lake as a water source since the construction of the dam at "The Partings", finally had to turn to Boston for water (Valeriani, 1979). Additional evidence comes from a 15

June 1883 Medford Mercury newspaper article which talks about massive fishkills of the migratory alewife along the Mystic River related to sewage-laden water exiting from the lake (Valeriani, 1979).

So pollution, a relative non-problem in the 1860's, became noticeable and significant by the 1870's, and ramped up rapidly such that by the 1890's it had reached poisonous levels. It remained at high levels for decades; for example, in 1910 it was prohibited to simply swim in the lake because it was considered "a menace to health," (Medford Mercury, 2 September 1910).

Recently, the author became aware of another significant pollution source that may also be implicated. Research by a local historian Richard Duffy provides documentation about the existence and activities of the Arlington Gasworks on the Arlington side (i.e. the west side) of the LML (R. Duffy, personal communication). The Arlington Gasworks operated a coal gasification plant that at times dumped its tarry, poisonous waste directly into Mill Brook, the small creek that feeds into the southwest corner of the lake. While the plant was operating in generally the same time frame, information about specific dates of operation, and details about the plant should be forthcoming from R. Duffy. A recent unpublished masters degree from Tufts University (Zubick, 2004) apparently links a spike in PAHs (polycyclic aromatic hydrocarbons) noted in a sediment core from the LML to this same coal gasification plant.

Thus, we suggest that the anomalous black/dark zone present in the LML stratigraphy may be related to a period of massive, poisonous pollution the lake experienced in the late 19th and early 20th centuries. Future research should be able to confirm or deny this suggestion.

5.6 Storm surge overwash record from Belle Isle Marsh

As documented in Chapter 4, a series of anomalous sand layers are found in the otherwise peaty, high marsh stratigraphy of Belle Isle Marsh (14 km ESE of LML). The sand layers are undoubtedly the result of storm surge overwash events that affected the marsh. Such events entrain sediment from the sandy ocean-facing beach to the northeast of the marsh, and then redeposit it on the marsh surface as they pass over. In general, sandy overwash layers like these are well-understood, and considered to be a good, straightforward proxy indicator for overwash events. In fact, the majority of hurricane activity reconstruction projects use similar overwash layers, whether they be in marshes or shallow coastal/backbarrier ponds, as the basis for developing their hurricane activity records.

A chronology of sand layers, classified as either continuous or local, was presented as Table 13 within the "4.2.8 Chronology of marsh sand layers" section of Chapter 4. That is reproduced below as Table 21 in this chapter. We examine that chronology now, and attempt to link the sand layers from historical times to actual known storms.

Table 21—Estimated age of deposition for sand layers in sediment core BIM-14SEP2002-PVC4-7. The year AD is given with a "+/-" error, if applicable. Continuous sand layers are listed in the left column, and sand layers of only local extent in the right column.

Continuous sand layers	Sand layers of only local extent
1978	1991
1870 +/- 40	1971
1840 +/- 54	1954
1812 +/- 70	1906 +/- 20
1235 +/- 88	1235 +/- 88
	824 +/- 101

5.6.1 Sand layers tentatively dated between 1954-1991

Given that the marsh sand layers are related to overwash during storm surge, a record of water level values for the Boston area could help link up these sand layers with known storms. In fact, hourly water level data for Boston Harbor does exist, and is freely available from the NOAA-NOS-CO-OPS website[82]. Coverage runs from 1921 to the present day. Approximately 727,000 data points are available between 1921 and 2004 given the hourly frequency, so the data was analyzed, and only high water events that fell greater than +2 standard deviations above the 1921-2004 mean value, and that were of at least 2 hours duration were used. Using this criteria, the data set was reduced to about 1020 data points. This data is presented in Figure 65 below.

The only continuous sand layer in this interval, the one tentatively dated to 1978 in Table 21, undoubtedly is a result of a great nor'easter, the memorable Blizzard of 1978. The water levels reached during this event are the highest ever recorded levels since the station began operating in 1921. In particular, this sand layer reaches a thickness of several centimeters which makes it the thickest and most prominent one in the core.

Regarding the three sand layers of only local extent tentatively dated to this interval according to Table 21 (years 1954, 1971, and 1991), at least two of those three appear to have an obvious link to known historical storms. In particular, the layer tentatively dated to 1991 is undoubtedly related to overwash during the Halloween Storm of 1991, sometimes referred to as the Perfect Storm since it inspired Sebastian Junger's 1997 novel, and eventually the 2000 Hollywood film, both of the same name.

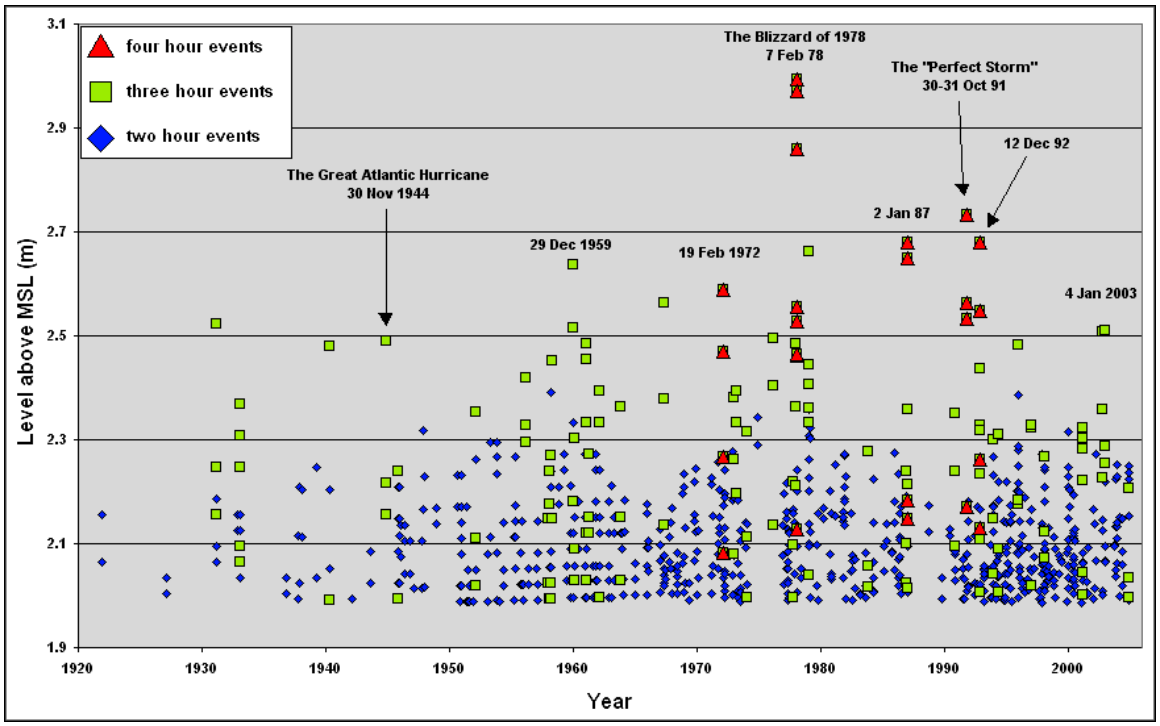

Figure 65—Excessive (> 2 standard deviations from 1921-2004 hourly mean) hourly water levels of at least two hours duration experienced at Boston Harbor from 1921-2004. The multi-shaped/-colored symbols indicate categories related to the continuous duration of the event. Blue diamonds represent high water events continuous for 2 hours, green square represent high water events continuous for 3 hours, and red triangles represent events continuous for 4 hours or more.

The sand layer of only local extent tentatively dated to 1971 is, in fact, probably the result of another large and intense nor'easter storm which affected the Boston area on 19 February 1972. Pore (1973) provides a meteorological analysis of the storm, and mentions that the surge almost coincided with one of the astronomical high tides of that day. With both forces working in coordination, an impressive storm surge was produced.

Finally, regarding the last sand layer of only local extent tentatively dated to 1954, a first expectation would be that it was related to the passage of Hurricane Carol on 31 August-1 September 1954 as storm surge is often mentioned in relation to that storm. However, the zone of strongest storm surge was along the southern New England coast.

---

[82] The current URL is "http://co-ops.nos.noaa.gov/cgi-bin/station_info.cgi?stn=8443970+Boston,+MA".

In the Boston area it was unspectacular as can be seen by its lack of appearance in Figure 65. Instead, it might be more appropriate to identify it with another unnamed nor'easter storm on 29 December 1959 that did produce a significant storm surge.

Thus, out of these four sand layers, it seems that all of them may have been deposited by nor'easter storms, and not hurricanes.

5.6.2 Sand layers tentatively dated between 1812-1906

Historical water level data for Boston Harbor is only available back to 1921. For the sand layers that are tentatively dated to earlier than this, but still within the historical period, we can partly rely on the Hurricane Research Division's Atlantic Hurricane Database Re-analysis Project (see "5.2 Brief history of historical Boston hurricanes" section above for more information), and the historical documentation from the storm summaries (in the "5.2 Brief history of historical Boston hurricanes" section above) in an attempt to link these sand layers to particular storms.

Regarding the sand layer of local extent tentatively dated as 1906 +/- 20 year, this gives a total age range from 1886-1926 when the error is expanded. Ludlum's (1963) hurricane volume ends in 1870, so we turn to the best estimate trajectory and intensity maps published by the Re-analysis Project. That database illustrates several tropical disturbances (mostly tropical depressions and tropical storms with a few Category 1 hurricanes included) that passed close by the Boston area within the 1886-1926 time frame. This includes storms during the years of 1886, 1889, 1894, 1896, 1897, 1900, 1902, 1904, 1907, 1908, and 1923. Unfortunately, the Re-analysis Project does not offer the same type of historical descriptions provided by Ludlum (1963), so it is not possible

to figure out which of these possible 11 candidate storms is the most likely event that deposited the sand layer in question. Note that all 11 of these candidate storms are of tropical nature—extratropical nor'easter storms have not even been considered as candidates which would expand the candidate pool greatly.

Regarding the three sand layers of continuous extent that are tentatively dated to all within the 1800's, we deal with these jointly as their ranges overlap completely, but their relative/stratigraphic order is absolute and unchangeable. The dates included are 1870 +/40, 1840 +/- 54, and 1812 +/- 70 years. When the error ranges are expanded, it gives a possible total age range from 1742 to 1910. Ludlum (1963) provides information about six different hurricanes that produce moderate to large storm surges within this timeframe. Those include the following storms:

- Benjamin Franklin's Eclipse Hurricane of 1743
- The Late Season Storm of October 1770
- New England's Snow Hurricane of 1804
- The Great September Gale of 1815
- Minot's Lighthouse Gale of 1851[83]
- The "Expedition" Hurricane of November 1861

Certainly, the last three storms (1815, 1851, and 1861) seem the most probable candidates for depositing the overwash sand layers given their dates, but at least four of the six candidate storms (1743, 1770, 1851, and 1861) would be good choices because of the exceptional storm surges they produced. Because of this, it is difficult to confidently associate any of the sand layers with a particular storm. Another important consideration is that this list of candidate storms includes only hurricanes with the exception of the

[83] This was actually a nor'easter storm, not a hurricane, but it produced the highest water level ever recorded in the Boston area. If a storm was going to deposit overwash in Belle Isle Marsh, there would not be a better candidate.

1851 storm, so there are probably many more extratropical nor'easter storms that could serve as candidates, and are simply not listed here.

5.6.3 Sand layers tentatively dated to prehistoric times

Sediment core BIM-14SEP2002-PVC4-7 contains three more sand layers tentatively deposited during prehistoric times. One of the sand layers is continuous, and is dated to AD 1235 +/- 88 years. The two other sand layers are discontinuous, and are dated to AD 1235 +/- 88 years, and AD 824 +/- 101 years. That two of these sand layers share a tentative age of AD 1235 +/- 88 years is a function of the fact that they both fall within an 8 cm vertical section of the core which underwent conventional radiocarbon dating. There is no way to know whether these sand layers actually represent deposition by a hurricane, or an extratropical storm given that even during the historic period, it is essentially impossible to confidently link up sand layers to particular storms because of flexibility of the chronologic control.

5.6.4 Summary of the BIM storm surge overwash record

Very few conclusive details about hurricane activity can be drawn from the BIM storm surge overwash record. Without a doubt, the major frustrating issue is the chronology that can be derived from a sedimentary archive such as a marsh. The handful of absolutely-dated horizons towards the top of the core (from ^{137}Cs dating, and the Logan Airport expansion clay bed) provide good chronologic control back about 60 years before present. But before that it is almost just a guessing game in attempting to assign a sand layer to a particular known historical storm.

There are some worrying aspects about the BIM record, particularly the fact that a few overwash layers start off the sequence at AD 824 +/- 101 years, and 1235 +/- 88 years, but then there is an apparent 600 year quiescent period, and several more sand layers appear over the most recent 200 years. We confidently know of large storm surges that affected Boston Harbor during the 1600s and 1700s from the historical record. And undoubtedly large storm surges were produced by at least a few of the hurricanes that are recorded in the LML varve record as graded beds during the prehistoric period.. But according to our chronology these portions of the BIM record are barren. This is probably related to a geomorphic change provoked by sea level rise during this span of the record. But given the ultimate goal of using such a record to interpret changes in storm frequency, it reaffirms the fact that considerable attention must be paid to the details of any system.

5.7 A brief comparison of the LML varve record and BIM marsh record, and their use for building a hurricane activity record

The hurricane activity records derived from the LML varve chronology and from the BIM record share a fundamental premise—the passage of a hurricane or large storm alters the sedimentation patterns that affect a specific sedimentary archive, be it an annually laminated lake or a coastal marsh. If that anomalous sedimentation pattern is preserved in the sedimentary archive, it can be used later to reconstruct a time series of the events that produced it. The similarity between the records stops here.

The main difference between the two records is the choice of sedimentary archive. The LML varve record offers an exquisite, (sub-)annually resolvable archive of sedimentation in the lake over the last millennium. It has been shown that the lake is

extremely sensitive to environmental change, and preserves such changes via subtle variations in sediment type or quantity.

The BIM record, in turn, offers a sedimentary archive of much lower resolution. No matter what quantity of tests or age-dating analyses are applied to the record, it can never approach the level of sub-annual resolution offered by the LML varve record. Even if the quantity of ^{14}C dates used to date the archive were tripled or quadrupled, the very nature of the radiocarbon dating technique is that every result is a range of values, not a single specific year. Certainly additional dating techniques could be used to help control the chronology. For example, pollen analysis or a chemical analysis could be used to identify certain absolutely dated horizons. But nonetheless, even between every absolutely dated horizon, the intervening ages must be interpolated. In comparison, the very architecture of the LML varves have a well-understood, built-in, chronological significance that is continuous over the length of the record—interpolation is not necessary.

Thus, it is nearly impossible to draw any conclusions of confidence from the BIM record concerning hurricane activity. The marsh is ideally situated to record high water events in Boston, and it has registered anomalous sand layers that are related to storm surge overwash. But the chronology is simply so poor, at least when compared to the exquisite LML chronology, that we cannot assign the sand layers to particular storms with any confidence. For example, for the tentatively dated 1906 +/- 20 years sand layer, there were 11 different possibilities for tropical storms that might have been responsible for it. And the same thing can be said for the three sand layers tentatively dated to the 1800's—

with six different choices to apply between the three, it would be hard to consider any of the dates confident.

Another complication, perhaps a function of the locality more than anything, is that a significant number of extratropical nor'easter storms also affect the Boston area, and are clearly capable of generating massive storm surges. There seems to be no way to distinguish their overwash from similar overwash produced by a true hurricane. If annual chronological resolution were available from a marsh locality, it might be possible to develop a statistical technique such as was possible for the LML[84]. Unfortunately, such resolution may never be possible for a marsh sequence. Furthermore, for the interval where we have a well-dated marsh sequence, all of the identifiable sand layers are associated with nor'easters, not hurricanes. We conclude that marsh records (at least in this location) are not very useful in determining the frequency of past hurricanes in the Boston area. It is likely that similar factors limit the usefulness of this type of archive in other coastal settings, and so chronologies of hurricanes based on such records must be treated with caution.

[84] In particular, we are referring to the statistical analysis of varve thickness for the LML with which it was observed than any varves with a thickness >3 standard deviations from the average contained a graded bed, and corresponded with a known hurricane year. See the "5.4.6 Can anomalous thickness be used to unequivocally identify a hurricane signal?" section above.

CHAPTER 6

CONCLUSION

6.1 Introduction

"Tempestites", or storm event-related sediment layers, have long been recognized in the geologic record. But until the pioneering work of Liu and Fearn (1993) at Lake Shelby in Alabama, the simple idea of using such indicators from a modern sedimentary environment to build a time series of (sub-)recent hurricane activity had simply never been undertaken.

Inspired by Liu and Fearn (1993), as the field of paleotempestology began to bloom, almost all studies followed the same tack, and used generally low resolution, coastal sedimentary archives such as marshes to undertake similar work. While useful, the geomorphic evolution of coastal environments is often quite rapid—the migration of a dune or channel could lead to an apparent change in hurricane-related sedimentation at one location which might be interpreted as a change in storm frequency or intensity. Furthermore, as with almost any paleo study, a robust, unambiguous chronology is critical for confident interpretations, but the level reachable with one of these coastal archives is simply not in the same category as a higher resolution archive. And critically, all of these subaerial or shallow subaqueous sedimentary environments are subject to bioturbation. Bioturbation may completely obliterate a thinner event layer related to a less intense event, or perhaps worse, it may homogenize two closely spaced event layers into a single layer which leads to an apparent single mega-event. Given the critical attention that such hurricane activity studies receive as we attempt to understand how hurricane activity

varies naturally and due to global change, we saw a significant opportunity to improve on preexisting work.

Thus, as this project was conceived in early 1996, our goal was to guide the field of paleotempestology to the next level by developing a similar hurricane activity record, but based on a sedimentary archive that does not suffer from the same critical limitations as the lower resolution coastal records. To do so, we turned to a varved (e.g. annually laminated) lacustrine record which completely eliminated the issue of bioturbation, and which offered exquisite and robust chronologic control that would have been simply impossible to obtain from lower resolution coastal records. We think that this project has shown the great potential that high resolution sedimentary archives can offer the field of paleotempestology. And we hope that it inspires future work in the field to use similar high resolution archives, whether they be varved lacustrine sediments, or a different medium, but with similar resolution.

6.2 Answers to research questions proposed in introduction

In the introduction to this dissertation, we proposed several research questions we hoped this project would help address. The results are provided here.

6.2.1 What is the average recurrence rate for large intense hurricane strikes near the Boston area during the last millennium?

We do not have a definitive answer to this question yet as we are not yet able to confidently estimate the intensity of a storm based on the graded bed it deposits.

As discussed in Chapter 5 (the "5.3 One if by land, and two if by sea—source of the graded beds" section), we have identified the mechanism behind the occasional,

anomalous graded beds. We hypothesize that intense, hurricane-strength rains saturate the watershed, resulting in erosive overland flow that entrains sediment, which is then carried into the lake where it is deposited as a graded bed. This is enhanced by hurricane-strength winds which disturb vegetation, and uproot trees to expose fresh, loose sediment.

We intuitively expected that the thickness of these graded beds would be proportional to the strength of the storm that produced it. Unfortunately, at least for the graded beds linked to known hurricanes during the historical period, the thickness of the graded bed does not seem to be linked to the intensity of the storm (see the "5.4.7 Does varve thickness have any relationship to storm intensity?" section in Chapter 5).

As discussed in Chapter 5, we believe at least two factors might play a role in this. First, it may be an indirect consequence of the effect of European colonists on the landscape. For example, as fields around the lake are either cultivated or left fallow, this will directly affect the ease with which siliciclastic sediment is entrained and carried into the lake. Second, an obvious natural/non-anthropogenic control that must always be considered is the simple storm trajectory. Two storms of equivalent intensity could produce graded beds of different thicknesses simply by varying their trajectories with respect to the lake.

Prior to the arrival of European settlers, we do think that graded bed thickness may more directly be related to storm intensity provided that trajectory plays a neutral role. Certainly, the native American population had some effect on the landscape during this time, but the intensity with which they affected the landscape was not comparable to the massive alterations produced by European settlement. That the thickness of pre-

European settlement graded beds may be more directly related to storm intensity seems difficult to prove, but future work will examine this relationship further.

While we cannot identify "intense" storms at this point, we can confidently identify significant storms that directly affected the Boston area. From the statistical analysis of varve thickness in Chapter 5 (the "5.4.4 LML varves of anomalous thickness deposited from AD 1060-1865" section), out of the entire record back to AD 1060, we identified 12 varves with thicknesses >3 standard deviations from the mean, and each of those varves had a prominent graded bed. Of these 12 excessively thick varves, 6 were from the historic period, and 6 were from the prehistoric period. Every one of the 6 historic period varves corresponded with years in which known hurricane events affected the Boston area. By analogy, the remaining 6 excessively thick varves from the prehistoric period probably represent similar events.

Regarding a recurrence rate for such events, as mentioned, 6 of the excessively thick varves were deposited during the historic period, and 6 in the prehistoric period. For the purposes of the statistical varve thickness analysis, the prehistoric period ran from the beginning of the record in 1060 up to 1630, or a total of 570 years. In turn, the historic period ran from 1630-1865, or 235 years total. Given 6 excessively thick varves in each period, this would suggest a recurrence rate of about 95 years between events (i.e. 570 years ÷ 6 events) during the prehistoric period, and ~39 years between events (i.e. 235 years ÷ 6 events) during the historic period.

We do not believe it is appropriate to take these recurrence rates at face value at this point. Importantly, no consideration was been given to storm trajectory. In hindsight, we also believe our initial statistical analysis of varve thickness may have been

biased against the prehistoric portion of the record because the entire time series up to 1865 was used in calculating the mean. Since there is a higher variability in the historic part of the record, the relative ability to identify anomalous thicknesses in the prehistoric portion of the record was decreased. Instead, it would be appropriate to undertake another statistical analysis of varve thickness in the future, but by treating both the prehistoric and historic portions as individual entities, and not mixing them together. We believe that type of analysis would offer a more valid perspective about the true recurrence rate for hurricanes during the prehistoric period.

6.2.2 Do the hyperactive and quiescent modes of hurricane activity reported in the Gulf of Mexico also exist for the eastern seaboard of the U.S., and are they anti-correlated between regions?

As mentioned in Chapter 1, Liu and Fearn (2000) and Elsner and other (2000) presented the idea of regional hyperactive and quiescent modes of hurricane activity—when the Gulf region is in hyperactive mode, the eastern seaboard of the U.S. is in quiescent mode, and vice versa. They identified a mode transition about 1000 years ago.

Based on an initial radiocarbon date towards the base of the varved sequence before the varve chronology was established, we estimated the chronology included about 1200 varves. This would have allowed the LML record to show about 200 years of the previous regime followed by a full 1000 years of the new regime with the transition sandwiched between them. However, after our varve chronology was constructed, and finally linked to sediment/water interface with the retrieval of oversized freeze core LML-19JAN2002-FRZ-1 core, we were able to determine the true number of varves available, and that is slightly less than 1000 as the record begins in 1060. Thus, we cannot answer

this question because it was formulated expecting the LML varve chronology would include about 1200 varves. Fortunately, we can at least examine frequency changes within the period of the record itself. As discussed above, future work will include another statistical analysis of thickness, but treating the prehistoric and historic portions and individual entities, not lumping them together.

6.2.3 Can any empirical relationship be detected between periods of globally warmer or cooler climate, and hurricane activity which simple atmospheric circulation models suggest should exist?

As mentioned in the answers to the two questions above, we are not satisfied with the statistical thickness analysis performed on the varve record. In hindsight, we believe that the analysis was partially biased against the prehistoric period because that period did not receive the thickness "benefit" that may have been afforded to the varves during the historical part of the record because of the indirect effect of humans on the landscape.

Nonetheless, if we exclude thickness for the moment, and simply tally up the number of graded beds per century (listed in Table 9 in Chapter 4), we do notice some differences (Figure 66). In particular, one might identify a broad high during the 11th-15th centuries, and then a ramp down in the 16th and 17th centuries to a final low value in the 18th century. In the loosest of definitions, the broad high in the 11th-15th centuries might be correlated with the Medieval Warm Period (Keigwin, 1996), and the ramp down in the 16th–18th centuries with the Little Ice Age (Grove, 1988).

We are hesitant to attach any significance to this temporal distribution of graded beds given this record is from just one locality. But as new records are developed, if a

plurality of records from different locations begins to show a similar distribution, then we would begin to assign it some significance.

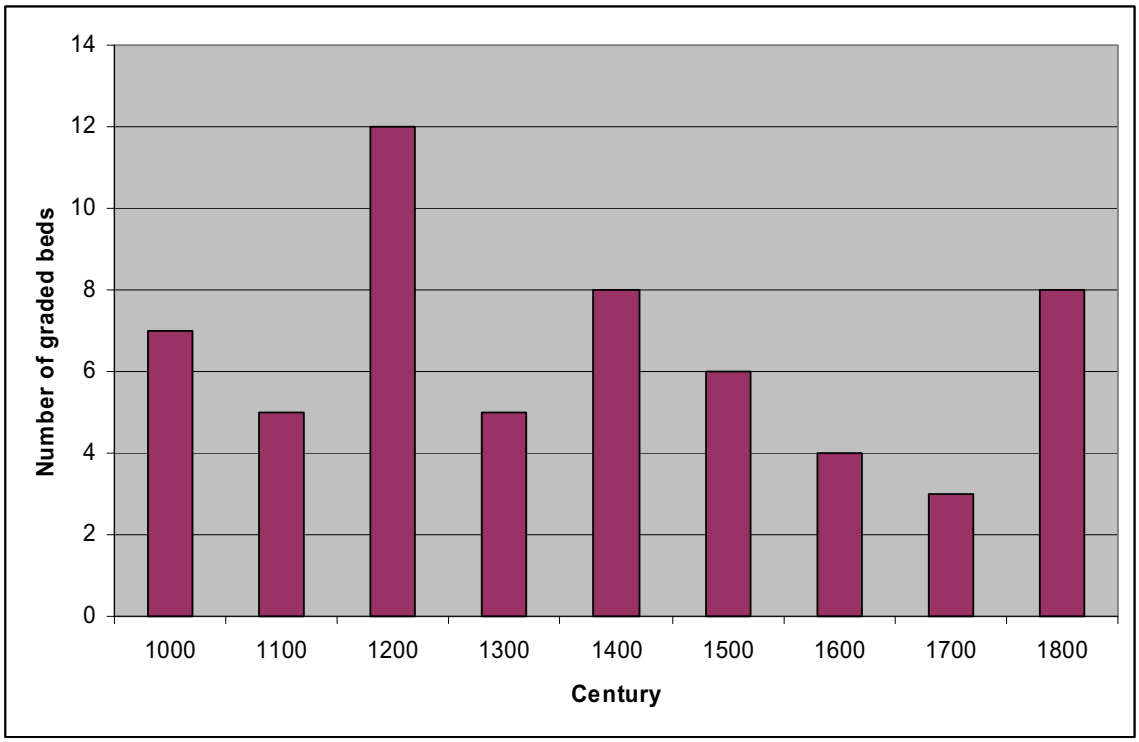

Figure 66—Histogram showing the number of graded beds per century found in the LML varve record. This plot entirely excludes varve thickness, and simply references the number of graded beds of varying sizes. Note that the tally for the 11th century only includes from 1060 onward as that is when the record begins. If the period from 1000-1059 existed as varves, it would undoubtedly contribute to an increased number of graded beds for the 11th century.

6.3 Suggestions for future work

The LML varve record holds tremendous potential to serve as a well-dated, high resolution archive of paleoenvironmental data for the Boston, and perhaps greater New England area. A tremendous portion of the energy devoted to this project was dedicated to understanding the nature of the archive, and developing the high resolution chronology. The hurricane activity record which has emerged is simply the first of many paleoenvironmental studies that can be built on the solid base we have established. We

offer some brief suggestions below about future that could/should be undertaken with the record.

6.3.1 Revised statistical analysis of varve thickness record

As we have mentioned several times above, in hindsight, we feel the statistical varve thickness analysis might have been biased against the prehistoric period since that portion of the record did not experience the indirect effects of human activity on the landscape. A new analysis should be performed, but treating both the prehistoric and historic periods as separate entities.

6.3.2 Grayscale densitometry analysis of X-ray imagery

As the LML varves are predominantly a mix of biogenic and siliciclastic components, the grayscale value of an X-ray image of those sediments essentially serves as an index of biogenic vs. siliciclastic content. Given this, a grayscale densitometry analysis over the length of the record could quickly provide a long-term index of siliciclastic input, or biogenic production, in the lake.

6.3.3 Continued BSEM analysis of selected sections of record

Continued BSEM analysis of select portions of the record could still provide important information about processes which affect the lake. For example, in Chapter 5, we identified yellowish varves in the freeze core, and noted that they perfectly corresponded with drought periods. Other zones which would also benefit from BSEM examination include the three zones of anomalous sedimentation discussed in Chapter 4.

6.3.4 Paleoenvironmental analyses

The LML varve record will serve as a great base for a variety of paleoenvironmental work including analyses of pollen, diatom assemblages, and many other paleoenvironmental indicators. In particular, the analysis of diatom assemblages should prove useful for confirming the landward source of the graded beds vs. the seaward source which was originally postulated[85].

6.3.5 Additional sediment core retrieval for possible record extension and long term archiving

The retrieval of additional sediment cores would be useful for filling in some of the small gaps left in the LML varve chronology. Importantly, the piston core (LML-23NOV1996-LIV-1) on which the majority of the chronology is based was retrieved from 20.3 m water depth whereas the lake actually reaches about 24 m depth. It is possible that sediment cores from the deepest part of the basin might preserve older varves that were not preserved at shallower water depths. If so, this may allow us to extend the varve record back in time.

Additionally, as Ludlam and Duval (2001) have estimated the monimolimnion in the lake will disappear by 2013-2014, it is imperative that we obtain multiple archive copies of the record before it is lost. When the monimolimnion disappears, bioturbation on the lake bottom will obliterate at least the upper 10-15 cm of the varved record, and possibly more.

---

[85] Diatom assemblage analysis was, in fact, planned as a component of this project, and approximately 160 diatom slides were prepared from samples over the length of the record. Unfortunately, time constraints did not allow this portion of the project to be realized.

APPENDIX A

VARVE CHRONOLOGY X-RAY AND OPTICAL IMAGERY

This appendix contains the X-ray and optical microscope imagery of the LML varve chronology.

For the "Bird" series impregnations which were produced from core LML-23NOV1996-LIV-1, each figure contains the raw X-ray thin slab imagery with sedimentary and stratigraphic defects, the palinspastically reconstructed X-ray thin slab imagery used as the base for the varve chronology and thickness record, and cross- and plane-polarized optical microscope imagery of the thin sections. The X-ray thin slabs were cut from the subsample blocks perpendicular to the plane of the thin sections. Thus, they a critical cross-check again the thin section imagery, and vice versa.

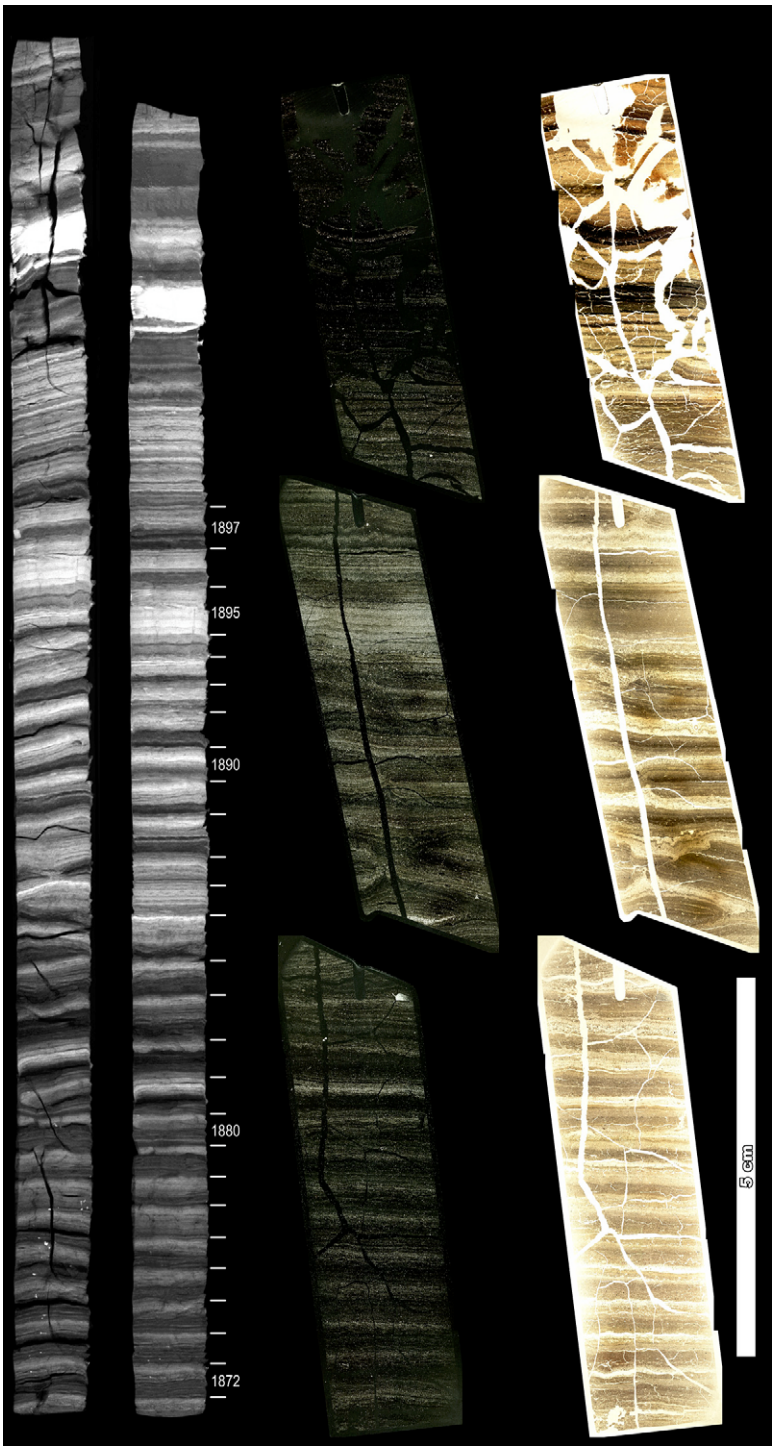

Figure 67—"Bird A" series X-ray and optical imagery. From the left to the right, the figure includes: 1.) raw X-ray imagery, 2.) palinspastically reconstructed X-ray imagery with the varve chronology ages, 3.) cross-polarized light optical imagery, and 4.) plane-polarized light optical imagery. Note the 5 cm scale bar in the image.

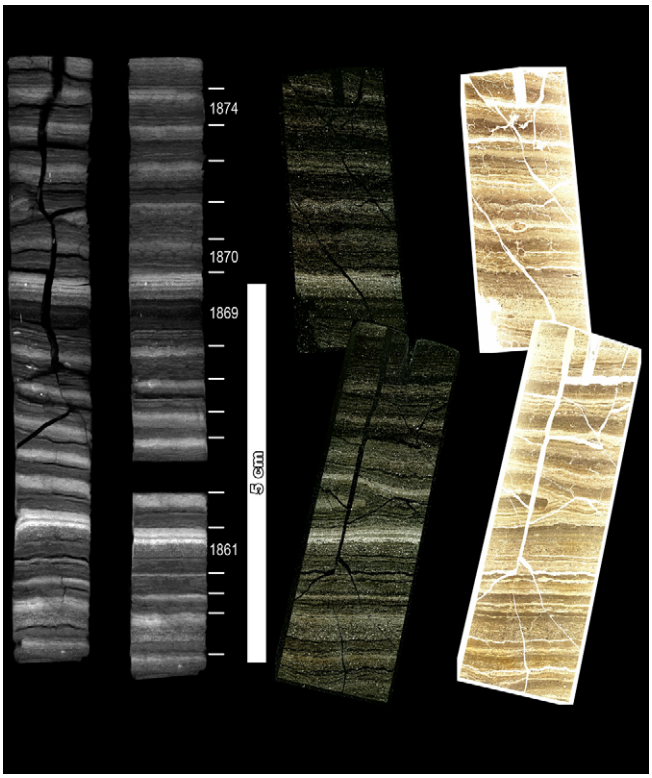

Figure 68—"Bird B" series X-ray and optical imagery. From the left to the right, the figure includes: 1.) raw X-ray imagery, 2.) palinspastically reconstructed X-ray imagery with the varve chronology ages, 3.) cross-polarized light optical imagery, and 4.) plane-polarized light optical imagery. Note the small gap in the chronology following the 1862 varve. The stratigraphic defect responsible for this gap is essentially unnoticeable in the X-ray imagery, but obvious in the optical imagery which was cut from a perpendicular plane. Note the 5 cm scale bar in the image.

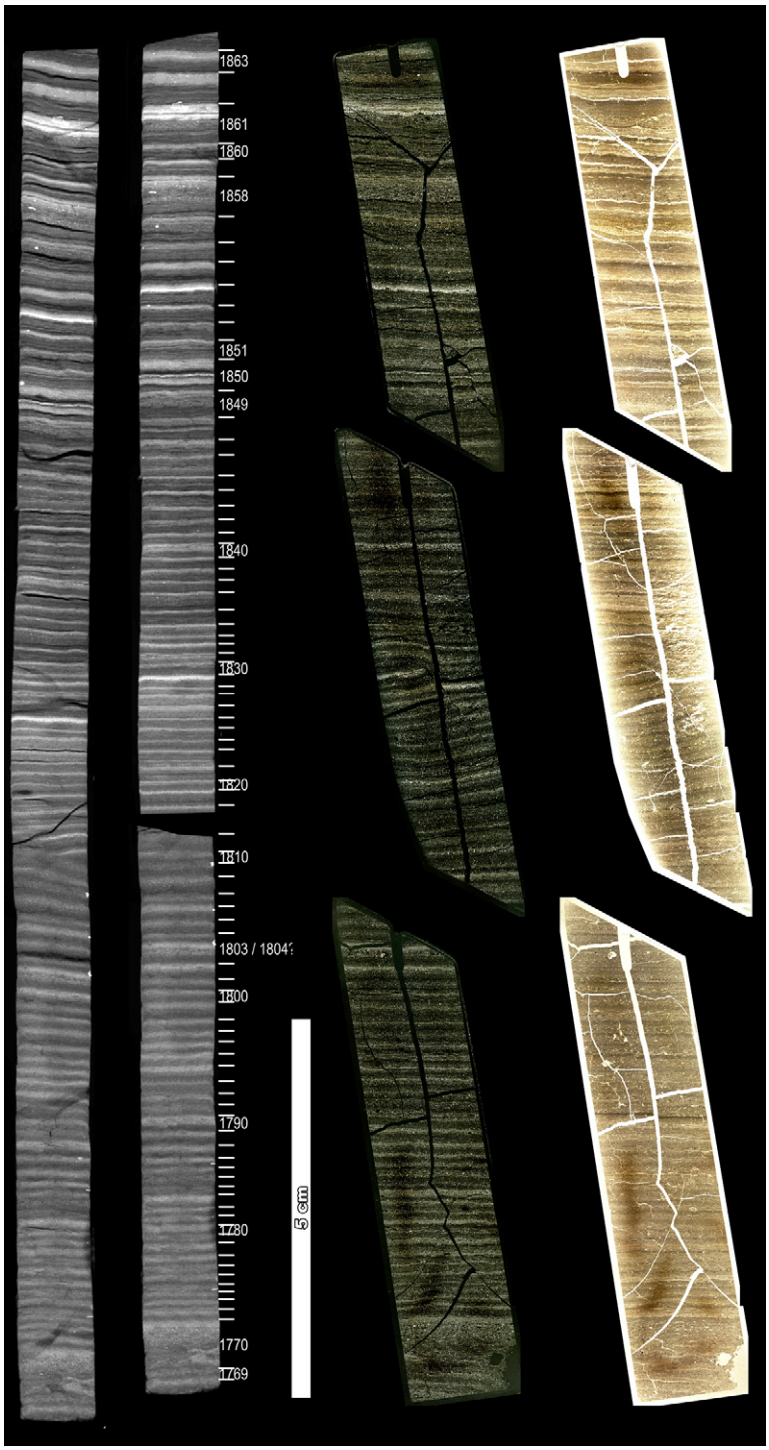

Figure 69—"Bird C" series X-ray and optical imagery. From the left to the right, the figure includes: 1.) raw X-ray imagery, 2.) palinspastically reconstructed X-ray imagery with the varve chronology ages, 3.) cross-polarized light optical imagery, and 4.) plane-polarized light optical imagery. Note the small gap in the chronology following the 1811 varve. The stratigraphic defect responsible for this gap is essentially unnoticeable in the optical imagery, but obvious in the X-ray imagery which was cut from a perpendicular plane. Note the 5 cm scale bar in the image.

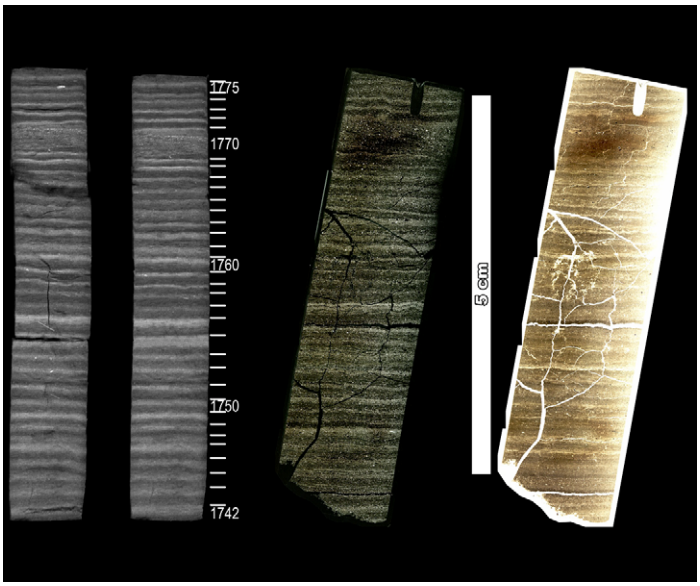

Figure 70—"Bird D" series X-ray and optical imagery. From the left to the right, the figure includes: 1.) raw X-ray imagery, 2.) palinspastically reconstructed X-ray imagery with the varve chronology ages, 3.) cross-polarized light optical imagery, and 4.) plane-polarized light optical imagery. Note the 5 cm scale bar in the image.

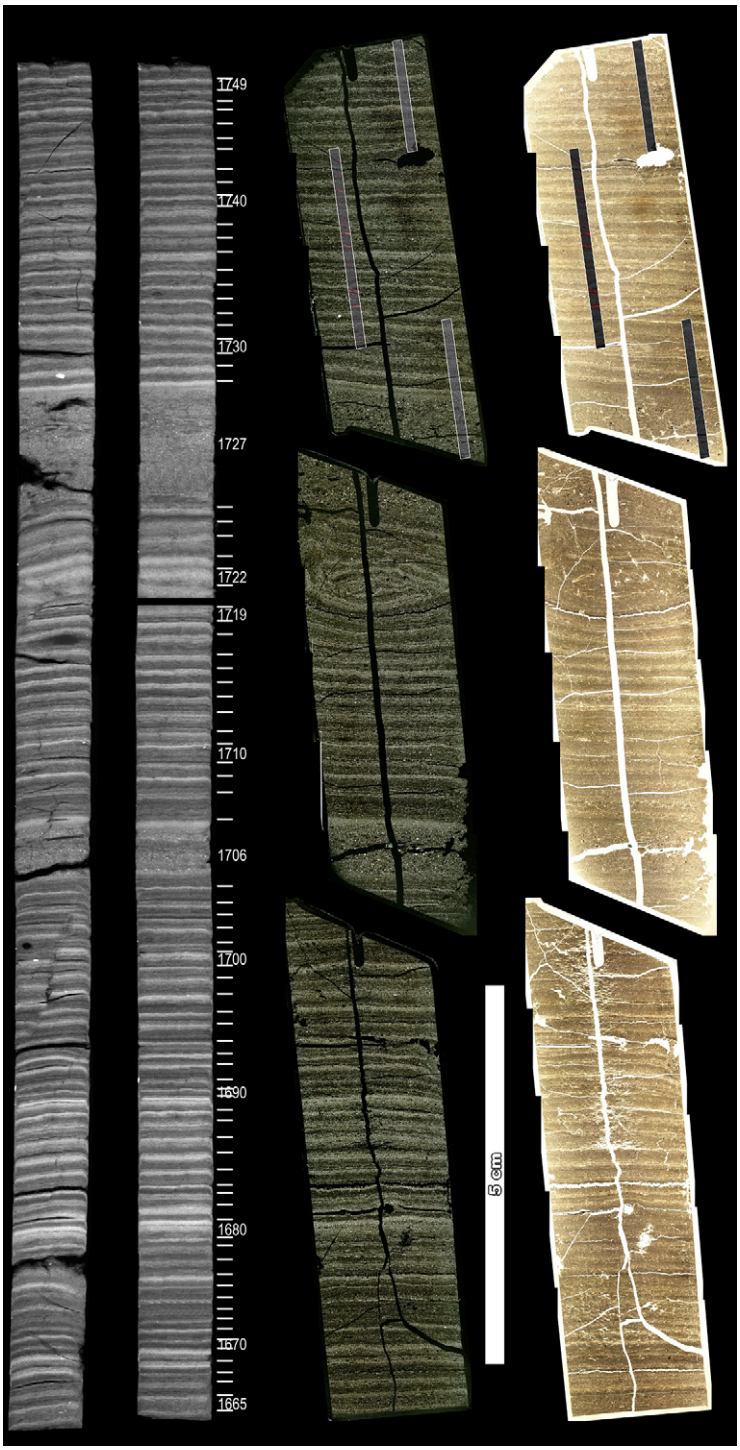

Figure 71—"Bird E" series X-ray and optical imagery. From the left to the right, the figure includes: 1.) raw X-ray imagery, 2.) palinspastically reconstructed X-ray imagery with the varve chronology ages, 3.) cross-polarized light optical imagery, and 4.) plane-polarized light optical imagery. The strips seen on the optical imagery are BSEM image transects. Note the small gap in the chronology following the 1719 varve. The stratigraphic defect responsible for this gap is noticeable in both the X-ray and optical imagery. Note the 5 cm scale bar in the image.

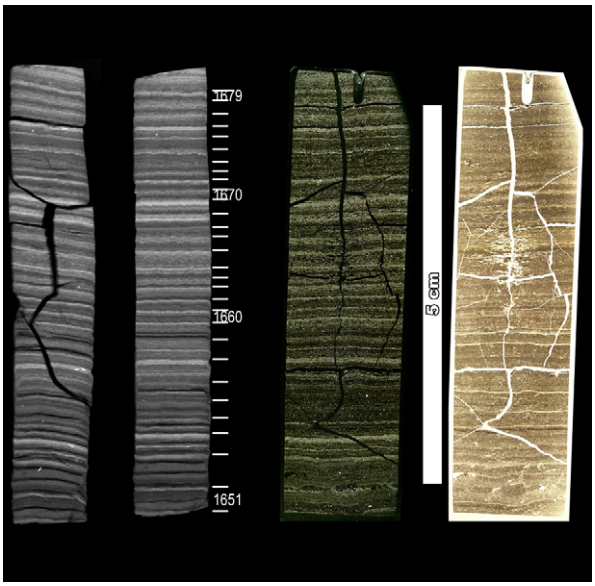

Figure 72—"Bird F" series X-ray and optical imagery. From the left to the right, the figure includes: 1.) raw X-ray imagery, 2.) palinspastically reconstructed X-ray imagery with the varve chronology ages, 3.) cross-polarized light optical imagery, and 4.) plane-polarized light optical imagery. Note the 5 cm scale bar in the image.

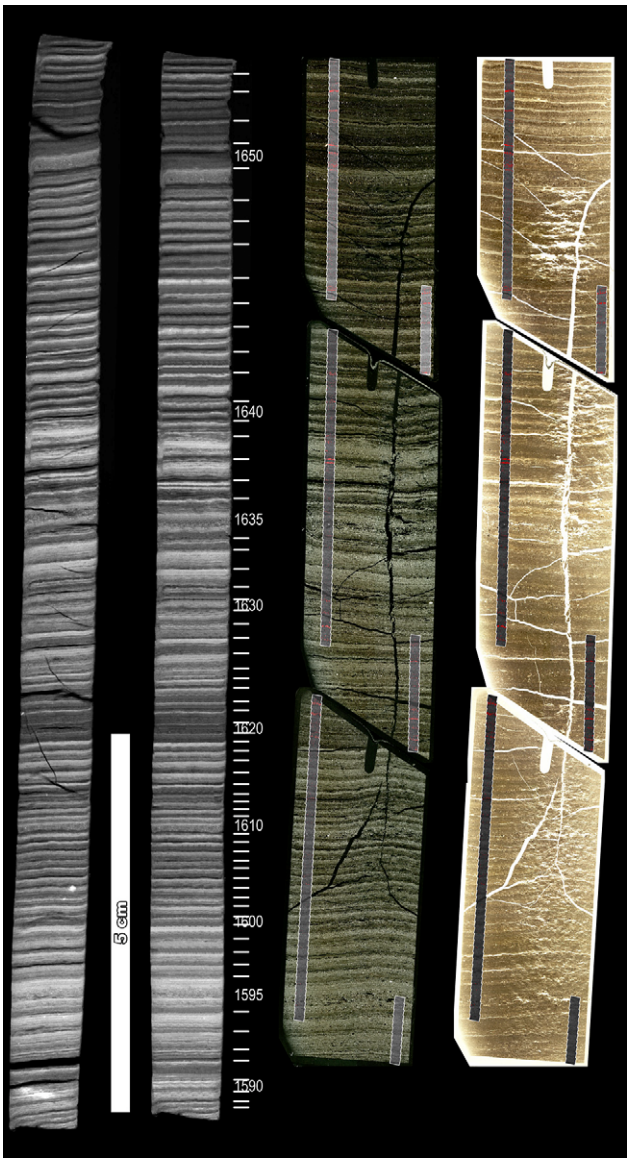

Figure 73—"Bird G" series X-ray and optical imagery. From the left to the right, the figure includes: 1.) raw X-ray imagery, 2.) palinspastically reconstructed X-ray imagery with the varve chronology ages, 3.) cross-polarized light optical imagery, and 4.) plane-polarized light optical imagery. The strips seen on the optical imagery are BSEM image transects. Note the 5 cm scale bar in the image.

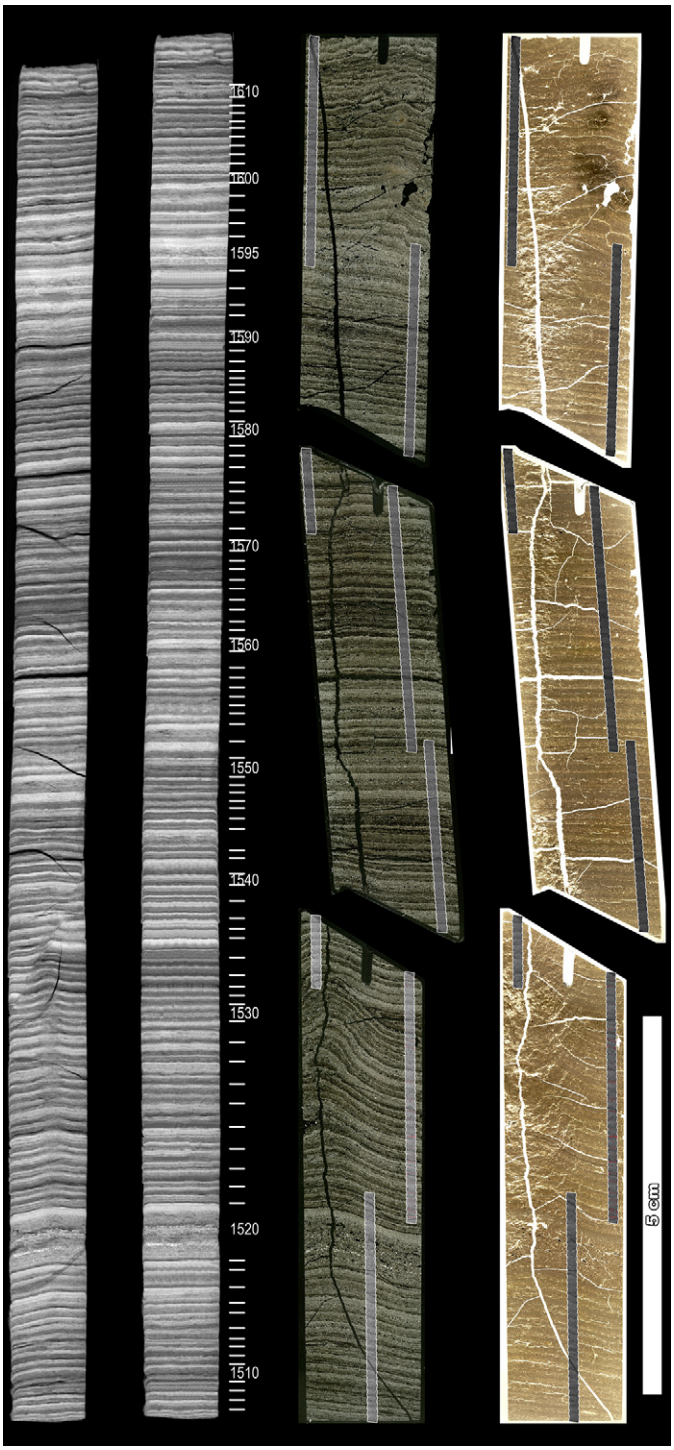

Figure 74—"Bird H" series X-ray and optical imagery. From the left to the right, the figure includes: 1.) raw X-ray imagery, 2.) palinspastically reconstructed X-ray imagery with the varve chronology ages, 3.) cross-polarized light optical imagery, and 4.) plane-polarized light optical imagery. The strips seen on the optical imagery are BSEM image transects. Note the 5 cm scale bar in the image.

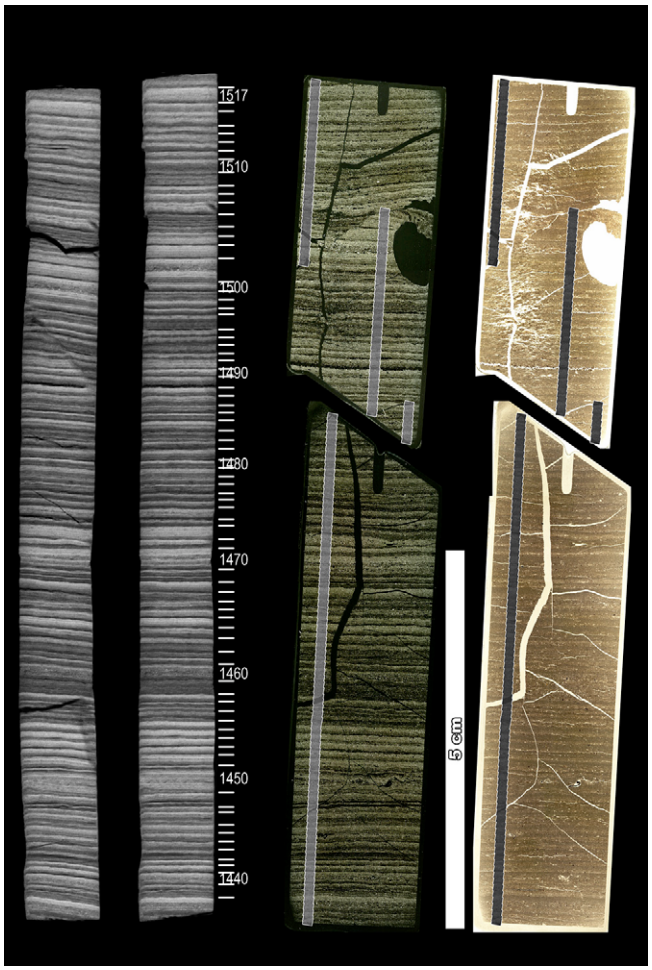

Figure 75—"Bird I" series X-ray and optical imagery. From the left to the right, the figure includes: 1.) raw X-ray imagery, 2.) palinspastically reconstructed X-ray imagery with the varve chronology ages, 3.) cross-polarized light optical imagery, and 4.) plane-polarized light optical imagery. The strips seen on the optical imagery are BSEM image transects. Note the 5 cm scale bar in the image.

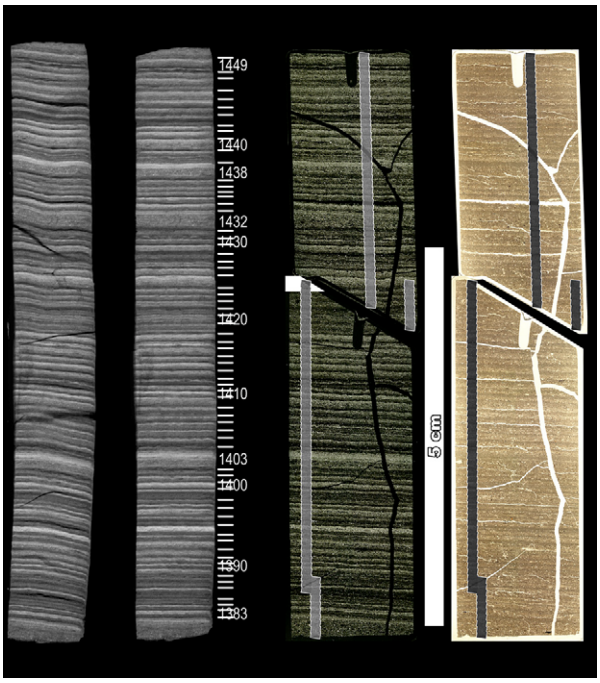

Figure 76—"Bird J" series X-ray and optical imagery. From the left to the right, the figure includes: 1.) raw X-ray imagery, 2.) palinspastically reconstructed X-ray imagery with the varve chronology ages, 3.) cross-polarized light optical imagery, and 4.) plane-polarized light optical imagery. The strips seen on the optical imagery are BSEM image transects. Note the 5 cm scale bar in the image.

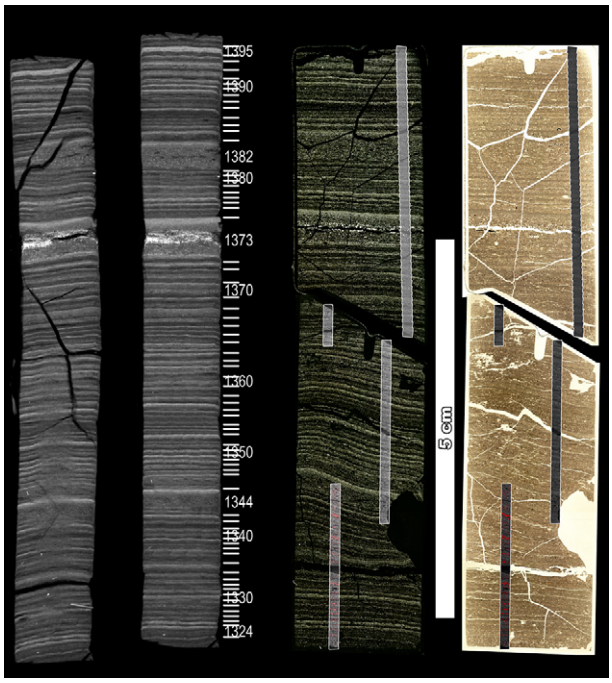

Figure 77—"Bird K" series X-ray and optical imagery. From the left to the right, the figure includes: 1.) raw X-ray imagery, 2.) palinspastically reconstructed X-ray imagery with the varve chronology ages, 3.) cross-polarized light optical imagery, and 4.) plane-polarized light optical imagery. The strips seen on the optical imagery are BSEM image transects. Note the 5 cm scale bar in the image.

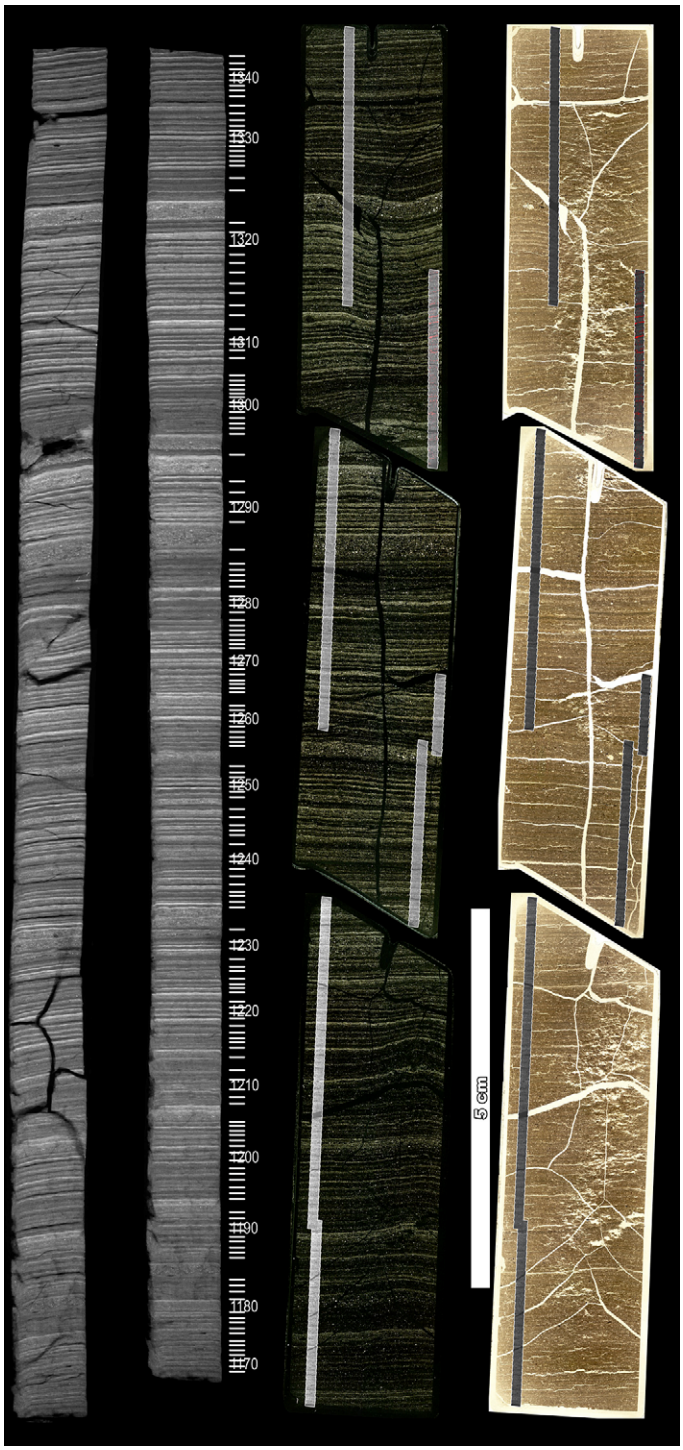

Figure 78—"Bird L" series X-ray and optical imagery. From the left to the right, the figure includes: 1.) raw X-ray imagery, 2.) palinspastically reconstructed X-ray imagery with the varve chronology ages, 3.) cross-polarized light optical imagery, and 4.) plane-polarized light optical imagery. The strips seen on the optical imagery are BSEM image transects. Note the 5 cm scale bar in the image.

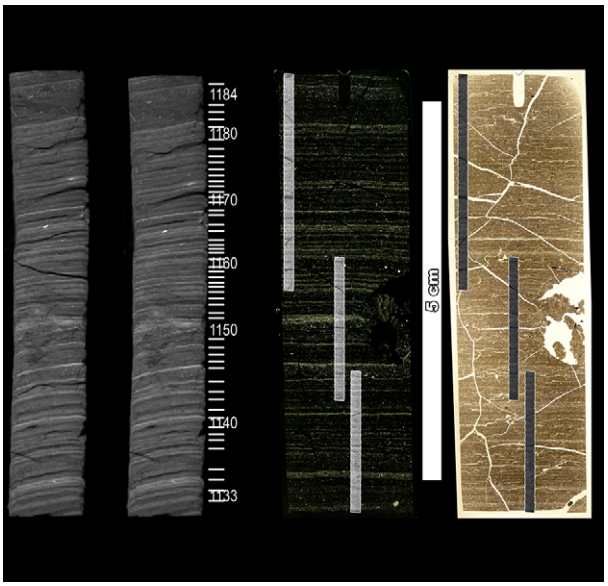

Figure 79—"Bird M" series X-ray and optical imagery. From the left to the right, the figure includes: 1.) raw X-ray imagery, 2.) palinspastically reconstructed X-ray imagery with the varve chronology ages, 3.) cross-polarized light optical imagery, and 4.) plane-polarized light optical imagery. The strips seen on the optical imagery are BSEM image transects. Note the 5 cm scale bar in the image.

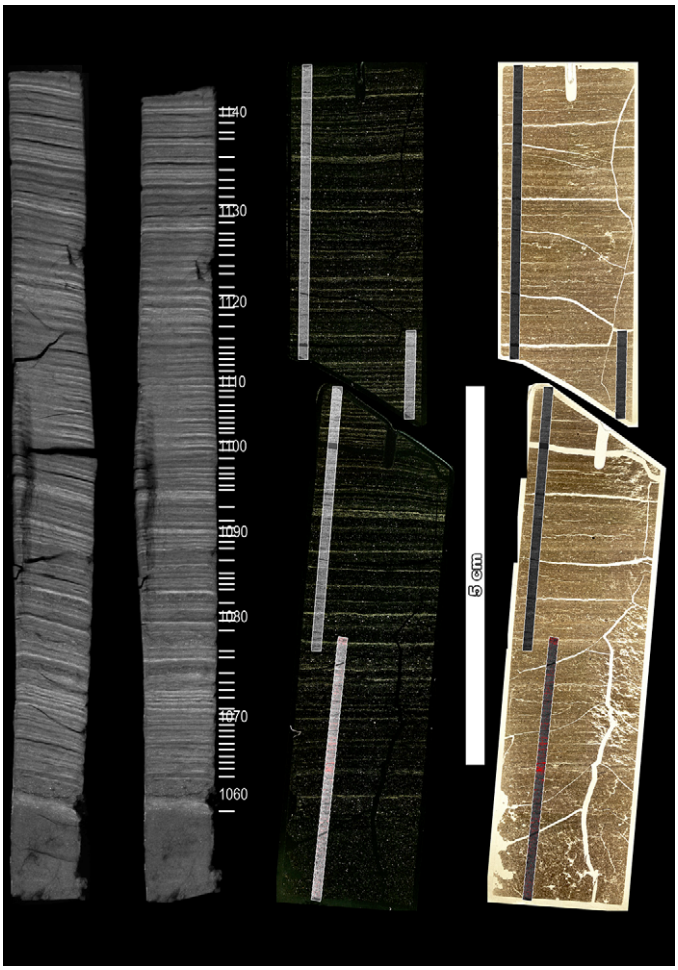

Figure 80—"Bird N" series X-ray and optical imagery. From the left to the right, the figure includes: 1.) raw X-ray imagery, 2.) palinspastically reconstructed X-ray imagery with the varve chronology ages, 3.) cross-polarized light optical imagery, and 4.) plane-polarized light optical imagery. The strips seen on the optical imagery are BSEM image transects. Note the 5 cm scale bar in the image.

BIBLIOGRAPHY

Abbott, M.B. and Stafford, T.W., 1996, Radiocarbon geochemistry of ancient and modern Arctic lakes, Baffin Island: Quaternary Research, v. 45, p. 300-311.

Appleby, P. and Oldfield, F., 1978, The calculation of lead-210 dates assuming a constant rate of supply of unsupported ^{210}Pb to the sediment: Catena, v. 5, p. 1–8.

Appleby, P.G., 2001, Chronostratigraphic techniques in recent sediments, *in* Last, W. and Smol, J., eds., Tracking environmental change using lake sediments, vol. 1, basin analysis, coring, and chronological techniques: Dordrecht, The Netherlands, Kluwer Academic Publishers, p. 171–203.

Bertness, M.D., 1991, Zonation of Spartina Patens and Spartina Alterniflora in a New England salt marsh: Ecology, v. 72, no. 1, p. 138-148.

Bloom, A.L., 1960, Late Pleistocene changes of sea level in southwestern Maine: Augusta, Maine, Dept. of Economic Development, Maine Geological Survey, 143 p.

Bloom, A.L., 1963, Late-Pleistocene fluctuations of sealevel and postglacial crustal rebound in coastal Maine: American Journal of Science, v. 261, p. 862-879.

Bloom, A.L., 1967, Pleistocene shorelines: a new test of isostasy: Geological Society of America Bulletin, v. 78, p. 1477-1494.

Bloom, A.L. and Stuiver, M., 1963, Submergence of the Connecticut coast: Science, v. 139, no. 3552, p. 332-334.

Broccoli, A.J. and Manabe, S., 1990, Can existing climate models be used to study anthropogenic changes in tropical cyclone climate?: Geophysical Research Letters, v. 17, p. 1917-1920.

Brooks, C., 1886, History of the town of Medford, Middlesex County, Massachusetts, from its first settlement in 1630 to 1855. Rev., enl., and brought down to 1885, by James M. Usher: Boston, Massachusetts, Rand Avery, 592 p.

Brown, S.L., Bierman, P.R., Lini, A., Davis, P.T, and Southon, J., 2002, Reconstructing lake and drainage basin history using terrestrial sediment layers: analysis of cores from a post-glacial lake in New England, USA: Journal of Paleolimnology, v. 28, p. 219-236.

Brown, S.L., Bierman, P.R., Lini, A., Southon, J., 2000, 10,000 yr record of extreme hydrologic events: Geology, v. 28: p. 335-338.

Campbell, C., 1998, Late Holocene lake sedimentology and climate change in southern Alberta, Canada: Quaternary Research, v. 49, p. 96–101.

Chapman, H.S., 1936, History of Winchester, Massachusetts: Winchester, Massachusetts, Town of Winchester, 396 p.

Chapman, V.J., 1974, Salt marshes and salt deserts of the world: Lehre, Germany, J. Cramer, 392 p.

Chesebrough, E.W. and Screpetis, A.J., 1975, Upper Mystic Lake water quality study, April 1974-April 1975: Westborough, Massachusetts, Water Quality Section, Division of Water Pollution Control, 75 p.

Chute, N.E., 1959, Glacial geology of the Mystic Lakes-Fresh Pond area, Massachusetts: Washington, United States Government Printing Office, United States Geological Survey Bulletin 1061-F, p. 182-216.

Collins, E.S., Scott, D.B., and Gayes, P.T., 1999, Hurricane records on the South Carolina coast: can they be detected in the sediment record?: Quaternary International, v. 56, p. 15-26.

Davis, R.A., Jr., Knowles, S.C., and Bland, M.J., 1989, Role of hurricanes in the Holocene stratigraphy of estuaries: examples from the Gulf coast of Florida: Journal of Sedimentary Petrology, v. 59, no. 6, p. 1052-1061.

Dean, W.E. Jr., 1974, Determination of carbonate and organic matter in calcareous sediments and sedimentary rocks by loss on ignition: comparison with other methods: Journal of Sedimentary Petrology, v. 44, no. 1, p. 242-248.

Desloges, J.R., 1994, Varve deposition and the sediment yield record at three small lakes of the southern Canadian Cordillera: Arctic and Alpine Research, v. 26, no. 2, p. 130-140.

Diaz, H.F. and Pulwarty, R.S., 1997, Preface, *in* Diaz, H.F. and Pulwarty, R.S., eds., Hurricanes: climate and socioeconomic impacts: Berlin, Springer-Verlag, p. IX-XII.

Dix, G.R., Patterson, R.T., and Park, L.E., 1999, Marine saline ponds as sedimentary archives of late Holocene climate and sea-level variation along a carbonate platform margin; Lee Stocking Island, Bahamas: Palaeogeography, Palaeoclimatology, Palaeoecology, v. 150, no. 3-4, p. 223-246.

Donnelly, J.P., Smith Bryant, S., and nine other authors, 2001a, 700 yr sedimentary record of intense hurricane landfalls in southern New England: Geological Society of America Bulletin, v. 113, p. 714-727.

Donnelly, J.P., Roll, S., and four other authors, 2001b, Sedimentary evidence of intense hurricane strikes from New Jersey: Geology, v. 29, p. 615-618.

Donnelly, J.P., Butler, J., and three other authors, 2004, A backbarrier overwash record of intense storms from Brigantine, New Jersey: Marine Geology, v. 210, p. 107-121.

Duffy, R.A., 1999, Commentary, *in* Trowbridge, J.T., The Tinkham Brothers' Tide-Mill: Arlington, Massachusetts, The Arlington Historical Society, 144 p.

Duval, B. and Ludlam, S.D., 2001, The black water chemocline of meromictic Lower Mystic Lake, Massachusetts, U.S.A.: International Review of Hydrobiology, v. 86, p. 165-181.

Eden, D. N., and Page, M. J., 1998, Paleoclimatic implications of a storm erosion record from late Holocene lake sediments, North Island, New Zealand: Palaeogeography, Palaeoclimatology, Palaeoecology, v. 139, p. 37–58.

Elsner, J.B., Liu, K.-B., and Kocher, B., 2000, Spatial variation in major U.S. hurricane activity: statistics and a physical mechanism: Journal of Climate, v. 13, no. 13, p. 2293–2305.

Emanuel, K.A., 1987, The dependence of hurricane intensity on climate: Nature, v. 326, p. 483-485.

Emanuel, K.A., 1997, Climate variations and hurricane activity: some theoretical issues, *in* Diaz, H.F. and Pulwarty, R.S., eds., Hurricanes: climate and socioeconomic impacts: Berlin, Springer-Verlag, p. 55-65.

Fairbanks, R.G., 1989, A 17,000 year glacio-eustatic sea level record: influence of glacial melting rates on the Younger Dryas event and deep-ocean circulation: Nature, v. 342, p. 637-642.

Fairbridge, R.W., 1961, Eustatic change in sea level, in Ahrens, L.H. et al., eds., Physics and chemistry of the earth, v. 4: New York, New York, Pergamon Press, p. 99-185.

Fetter, C.W. Jr., 1980, Applied Hydrogeology: Columbus, Ohio, Charles E. Merrill Publishing Co., 488 p.

Fisher, T.J., Allison, D.T., Haywick, D.W., Blackwell, K.G., and Grace, M.L., 1998, Storm-driven sedimentation in a Gulf Coast estuary; an undergraduate GIS and grain size mapping project of Weeks Bay, Alabama, *in* Abstracts with Programs, Geological Society of America, v. 30, no. 7, p. 227-228.

Flanagan, S.M., Nielsen, M., and two other authors, 1999, Water-quality assessment of the New England coastal basins in Maine, Massachusetts, New Hampshire, and Rhode Island: environmental settings and implications for water quality and aquatic biota: Pembroke, New Hampshire, United States Geological Survey Water-Resources Investigations Report 98-4249, 56 p.

Flowers, G.C., Klopitz, L.V., and McPherson, G.L., 1995, The impact of Hurricane Andrew; changes in the texture and chemistry of Barataria Estuary bottom sediments: AAPG Bulletin, v. 79, no. 10, p. 1558.

Francus, P., Keimig, F., and Besonen, M., 2002, An algorithm to aid varve counting and measurement from thin-sections: Journal of Paleolimnology, v. 28, p. 283-286.

Garrison, T., 1993, Oceanography: an invitation to marine science: Belmont, California, Wadsworth Publishing Company, 540 p.

Gehrels, W.R., 1999, Middle and late Holocene sea-level changes in eastern Maine reconstructed from foraminiferal saltmarsh stratigraphy and AMS ^{14}C dates on basal peat: Quaternary Research, v. 52, p. 350-359.

Gehrels, W.R., 2002, Intertidal foraminifera as palaeoenvironmental indicators, *in* Haslett, S.K., ed., Quaternary environmental micropalaeontology: London, Great Britain, Arnold, p. 91-114.

Gehrels, W.R. and Belknap, D.F., 1993, Neotectonic history of eastern Maine evaluated from historic sea-level data and ^{14}C dates on salt-marsh peats: Geology, v. 21, p. 615–618.

Gillette, A., 1996, Analysis of salt marsh foraminifera in a core at Short Beach marsh, Revere, Massachusetts in relation to relative rates of sea level change [Unpublished senior project report]: Medford, Massachusetts, Dept. of Geology, Tufts University, 6 p.

Glew, J.R., 1991, Miniature gravity corer for recovering short sediment cores: Journal of Paleolimnology, v. 5, p. 285-287.

Godwin, H., Suggate, R.P., and Willis, E.H., 1958, Radiocarbon dating of the eustatic rise in ocean level: Nature, v. 181, p. 1518-1519.

Gould, H.R. and McFarlan, E. Jr., 1959, Geologic history of the chenier plain, southwestern Louisiana: Gulf Coast Association of Geologic Societies Transactions, v. 9, p. 261-270.

Grove, J.M., 1988, The Little Ice Age: London, Methuen, 498 p.

Hammer, B.K. and Stoermer, E.F., 1997, Diatom-based interpretation of sediment banding in an urbanized lake: Journal of Paleolimnology, v. 17, p. 437-449.

Heiri, O., Lotter, A.F., and Lemcke, G., 2001, Loss on ignition as a method for estimating organic and carbonate content in sediments: reproducibility and comparability of results: Journal of Paleolimnology, v. 25, p. 101-110.

Hilterman, J., 1998, Taxonomic composition, distribution and hurricane effects on diatom assemblages on Masonboro Island, NC: Master's Thesis, University of North Carolina (Wilmington), 97 p.

Hornbeck, J.W., Bailey, S.W., Buso, D.C., and Shanley, J.B., 1997, Streamwater chemistry and nutrient budgets for forested watersheds in New England: variability and management implications: Forest Ecology and Management, v. 93, p. 73-89.

Horsford, E.N., 1860, On the relation of Mystic Pond and River to Boston Harbor, *in* Totten, J.G., Bache, A.D., and Davis, C.H., 1861, City Document No. 12, 1861: Special report of the United States Commissioners on Boston Harbor, on the relation of the Mystic Pond and River to Boston Harbor: Boston, Massachusetts, Geo. C. Rand and Avery, City Printers, 72 p., with Figures and Appendix.

Hughen, K.A., Overpeck, J.T., and two other authors, 1996, The potential for palaeoclimate records from varved Arctic lake sediments: Baffin Island, Eastern Canadian Arctic, *in* Kemp, A.E.S., ed., Palaeoclimatology and palaeoceanography from laminated sediments: Bath, United Kingdom, The Geological Society Publishing House, Special Publication No. 116, p. 57-71.

Hughes, J.W. and Fahey, T.J., 1994, Litterfall dynamics and ecosystem recovery during forest development: Forest Ecology and Management, v. 63, p. 181-198.

Insurance Institute for Property Loss Reduction and Insurance Research Council, Inc. (IIPLR and IRC), 1995, Coastal exposure and community protection: Hurricane Andrew's legacy: Wheaton, Illinois, Insurance Research Council, Inc. and Insurance Institute for Property Loss Reduction, 45 p.

Integovernmental Panel on Climate Change (IPCC), 2001, Climate change 2001: synthesis report. A contribution of working groups I, II, and III to the Third Assessment Report of the Integovernmental Panel on Climate Change [Watson, R.T. and the Core Writing Team (eds.)]: Cambridge, United Kingdom and New York, New York, Cambridge University Press, 398 pp.

Johnson, D.W., 1925, The New England-Acadian shore line: New York, John Wiley, 608 p.

Johnson, D.S. and York, H.H., 1915, The relation of plants to tidal levels: Washington, D.C., Carnegie Institute, Publication 206.

Kalbfleisch, W.B.C and Jones, B., 1998, Sedimentology of shallow, hurricane-affected lagoons; Grand Cayman British West Indies: Journal of Coastal Research, v. 14, no. 1, p. 140-160.

Kaye, C.A., 1959, Shoreline features and Quaternary shoreline changes, Puerto Rico: U.S. Geological Survey Professional Paper 317-B, p. 49-140.

Kaye, C.A. and Barghoorn, E.S., 1964, Late Quaternary sea-level change and crustal rise at Boston, Massachusetts with notes on the autocompaction of peat: Geological Society of America Bulletin, v. 75, p. 63-80.

Keen, T. R. and Slingerland, R.L., 1993, Four storm-event beds and the tropical cyclones that produced them: a numerical hindcast: Journal of Sedimentary Petrology, v. 63, no. 2, p. 218-232.

Keigwin, L.D., 1996, The Little Ice Age and Medieval Warm Period in the Sargasso Sea: Science, v. 274, p. 1504–1508.

Kelley, J.T., Gehrels, W.R., and Belknap, D.F., 1995, Late Holocene relative sea-level rise and the geological development of tidal marshes at Wells, Maine, U.S.A.: Journal of Coastal Research, v. 11, no. 1, p. 136-153.

Knutson, T.R., Tuleya, R.E., and Kurihara, Y., 1998, Simulated increase of hurricane intensities in a CO_2-warmed climate: Nature, v. 279, p. 1018-1020.

Krishnaswami, S. and Lal, D., 1978, Radionuclide limnochronology, *in* Lerman, A., ed., Lakes: chemistry, geology, physics: New York, Springer-Verlag, p. 153–177.

Lamoureux, S.F., 1994, Embedding unfrozen lake sediments for thin section prepartion: Journal of Paleolimnology, v. 10, p. 141-146.

Liu, K.-B., 2000, Paleotempestology: reconstruction of past hurricane landfalls from sedimentary proxy records, *in* Science in an Uncertain Millennium: 2000 AAAS Annual Meeting and Science Innovation Exposition, American Association for the Advancement of Science.

Liu, K.-B. and Fearn, M.L., 1993, Lake-sediment record of late Holocene hurricane activities from coastal Alabama: Geology, v. 21, no. 9, p. 793-796.

Liu, K.-B. and Fearn, M.L., 2000, Reconstruction of prehistoric landfall frequencies of catastrophic hurricanes in northwestern Florida from lake sediment records: Quaternary Research, v. 54, p. 238-245.

Long, S.P. and Mason, C.F., 1983, Saltmarsh ecology: Glasgow, Scotland, Blackie and New York, New York, Chapman and Hall, 160 p..

Ludlam, S.D. and Duval, B., 2001, Natural and management-induced reduction in monimolimnetic volume and stability in a coastal, meromictic lake: Journal of Lake and Reservoir Management, v. 17, no. 2, p. 71-81.

Ludlum, D.M., 1963, Early American hurricanes 1492-1870: Boston, Massachusetts, American Meteorological Society, 198 p.

Lyles, L.D., Hickman, L.E. Jr., and Debaugh, H.A. Jr., 1988, Sea level variations for the United States 1855-1986: Rockville, Maryland, NOAA, U.S. Department of Commerce.

Mann, M.E., Bradley, R.S., and Hughes, M.K., 1998, Global-scale temperature patterns and climate forcing over the past six centuries: Nature, v. 392. p. 779-787.

Mann, M.E., Bradley, R.S., and Hughes, M.K., 1999, Northern hemisphere temperatures during the past millennium: inferences, uncertainties, and limitations: Geophysical Research Letters, v. 26, no. 6, p. 759.

Martin, C.W. and Hornbeck, J.W., 1994, Logging in New England need not cause sedimentation of streams: Northern Journal of Applied Forestry, v. 11, no. 1, p. 17-23.

May, J.P., 1990, The effects of Hurricane Hugo in the sedimentology and bathymetry of the Charleston shoal area, South Carolina: South Carolina Geology, v. 33, no. 2, p. 17-24.

McFarlan, E. Jr., 1961, Radiocarbon dating of late Quaternary deposits, south Louisiana: Geological Society of America Bulletin, v. 72, p. 129-158.

McIntire, W.G. and Morgan, J.P., 1964, Recent geomorphic history of Plum Island, Massachusetts and adjacent coasts: Baton Rouge, Louisiana, Louisiana State University Press, 44 p.

Merkt, J. von, 1971, Zuverlässige Auszählungen von Jahresschichten in Seesedimenten mit Hilfe von Gross-Dünnschliffen: Archiv für Hydrobiologie, v. 69, p. 145-154.

Merrens, E.J. and Peart, D.R., 1992, Effects of hurricane damage on individual growth and stand structure in a hardwood forest in New Hampshire, USA: Journal of Ecology, v. 80, no. 4, p. 787-795.

Michaels, A., Malmquist, D., Knap, A., and Close, A., 1997, Climate science and insurance risk: Nature, v. 389, p. 225-227.

Miller, W.R. and Egler, F.E., 1950, Vegetation of the Wequetequock-Pawcatuck tidal-marshes, Connecticut: Ecological Monographs, v. 20, no. 2, p. 143-172.

Niering, W.A. and Warren, R.S., 1980, Vegetation patterns and processes in New England salt marshes: BioScience, v. 30, no. 5, p. 301-307.

Nixon, S.W., 1982, The ecology of New England high salt marshes: a community profile: Washington, D.C., United States Department of the Interior.

National Oceanic and Atmospheric Administration (NOAA), 1998 (on-line), Population: distribution, density and growth: NOAA's State of the Coast Report: Silver Spring (MD), prepared by Thomas J. Culliton, URL: http://state-of-coast.noaa.gov/bulletins/html/pop_01/pop.html.

Noren, A.J., Bierman, P.R., Steig, E.J., Lini, A., Southon, J., 2002, Millennial-scale storminess variability in the northeastern United States during the Holocene epoch: Nature, v. 419, p. 821-824.

Nydick, K.R., Bidwell, A.B., and two other authors, 1995, A sea-level rise curve from Guilford, Connecticut, USA: Marine Geology, v. 124, p. 137-159.

Nyman, J.A., Crozier, C.R., and DeLaune, R.D., 1995, Roles and patterns of hurricane sedimentation in an estuarine marsh landscape: Estuarine, Coastal and Shelf Science, v. 40, p. 665–679.

Oldale, R.N., 1985, Late Quaternary sea-level history of New England: a review of the published sea-level data: Northeastern Geology, v. 7, p. 192-200.

Oldale, R.N., Colman, S.M., and Jones, G.A., 1993, Radiocarbon ages from two submerged strandline features in the western Gulf of Maine and a sea-level curve for the northeastern Massachusetts coastal region: Quaternary Research, v. 40, p. 38-45.

Page, M.J., Trustrum, N.A., and DeRose, R.C., 1994, A high resolution record of storm-induced erosion from lake sediments, New Zealand: Journal of Paleolimnology, v. 11, p. 333-348.

Pardo, L.H., Driscoll, C.T., and Likens, G.E., 1995, Patterns of nitrate loss from a chronosequence of clear-cut watersheds: Water, Air, and Soil Pollution, v. 85, p. 1659-1664.

Parsons, M.L., 1998, Salt marsh sedimentary record of the landfall of Hurricane Andrew on the Louisiana coast; diatoms and other paleoindicators: Journal of Coastal Research, v. 14, no. 3, p. 939-950.

Patton, P.C. and Horne,G.S., 1991, A submergence curve for the Connecticut River estuary: Journal of Coastal Research Special Issue, v. 11, p. 181-196.

Pennington W., Cambray, R.S., and Fisher, E.M., 1973, Observations on lake sediments using fallout ^{137}Cs as a tracer: Nature, v. 242, p. 324–326.

Perley, S., 1891, Historic storms of New England: Salem, Massachusetts, Salem Press Publishing and Printing Co., 341 p.

Pore, N.A., 1973, Marine conditions and automated forecasts for the Atlantic coastal storm of February 18-20, 1972: Monthly Weather Review, v. 101, n. 4, p. 363-370.

Pu, M., Fahey, T.J., and Hughes, J.W., 1993, Effects of soil disturbance on vegetation recovery and nutrient accumulation following whole-tree harvest of a northern hardwood ecosystem: Journal of Applied Ecology, v. 30, p. 661-675.

Rasband, W.S., 2006, ImageJ, U. S. National Institutes of Health, Bethesda, Maryland, USA, http://rsb.info.nih.gov/ij/.

Redfield, A.C., 1967, Postglacial change in sea level in the western North Atlantic Ocean: Science, v. 157, no. 3789, p. 687-692/

Redfield, A.C., 1972, Development of a New England salt marsh: Ecological Monographs, v. 42, no. 2, p. 201-237.

Redfield, A.C. and Rubin, M., 1962, The age of salt marsh peat and its relation to recent changes in sea level at Barnstable, Massachusetts: Proceedings of the National Academy of Sciences of the United States of America, v. 48, no. 10, p. 1728-1735.

Rejmanek, M., Sasser, C.E., and Peterson, G.W., 1988, Hurricane-induced sediment deposition in a Gulf Coast marsh: Estuarine, Coastal and Shelf Science, v. 27, no. 2, p. 217-222.

Renberg, I., 1981, Improved methods for sampling, photographing and varve-counting of varved lake sediments: Boreas, v. 10, p. 255-258.

Rodbell, D.T., Seltzer, G.O., Anderson, D.M., Abbott, M.B., Enfield, D.B., and Newman, J.H., 1999, An ~15,000-year record of El Niño-driven alluviation in southwestern Ecuador: Science, v. 283, p. 516-520.

Risk Prediction Initiative (RPI), 1997 (online), Tropical cyclones and climate variability: a research agenda for the next century: Bermuda, Risk Prediction Initiative, URL: http://www.bbsr.edu/rpi/tcdoc/tclong.html.

Scott, D.B. and Collins, E.S., 1999, Hurricane records on the South Carolina coast: patterns of periodicity over the last 5000 years, *in* Abstracts with Programs, Geological Society of America, v. 31, no. 7, p. A382.

Scott, D.K. and Leckie, R.M., 1990, Foraminiferal zonation of Great Sippewissett salt marsh: Journal of Foraminiferal Research, v. 20, p. 248-266.

Scott, D.B. and Medioli, F.S., 1978, Vertical zonations of marsh foraminifera as accurate indicators of former sea-levels: Nature, v. 272, p. 528–531.

Scott, D.B. and Medioli, F.S., 1980, Quantitative studies of marsh foraminiferal distributions in Nova Scotia: implications for sea-level studies: Cushman Foundation for Foraminiferal Research Special Publication 17, 57 p.

Scott, D.B., Collins, E.S., and two other authors, 2003, Records of prehistoric hurricanes on the South Carolina coast based on micropaleontological and sedimentological evidence, with comparison to other Atlantic Coast records: Geological Society of America Bulletin, v. 115, no. 9, p. 1027-1039.

Socolow, R.S., Girouard, G.G., and Ramsbey, L.R., 2003, Water Resources Data for Massachusetts and Rhode Island, 2002, Water-Data Report MA-RI-02-1, 340 p.

Stanley, D.J., 1995, A global sea-level curve for the late Quaternary: the impossible dream?: Marine Geology, v. 125, p. 1-6.

Stuiver, M. and Reimer, P. J., 1993, Extended ^{14}C database and revised CALIB radiocarbon calibration program: Radiocarbon, v. 35, p. 215-230.

Thomas, E. and Varekamp, J.C., 1991, Paleoenvironmental analyses of marsh sequences (Clinton, Conn.): evidence for punctuated sea-level rise during the latest Holocene: Journal of Coastal Research Special Issue, v. 11, p. 125-158.

Thompson, W.B., 1982, Recession of the late Wisconsinan ice sheet in coastal Maine, *in* Larson, G.J. and Stone, B.D., eds., Late Wisconsinan glaciation of New England: Dubuque, Iowa, Kendall/Hunt, p. 211-228.

Thorndycraft, V., Hu, Y., Oldfield, F., Crooks, P.R.J., and Appleby, P.G., 1998, Individual flood events detected in the recent sediments of the Petit Lac d'Annecy, eastern France: The Holocene, v. 8, p. 741-746.

Totten, J.G., Bache, A.D., and Davis, C.H., 1861, City Document No. 12: Special report of the United States Commissioners on Boston Harbor, on the relation of the Mystic Pond and River to Boston Harbor: Boston, Massachusetts, Geo. C. Rand and Avery, City Printers, 72 p., with Figures and Appendix.

Ulrich, K.E., Burton, T.M., and Oemke, M., 1993, The effects of whole-tree harvest on benthic algae in headwater streams in New Hampshire: Journal of Freshwater Ecology, v. 8, no. 2, p. 83-92.

United States Geological Survy (USGS), 1985, Boston North, Massachusetts, 1:25,000 scale metric topographic map, 42071-D1-TM-025.

Valeriani, J.V., 1979, The history of Medford: a study of local history [Ed.D. thesis]: Boston, Massachusetts, Boston University, 148 p.

van de Plassche, O., 1986, Introduction, *in* van de Plassche, O., ed., Sea-level research: a manual for the collection and evaluation of data: Norwich, United Kingdom, Geo Books, p. 1–26.

van de Plassche, O., 1991, Late Holocene sea-level fluctuations on the shore of Connecticut inferred from transgressive and regressive overlap boundaries in salt-marsh deposits: Journal of Coastal Research Special Issue, v. 11, p. 159–180.

van de Plassche, O., van der Borg, K., and de Jong, A.F.M., 1998, Sea level–climate correlation during the past 1400 yr: Geology, v. 26, p. 319–322.

van de Plassche, O., van der Borg, K., and de Jong, A.F.M., 1999, Sea level–climate correlation during the past 1400 yr: Reply: Geology, v. 27, p. 190.

Varekamp, J.C., Thomas, E., and van de Plassche, O., 1992, Relative sea-level rise and climate change over the last 1500 years: Terra Nova, v. 4, p. 293–304.

Varekamp, J.C., Thomas, E., and Thompson, W.G., 1999, Sea level–climate correlation during the past 1400 yr: Comment: Geology, v. 27, p. 189–190.

Williams, H.F.L., 1995, Foraminiferal record of recent environmental change: Mad Island Lake, Texas: Journal of Foraminiferal Research, v. 25, no. 2, p. 167-179.

Wright,H.E. Jr., Mann, D.H., and Glaser, P.H., 1983, Piston corers for peat and lake sediments: Ecology, v. 65, p. 657-659.

Zubick, M.N., 2004, title unknown [MSc thesis]: Medford, Massachusetts, Tufts University, Dept. of Civil and Environmental Engineering, degree completed under the supervision of Dr. John Durant.